UNIVERSITY OF SOUTHAMPTON

FACULTY OF ENVIRONMENTAL AND LIFE SCIENCES

Ocean and Earth Science

Compound Flooding in the UK: Past, Present and Future Co-occurring Extreme Flooding Hazard Sources

By

Alistair Jamie William Hendry

Thesis for the degree of Doctor of Philosophy

August 2021

Abstract

Flooding is one of the most dangerous and costly natural disasters with wide ranging social, economic and environment impact. In low-lying coastal areas, flooding typically arises through four main sources; at the coast as a result of (1) storm surges and (2) waves, and terrestrially, through (3) fluvial (river) and (4) pluvial (surface water) flooding. When two or more of the sources combine, compound flooding can occur, and the catastrophic results can be magnified greatly, leading to some of the worst flood events (such as Hurricane Harvey in Houston, USA). Despite the increased consequences, compound flooding is far less well understood compared to the individual sources, particularly in the UK. The overall aim of this thesis is therefore to determine which regions of the UK coast are most subject to compound flooding, which combination of source variables are most apparent, and what variables (e.g., meteorological conditions, catchment characteristics) control the spatial patterns evident in compound events, to help inform future compound flood defence and response strategies.

The first objective is to assess the potential for compound flooding arising from the joint occurrence of extreme sea levels and river discharge around the coast of UK and investigate the driving mechanisms involved. The west coast is identified as having a far greater number of joint occurring events compared to the east coast (3-6 events per decade compared to 0-1). The primary cause of this spatial variability is found to be the meteorological conditions leading to extreme surge and river discharge on the west coast are similar storm types, whereas on the east coast, the storms typically follow different weather patterns and tracks. The strength and phase of dependence between extreme surge and river discharge is compared to river catchment characteristics (i.e., flashiness, catchment size and elevation gradient). It's found that high skew surges tend to occur more frequently with high river discharge at catchments with a lower base flow index, smaller catchment area, and steeper elevation gradient.

The second objective is to quantify the risk of underestimating compound flooding around the coast of the UK arising from the joint occurrence of all possible pairs of the four main flood sources. The most extreme events joint occurrences were found between surge and waves (at Liverpool with 17 events per decade) whilst the strongest dependence was between wave and river discharge. All flood combination pairs showed a stronger dependence on the west coast compared to the east (for example, for wave vs river discharge, on the west coast, τ =0.35-0.5, whilst on the east coast τ = 0.05-0.2). Furthermore, it is shown that ignoring the relationship between the flood sources can lead to an underestimation of the flood risk by 5-6 times when compared to considering the flood sources dependent on each other.

Finally, a novel methodology is developed to extend compound flood records beyond the observed overlapping datasets, using the weather patterns likely to lead to compound flood events. In a historical meteorological reanalysis (1851-2017), no increasing or decreasing long-term trend was found in compound flood events (involving extreme surge and river discharge). Similar interannual and decadal variability was seen in the meteorological record compared to long-term individual surge and river discharge records. Clustering of surge events found in the periods 1925-1945 and 1995-2005 and fewer events in the mid 20th century (1945-1985) which matched to the compound events identified using the meteorological approach.

Based on these findings, the areas of the UK most at risk to compound flooding have been located and therefore, flood defences and responses can be designed to cope much more effectively with compound flood events. The identification of the meteorological conditions leading to compound flood events can be implemented into forecasting capabilities, reducing emergency response reaction times and potentially reducing deaths, injuries and damages. Furthermore, these weather patterns could be used to better understand the future risk of compound flooding, by examining their occurrence in future climate predictions.

Table of Contents

List of Figures

List of Tables

Declaration of Authorship

I, Alistair Jamie William Hendry, declare that this thesis "Compound Flooding in the UK: Past, Present and Future Risk of Co-occurring Extreme Flooding Events" and the work presented in it are my own and has been generated by me as the result of my own original research.

I confirm that:

1. This work was done wholly or mainly while in candidature for a research degree at this University;
2. Where any part of this thesis has previously been submitted for a degree or any other qualification at this University or any other institution, this has been clearly stated;
3. Where I have consulted the published work of others, this is always clearly attributed;
4. Where I have quoted from the work of others, the source is always given. With the exception of such quotations, this thesis is entirely my own work;
5. I have acknowledged all main sources of help;
6. Where the thesis is based on work done by myself jointly with others, I have made clear exactly what was done by others and what I have contributed myself;
7. Parts of this work have been published as:
    a. *Hendry, A., Haigh, I. D., Nicholls, R. J., Winter, H., Neal, R., Wahl, T., Joly-Laugel, A. and Darby, S. E.: Assessing the characteristics and drivers of compound flooding events around the UK coast, Hydrol. Earth Syst. Sci., 23(7), 3117–3139, doi:10.5194/hess-23-3117-2019, 2019.*

Signed:

Date:

Acknowledgements

I'd firstly like to offer a huge thank you to my primary supervisor Dr Ivan Haigh. I had initially wanted to experience a new university when I looked into doing a PhD. However, having worked with Ivan at an undergraduate level, I knew of his dedication, compassion and understanding for his students. He was the main reason I returned to Southampton, and I'm very glad of that decision. To Prof Robert Nicholls, I owe thanks for providing great steering during this journey. His excellent eye for the bigger picture always helped keep me on track.

To the University of Southampton, I acknowledge the receipt of a studentship, enabling the project to take place. To EDF R&D UK I acknowledge the receipt of funding. I would also like to thank my supervisors at EDF, Dr Hugo Winter, whose knowledge of statistics was an invaluable asset; Amélie Joly-Laugel, for help with the extreme weather and hindcasts; as well as Pietro Bernardara, who's input at the beginning helped get the project started. I would also like to thank Dr Dafni Sifnioti for providing valuable comments in the closing stages of my thesis.

I would also like to thank the following for their input in both the PhD and publications; Dr Thomas Wahl, who's extensive knowledge of compound flooding, statistics and sea level was invaluable. Prof. Stephen Darby provided great support on riverine flooding, and what variables I should focus on. Robert Neal at the Met Office provided much guidance on weather patterns and their applications to flooding. Prof. Philip Ward, for inviting me to participate in his research, and allow me to consider compound flooding on a global scale.

I owe an enormous debt of gratitude to my partner, Emily who has helped keep me sane during this process, made sure I kept some form of work-life balance, and always helped keep things in perspective. Finally, I'd like to thank Norman, who came into our lives part way through this journey, and showed me that no matter how bad your day is going, it can always be improved by chasing a ball.

Abbreviations

Abbreviation	Definition
AMAX	Annual maximum
AMO	Atlantic multi-decadal oscillation
AO	Arctic oscillation
BFI	Base flow index
BODC	British Oceanographic Data Centre
CaMa	Catchment-based macro-scale floodplain model
CC	Correlation Coefficient
CCO	Channel Coastal Observatory
CDAS	Climate Data Assimilation System
CEDA	Centre for Environmental Data Analysis
CEFAS	Centre for Environment, Fisheries and Aquaculture Science
CEH	Centre for Ecology & Hydrology
CF	Compound flooding
CFG	Capéraá-Fougéres-Genest
CMIP5	Coupled Model Intercomparison Project Phase 5
CPC	Climate Prediction Center
DEFRA	Department for Environment, Food and Rural Affairs
DEM	Digital elevation model
DJFM	December January February March
EA	Environment Agency
ECMWF	European Centre for Medium-Range Weather Forecasts
ERA-5	European Reanalysis-5
EVA	Extreme value analysis
FES2012 model	Finite Element Solution tide model
GCM	Global climate model
GDP	Gross domestic product
GEV	Generalised extreme value distribution
GOW2	Global ocean waves 2
GPD	Generalised pareto distribution
GWL	Grosswetterlagen weather regimes
H&T	Heffernan and Tawn method
HADGEM2-ES	Hadley Centre Global Environment Model version 2 Earth-System configuration
Hmo	Spectral significant wave height
Hs	Significant wave height
IPCC	Intergovernmental Panel on Climate Change
MIDAS	Met Office Integrated Data Archive System
MSL	Mean sea level
MSLP	Mean sea level pressure

NAO	North Atlantic oscillation
NRFA	National River Flow Archive
NTR	Non-tidal river
NTSLF	National Tidal and Sea Level Facility
PC	Pearson's correlation
POT	Peaks over threshold
PWC	Precipitable water content
RA	Rainfall
RCP	Representative Concentration Pathway
RD	River discharge
RDvsRA	River discharge vs rainfall
RMSD	Root mean square difference
RMSE	Root mean square error
RPCA	Rotated principal component analysis procedure
SD	Standard deviation
SL	Sea level
SSD	Sum of square differences
SU	Surge
SUvsRA	Surge vs rainfall
SUvsRD	Surge vs river discharge
SUvsWA	Surge vs wave
SWEEP-OWWL	South West Partnership for Environment and Economic Prosperity - Operational Wave and Water Level
Tp	Peak wave period
TWL	Total water level
Tz	Mean zero-upcrossing period
WA	Wave
WAvsRA	Wave vs rainfall
WAvsRD	Wave vs river discharge
WCRP	World Climate Research Program
wNAO	Winter North Atlantic oscillation
WP	Weather pattern
WS	Wind speed

1. Introduction

1.1 Background, motivation and justification

Flooding is one of the most dangerous and costly natural disasters. From 1980 to 2013, floods accounted for more than 1 trillion USD in losses and resulted in at least 220,000 fatalities globally (Munich Re, 2017). More than 50% of these deaths and a large proportion of the economic losses occurred in densely populated low-lying coastal regions. Globally, coastal areas are home to more than 600 million people and constitute strategic economic centres (McGranahan et al., 2007). Recent flood events, for example, Cyclone Nargis in Myanmar (Fritz et al., 2009), Hurricane Katrina in the US (Jonkman et al., 2009), Storm Xynthia in France (Lumbroso & Vinet, 2011), flooding in the UK over the winter of 2013–2014 (Haigh et al., 2016), and Hurricane Harvey in the US (Emanuel, 2017), have demonstrated the ever-present threat of serious flood impacts in coastal regions despite improvements in levels of flood protection and advancements in flood forecasting and warnings. Furthermore, coastal flooding is a growing threat due to mean sea-level rise and changes in storminess (Church et al., 2013; Nerem et al., 2018), ongoing vertical land movement, especially subsistence (Brown & Nicholls, 2015; Nicholls et al., 2021), and rapid population growth and accompanying development in flood-exposed areas (Brown et al., 2018; Hallegatte et al., 2013)

Flooding in coastal regions arises from four main source mechanisms (and their interactions):

(1) storm surge combined with high astronomical tide (storm tides);

(2) locally (wind) or remotely (swell) generated waves;

(3) river discharge (fluvial); or

(4) direct surface run-off (pluvial).

The first two sources are oceanographic in origin, while the latter two mainly arise from heavy precipitation but can also be caused by snow melt. Flooding can also be caused by tsunami's; however, they are not considered in this thesis as they're 1) extremely uncommon in the UK and 2) geological in origin rather than climatic. Erosion can also lead to flooding via a breach of a natural barrier or damaging the structure integrity of a hard engineered defence; or by mediating the source of flooding (e.g. beach lowering increasing overtopping). As erosion is geological in nature it's not considered further. Most existing flood risk assessments consider these four main drivers of flooding separately. However, in coastal regions, floods are often

caused by more than just one factor because they may be correlated (i.e., with storms). Furthermore, the adverse consequences of a flood can be greatly exacerbated when the oceanographic (storm tides and waves), fluvial, and/or pluvial drivers occur concurrently or in close succession (i.e., a few hours to days apart). Depending on local characteristics (which influence lag times between variables), this can result in disproportionately extreme events, referred to as compound flood events. Compound events are defined by the Intergovernmental Panel on Climate Change (Seneviratne et al., 2012) as *"(1) two or more extreme events occurring simultaneously or successively, (2) combinations of extreme events with underlying conditions that amplify the impact, (3) and combinations of events that are not them- selves extremes but lead to an extreme event when combined".* With the potential to create considerable destruction, the World Climate Research Program (WCRP) Grand Challenge on Weather and Climate Extremes has recently identified compound events as an international research priority (Zscheischler et al., 2018). Recently, Zscheischler et al., (2020) more specifically defined compound weather/ climate events as *"the combination of multiple drivers and/or hazards that contributes to societal or environmental risk".* Drivers include the processes, variables and phenomena present in climate/weather which can span over varying spatial and temporal scales; whilst hazards are the immediate physical precursor to negative impact (e.g. floods, wildfires or drought). Finally, the risk is simply defined as the probability of hazards occurring multiplied by the consequences.

A recent example of compound flooding occurred during Hurricane Harvey in 2017 in the USA. Record-breaking rainfall, river discharge, and run-off, combined with a moderate but long-lasting storm surge, resulted in disastrous flooding in Houston (USA) (Emanuel, 2017). It was the second-costliest natural disaster in US history (Blake & Zelinksy, 2018). Hurricane Irma in 2017 was also a prime example of compound flooding, where significant flooding occurred along the St Johns River in Jacksonville (US) as a result of a combined storm surge and extensive rainfall run-off (Cangialosi et al., 2017). Compound flooding can also arise from extratropical storms. For example, a storm surge on the Adriatic coast of Italy obstructed large amounts of freshwater run-off (generated by the same storm) from draining, causing major compound flooding in Ravenna, Italy (Bevacqua et al., 2017). It is now recognised that by not considering compound flooding, the risk may be greatly underestimated (Wahl et al., 2015).

Northern Europe, and specifically the UK, has a long history of coastal flooding, resulting in large numbers of fatalities, damage to property and infrastructure as well as environmental consequences (Lamb, 1991). Whilst tropical cyclones do not impact the British Isles, extra-

tropical storms frequently hit the UK during the winter season (Wolf et al., 2020). The most severe coastal flooding event in living memory (in Northern Europe) was the North Sea flood of 1953, which killed 307 along the east coast of England, 30 in Scotland, 1836 people in the Netherlands, 40 in Belgium and resulted in more than 250 boating related deaths (Baxter, 2005; Wadey et al., 2015). The total damage in England and Scotland was estimated to be £50 million (or £1.5 billion today). This event triggered a far greater interest in flood risk management, with sophisticated flood defences (such as the Delta Works programme in the Netherlands and the Thames barrier in the UK), forecasting systems and monitoring systems (such as tide gauges) all being developed (Lumbroso & Vinet, 2011; Wadey et al., 2015).

The most notable flooding in the UK since 1953, occurred during the 2013-14 storm season, notably Storm Xaver which occurred during 5th-6th December 2013. Unlike the 1953 event, which only caused flooding along the east coast, Xaver impacted coastlines in Ireland, Scotland, Wales, northwest England, the east coast and English Channel. Measures taken after the 1953 event resulted in only 2800 properties flooded in December 2013, compared to 24,000 in 1953, but importantly the 2013 event resulted in no fatalities. Despite this, the 2013-14 storm season still cost £1.3 billion, highlighting a continued need to develop monitoring, forecasting and defensive schemes (Chartteron et al., 2016).

The UK is not only susceptible to marine based flooding, but also has a long history of pluvial and fluvial flooding. In recent times, the 2007 summer floods were generated by Britain's wettest May-July period since records began in 1776. Flooding occurred across the Midlands and north England, Wales and Scotland (Marsh et al., 2007). The Environment Agency estimated damage costs of ~£3.2 billion (Environment Agency et al., 2013). The 2013-14 storm season also had considerable inland flooding. Whilst the total number of properties flooded was less than the 2007 events, the combined impact with coastal flooding stretched the response teams' abilities. Notable areas flooded included the Somerset Levels, where 6900 ha of agriculture land were affected (Kendon & McCarthy, 2015). More recently, Storms Ciara and Dennis in 2020 produced the wettest February since records began in 1776, causing wide spread flooding across the UK with estimated insurance losses of £150-200 million and £175-225 million for Storms Ciara and Dennis, respectively (Finlay, 2020).

Flooding can also have a huge impact on critical infrastructure, such as power and transportation networks. This can directly hamper recovery efforts, for example, loss of power can prevent urban waste water pumps functioning to remove water (Burzel & Becker, 2014) and loss of transportation networks can prevent emergency services attending the area affected

(Lu et al., 2015). Once the immediate danger has passed, the cost of repairing such infrastructure can be considerable; for example, during the 2013/14 winter storms in the UK, the Dawlish rail line to Plymouth and Cornwall, collapsed in the sea as a result of waves and a storm surge overnight on 4th and 5th February 2014. The closure and repair of the line was estimated to be up to £1.2 billion (Dawson et al., 2016; Dawson et al., 2018; Devon Maritime Forum, 2014)

The need to consider compound events in the design of flood protection schemes in the UK is strongly illustrated by the flood event on the 24th–25th December 1999 in Lymington, on the southern coast of England where significant flooding occurred despite a significant recent upgrade in flood defences. On the 16–17 December 1989, Lymington was flooded by high sea levels and waves, with considerable damage to 50 houses and the railway line (Haigh et al., 2015; Ruocco et al., 2011; Wadey, 2013) This event was the driving force for a large upgrade of coastal flood defences for the town, including new sluice gates which allowed the Lymington River to drain at low tide but sealed it from tidal flooding during high sea levels. However, no allowance or consideration of compound flooding appears to have been made in the design. Ten years later, on 24 December 1999, a storm surge was generated that did not directly cause flooding itself because of the raised defences. However, the storm surge prevented the sluice gates from opening for a prolonged period, while large volumes of rainfall in the Lymington River catchment during the storm raised the river flow. Combined with the lack of drainage, this caused flooding from the river on the upstream side of the sea defences (Ruocco et al., 2011b). After 1999, the Lymington flood defences were upgraded again. This experience strongly highlights the importance of considering compound flooding when assessing and designing flood management.

In the last two decades, there has been a rapid increase in the number of studies starting to look at compound flooding. These are reviewed in detail in Chapter 2. Key papers include those which have looked at compound flooding globally (Ward et al., 2018); developed new methods of assessing joint probability (Wahl et al., 2015); studied future compound flooding risk (Bevacqua et al., 2019, 2020); and carried out sensitivity test on the range of approaches to assess compound flooding (Camus et al., 2021). Within the UK, Svensson and Jones (2002 and 2004) provided the most spatially comprehensive appraisal of compound flood around the UK for extreme river discharge and water level. A joint probability method was developed for the Department for Environment, Food and Rural Affairs (DEFRA) in the UK, JOIN-SEA (Hawkes et al., 2002), which formed the primary method of compound flooding assessment

through the early 2000. JOIN-SEA is likely to be superseded by new multivariate approaches (Gouldby et al., 2017) for coastal design. There are still key knowledge gaps relating to compound flooding however.

Thus far, no study has considered how compound flood occurrences in different areas of the UK vary. Svensson and Jones (2002 and 2004) consider the western and eastern coasts of the UK separately, and so do not identify any variability. Furthermore, no study has considered the driving forces behind compound flooding in the UK, either at a national scale (such as meteorological conditions) or at a localised catchment scale (such as catchment size, elevation or geology).

To date, no studies have considered the four main sources of flooding in the UK (water level, waves, fluvial and pluvial) in a single study, with most focusing on occurrences of two sources. By not taking all flood sources into account, an underestimation of the total flood risk can occur.

Finally, a key limit on studying compound flooding is the lack of data. Overlapping observed (or modelled) datasets for each variable are required, which typically limits studies to the last 50 years. The conclusions which can be drawn on temporal trends in compound flooding are therefore reduced, and so far, no studies have analysed long term compound flooding trends.

1.2 Aims and Objectives

The overall aim of this thesis is **to determine which regions of the UK coast are most subject to compound flooding, which combination of source variables are most apparent, and what variables (e.g. meteorological conditions, catchment characteristics) control the spatial patterns evident in compound events**. This aim will be addressed through the following three thesis objectives:

- **Thesis Objective 1:** To assess the potential for compound flooding arising from the joint occurrence of high sea levels and high river discharge around the coast of UK and investigate the driving mechanisms involved;
- **Thesis Objective 2:** To quantify the hazard of underestimating compound flooding around the coast of the UK arising from the joint occurrence of all possible pairs of the four main flood sources; and

- **Thesis Objective 3:** To evaluate how the frequency of compounding flooding has varied in the past and might vary in the future.

Objective 1 focuses on only two drivers of flooding in coastal regions, high sea levels and high river discharge and develops a comprehensive novel frame work to identify spatial patterns of compound flooding and driving mechanisms, beyond that undertaken to date. Tide gauge data and river discharge records, covering the period from 1915 to 2018, are used to map where on the coast high sea levels can occur at the same time as high river discharge. Then, weather patterns and catchment characteristics are examined to assess why large storm surges and high river discharge are more likely to coincide along certain stretches of coastline compared to others. Building on Thesis Objective 1, Thesis Objective 2 assesses all four drivers of compound flooding around the UK coast. Statistical approaches are used to quantify if flood likelihood is under-estimated if compound flooding is not considered, for the period 1915 to 2018. In Thesis Objective 3, the weather patterns, identified in Thesis Objective 1, that typically cause compound flooding are used to evaluate how the frequency of compounding flooding has varied historically from 1851 to 2017 and might vary in the future for different climate projections up to the year 2095.

1.3 Structure of Thesis

The structure of the thesis is as follows. **Chapter 2** provides a comprehensive literature review which defines what compound flooding is, discusses the state-of-the-art research undertaken in recent decades, and describes what the key knowledge gaps are. **Chapter 4** focuses on Thesis Objective 1, which assesses the joint occurrence of extreme storms surges and river discharge occurring around the UK coastline. **Chapter 0** is based on Thesis Objective 2, which focuses on the compound flood risk from the joint occurrence of all four major flooding sources around the UK coast. **Chapter 6** focuses on Thesis Objective 3, which uses weather patterns as a proxy to expand the records of compound flood events beyond the observed datasets. In **Chapter 7**, the conclusions, implications and further work are discussed.

2. Literature Review

This chapter provides a background and literature review of compound flooding. Section 2.1 explains the individual source components that can give rise to flooding in coastal regions. In particular, it outlines their relevance to the UK. The definitions and types of compound flooding are described in Section 2.2. Section 2.3 reviews important past compound flooding events that have occurred in the UK and internationally. Section 2.4 provides a simple overview of all relevant studies that have assessed compound flooding to date. A definition of the different variables that have been used in past studies is discussed in Section 2.5 to aid in the comparison among studies. Section 2.6 discusses the methods of extreme sampling and event definitions. A review of the approaches used is discussed in Section 2.7. Finally, the key knowledge gaps are highlight in Section 2.8.

2.1 Individual flood sources

Flooding in a coastal environment can occur through a variety of distinct source mechanisms, as follows: (i) as a storm generated surge, combined with high astronomical tide; (ii) through wind driven wave setup and runup; and through precipitation (or snow melt), either through (iii) increased river discharge (fluvial) of directly as (iv) runoff (pluvial). Each of these four sources is briefly described in the following sub-sections. Flooding can also arise due to ground water, tsunamis or breach flood barriers (natural or engineered), but these are not considered in this thesis. A summary of the different variables can be seen in Figure 2.1.

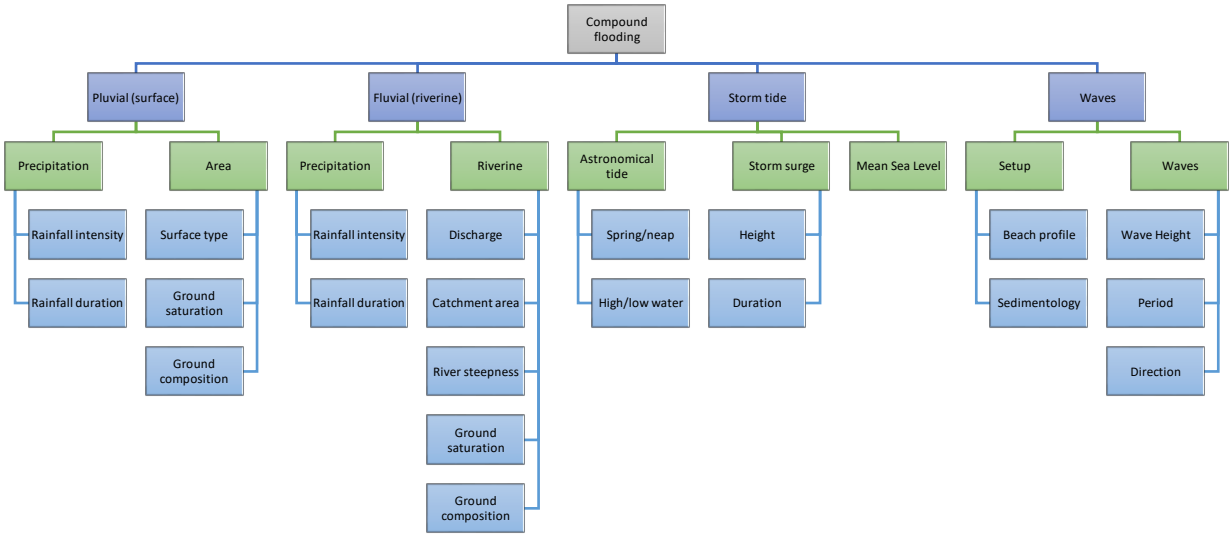

Figure 2.1: The major compound flooding sources and their variables.

2.1.1 Storm tides

Extreme still sea levels are caused by the combination of three principle factors, as follows :(1) mean sea level (MSL), the long term (monthly to yearly) variations in sea levels primarily due to the thermal expansion of the oceans and melting of continental ice sheets and glaciers; (2) astronomical tides, created by the gravitational attraction and rotation of the Earth, Moon and Sun system; and (3) storm surges, which are generated by strong winds and low air atmospheric pressures (Pugh, 2004). Tides are deterministic and can be predicted accurately into the future, whereas storm surges are stochastic. Storm tides arise when a large storm surge coincides with high water of a spring astronomical tide (when the Moon and Sun are in phase and create the largest high water), producing extreme high still sea levels.

Storm surges in the UK are generated by extra-tropical storms (those which formed between 30-60° latitude). These typically differ from those created by tropical cyclones, lasting longer (several days rather than hours to days). They have a larger spatial scale (~1000km compared to ~500km) but smaller amplitude (typically 2-3m compared to 5-10m) (Haigh et al., 2016; Pugh & Woodworth, 2014). Haigh et al. (2016) looked at the distribution of extreme water

levels and surges around the UK. They found that most extreme sea level events were generated by moderate, rather than extreme storm surges, coinciding with spring high tides. They also found four distinct footprint categories, with the storm tracks and location of storm centre defining which of the four footprints occurred. Brown et al. (2010) modelled present and future surges in the eastern Irish sea, finding that sea level rise was found to have a greater impact on the surge height compared to increased wind velocities.

2.1.2 Waves

Wind waves are generated by wind stress causing variations in the sea surface height, which develop into waves propagating in the wind direction. As the waves travel towards the coastline the seabed shoals, a process known as wave set-up may occur. The reduced depth causes the waves to be slowed down and compressed, resulting in an increase in amplitude and this can result in waves overtopping sea defences (Pugh & Woodworth, 2014). Wave run up is the additional height that broken waves attain as the run up the shore and can lead to defence over wash (Poate et al., 2016). Wave setup is important because it can increase water depth in the order of tens of centimetres during a storm surge, which is not observed in tide gauge records. This can be of particular significance as a storm tide might not necessarily lead to flooding, however the waves generated by the storm may lead to overtopping of the sea defences. Despite their impact, there are currently no national operational flood forecasting systems which include wave setup. This is because of the complexity involved, as waves and set-up would need to be modelled in great detail for every beach, harbour and bay along a coastline (Pugh & Woodworth, 2014). More recently however, a forecasting tool (South West Partnership for Environment and Economic Prosperity -Operational Wave and Water Level model or SWEEP-OWWL, https://sweep.ac.uk/owwl/) has been developed to accurately forecast run up and set up in the southwest of the UK for 1000 km of coastline using computationally efficient models (Stokes et al., 2021). Infragravity waves (those with a period 20-200 seconds) can also pose a hazard and are not currently in forecast services. For example, in the Bay of Biscay in the 2013-14 winter, infragravity waves lead to dune breaching and wash over deposition at many locations (Baumann et al., 2017).

Malagon Santos et al., (2017) looked at the spatial distribution of extreme wave events using similar technique to Haigh et al., (2016). Six main spatial footprint types of extreme storm-wave events were identified, whilst Haigh et al. (2016) found four for storm-tides. Additionally,

no clear pattern was found between storm centre and the occurrence of extreme waves, in contrast to Haigh et al. (2016) which found a link between storm centres and extreme sea levels. This study, however, was severely limited by data availability (between 6 and 13 years of data at each site). Localised studies agree, for example in the northwest of England, that the largest waves are formed from depressions tracking across the UK from a south-westerly direction. This makes future extreme wave events closely linked to future North Atlantic storm tracks. Fetch limitation in enclosed seas may limit future change of the wave climate however. For example in the Eastern Irish Sea, the wave heights are limited by fetch, so the frequency of events from different directions and duration of events are of greater concern (Wolf et al., 2011).

Waves have numerous parameters that can change how they might impact a coastline. These include height, length, period and propagation direction, which will all have an impact on the potential damage caused when the waves break on the coast. It is therefore important to take into account all covariates when assessing wave impacts. Callaghan et al. (2008) highlighted this when looking at the joint probability of wave height, period and direction, event duration, tidal anomalies and event clustering in the context of beach erosion.

2.1.3 River flooding

River (or fluvial) flooding occurs when excessive precipitation (or snow melt) over an extended period of time causes a river to exceed its capacity. In hilly or mountainous areas, floods can occur very shortly (within minutes) after heavy rain. In flatter areas, the flood water tends to rise more slowly and generally be shallower but may remain for days and be more far spread (Shaw et al., 2011).

Long term trends in fluvial flooding in the UK were investigated from 1884-2013 in Stevens et al. (2016). An increase in reported flood events is seen, associated with increased exposure due to development on floodplains. When the data was detrended for exposure, no trend is observed over time, however significant decadal variability is seen.

Tidal blocking in estuaries (where a high tide reduces the fluvial outflow) can also cause rivers to back up and flood. This highlights the need to include tidal regimes in hydrographical modelling (Robins et al., 2018).

2.1.4 Surface flooding

Surface flooding (or pluvial flooding), often occurs during short intense period of rainfall that cannot be displaced via drainage systems or groundwater sources quickly enough and can often happen in areas not frequently affected by flooding (Houston et al., 2011).Urban areas are most likely to be at risk due to their built-up nature. Pluvial flooding risk accounts for approximately one-third of flood risk from all sources in the UK. Approximately two million people (5% of the urban UK population) are at risk of an annual 0.5% risk of surface flooding (1 in 200 return period) (Houston et al., 2011).

Assessing the hydrological risk of flooding is made difficult by the numerous variables to be considered. For example, pluvial flooding could be influenced by soil saturation and rainfall intensity and duration, whilst riverine flooding could be measured by peak flow, duration of peak and extent of flooding area. A univariate case in hydrological applications, such as frequency analysis, therefore may lead to underestimation or overestimation of the risk (Hao & Singh, 2016). In many compound flooding studies, rainfall is used as a proxy for pluvial flooding (e.g. Wahl et al., 2015). Whilst this is acceptable on a large scale, true pluvial flooding should take into account parameters such as elevation, drainage and surface type, typically through hydrodynamic modelling.

2.2 Definitions and mechanisms of compound flooding

There are currently only broad definitions on what a compound flooding event is. As mentioned previously, compound events are defined by the IPCC (Seneviratne et al., 2012) as: (1) two or more extreme events occurring simultaneously or successively; (2) combinations of extreme events with underlying conditions that amplify the impact; (3) combinations of events that are not themselves extremes but lead to an extreme event when combined. These, however, are not specific to flooding. Coastal compound flooding can occur through various combinations of the four source mechanisms. Mazas & Hamm (2017) refer to three generalised multivariate cases: Type A – a single metocean process which can be described by multiple parameters, for example, a sea state can be described by variables including significant wave height; peak period and peak direction; Type B – a single metocean process which is made up of several base processes, for example, total sea level is made up of MSL, astronomical tides, meteorological surge and wave set up; and Type C – the joint occurrence of several distinct metocean processes such as waves, sea level, wind, rainfall and river flow. Recently

Zscheischler et al. (2020) more specifically defined compound weather/ climate events as "the combination of multiple drivers and/or hazards that contributes to societal or environmental risk".

Five different event mechanism have been defined for this review which can lead to a compound flooding event, as follows:

1. Two or more variables are extreme.
2. One variable is extreme by the other(s) is(are) moderate.
3. Combinations of variables that are not themselves extreme but lead to an extreme event when combined.
4. One or more variables interacting with a human element.
5. Clustering or sequences of repeated events.

These five types are discussed in more detail in the sections below.

2.2.1 Two or more variables are extreme

The first type of compound events is when two or more variables are extreme. An example of this type of event is, in an estuarine region, when the joint occurrence of both a storm tide and extreme river discharge results in water levels being increased to the point where inundation occurs or is exacerbated. Another example is that of tropical cyclones that are more likely to result in a joint occurrence of extremes flooding sources, when compared to extratropical cyclones. This is because tropical cyclones are typically small in diameter and very intense. The strong winds associated can produce large storm surges and waves, whilst also delivering large quantities of rainfall in the same area (Pugh, 2004).

2.2.2 One variable is extreme but the other(s) is (are) moderate

Compound flooding does not necessarily require both source mechanisms to be extreme. For example, in an area lying at a similar altitude to the MSL, a moderate storm surge (or spring tide) might not cause flooding. However, it may be high enough to prevent or slow down a river from draining, such that any heavy precipitation in the area is then more likely to cause flooding (Wahl et al., 2015).

2.2.3 Combinations of variables that are not themselves extremes but lead to an extreme event when combined

Unlike events in Section 2.2.2, this category involves no extreme variables. This type of event may arise, for example, when a moderate storm surge combines with a moderate wave height or period to produce water levels which may produce overtopping. As described further in Sections 2.6 and 2.7, the lack of extremes makes this type of compound event particularly difficult to classify and identify. Localalised overtopping events however have been identified due to a combination of moderate waves and spring tides, using a novel overtopping monitoring system "WireWall" in Crosby, northwest England (Brown et al., 2018).

2.2.4 One or more variables interacting with a human element

A compound flood event may also occur due to the presence of man-made environmental adaptations or engineering solutions. For example, in a scenario where a human settlement is close to MSL and precipitation flows out from man-made storm drains at low tide; should a moderate storm surge occur, it may not cause seaward flooding, however if the sea level is held above the storm drains over multiple tidal cycles, precipitation may not drain away, resulting in terrestrial flooding. An example of this would by the flooding in Lymington, UK in 1999 (described in Section 2.3.2).

2.2.5 Clustering or sequences of repeated events

It is important to note that compound flooding can also be produced by only one flooding source type. For example, an extreme rainfall event might be followed by another before the initial precipitation has been carried away and the system recovered. The cumulative water then results in flooding. As an example of this would be Brisbane, Australia flooding (January 2011) described in Section 2.3.1. Two storms arrived two days apart, the flood defences could handle the individual storms, however the combined rainfall created a flood event. (Leonard et al., 2014).

2.3 Past compound flooding events

Compound events are typically less well recorded compared to single source events, due to their complicated nature or lack of measurements for all the flood sources responsible. However, some of the worst flooding events around the globe have been due to compound flooding. This section briefly describes a selection of the more recent and significant events.

2.3.1 Global events

A recent example of compound flooding was Hurricane Harvey in 2017, in the USA. The stationarity of the storm track led to record levels of rainfall (a return period of 100-2000 years (Emanuel, 2017). The hurricane also generated a moderate storm surge, which resulted in elevated water levels over 5 days. The surge prevented the rainfall from draining into the sea, causing much of Houston to be inundated, leading to the second most costly hurricane to impact the USA (NOAA, 2018b).

Cyclone Idai was a long-lived tropical cyclone travelled within the Mozambique Channel in March 2019, causing catastrophic damage along its path in Madagascar, Malawi, Zimbabwe, and most importantly in Mozambique where it made landfall twice. The second landfall on 14th March 2019 devastated the city of Beira and neighbouring communities. Severe rainfall over several days prior to and before the landfall combined with extreme winds of more than 160 km/h. No precise measurements are available, however it is estimated a maximum storm surge of 4.4m was produced, along with 600 mm of accumulated rainfall over a 2 week period (Probst & Annunziato, 2019). It's estimated that at least 1000 people were killed and ~$1 billion of infrastructure was destroyed. Furthermore, the resultant conditions lead to outbreaks of diseases such as Cholera and Malaria (Mongo et al., 2020).

Hurricane Matthew was, at its peak, a category 5 tropical cyclone which made landfall in Haiti, Cuba, Grand Bahama Island and USA in 2016. In Cuba, a surge of up to 13 ft was observed, coupled with waves of 30 ft, resulted in sea water inundation 300 ft inland (Stewart, 2017). In Florida, USA, the combined effect of the surge and tide produced maximum inundation levels of 5 to 7 ft, the region also received 10 inches of rain. 585 deaths were attributed to the hurricane and in Haiti alone estimated damages were $1.9 billion USD, equal to more than 10 percent of the country's GDP. The damage caused by Matthew in USA totalled approximately $10 billion

USD and the 10th most destructive hurricane to affect the United States (at the time) (Stewart, 2017).

Hurricane Sandy (October-November 2012) featured an unusual path, which resulted from multiple weather systems coinciding over the North American continent and the North Atlantic that steered Sandy back towards the coast, leading to substantial inland rain and flooding. Coming almost directly from the east, the storm caused the highest storm surge in at least 300 years and coinciding with a high (spring) tide as well as inland precipitation (pluvial flooding), the storm led to widespread flooding in New York City and surrounding areas (Zscheischler et al., 2018).

A high storm tide brought by Typhoon Longwang in 2005 impeded the discharge of the rain runoff resulting in the inundation of a 13.69 km^2 area in Fuzhou city, China, and over 62 people died (Lian et al., 2013). Fuzhou was struck by tropical cyclones 56 times in the historical period 1949–2011.

The 2010/2011 wet season in Queensland, Australia resulted in a series of floods during a La Nina event; Brisbane City was flooded by two storms separated by two days (11th-13th January 2011). The rainfall from the first storm was absorbed by Wivenhoe Dam; however, the second resulted in the dam releasing floodwater onto downstream Brisbane, producing A$2.39 billion if damage and affecting 200,000 people. This flood event can be considered a compound event as either storm on its own could have been contained by the city's flood defences, but once combined, proved to be too much (Leonard et al., 2014).

It is not just regions affected by tropical cyclones that are at risk of compound flooding. In 2015, a low-pressure system in the Adriatic Sea drove strong wind at the Italian coast. The resultant storm surge generated the highest sea levels seen in 18 years in the coastal area of Ravenna. The surge was combined with 80 mm of rainfall on the day prior to the storm and 90 mm on the day of the storm. Rainfall runoff was blocked by the surge, producing major flooding in the area (Bevacqua et al., 2017).

In the northern Netherlands, a slow-moving low-pressure system resulted in the free gravity drainage being blocked over five consecutive tidal cycles. Combined with high rainfall (60 mm in 5 days), this resulted in high inland water levels and precautionary evacuation (van den Hurk et al., 2015).

In the eastern Baltic Sea, compound flooding occurred along the Polish coast in 2009. Strong northerly winds did not generate an extreme storm surge, however it did push seawater

upstream of the Odra and Vistula rivers at the time of increased runoff from rainfall and caused inundation along several rivers (Kowalewska-Kalkowska, 2018; Paprotny et al., 2020).

On 28th February 2010, Storm Xynthia wreaked havoc on the French Atlantic coastline, causing more than 30 casualties because of coastal flooding through a combination of a storm surge occurring at the high water of a spring tide. But an in-depth analysis also shown the role played by the waves, that increased the ocean roughness and whose breaking added a set-up component (Mazas & Hamm, 2017).

2.3.2 UK events

In the UK, compound flooding events were not systematically documented and resulted in flooding in coastal regions. Lymington, a coastal town in the western Solent, has strong fluvial influence (from Lymington River) and in 1989 the town suffered a major flood event, with damage to 50 houses and the railway line (Haigh et al., 2015). This led to a large investment in coastal flood defences in the town, including sluice gates which allowed the river to drain at low tide, but protected it from tidal flooding during high waters and surges. In 1999, a winter storm generated a storm surge which did not directly cause a flood; however, it prevented the flood gates opening over several tidal cycles. Large volumes of rainfall caused increased river flow, resulting in flooding on the fluvial side of the sea defences (Ruocco et al., 2011b). This series of flooding events has been poorly categorised in studies yet highlights the hazard of not taking into account multiple sources when planning flood defences.

On the southwest UK coast, the 2013-14 winter storm season produced the largest storm surge for 60 years combined with waves and rainfall to cause some of the worst coastal flooding for 20 years. Significant damage occurred, including the destruction of the main railway line in Dawlish, Devon. Estimated cost of the railway closure alone is between £60 million up to £1.2 billion (Devon Maritime Forum, 2014). The 2013-14 winter seasons was also one of the wettest on record (Kendon & McCarthy, 2015). The sustained heavy rainfall combined with the high spring tides in the Severn Estuary resulted in extensive flooding in the Somerset Levels (Met Office & CEH, 2014).

2.4 General review

Due to the complexities involved and often the lack of long-term observation data, the assessment of compound flooding is a relatively young science, with most advancements being

made in the past 15 years (Figure 2.2) As part of this review, 68 papers were identified that assessed compound flooding in different parts of the world and these are listed in Table 8.1 and Figure 2.3. The majority of studies have considered sea level and river discharge or rainfall. Across the papers, 12 examined coincidence of surge and precipitation; 18 investigated surge and river discharge; 18 assessed surge and waves; 1 paper analysed surge, precipitation, river discharge and waves; 1 precipitation and runoff; and 1 precipitation and river discharge. 12 papers included modelling of compound events. Study areas have predominantly included the UK (Svensson & Jones, 2004; Svensson & Jones, 2002) and Europe (Petroliagkis et al., 2016), USA (Wahl et al., 2015), Australia (Zheng et al., 2013, 2014), and China (Fang et al., 2020). Recently there have been 2 studies that focused globally (Couasnon et al., 2019; Ward et al., 2018).

Across these 68 studies, there were large variations in definition of variables and the approaches used. In the two sections below, the different methodologies and approaches (Sections 2.6 and 2.7 respectively) are reviewed and compared to highlight the impact they can have on compound flooding assessments.

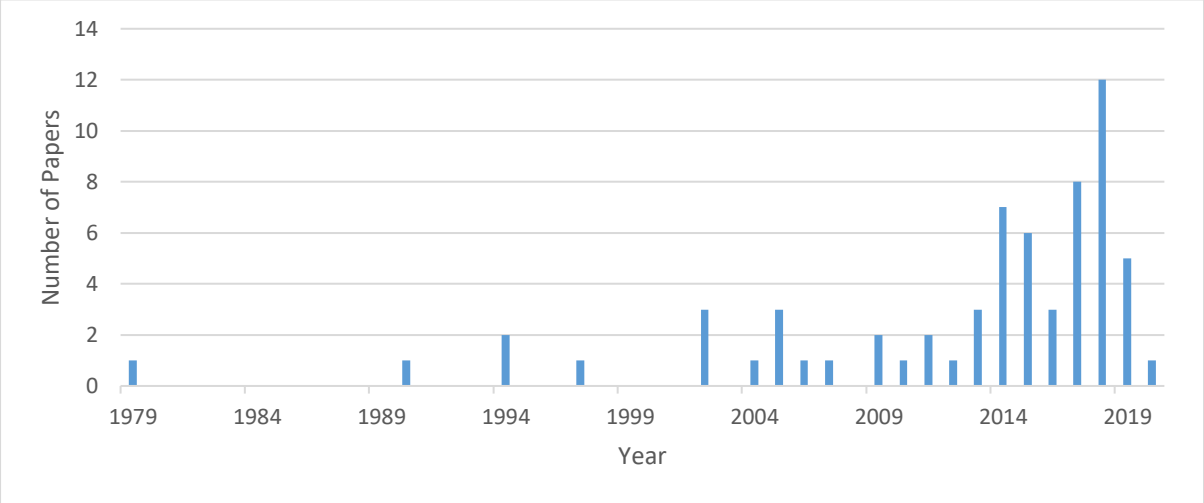

Figure 2.2: timeseries of compound flooding paper publications

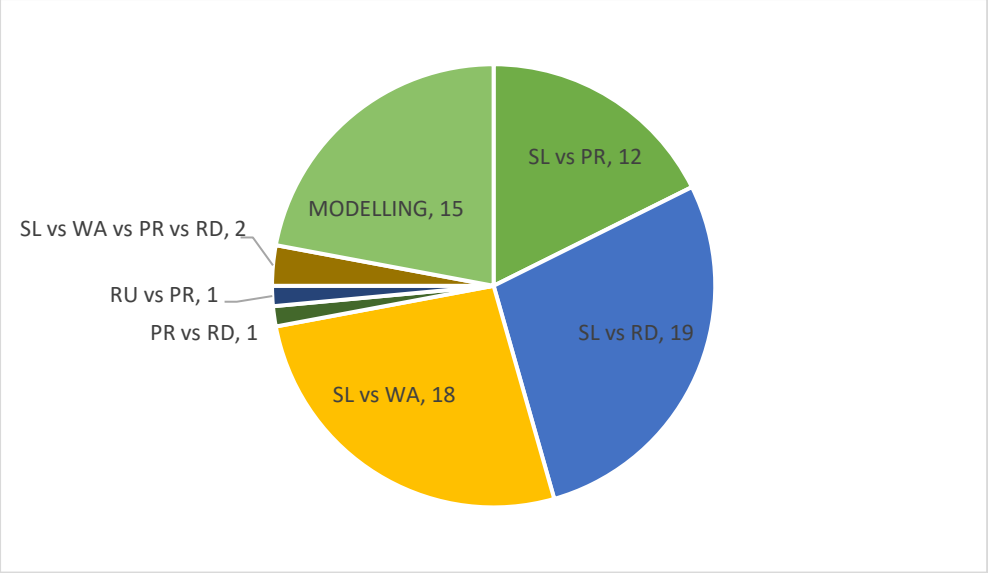

Figure 2.3: Distribution of compound flooding paper source variations; Sea Level (SL); Waves (WA); River Discharge (RD); Precipitation (PR) and Hydrodynamic modelling (MODELLING)

2.5 Measurement of variables

In addition to variation in methodology, there is a lot of disparity in definition of source variables throughout the 68 studies identified above that have assessed compound flooding to date. This can be due to the disparity in data availability or the lack of a standard measurement method within the variables. This variability makes it difficult to directly compare studies. In the sections below, a brief overview is given of which specific variables were assessed for each of the four source drivers of flooding, across the different studies.

2.5.1 Sea level

Sea level is typically recorded using a tide gauge. The data recorded contains the various components of sea level; astronomical tide, surge level (excluding waves) and mean sea level. Compound flooding studies have varied in how they separate these components, and whether they use the total recorded water level or just the storm surge component. Studies which use the total water level (TWL) (For example, Lian et al., 2013), include the deterministic astronomical tide, and so reduce the statistical relationship found between TWL and the other variable depending on the state of tide (high/low or spring/neap). However, using the TWL

will show water level likely to cause flooding, which could be more useful for coastal management decisions. Conversely, considering just the surge component could increase the dependence or correlation, and so demonstrate compound flooding occurrences where the effects of tides might hide it. In the UK, the National Tide and Sea Level Facility (NTSLF) has been maintaining a network of 44 tide gauges for over 100 years.

Furthermore, studies differ in their method of separating out the sea level components. For example, Svensson and Jones (2002) use the non-tidal residual (NTR, the measured water level minus the astronomical tide) for the surge component. This method, however, as shown by (Horsburgh & Wilson, 2007) can lead to harmonic prediction errors or timing errors and non-linear interactions, which can artificially bias the surge. A more accurate method used is to extract the skew surge (the difference between the maximum observed water level and the maximum predicted tidal level regardless of their timings within the tidal cycle), as used in Ward et al. (2018). With the skew surge extraction, there is only one surge value per tidal cycle, this results in a temporal scale variability when comparing to studies using the NTR which will contain a value for every water level measurement.

2.5.2 Waves

The most commonly used variable to describe waves in compound flooding studies is significant wave height (H_s). Traditionally this is defined as the mean of the highest third of the measured waves ($H_{1/3}$) but can also be computed from the wave energy spectrum (H_{m0}). Whilst equal in deep water, H_{mo} can be found to overestimate significant wave height by approximately 5% in shallow water (Mangor et al., 2017). Wave height is not the only parameter that can affect the flooding resulting from waves. Wave period (typically defined as mean zero-crossing period (Tz) or peak energy period (Tp)) can often have a greater impact. For example, long period swell waves have been found to cause significant flooding along the English Channel coastline (Sibley & Cox, 2014). These waves may have lower wave heights but longer run-up, resulting in overtopping of sea defences. Wave direction can also have a huge bearing on the flooding impact, particularly at a local scale. For example, Mazas & Hamm (2017) developed a bivariate method for determining extreme joint probabilities of wave height and period for sea states; however, for determining the extreme joint probability of waves and sea level, just significant wave height was used. Finally, the Atlantic facing coasts of the British Isles can also see combination of wind-sea and swell-sea waves (known as a bimodal sea state),

further complicating wave analysis (Mason & Dhoop, 2018; Orimoloye et al., 2021) These properties of a wave are more complicated to analyse and require wave energy spectra data, which are typically limited in data length. As a result, these wave parameters are typically ignored in compound flood studies, particularly at larger spatial scales.

In the UK, a network of wave buoys is maintained by organisations including the Environment Agency (EA), Met Office, Coastal Channel Observatory (CCO), which feed into wave forecasting and CEFAS's WaveNet datahub (http://wavenet.cefas.co.uk).

2.5.3 Riverine

Riverine output can be described using river level (stage) or flow. Typically, flow is used for studies, however, this can be measured over different periods. Studies have used hourly discharge (Serafin et al., 2019); daily total flow (Moftakhari et al., 2017) or mean daily flow (Couasnon et al., 2019; Ward et al., 2018). Ikeuchi et al., (2017) ran a global model to simulate coupled fluvial floods and storm surges whilst river flow and a Digital Elevation Model (DEM) were used to produce inundation depths. In the UK, the National River Flow Archive (NRFA) supplies the gauged daily flow as the mean daily flow. However is should be noted that the gauging stations might not be at the point of impact and miss the downstream inflow.

2.5.4 Pluvial

In compound flooding studies (e.g., Wahl et al., 2015), pluvial flooding is typically represented using precipitation as a proxy. These studies use either observed weather station data or gridded modelled datasets. As with river flow, difficulty in comparison among studies arises because studies use different temporal scales. Cumulative daily precipitation is the most commonly used (e.g. Bevacqua et al., 2019; Wahl et al., 2015; Wu et al., 2018), however, cumulative hourly has also been used when available (van den Hurk et al., 2015). In more localised modelling studies, pluvial flooding, will be modelled as an extent with regards to area affected (Ray et al., 2011). In the UK, a network of weather stations measuring precipitation is maintained by the EA and the Met Office for forecasting and data access is provided by the Centre for Environmental Data Analysis (CEDA).

2.5.5 Weather Patterns and systems

Weather patterns have been used to define compound flooding in a number of studies using different methodology, however all studies have used low pressure system as the weather pattern. Svensson and Jones (2002 and 2004) tracked several low-pressure systems which led to joint extreme river and surge events. Wu et al. (2018) used sea level pressure to define rain only, surge only and compound events, however did not use a rainfall component when producing their synoptic maps. Wahl et al. (2015) is the only study so far to use different variables (sea level pressure, wind speed and rainfall) to classify the meteorological conditions leading to compound events.

2.5.6 Site selection criteria

Studies also vary in how they select the data locations used. Studies using observed data typically use the wave/sea level sites as the reference gauge and select the river/precipitation gauges within a certain radius (Wahl et al., 2015; Ward et al., 2018), or nearest gridded node when using modelled data (Couasnon et al., 2019). This is primarily because the marine measuring sites are usually fewer in number. As with defining the variables, there is no set guidance for matching variable measurement sites. Studies use a combination of the following selection criteria; within a certain radius of reference gauge; minimum upstream basin area; minimum discharge of river; maximum distance between river basin and tide gauge Conversely, (Svensson & Jones, 2004; Svensson & Jones, 2002) measured the dependence between every tide gauge and river gauge, this can produce result which are not relevant due to the location of the corresponding gauges.

2.6 Definitions of extreme sampling and compound event extraction

In this section, the methods of extracting a subset of extreme values from a time series are discussed, as well as how compound events can be sampled from two time series.

2.6.1 Extreme sampling

When using extreme value analysis (EVA) (both for a single source or multi-hazards), there are numerous methods for extracting extreme events. Two main approaches have been typically

applied in the literature. The first method relies on deriving a block maximum (or minimum), whereby the maximum value is chosen within a time period (or block), typically looking at the annual maximum (AMAX). The second method involves extracting peak values above (or below a certain threshold, from a continuous record (peaks over threshold, POT) (Bezak et al., 2014). A third approach, the r-largest approach can also be used whereby a set number (r) of samples is extracted. This can provide more information than a block maxima approach, however the size of r is critical. If r is too large, a bias can occur, the variance of the estimator can be high. (Smith, 1986).

If the dataset is sufficiently long enough, the empirical distribution of the annual maximum can be obtained directly from the time series. To extrapolate to very high values, an extreme distribution is fitted. The statistical theory of extremes says that the maximum of n independent identically distributed random variables, as n is high, is a random variable with a distribution of only three types which have a unified distribution under the GEV (Generalized Extreme Value) (Coles et al., 2001).

Samples extracted from the timeseries using POT must be sufficiently separated in time to be considered independent. For example, a storm surge generated peak water level, must be spaced far enough from the next peak to ensure they are not generated by the same storm. In contrast to the AMAX method, these are not the maximum value during a particular period, instead chosen based on their exceedance of a set threshold. An asymptotic result of the theory of extremes states the conditional distribution of a random variable, for high threshold, tends to the Generalised Pareto Distribution (GPD). Instead of considering the maximum in a block as in the AMAX, the r-largest approach can be used to estimate the empirical distribution if events are found to be independent, the GEV distribution can be used.

2.6.2 Extreme compound event extraction

A number of multivariate statistical methods are available to represent the relationship between extremes. The choice of methods can have great implications on the results. Methods used include a threshold excess (AND), point processes methods and conditional method (OR) (Coles et al., 2001; Zheng et al., 2013) (Figure 2.4).

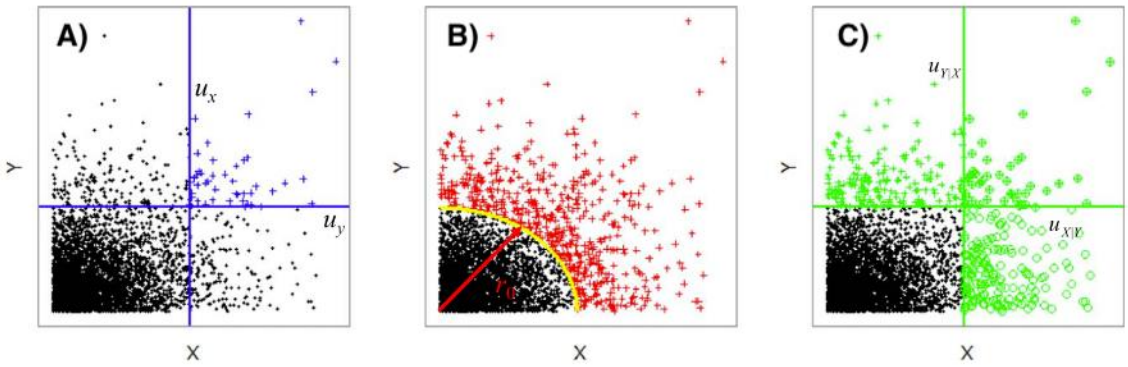

Figure 2.4: Graphical representation of the different multivariate statistical methods (where X and Y are representative variables) A) threshold excess (AND) B) point process, C) conditional method (OR) (Zheng et al., 2013).

Ward et al. (2018) used a threshold excess method, extracting events where both storm surge and river discharge are extreme. Wahl et al. (2015) used a conditional approach, taking the highest storm surge, and identifying the precipitation in the same time frame. Zheng et al. (2014) compared the three different extraction methods, finding the point process method was the most suitable in their case study, as the bias from the threshold was lowered.

2.7 Review of approaches to analysing compound flooding

Across the different relevant studies, six main methods have been used to assess compound flooding. These methods, are discussed in the sections below, starting with the simplest (conceptual assessments), moving to statistical descriptions and joint probability extreme value analysis; then taking a deeper look at the drivers of compound flood events and finally using hydrodynamic modelling.

2.7.1 Approach 1: Conceptual assessments

The first approach is to simple construct a conceptual understanding of which variables might occur concurrently or be statistically linked in some way. For example, (Gill & Malamud, 2014, 2017) considered 21 natural and 18 anthropogenic hazards (including flooding) in a purely theoretical concept, by synthesising the identified interaction relationship between the hazards rather than measuring the relationship between the hazards (Figure 2.5). They found flooding

was the third most linked secondary hazard (i.e. triggered by the primary hazard) after landslides and volcanic eruptions.

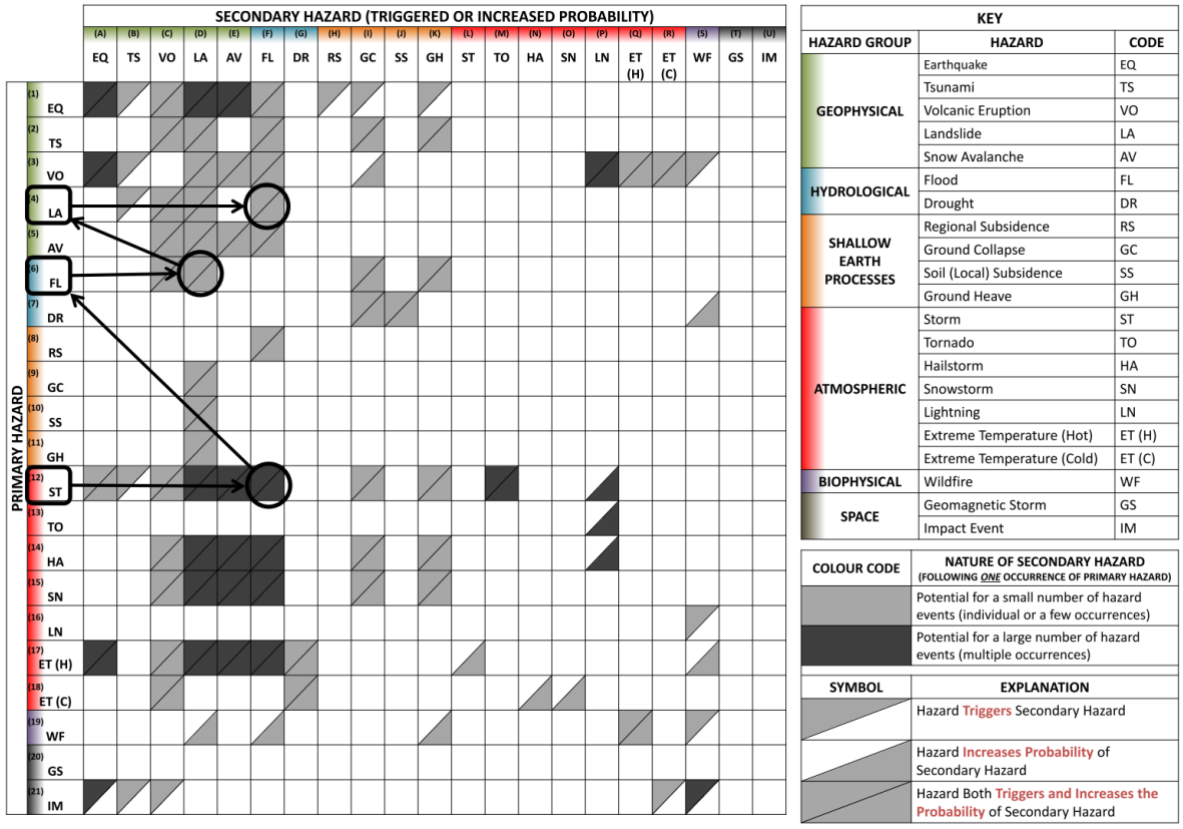

Figure 2.5: An example of a network of hazard interactions (a cascade system) (Gill & Malamud, 2014).

Kew et al. (2013) used a simplistic approach to assess dependence of surge and river discharge in the Rhine delta in the Netherlands. North-north-westerly winds and long duration precipitation were used as proxies to represent surge and river discharge respectively. They found the probability of extreme surge conditions following extreme 20-day precipitation to be around 3 times higher than if the variables were considered independent.

2.7.2 Approach 2: Case study of an individual compound flooding event

The second approach is to study a specific compound event, rather than looking for events within a time period. For example, this approach was taken by van den Hurk et al., (2015). They modelled an event in the Netherlands in 2012, which came close to causing major flooding. A series of low-pressure systems passed over the North Sea producing >60mm of

rain over a 5-day period. During this period the storm surge which was generated, prevented gravity drains to reduce the fresh water in the system. They used an ensemble of regional climate model simulations (simulating 800 years of current climate conditions) to show combined occurrence of extreme rainfall and storm surge are physically linked by the same mechanisms.

2.7.3 Approach 3: Statistical dependence description

The third approach is to use statistical dependence methods to quantify the relationship between the difference flooding sources and thus far this has been the most common approach to analyse compound flooding. Studies have used observed or modelled reanalysis data to look at the dependence between variables, at individual sites or many sites in a region. There are a variety of methods, including; Kendalls Rank Correlation Tau; Spearman's rank correlation coefficient; the Chi statistics of (Coles et al., 1999); the empirical upper tail dependence coefficient CFG (Capéraá-Fougéres-Genest) estimator; or measuring the number of events (through a joint occurrence count or co-occurring annual maxima). Frequently, studies will use more than one of these methods, allowing a comparison.

Ganguli & Merz (2019) used both Kendall's Tau and the CFG estimator to assess the relationship between high coastal water levels and peak river discharge over northwestern Europe. They find an upward trend in compound hazard ratio frequency at midlatitudes (gauges from 47°N to 60°N) and a downward trend along the high latitude (>60°N) regions of northwestern Europe.

Svensson & Jones, (2002, 2004) have conducted the most comprehensive study on the joint probability of storm surges, river flow and precipitation around Britain to date. They used techniques from Buishand (1984) and Coles et al. (1999) for measuring the dependence as the variables reach their extreme. On the east coast, they found that the strongest river flow–surge dependence occurs between river flow on the north shore of the Firth of Forth and surge at Aberdeen, Wick and Lerwick. The Firth of Forth is not sheltered from south-westerly winds by any topographic barrier (unlike most estuaries on the east coast). Precipitation from this direction may therefore be enhanced as it falls on the hills on the northern side of the firth, resulting in high river flow. Along the south and west Coasts, areas of high dependence were found in southwest Britain, southern Wales, the Solway Firth (western Scotland). Higher dependence was frequently found in hilly catchment areas. Seasonality was also found to have

an impact, with more dependence being seen in the winter compared to the summer. When the analysis was lagged, the dependence was found to be strongest when rainfall occurred 1 day before the peak river flow and surge.

Petroliagkis et al. (2016) performed the most comprehensive joint probability study for the European coast lines. They analysed the statistical dependence of storm surge and wave; storm surge and river discharge; and wave and river discharge using techniques developed by Svensson & Jones (2002) and Hawkes (2005). 32 sites from across Europe (including rivers draining into Atlantic Ocean, Mediterranean, North and Black Seas) were analysed. Due to the lack of long-term observational data, hindcast simulations were used for the primary variables. Approximately 23 years of river discharge and 35 years of surge and wave simulation data were used. Validation of the hindcasts were conducted using <5 years of data from just one site at the mouth of the Rhine River in the Netherlands, with no long-term series validation in the UK. When comparing surge and waves, they found that east coast sites were led by waves (i.e. the surge lagged behind waves) and were modest to well correlated ($0.38<p<0.53$). For sites along the south and west coasts, it was predominantly surge led between modest and strong correlation ($0.54<P<0.69$). For surge and river discharge, only one site was found to be discharge-led (Thames) at 1 day of lag with zero correlation. All other sites around the British Isles are surge-led with moderate correlation ($0.12<p<0.37$) with the maximum found at 1-5 days. When looking at wave and discharge, all British sites are wave-led.

Statistical approaches have also been used on a global scale, assessments of the dependence include between storm surge and waves (Marcos et al., 2019) and storm surges and river discharge using observed data (Ward et al., 2018) and modelled data (Couasnon et al., 2019). However, whilst Ward et al. (2018) and Marcos et al. (2019) use Kendall's Tau and copulas to measure dependence, Couasnon et al. (2019) use Spearman's rank correlation. When comparing the results from Ward et al. (2018) and Couasnon et al. (2019), the global spatial pattern is broadly similar, with strong dependence being found on the east and west coasts of USA, northwestern Europe, Japan and Australia. The study using modelled data (Couasnon et al., 2019) also found areas with no observed data to have a strong relationship, highlighting the requirement for data, when assessing compound flooding. Ward et al. (2018) and Marcos et al. (2019) both also use copula model to assess the joint exceedance probability, finding the joint return period (50-year) conditions have a higher return period when analysed in independence.

2.7.4 Approach 4: Joint probability extreme value analysis

The fourth approach goes a step further than approach three and quantifies the likelihood of the flood sources being extreme at the same time, rather than just measuring the relationship. This provides a far more useable data product to flood and coast risk management agencies when calculating design levels. In the UK, the R&D joint probability programme (funded by Department for Environment Food and Agricultural Affairs; DEFRA) commissioned a number of studies looking at joint probability of a variety of flooding risks. This resulted in a product called 'JOIN-SEA' (HR Wallingford, 1998), a software package designed to calculated joint probability between waves at high water and storm-tide. It was found that dependence should be expected between surge and wave, as both are generated by the same weather systems. The degree of statistical dependence differed from one site to another (due to local topographical features and atmospheric circulation). The software (produced in 1998) was written in FORTRAN-77, which limits it's use on modern operating systems (Petroliagkis et al., 2016). Hawkes et al., (2002) expanded on this method by introducing the joint probability density of three variables (storm tide, wave height and period) which highlighted the need to take into account different wave variables. Hawkes et al. (2002) used JOIN-SEA to run dependence and joint probability on surge and wave height; surge and tide; surge and river flow; and surge and precipitation. Results showed that surge and river flow were generally more correlated on the west coast than east and generally on short steep rivers, rather than long flat ones. Less correlation was found between rainfall and surge. Whilst this study is the most comprehensive joint probability study for the UK, it was again limited by data. 24 tide gauges were used, whilst today over 40 are available in UK Tide Gauge network (National Tidal and Sea Level Facility, 2018). Waves data was extracted from a model run covering 12 years, with no validation using observation data.

Samuels & Burt (2002) looked at dependence between peak sea levels at the Cardiff, UK and peak river flow on the Taff at Pontypridd using the JOIN-SEA approach. They concluded that there was no correlation between the two variables. This is in contrast to Svensson & Jones, (2004), who found dependence between daily mean river flow and surge. This is due to using peak sea level, which in the Bristol channel is dominated by astronomical tide. This can lead to lower dependence as only the surge is physically associated with intense rainfall under the same weather patterns. This highlights how critical data selection is for joint probability studies (Hawkes, 2008).

The Heffernan & Tawn, (2004) (H&T) approach entails of modelling pairwise dependencies on common scales using a single variable above a high threshold and all remaining transformed variables and has been used by multiple studies. Keef et al. (2009) used the H&T approach to measure the spatial dependence of extreme precipitation and river discharge separately in Great Britain. Precipitation was found to have a weaker spatial dependence in upland areas, whilst river flow spatial dependence was predominantly affected by catchment characteristics. Similarly, (Lamb et al., 2010) used the same techniques to measure the joint probability of extreme river flow or sea level at multiple locations across England. This was then used to model economic damages and calculate a risk profile. It should be noted, neither study compared the relationship between the different variables (i.e. precipitation vs river flow (Keef et al., 2009) or river flow vs sea level (Lamb et al., 2010)). Gouldby et al. (2014) and Wyncoll et al. (2016) developed an approach using H&T to model the joint probability of wind, waves and surge in Santander, Spain and England respectively. Both involved generating synthetic events to identify the boundary conditions for coastal flood simulations

White, (2007) used the techniques from Heffernan and Tawn (2004) to assess compound flooding in the River Ouse, Sussex. He found that river flow and tidally dominated water levels acted independently in different parts of the river system. However, there was a part of the river where the combination of surge and river flows were likely to act together. White (2007) also demonstrated that in some estuaries, fluvial, surge and tide components may all have an important impact on water levels. Such that a trivariate joint probability method may be necessary. The introduction of a third variable however, could make probability calculations extremely complex (Petroliagkis et al., 2016). The approaches based on Heffernan & Tawn (2004) however can suffer from the drawback that the marginal parameters need to be independent from each other or that the marginal distributions need to be from the same family.

Zheng et al. (2013) used a bivariate logistic threshold-excess model to look at the dependence between rainfall and storm surge around the Australia coast. They found that the probability of an extreme surge coinciding with an extreme rainfall event can be up to 35 times higher than if one would assume independence.

The second approach uses copula, which are joint distributions able to handle mixed marginal distributions and to account for the structure of dependence overlooking the margins. When using copulas, the dependence function is studied separately from the marginal distributions. There are a number of different families of copula, each with its own benefits and drawback

(Hao & Singh, 2016); including empirical, meta-elliptical, Archimedean, extreme value, vine and entropy copulas.

Bevacqua et al. (2017) used paired copula construction (vine copula) to investigate the compound flooding in Ravenna, Italy caused by surge and river discharge. A vine copula allowed the input of multiple rivers, tide gauges and meteorological forcing's to produce a 5-dimensional model. It is shown that ignoring the dependence between sea and river levels underestimates the risk, the 20-year return period became 32-years when moving from dependent to independent.

Masina et al. (2015) used a copula approach to estimate the joint probability of water levels and wave heights of the Ravenna coast, taking into account seasonality and direction. They found 3 to 4 events are predicted to exceed the threshold of 2.5 m at the Ravenna coast in a 100-year period.

Lian et al. (2013) estimated the joint probability for a combination of extreme precipitation and storm tide in Fuzhou, China using copula techniques. They show that the joint probability has increased by more than 300% on average after 1984.

Bengtsson (2016) found that extreme sea level and rainfall events occurring simultaneously were very rare in Malmo, Sweden. Copula and conditional probabilities were used and found the combination of 1-year rainfall and 1-year sea level has a return period of more than 200 years.

Wahl et al. (2012) introduced higher dimension copula models, using wave height and two storm surge parameters (intensity and highest turning point) in the German Bight, finding realistic exceedance probabilities and improving the overall results from integrated flood risk analyses in the area.

Li et al. (2014) compared a variety of copula-based methods (the Archimedean copula method, the Gaussian copula method, the physics-combined Gaussian copula and the Logistic model) looking at significant wave height, storm duration, surge level and peak wave period. It was found the Gaussian copula were the most suitable option for the Dutch coastline.

The most spatially comprehensive copula-based approach was conducted by (Wahl et al., 2015), who looked at the dependence between storm surges and rainfall for the entire mainland USA coastline. A range of copula functions were used (Frank, Gumbel, Clayton, Galambos and Hüsler-Reiss) depending on their fit. Compound flooding was found more likely on the Atlantic and Gulf coasts when compared the Pacific. There is also evidence that the number of

events has increased significantly over the last decade. Whilst this is primarily due to long-term sea-level rise, in the case study (New York City), the increase in compound events was attributed to a shift toward surge causing weather patterns which also favours increase precipitation.

Mazas & Hamm (2017) used an event-based copula method (Gumbel-Hougaard, Galambos and Hüsler-Reiss) to simulate the joint probability of waves and sea level. They compare their methodology to that of JOIN-SEA (HR Wallingford, 1998). Whilst there was good agreement in the marginal distributions, there is less good agreement in the upper tail. JOIN-SEA is constrained to assume a constant level of dependence past the chosen threshold, whilst extreme value copulas makes the dependence between extreme waves and sea levels continue to increase in the upper tail. They note that the correlation coefficient in JOIN-SEA is seen to continue to increase in the upper tail, suggesting the use of copulas is more appropriate in this scenario.

More recently, several studies have used copula based approaches to analyse future compound flood risk. Moftakhari et al. (2017) used copula and bivariate dependence to characterise the compounding effects of sea level rise and fluvial flooding around the USA, one of the few papers to model non-stationary compound flooding. They quantify the flooding probabilities for 2030 and 2050 under RCP. 4.5 and 8.5, finding an increasing likelihood of river flooding under SLR. Bevacqua et al. (2019) analyse the future compound flood risk of high sea level and precipitation in Europe. the datasets of future storm surge and precipitation levels are simulated using climate models through a DFLOW FM model. A copula-based joint probability model is then applied to the datasets. They find an increasing future compound flood risk across the northern Europe coast, whilst southern Europe and the Mediterranean reduces. Arns et al. (2017) also look at future compound flooding risk, however they used a Mike21 hydrodynamic model to produce the wave and surge heights under various RCP projections, and then use copulas to identify the joint return periods in the German Bight.

2.7.5 Approach 5: Assessment of compound flood drivers

The fifth approach is to analyse the drivers associated with the flooding sources. Primarily, this means the meteorological conditions leading to flooding conditions. For example, Rueda et al. (2016) looked at the relationship between extreme wave and surges using weather patterns. For each of their prescribed weather patterns, significant wave height, mean wave period and surge

level were modelled for Santander, Spain. The variables of interested were modelled used the GEV distributions and Gaussian copulas to model the interdependence. This method allowed the identification of weather types responsible for flooding events.

Wu et al. (2018) use a bivariate threshold model to analyse dependence between rainfall and storm surge, in Australia similarly to Zheng et al. (2013). They then extracted the mean sea level pressure (MSLP) which occurred on rain-only, surge only and coincident extreme events. A Pearson product-moment correlation was used to establish spatially similar conditions throughout the meteorological dataset. They identified different synoptic patterns were responsible for each combination at each site. However, by only considering MSLP, they ignored other meteorological drivers such as wind strength and direction and precipitation.

An alternative approach is to infer storm surges, for example, using metrological data and weather pattern analysis, which often extends much further back in time. This technique involves deriving the key driving weather patterns in an area of interest, by grouping historic weather patterns into sets. The primary application of this methodology has been meteorological forecasting. One of the earliest examples being the Grosswetterlagen (GWL) weather regimes (Hess & Brezowsky, 1969). In the GWL approach, 29 large scale circulation weather types were derived centred over Germany and mainland Europe. They were designed to represent weather regimes which persist for at least three days, however the GWL patterns were derived subjectively. James (2007) subsequently developed an objective classification for deriving the GWL patterns. In the UK, a set of circulation patterns, the Lamb weather types (Lamb, 1972), reflected the daily changes in British Isles at a more localised scale compared to the GWL. Seven basic weather types were originally derived: cyclonic, anticyclonic, northerly, easterly, southerly, westerly and north-westerly. These were subsequently reclassified, expanded and selected more objectively through work by Jenkinson & Collinson (1977) and Santer et al. (1993). More recently, Neal et al. (2016), derived a set of 30 and 8 weather patterns, through k means clustering of daily mean sea level pressure. These patterns are for use on medium-range (30 days) and monthly/seasonal timescales, providing a probabilistic insight into which pattern is most likely, and the key aspects of the pattern. The forecasting tool has been used in predicting climatic extremes including: droughts (Richardson et al., 2018); coastal flooding through storms surges or waves (Neal et al., 2018); and flooding through extreme precipitation (Richardson et al., 2020). The use of weather pattern forecasting for compound flooding was undertaken in Chapter 3.

Weather patterning approaches have started to be assessed for compound flooding studies. For example, Wahl et al. (2015) identified the prevailing synoptic weather patterns in compound events (extreme storm surge and extreme precipitation) and non-compound events (extreme storm surge and low precipitation) for New York City, USA. The number of each storm type was identified within the 20th Century hindcast dataset using the centred pattern correlation technique. They found an increase in the ratio of storms leading to compound events compared to non-compound events in the first 30 years of data (1850-1870) compared to the most recent 30 years of data.

Rueda et al. (2016) created 100 different weather pattern classifications for Santander, Spain using SLP. For each weather type, the skew surge, Hs and Tp were modelled using GEV distributions and a Gaussian copula, to measure the relationship between the variables. This allowed the joint probability of the variables to be analysed per weather type, providing insight into the relationship between weather patterns and extreme sea states. Whilst this methodology did not take into account tides, for coastal flooding forecasting, they could be added for other sites.

Wu et al. (2018) mapped the dependence of extreme rainfall and storm surges in Australia. A Bivariate Logistic Threshold Excess model (Coles, 2001, Zheng et al., 2013) was used to identify compound and non-compound events. The MSLP data from each event were extracted and their similarity was established using Pearson's Correlation to compare the grid point of each event against the other events. This produced a reference conditions for each event type. A second pass over the meteorological data was then made, identifying potential compound and non-compound events. Their methods highlighted the ability to supplement the observed data record with different sources (meteorological in this instance). However, the use of just MSLP as a variable reduces its effectiveness, as other variables (namely windspeed, WS and precipitable water content, PWC) can have a huge impact on the likelihood of compound events.

2.7.6 Approach 6: Hydrodynamic modelling

The final approach is to use a hydrodynamic model to simulate a region flooding from multiple sources, providing more data on the extent of a flood event. Compound hydrodynamic modelling typically examines the water levels on much smaller scales due to the labour and processing power involved. Thus far, all compound hydrodynamic modelling studies have

involved storm surge/water level combined with either rainfall or river discharge. For example, Klerk et al. (2015) explored the relationship between high sea levels at Hoek van Holland and high river discharge at Lobith (both in the Netherlands). They use physical models forced by the same atmospheric conditions leading to cooccurring storm surge and river discharge. The the strongest dependence was found at a lag of 6 days, concluding no significant threat was present and dependence in flood protection wasn't needed. Although they noted climate change may lead to more extreme conditions. Khanal et al. (2018) reinvestigated the region using extended data sets from a storm surge model and 2 river discharge models. They found the probability of finding a co-occurrence of extreme river discharge and storm surge conditions were 4 times higher, compared to random chance, highlighting the need for robust datasets.

Lian et al. (2013) combined two approaches, developing a complex hydrodynamic model of the river system in Fuzhou, China combined with a copula based joint probability assessment of rainfall and tidal level. Merging these two methods allowed quantification of the effectiveness of outlet pumps, creating useable data for flood risk management.

Another use of hydrodynamic modelling is in representing previously observed compound flood events. For example Olbert et al. (2017) used multiple nested models to simulate a flood event in November 2009, which impacted Lee Estuary and flooded Cork City Ireland. Flood wave propagation was simulated on a 2 m grid, creating a high-resolution model useful for flood planning. Kumbier et al. (2018) investigated the impacts of a compound flooding event (riverine flooding and storm tide) using Delft3D on Shoalhaven Estuary, Australia in 2016. The model found that a flood risk assessment only accounting for the storm tide would have underestimated the flood extent of the storm event by 30%.

Hydrodynamic modelling has also frequently been used to analyse the inundation extent of compound flooding from hurricanes and typhoons. Some have modelled previous events. For example, Torres et al. (2015) modelled Galveston Bay, USA, using simulated tracks of hurricanes which have hit the area (E.g. Hurricanes Katrina, Ike and Isaac). A relationship was found between rainfall-runoff and storm surge in region, with peak surge and peak runoff being separated by less than 24 hours in most modelled scenarios. Silva-Araya et al., (2018) used similar methodology to model Hurricane Georges (1998) and its impact on the east coast of Puerto Rico. They found the peak freshwater runoff did not coincide with the peak storm surge, however the increased runoff was enough to increase flood levels compared to storm surge alone. An issue with hydrodynamic modelling is the limitations in region size. Ikeuchi et al. (2017) showed that a global model (CaMa flood river model) can be used to represent a large-

scale region (the Ganges-Brahmaputra-Meghna Delta) for Cyclone Sird in 2007, this in contrast to previous studies which had investigated far smaller regions due to the processing requirements of running a high scale model over larger areas.

Saleh et al. (2017) looked to understand how uncertainties in meteorological drivers are translated into uncertainties in compound flood inundation models, using Newark Bay in New Jersey, USA during Hurricanes Irene and Sandy. It highlighted the propagation of uncertainty in meteorological forecasts of hurricanes can lead to large errors in flood maps.

Other studies have used hypothetical events to model the potential compound flooding extent, for example Chen & Liu (2014) simulated a Typhoon Haiyan sized event in the Tsengwen River basin, Taiwan to generate surge and river discharge at 200 year return period. Bilskie & Hagen (2018) modelled a hypothetical hurricane hitting the Louisiana coastline, similar to Hurricanes Harvey, Irma and Maria and found that the combination of rainfall and storm surge were less than the individual components on their own, in contrast to previous studies.

2.8 Summary and knowledge gaps

This chapter has undertaken a comprehensive literature review of compound flooding: starting with the individual flood sources themselves (surges, waves, fluvial and pluvial); the mechanisms leading to compound floods; previous compound flood events. The impact of how variables and extremes were defined was highlighted; and ending with a review of the different approach to assessing compound flooding, from simple conceptual models, to detailed localised hydrodynamic models.

Around the UK there have been several national scale studies, however, all have their drawbacks. Petroliagkis et al. (2016) used only hindcast model data with no validation in the UK. Svensson & Jones (2002, 2004) showed dependence around the UK, however made no comparison between different coastlines. Mazas & Hamm (2017) demonstrated that using traditional statistical methods might not yield as accurate results as using copulas. Thus far no study has looked at the spatial variability of compound flooding around the entire UK coastline. Svensson & Jones (2002, 2004) split their papers into east coast and the west and south coast. As a result, they do not compare between the two coastlines. Furthermore, whilst they assess the meteorological conditions causing both occurrences, no nationwide comparison is done of these drivers. Finally, there have been no studies which categorise the impact catchment

characteristics have on compound flooding. Therefore, first object of this thesis is to assess compound flooding due to high sea levels and river flow around the UK coast and determine their drivers.

Another key knowledge gap is that no study has assessed the joint occurrence of all of the variables (i.e. surges, waves, river flow and precipitation) around the UK. Svensson & Jones (2002, 2004) used surges, rainfall and precipitation. Hawkes (2005) collated studies on joint probability at the time in the UK, to look at the dependence and joint probability of wave height and surge, tide and surge, river flow and surge and precipitation and surge. Petroliagkis et al. (2016) produced a similar report for Europe, looking at surges, river flow and waves. However as mentioned previously, this was limited by the lack of observed data was used. Comparison of the two studies highlighted the difficulty using modelled data, with results varying based on the location of the modelled grid point used. The second objective of this thesis, is to determine the characteristics and likelihood of all coastal flood sources (storm tides, waves, river discharge (fluvial), precipitation (pluvial)) occurring concurrently.

Finally, no study has assessed the changes in compound flooding in the UK temporally. During their study on compound flooding in the USA, Wahl et al. (2015) used New York City as a case study and found that meteorological conditions favouring compound flooding had increased over the 20th century. No such work has been conducted in the UK. Furthermore, no study has looked at future risk from compound flooding. Therefore, my third objective, is to identify past and future changes in the meteorological conditions leading to compound flooding around the UK coastline.

3. Data

Five main data types were used in this study, namely: (1) sea- level timeseries; (2) wave timeseries; (3) river discharge records; (4) rainfall data; (5) North Atlantic Oscillation (NAO) Index; and (6) meteorological datasets. These are described in the following six sub-sections. In Section 4.2.7, the site selection methods are described, with the subsequent analysis outlined in Section 4.3.

This chapter describes datasets used within this thesis; the four main flood sources (sea level, wave, river discharge and rainfall (as a proxy for surface flooding). Meteorological data is used to analyse the flood source co-occurrences.

3.1 Sea level data

Sea level time-series from the UK National Tide Gauge network were obtained from the British Oceanographic Data Centre (British Oceanographic Data Centre, 2018). Data is available for 43 tide gauge sites around the UK coast. Sea level records are available as hourly measurements before 1993 and quarter hourly after 1993. The longest sea level record (Newlyn) starts in 1915, whilst the shortest (Portrush) begins in 1995. Data up to the end of 2016 is considered. The data has been previously quality controlled by the BODC, with questionable values flagged as improbable, null or interpolated (Mcgarrigle et al., 2015). Any values that were flagged as improbable or null have been removed from the analysis.

3.2 Wave data

Observed wave data is limited temporally in the UK, with an average data length of ~10 years per wave buoy. Therefore, a global wave hindcast, GOW2, was used instead (Perez et al., 2017). Data is available from 1979 to 2018 (39 years of data). Outputs include hourly sea state parameters (significant wave height, peak period and mean wave direction) and 3-hourly spectra (in shallow coastal locations). The modelled data is validated against observed wave buoy data acquired from the Channel Coastal Observatory (CCO, 2020) and Wavenet from the Centre for Environmental, Fisheries and Aquaculture Science (CEFAS, 2020a). Buoy data is quality controlled by the respective institutes (CEFAS, 2020b; Mason & Dhoop, 2017). Wave buoys were selected nearest to each GOW2 node used (see Section 4.2.7.). Data at every site

using the Pearson correlation coefficient, root mean square difference (RMSD) and standard deviation (Figure 3.1 Figure 3.2). Only significant wave height was found to be performed satisfactorily, showing correlation between 0.5-0.95, and RMSD and standard deviations below 1 for most sites, therefore peak period and wave direction were not considered in this study. On a global grid, the spatial resolution is half a degree (~55km), however in shallow coastal locations (such as those in this study), a spatial resolution of around 25km is available. The model's performance is reduced in water depths less than 5m, therefore sites below this depth were not selected.

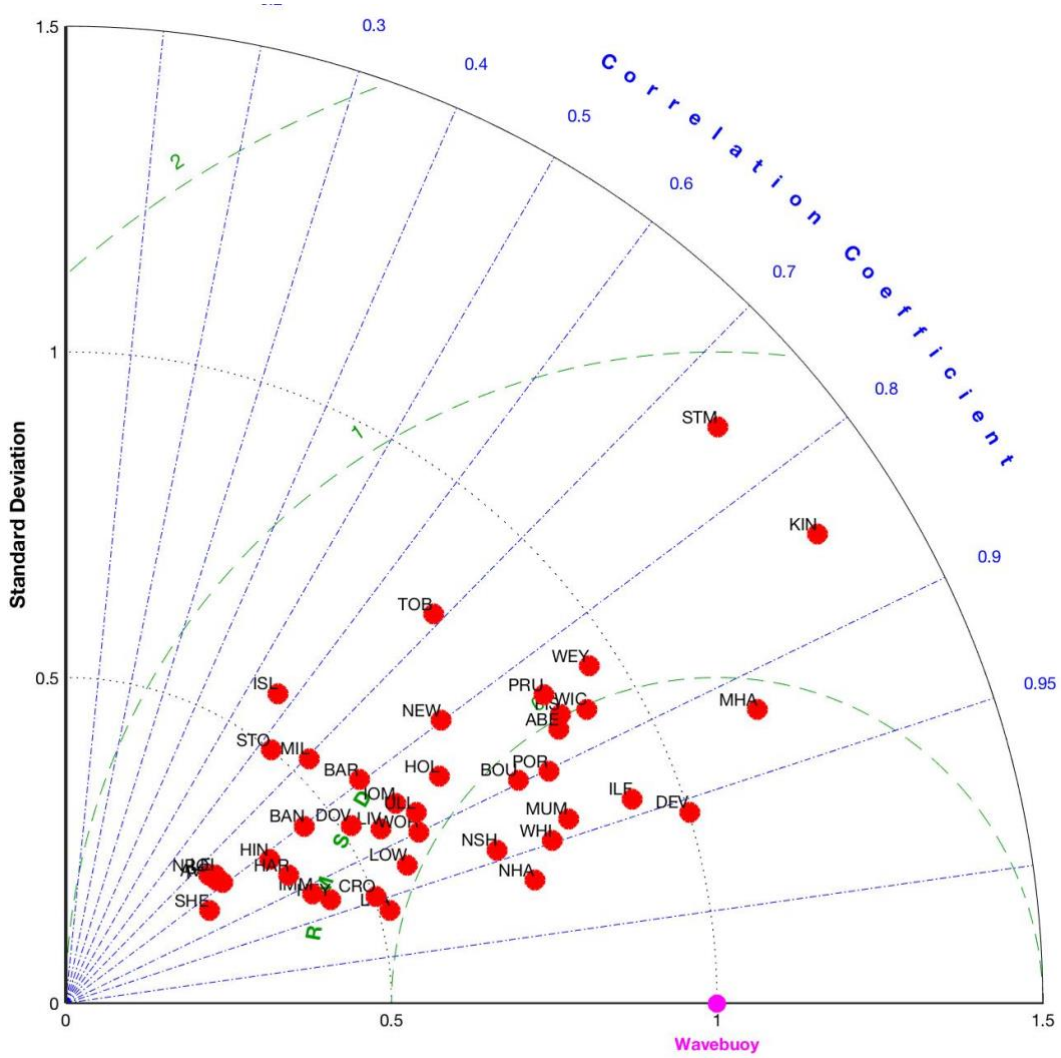

Figure 3.1: Taylor plot (Taylor, 2001) of GOW2 wave model performance vs the nearest local wavebuoy reference for significant wave height (Hs) at all study sites, showing standard deviation in black, root mean square difference (RMSD) in green and correlation coefficient in blue.

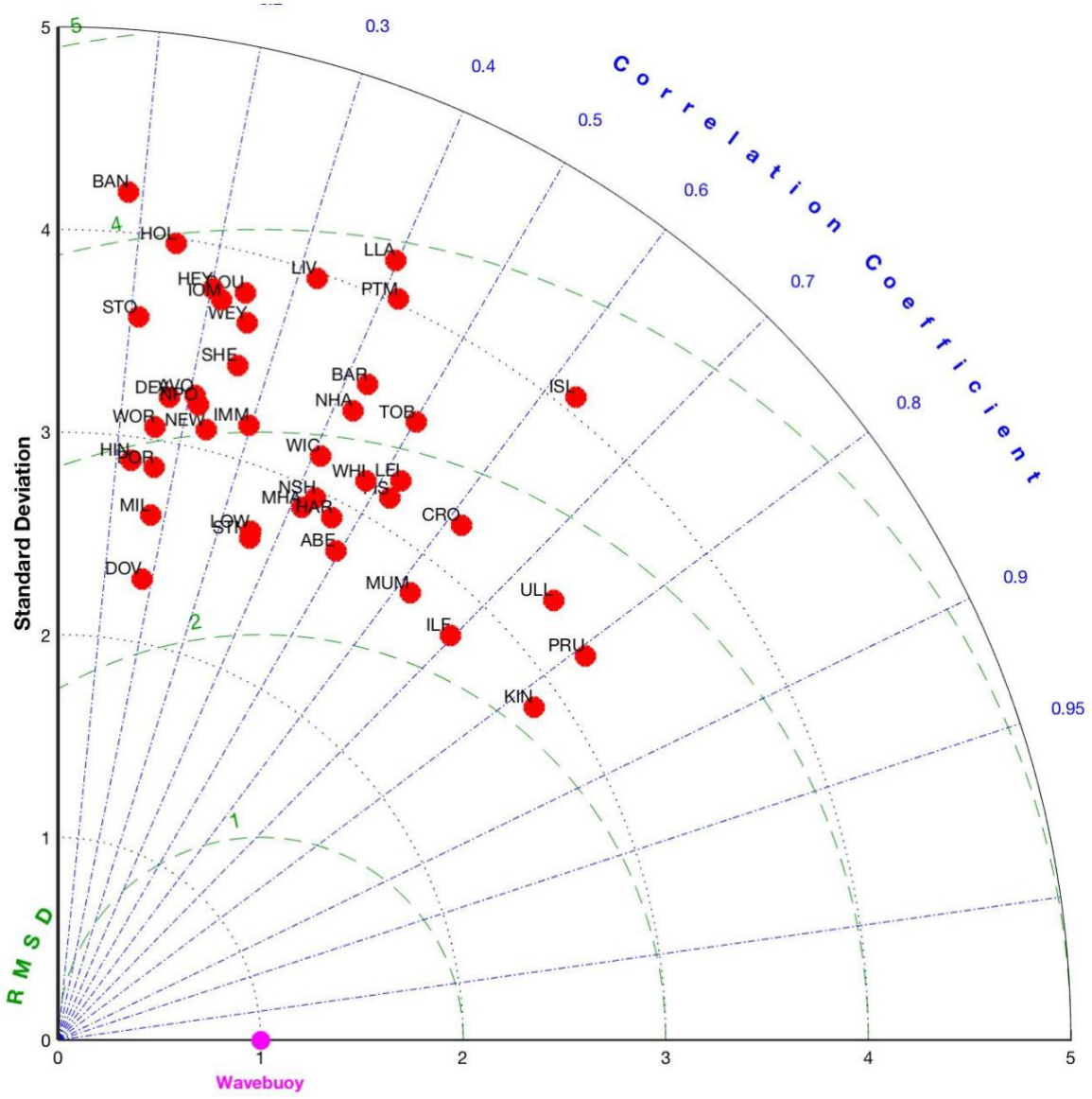

Figure 3.2: Taylor plot (Taylor, 2001) of GOW2 wave model performance vs the nearest local wavebuoy reference for peak period (Tp) at all study sites, showing standard deviation in black, root mean square difference (RMSD) in green and correlation coefficient in blue.

3.3 River discharge data

River discharge data was obtained from the UK's National River Flow Archive (CEH, 2018). Data is available for more than 1,500 river gauge sites (see Sections 3.2.1 and 4.2.1 for selection criteria). The measurements are available as daily mean rates. The longest river discharge record (Kingston, on the Thames) starts in 1883, whilst the shortest (Deerhurst on the Severn), begins in 1995. Again, data up to the end of 2016 are considered. The data has been previously

quality controlled by the Centre for Ecology & Hydrology (CEH), and data that was flagged as suspect is excluded (Dixon et al., 2013).

3.4 Rainfall data

Daily rainfall totals were obtained from the Met Office Integrated Data Archive System (MIDAS) Land and Marine Surface Stations Data (CEDA, http://archive.ceda.ac.uk last access: 1st February 2019). The dataset comprises daily and hourly weather measurements, for the period of 1853 to present at over 5,000 weather station, with almost 4,000 providing daily rainfall data. Sites are selected closest to the 43 tide gauges (see Section 4.2.7 for selection criteria). Data is checked for quality by both the Met Office and Environment Agency (who manage the weather stations).

3.5 Meteorological data

Gridded mean sea level pressure (MSLP), near-surface U and V wind and precipitable water content (PWC, entire atmosphere considered as a single layer) fields are used to investigate the meteorological conditions that drive compound and non-compound events in Chapters 4 and 5. Data from the 20th Century global meteorological Reanalysis (A blend of observations and past short range weather forecasts rerun with modern forecasting models) are used, Version 2c (Compo *et al.*, 2011), obtained from the National Oceanic and Atmospheric Administration website (NOAA; https://www.esrl.noaa.gov/psd/data/20thC_Rean/). The fields have a spatial and temporal resolution of 2 degrees (222km) and 6 hours, respectively and are available from 1851. Whilst the spatial resolution is relatively coarse, the 20th Century Reanalysis was chosen to encompass the full time series of the datasets used. Finer resolution reanalysis datasets (such as ERA-5) have shorter timeseries. The area is focused on 34˚N to 70˚N and 60˚W to 20˚E, which encompasses the region where storms affecting the UK are generated and influence the region.

The results in Chapter 4 are also compared to Coastal Decider (Neal et al., 2016). This is based on probabilistic weather-pattern forecasts and helps in identifying periods with an increased likelihood of coastal flooding from high sea levels around the UK. Coastal Decider uses a set of 30 distinct weather patterns (referred to as the “Met Office weather patterns”) which were derived by Neal et al. (2016) using k-means clustering techniques. These weather patterns

represent the large-scale meteorological conditions experienced over the UK and surrounding European area. Neal et al. (2018) used a daily historical weather-pattern catalogue to show that particular weather patterns tend to relate to high sea level events at different sites around the UK, with this analysis forming the basis for Coastal Decider. Other research which relates the Met Office weather patterns to meteorologically induced hazards includes that of (Richardson et al., 2018) who related the weather patterns to precipitation observations for the application of drought forecasting.

3.6 Catchment Characteristics

River catchment characteristics were obtained or calculated from information on the NRFA website for each of the river discharge sites analysed. Three catchment characteristics were considered as follows: (i) the base flow index (BFI), (ii) catchment area, (iii) and catchment elevation variation. The BFI is a measure of the proportion of the river run-off that derives from stored sources (Gustard et al., 1992) and gives an indication of the flashiness (how quickly a river responds to precipitation) of a catchment. The more permeable the rock and soils in a catchment, the higher the base flow. Rivers draining impervious clay catchments (with minimal lake or reservoir storage) typically have baseflow indices in the range 0.15 to 0.35, whilst chalk streams have a BFI greater than 0.9 as a consequence of the high ground- water component in the river flow. The catchment area is the size of the drainage basin of a particular river. Both the BFI and catchment area are provided directly on the NRFA website for each catchment (CEH, 2018). The catchment elevation variation is a measure of the steepness of a catchment. The NRFA provides statistics on the elevation of the minimum and maximum elevations in a catchment along with the elevations at the 10, 50, and 90 percentiles of the river catchment. An elevation variation index was calculated by taking the difference between the 90 and 10 elevation percentiles and normalising these about the mean of all sites; values close to 1 indicate a catchment with a steep elevation gradient, and values close to 0 indicate a catchment with a gentle gradient.

3.7 Climatic indices

The NAO has been selected to compare to compound flooding in Chapter 5 as the primary driving teleconnection which influences the UK (and Northern Europe) climate (Hurrell &

Deser, 2010). Other oscillations considered were the Arctic Oscillation (AO) and Atlantic Multidecadal Oscillation (AMO). These were discounted due to the lack of influence over the UK compared to the NAO (in the case of the AO, Ambaum et al., 2001); or due to the relative shortness of observed data masking any long term influence the AMO may have. The NAO index is used to examine the connection between the phase of NAO and compound flooding. The NAO index has been obtained from the Climate Prediction Centre, National Oceanic and Atmospheric Administration (CPC, NOAA; https://www.cpc.ncep.noaa.gov/products/precip/CWlink/pna/nao.shtml). The index is obtained by applying the Rotated Principal Component Analysis procedure (RPCA) (Barnston & Livezey, 1987), to monthly standardized 500-mb height anomalies obtained from the (Climate Data Assimilation System) CDAS in the analysis region 20N-90N from January 1950 to present. The winter NAO index was calculated from averaging NAO for the winter months, with winter defined as December, January, February and March (DJFM), in line with Hurrell (1995), who identified decadal trends in the NAO winters.

In addition to the NAO, the AMO was selected for use due to the longer time scales being examined. The AMO is a mode of natural variability in the North Atlantic with a period of 60-80 years. The AMO index is based upon sea surface temperature anomalies in the North Atlantic basin over 0-80N, from 1856 to present (Enfield et al., 2001). The index was obtained from the Physical Science Laboratory, NOAA (PSL, NOAA; https://www.esrl.noaa.gov/psd/data/timeseries/AMO/). The annual winter AMO index was calculated from the average monthly AMO between December, January, February and March (DJFM), in line with the winter NAO.

3.8 Future Projections

To understand future risk of compound flooding, outputs from a global climate model (GCM) were used. HADGEM2-ES (Met Office Hadley Centre, 2012) was selected as it is known to accurately reproducing UK climate from the CMIP5 models (Zappa et al., 2013). Although 3 and 6 hourly data are available for some parameters, the three variables required here (i.e., MSLP, WS and PWC) were only available together at a daily frequency. Data was used for the period from 2005-2095. The projected data had a different resolution (1.25 degrees latitude by 1.875 degrees longitude), compared to the reference conditions based on the 20th Century data (2.0 degrees latitude by 2.0 degrees longitude). Therefore, the reference conditions were

interpolated to same resolution as the projection data. The Hadley Centre family of GCM's (including HADGEM2-ES) uniquely use a "360 day" calendar, where by each year has 360 days (conceptualized as 12 months of 30 days each). Other studies (e.g. Ruosteenoja et al., 2016) have inserted 5 days (6 on leap years) of data interpolated data from other periods, spread equally across the year. This results in an average of 1.4% of data being interpolated. As this thesis is looking at extreme tail events, interpolating temporally could result in undesirable data. For this reason, coupled with the fact this study is not comparing different GCM's, a decision was made to keep the calendar year as it is.

Two different projections were used, Representative Concentration Pathways (RCP) 2.6 and RCP8.5. These refer to the radiative forcing's in the year 2100 (2.6 and 8.5 W/m^2, respectively). These represent the climate modelling scenarios depending on different volumes of greenhouse gases released. RCP2.6 is a "stringent pathway" with CO_2 emissions declining by 2020 and reaching zero by 2100. In RCP8.5, emissions will continue to rise through to 2100 and typically taken as the worst-case scenario (IPCC, 2014). These two pathways were chosen to test the viability of this method, as the most chance of showing variation on future compound flooding. Another variation from the reference conditions is the use of precipitation flux (the rainfall falling), as opposed to PWC within the reference conditions.

4. Assessing the characteristic and drivers of storm surge and fluvial compound flooding events around the UK coast

This chapter has been adapted from the following publication:

> *Hendry, A., Haigh, I. D., Nicholls, R. J., Winter, H., Neal, R., Wahl, T., Joly-Laugel, A. and Darby, S. E.: Assessing the characteristics and drivers of compound flooding events around the UK coast, Hydrol. Earth Syst. Sci., 23(7), 3117–3139, doi:10.5194/hess-23-3117-2019, 2019.*

4.1 Introduction

This chapter focuses on the dependence between coastal and river flooding around the UK. As underlined in Chapter 2, previous studies have investigated the spatial difference in the likelihood of extreme storm surges to occur simultaneously with extreme river discharge, however no study has been comprehensive. Svensson and Jones (2002 and 2004) examined the west and east coasts independently and briefly examined the storm tracks (following the centre of the low pressure systems) associated with compound events. Petroliagkis et al. (2013), examined dependency between storm surge and river discharge in Europe, and used 10 sites in the UK, but did not investigate variation between different areas of the UK. More recently in their global study; Ward et al. (2018) identified a west-east difference in the strength of dependence between extreme storm surges and river discharge. Crucially however, none of the studies identified the reason or reasons for this spatial variability. A key knowledge gap is therefore to identify the meteorological conditions which lead to compound and non-compound events and if they are the driver behind any potential spatial variability. Finally, those studies which did identify a spatial pattern in the UK (Petroliagkis et al., 2016; Ward et al., 2018), were working at larger resolutions (European and globally respectively) and so only featured a handful of sites within the UK. Therefore, a key knowledge gap is how compound flooding varies at a more localised scale, and the impact of riverine catchment characteristics (i.e. flashiness, size, and elevation gradient) on compound flooding.

The overall objective of this chapter is to assess the potential for compound flooding arising from the joint occurrence of high storm surge and high river discharge around the coast of UK. To achieves this, the sub-objectives in this study are as follows:

1. To map the spatial dependence between storm surges and high river discharge around the UK
2. To investigate the meteorological conditions that drive compound and non-compound events across the UK.
3. To examine how the strength and phase of dependence between storm surge and river discharge are influenced by the characteristics (i.e. flashiness, size, and elevation gradient) of the corresponding river catchments

4.2 Methodology

The analysis was undertaken in three main stages, each addressing one of the three sub-objectives outlined above. These stages are described in turn in the sections below.

4.2.1 Site Selection

From the available datasets, described above in Sections 3.2.1 and 3.2.2, combinations of tide gauge and river discharge sites were matched that satisfied the following criteria: (1) there are at least 15 years of overlapping records and (2) daily mean river discharge is at least 5 $m^3 s^{-1}$ at the river site. Previous studies often matched river gauge sites to the nearest tide gauge sites (Paprotny et al., 2018) or every river gauge to every tide gauge site (Svensson and Jones, 2002, 2004). However, because of the complex topography of the coastline, this does not always associate a river gauge site to the hydrologically relevant tide gauge (and coast) for that river system. Therefore, each river site was matched visually to the tide gauge site nearest to the appropriate river mouth. Nine tide gauge sites – (1) Dover; (2) Newhaven; (3) Port Erin, Isle of Man; (4) St Helier, Jersey; (5) St Mary's, Isles of Scilly; (6) Stornoway, Isle of Lewis and Isle of Harris; (7) Lerwick, Shetland Islands; (8) Lowestoft; and (9) Harwich – were excluded from the analysis, as there were no appropriate nearby river systems with discharge measurements or the corresponding overlapping record length was less than 15 years for that specific combination of sites.

Following this selection, there are 326 combinations of discharge stations and tide gauges, the locations of which are shown in Figure 4.1, linked to 33 tide gauge sites. In Figure 4.1a, and

subsequent figures of this nature hereafter, river sites discharging onto the western, eastern, and southern coasts of the UK are plotted as triangles, circles, and squares, respectively. There is good spatial coverage across most of the country, except in the south-east. The river sites discharging along the south-east tend to have discharges below 5 $m^3 s^{-1}$ or the overlapping data lengths are less than 15 years. Some tide gauge sites (e.g. Newlyn (5) and Wick [26]) are not in the near vicinity of where corresponding rivers drain into the sea. However, as storm surges have large spatial extents, they are close enough to be considered representative of the broader-scale storm surge characteristics in that area.

The number of years for which overlapping data are available for both sites is also shown in Figure 4.1a. The tide gauge data were typically the shorter of the two sets. The mean overlapping length across all sites was 24 years, with a maximum of 50 years. Tide gauges had an average of 10 river gauges linked to them (Figure 4.1b), with a minimum of 1 (Newlyn [5], Fishguard [12] and Holyhead [14]) and a maximum of 37 (Immingham [31]). At some tide gauge sites, multiple sub-catchments have been used, sometimes with multiple discharge stations on the same river. Details of the location of the combination of sites and their overlapping data lengths are given in Table 9.1.

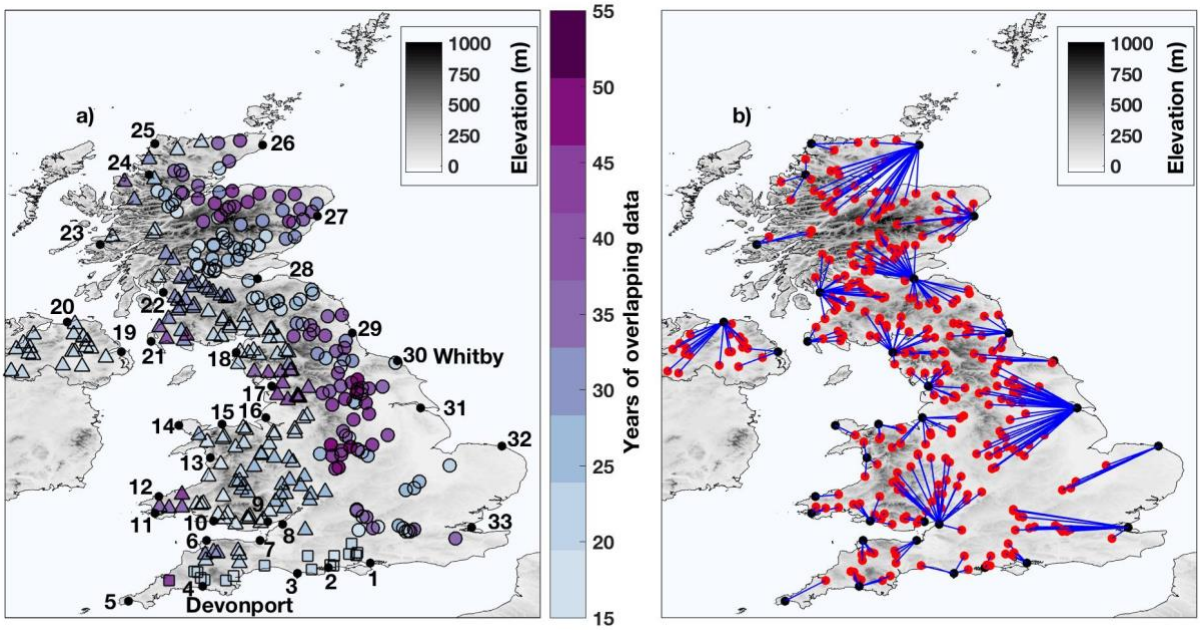

Figure 4.1: (a) Location and overlapping data length (in years) of the 33 tide gauge sites (black dots) and 326 river discharge stations (triangles, circles and squares show the river stations that discharge onto the west, east and south coasts, respectively); and (b) pairing of the tide gauge and river discharge stations.

4.2.2 Joint Occurrence and dependence

The first sub-objective is to map the dependence between storm surge and river discharge, comparing different methods for quantifying the dependence between these two variables. For sea level, two parameters were considered: (1) total still sea- level and (2) storm surge (i.e. the meteorological component of sea level). To represent the latter, the skew surge parameter is used, which is the difference between the maximum observed high water and the maximum predicted (astronomical) high water, in each tidal cycle, regardless of its timing. To extract time series of skew surges from the sea-level records at each tide gauge site, the approach of Haigh et al., (2016) is followed. To do this, first a harmonic analysis is performed for each calendar year, using the T-Tide harmonic analysis package (Pawlowicz et al., 2002) with the standard 67 tidal constituents. Each instance of observed and predicted high water was identified, and the difference between the two was computed to give time series of skew surges. Daily maxima of total still sea level and skew surge time series were then extracted at each tide gauge site. The exact time of the daily maxima was retained for the meteorological analyses, described later in Sect. 4.2. The river discharge records were obtained in the format of daily mean values, and so no pre-processing was necessary on these records.

Extreme levels were extracted for each of the three (i.e. total sea level, skew surge, and river discharge) daily time series, at each site, using a peaks-over-threshold (POT) approach. A declustering algorithm was used, with a storm length of 48 h (Haigh et al., 2016, found that storms in the UK typically affect sea level for 3.5 days) to guarantee independent events. The threshold was varied at each site to ensure that each of the three time series had on average 2.3 to 2.5 extreme levels per year. This threshold range ensured that (1) there were enough data points to estimate dependence between the variables reliably and (2) the threshold was high enough for the exceedances to be considered “extreme” (Svensson & Jones, 2005). The average thresholds across all sites were the 99, 99.1, and 99.2 percentiles for total sea level, skew surge and river discharge, respectively.

Two different approaches were used to assess the dependence between total sea level or skew surge and river discharge. The first approach is hereafter known as the “dependence method”. Here, dependence is calculated between the daily maximum total sea-level or skew surge and discharge time series using Kendall’s rank correlation τ (Kendall, 1938), which, unlike Pearson’s correlation coefficient, captures non- linear relationships. Significance was assessed

at $\alpha = 0.05$ (i.e. 95 % confidence level), using corresponding p values estimated from exact permutation distributions. The analysis is repeated using time lags from −5 to +5 days. For example, for daily maximum skew surge, corresponding daily maximum discharge values are selected with time lags of −5, −4, −3, −2, −1, 0, +1, +2, +3, +4, and +5 days. This is to allow for that fact that when a storm approaches the coast, for example, it might first generate a high storm surge be- fore travelling inland and generating high precipitation and therefore elevated river discharge sometime afterwards.

The second approach is hereafter known as the "joint occurrence method". Here, the number of times extreme total sea-levels events, or skew surges events, above the chosen threshold for that site, occurring on the same day as extreme river discharge are counted. Each pair of sites has varying overlapping data lengths. Therefore, to standardise the results, the number of joint occurrences per decade were determined. Again, the analysis is repeated but lag the discharge using time lags of −5 to +5 days.

To illustrate the approaches, time series of daily maximum skew surges are plotted against records of daily maximum river discharge at the 0-day lag for Devonport (south- western coast) and Whitby (eastern coast) in Figure 4.2a and b length of 48 h (which is appropriate, as Haigh et al., 2016, found that storms in the UK typically affect sea level for 3.5 days) to guarantee independent events. The threshold is varied at each site to ensure that each of the three time-series had on average 2.3 to 2.5 extreme levels per year. This threshold range ensured that (1) there were enough data points to estimate dependence between the variables reliably and (2) the threshold was high enough for the exceedances to be considered "extreme" (Hawkes et al., 2005). The average thresholds across all sites were the 99, 99.1, and 99.2 percentiles for total sea level, skew surge and river discharge, respectively.

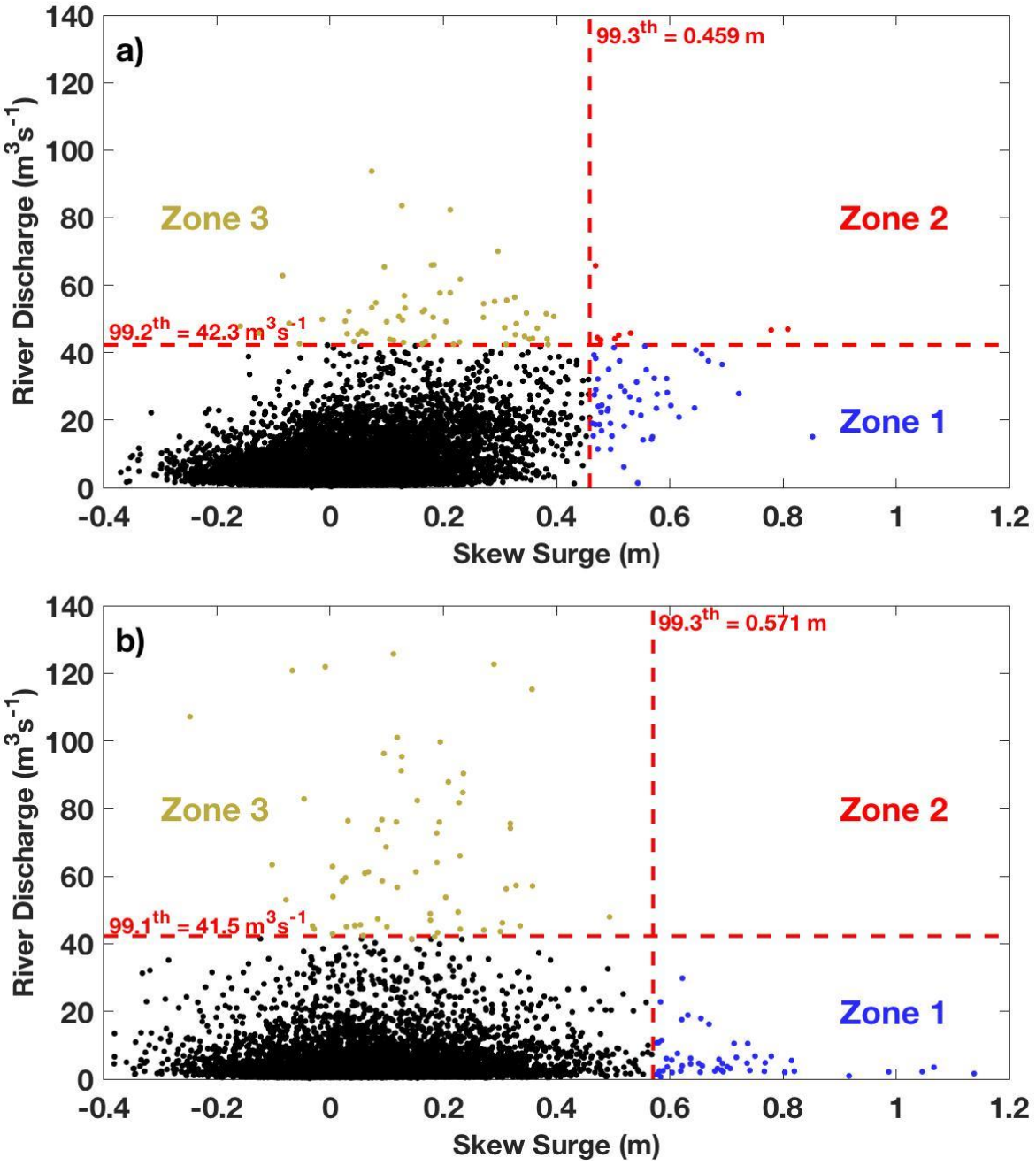

Figure 4.2: Daily maximum skew surge plotted against daily maximum river discharge for (a) Devonport; and (b) Whitby. The dotted red lines indicate the high percentiles chosen in the analysis for the two variables at these sites. Red dots (plotted in Zone 2) show the events with potential for compound flooding (i.e., joint occurrence of high storm surge and large river discharge) whereas blue (Zone 1) and green (Zone 3) define the non-compound events (i.e., high storm surge or high river discharge only, respectively).

4.2.3 Meteorological analysis

The second sub-objective of this chapter is to investigate the meteorological conditions that drive compound (i.e. joint occurrence of high skew surges and large river discharge) and non-compound (i.e. high skew surge or high river discharge only) events across the UK. For each site, fields of MSLP, wind speed, and PWC were extracted for the 6 h period closest to the peak of each (1) extreme total sea level or skew surge event (i.e. all the events in Zone 1 in Figure 4.2), (2) each joint-occurrence event (i.e. all the events in Zone 2 in Figure 4.2), and (3) each extreme river flow event (i.e. all the events in Zone 3 in Figure 4.2). For each site, and each of these three types of events, composite plots of MSLP, wind speed, and PWC were extracted by taking an arithmetic mean and standard deviation of the data at each hindcast grid cell through the time of the corresponding events. The composite plots thus represent the mean (with variance around the mean) conditions of the storms that generate compound and non-compound events. Tracks of all responsible storms were digitised for the three different event types, using the storm tracking algorithm developed by Haigh et al. (2016). This captures the location of the storm centre for each 6-hourly time step of the metrological reanalysis, from cyclogenesis to storm dissipation or when the storm leaves the area of interest (defined above). The mean storm track were calculated for each event type at each site. This allows a comparison and contrast of the weather patterns which cause the compound and non- compound events.

4.2.4 Catchment Correlations

The final chapter sub-objective is to briefly examine how the strength and phase of dependence between total sea level or skew surge and river discharge are influenced by the characteristics of the corresponding river catchments. To do this correlation coefficients were calculated between the strength of dependence (or number of joint occurrences per decade) and the maximum phase lag, with the three selected catchment variables (BFI, catchment area, and catchment elevation variation). Again, significance was assessed at $\alpha = 0.05$. It's hypothesised that the lower the BFI, the smaller the catchment area, and the greater the average elevation gradient, the more likely that high total sea levels or skew surges will occur around the same time as high river discharge. The higher the BFI, the larger the catchment area, and the gentler the elevation gradient of the catchment, the more likely it is that high river discharge will occur several days after high total sea level or skew surge for the sites closest to the coast.

4.3 Results

4.3.1 Dependence and Joint Occurrences

Two methods were used to assess the dependence between high total sea level or high skew surge with high river discharge, across the 326 combinations of discharge stations and tide gauge sites. The results of the first method, the dependence method, are shown in Figure 4.3aFigure 4.4a for daily maximum total sea level and daily maximum skew surge, respectively, with daily maximum river discharge for the 0-day lag. As expected, there is generally greater dependence between skew surges and river discharge (Figure 4.4a) than between total sea level and river discharge (Figure 4.3a). This is because total sea levels are strongly influenced by the deterministic tidal component around the majority of the coastline of the UK (Haigh et al., 2016). Interestingly, the dependence is stronger for total sea levels for sites linked to tide gauges in the northern Irish Sea (e.g. Portrush [20] and Bangor [19] in North Ireland and Portpatrick [21] and Millport [22] in Scotland), and this is most likely because tidal range is small here and not such a dominant factor on total sea levels compared to other sites. A clear spatial variation in the dependence between high sea levels or skew surges with high river discharge is evident in Figs. 3a and 4a. For many of the sites along the south- western and western coasts of the UK, τ typically ranges from 0.1 to 0.35, whilst along the eastern coast, this drops to 0.0 to 0.15. The greatest dependence is found at river gauges linked to the Millport [22] and Portpatrick [21] tide gauges in south-western Scotland. The lowest dependence is located at river gauges near Cromer [32] on the eastern coast. Two river sites linked to the Bangor [19] tide gauge in Northern Ireland show negative dependence.

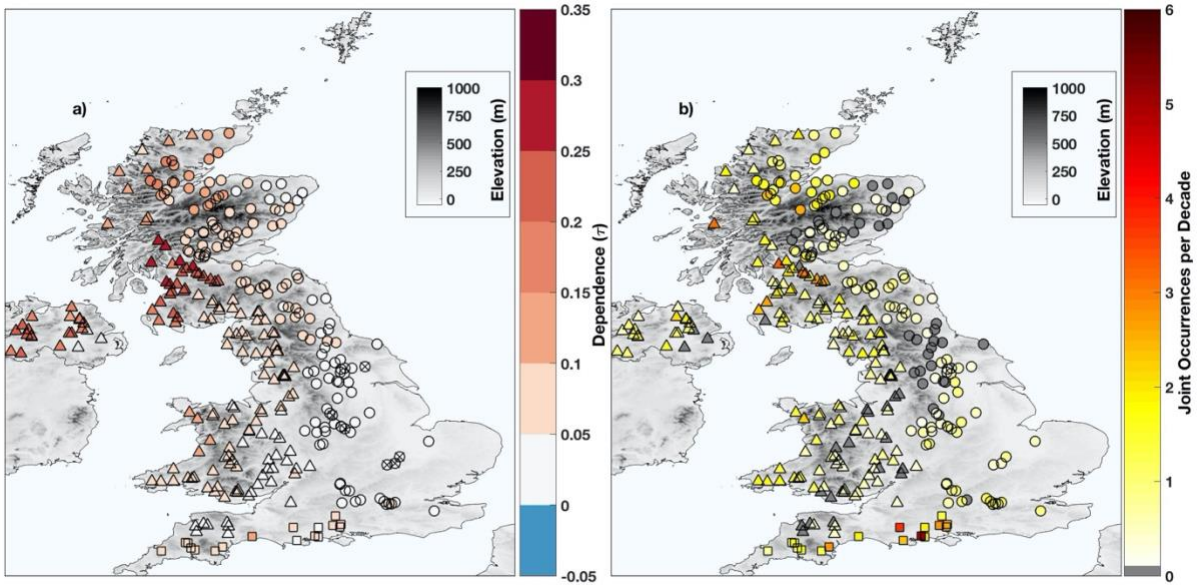

Figure 4.3: (a) Kendall's Rank Correlation τ between daily maximum total sea level and daily maximum river discharge; and (b) number of joint occurrences per decade between extreme total sea levels and river discharge, at 0-day lag. Thick black lines in (a) represent that the dependence is statistically significant (95% confidence) at these sites. Note that the triangles, circles and squares show the river stations that discharge onto the west, east and south coasts, respectively.

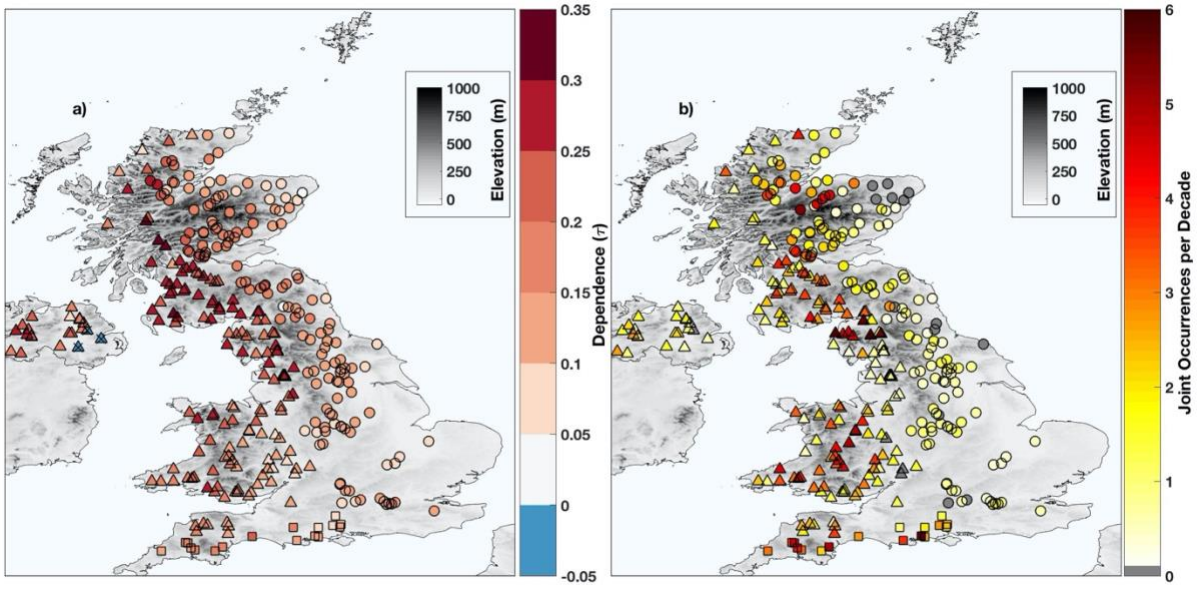

Figure 4.4: (a) Kendall's Rank Correlation τ between daily maximum skew surge and daily maximum river discharge; and (b) number of joint occurrences per decade between extreme skew surge and extreme river discharge, at 0-day lag. Sites with across through them in (a) represent that the dependence is not statistically significant (95% confidence) at these sites.

Note that the triangles, circles and squares show the river stations that discharge onto the west, east and south coasts, respectively.

The dependence is also calculated between daily maximum total sea level or skew surge and daily maximum river discharge using time lags from −5 to +5 days. Dependence is typically weak until the −1-day lag. Interestingly the dependence is higher for +1-day to +5-day lags compared to −5-day to −1-day lags. This is illustrated in Figure 4.5 for the six river sites closest to the tide gauges of Bournemouth [2], Devonport [4], Workington [18], Ullapool [24], Whitby [30], and Cromer [32]. The distributions are typically skewed to the right, and this is probably because river levels remain elevated for several days after a storm event. The lag day when there is the maximum dependence between daily maximum skew surge and daily maximum river discharge is shown in Figure 4.6a for all sites. Interestingly, 42 inland sites (13 % of the 326 sites) on the eastern coast have a maximum correlation at the −1-day lag. The majority of the sites (188; 58 %) have maximum correlation at the 0-day lag. Sites on the south-western and western coast typically have maximum correlations between +1 and +5 days. The number of sites on each day of maximum dependence can be seen in Table 4.1. The sites with maximum correlations at the +4-day and +5-day lag are mostly situation in the Severn River, which has a large catchment area (see Sect. 3.4.3).

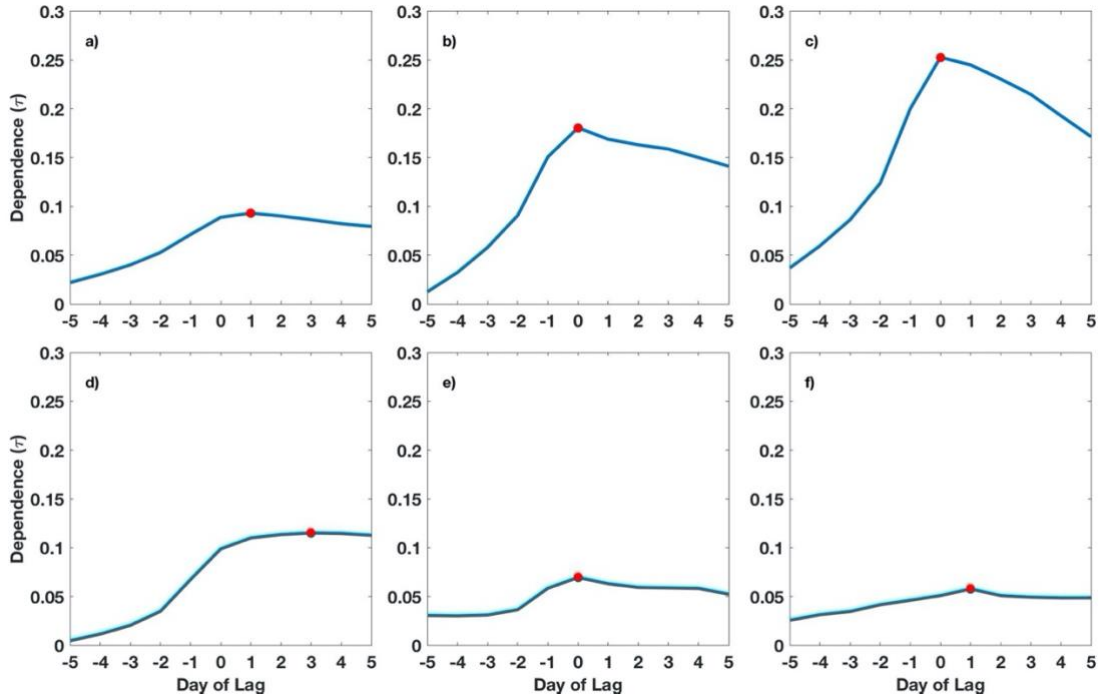

Figure 4.5: Kendall's Rank Correlation τ plotted against day of lag at the follow sites: (a) Bournemouth [2]; (b) Devonport [5]; (c) Workington [18]; (d) Ullapool [24]; (e) Whitby [30]; and (f) Cromer [32]. The red dot shows the day with maximum lag.

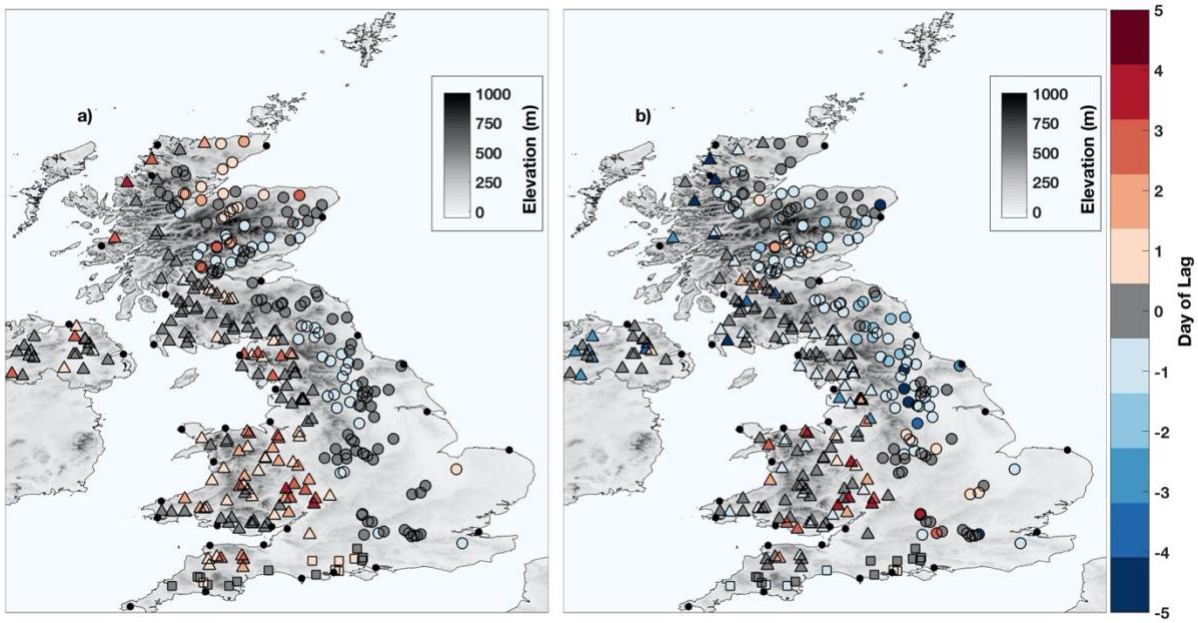

Figure 4.6: (a) The lag day when the Kendall's Rank Correlation τ is maximum between daily maximum skew surge and daily maximum river discharge; and (b) when the lag day when the number of joint occurrences between high skew surge and high river discharge is maximum. Note that the triangles, circles and squares show the river stations that discharge onto the west, east and south coasts, respectively.

Table 4.1: Day of maximum dependence between high skew surges and river discharge; in number of sites and percentage of sites

Day of maximum dependence	-5	-4	-3	-2	-1	0	+1	+2	+3	+4	+5
Number of sites	0	0	0	0	42	188	50	19	21	3	3
Percentage of sites	0%	0%	0%	0%	13%	58%	15%	6%	6.4%	1%	1%

The results for the second method, the joint-occurrence method, are shown in Figure 4.3bFigure 4.4b for high total sea levels and high river discharge and high skew surges and high river discharge, respectively, at the 0-day lag. The spatial patterns are very similar to those of the daily dependence results. For many of the sites along the south-western and western coasts of the UK, there are a higher number of joint occurrences between high skew surges and high river discharge (between three and six joint events per decade) than for sites along the eastern coast (between zero and one joint events per decade). Sites with the largest numbers of joint occurrences (five to six events per decade) include river discharge sites linked to Millport

[22], Workington [18], Mumbles [10], Devon- port [4], and Bournemouth [2] tide gauges. There are several sites along the south-western and western coasts which show low (< 1 event per decade) or zero joint occurrences at the 0-day lag. These include river discharge sites linked to tide gauges at Heysham [17] and Portsmouth [1] in England; Bangor [19] in Ireland; Barmouth [13] and Milford Haven [11] in Wales; and Portpatrick [21], Ullapool [24], and Kinlochbervie [25] in Scotland. Interestingly, there is large variation on a regional or local scale, particularly in areas which mostly have high numbers of joint occurrences. For example, at many sites around the Bristol Channel, the number of joint occurrences varies between one to four per decade at river discharge sites less than 80 km apart. The number of sites with joint occurrences per decade between (i) total water level and river discharge and (ii) skew surge and river discharge can be seen in Table 4.2.

Table 4.2: The number of sites with joint occurrences per decade between (i) total water level and river discharge; and (ii) skew surge and river discharge.

Total number of sites with joint occurrences per decade between:	0	0-1	1-2	2-3	3-4	4-5	>5
Extreme total water level and river discharge (percentage of sites)	61 (19%)	169 (52%)	76 (23%)	17 (5%)	2 (1%)	1 (0.3%)	0
Extreme skew surge and river discharge (percentage of sites)	24 (7%)	97 (30%)	97 (30%)	56 (17%)	31 (10%)	14 (4%)	7 (2%)

The lag day when there are the maximum number of joint occurrences between high skew surge and high river dis- charge is shown in Figure 4.6b for all study sites. The results are similar to those seen for the daily maximum dependence approach (Figure 4.6a). Inland sites on the eastern coast typically have a maximum number of joint occurrences at the −1-day to −3-day lag, whereas several sites on the western coast have a maximum number of joint occurrences at the +1-day to +5-day lag.

4.3.2 Meteorological analysis

The next step is to investigate the meteorological conditions that drive compound (i.e., joint occurrence of high skew surges and large river discharge) and non-compound events (i.e. high skew surge or high river discharge only) events across the UK. Here the focus is on skew surge rather than total sea level, as the dependence between skew surges and river discharge is

stronger. At each of the 326 river discharge sites, composite plots have been derived of SLP, wind speed, and PWC through the time of the events that have led to (1) high skew surge events only, (2) joint-occurrence events, and (3) high river discharge events only. To illustrate the results of this component two contrasting sites are focused on: Devonport [4] on the UK south-western coast, where high storm surges and high river discharge have occurred at similar times in the past (Figure 4.2a), and Whitby [30] on the UK eastern coast, where high storm surges have never occurred (during the period of record) at times of high river discharge (Figure 4.2b).

Composite plots are shown in Figure 4.7 and Figure 4.8 for Devonport [4] and Whitby [30], respectively, for SLP (Figure 4.7a, d, and g and Figure 4.8a, d, and g), wind speed (Figure 4.7b, e, and h and Figure 4.8b, e, and h), and PWC (Figure 4.7c, f, and i and Figure 4.8c, f, and i) for the events that had (1) only high skew surge (Figure 4.7a, b, and c and Figure 4.8a, b, and c), (2) both high skew surge and high river discharge (Figure 4.7d, e, and f and Figure 4.8d, e, and f), and (3) only high river discharge (Figure 4.7g, h, i and Figure 4.8g, h, and i). The number of events recorded for each type is listed, and the average standard deviation (SD), across all grid cells, is also reported. The latter gives an indication of the spread of the spatial patterns across all the corresponding events (i.e. a low SD indicates that the storms across all events have very similar spatial patterns).

At Devonport (Figure 4.7), the meteorological patterns in SLP are similar across the three event types. All three event types feature a low-pressure system to the north-west of Ireland (Figure 4.7a, d and g), with strong south-westerly winds affecting the south-western coast. As expected, the wind speed is more intense along the southern coast for the skew surge- only (Figure 4.7b) and joint event types (Figure 4.7e) compared to the events with river discharge only (Figure 4.7g). The differences in PWC patterns are more pronounced. There is low PWC over the south-west for the surge only events (Figure 4.7c) and higher PWC for the joint and river only event types (Figure 4.7f and j). The composite plot of PWC is characterised by a higher SD for surge-only events (e.g. there is more spread across the range of events) in comparison to the event types that are joint and river only.

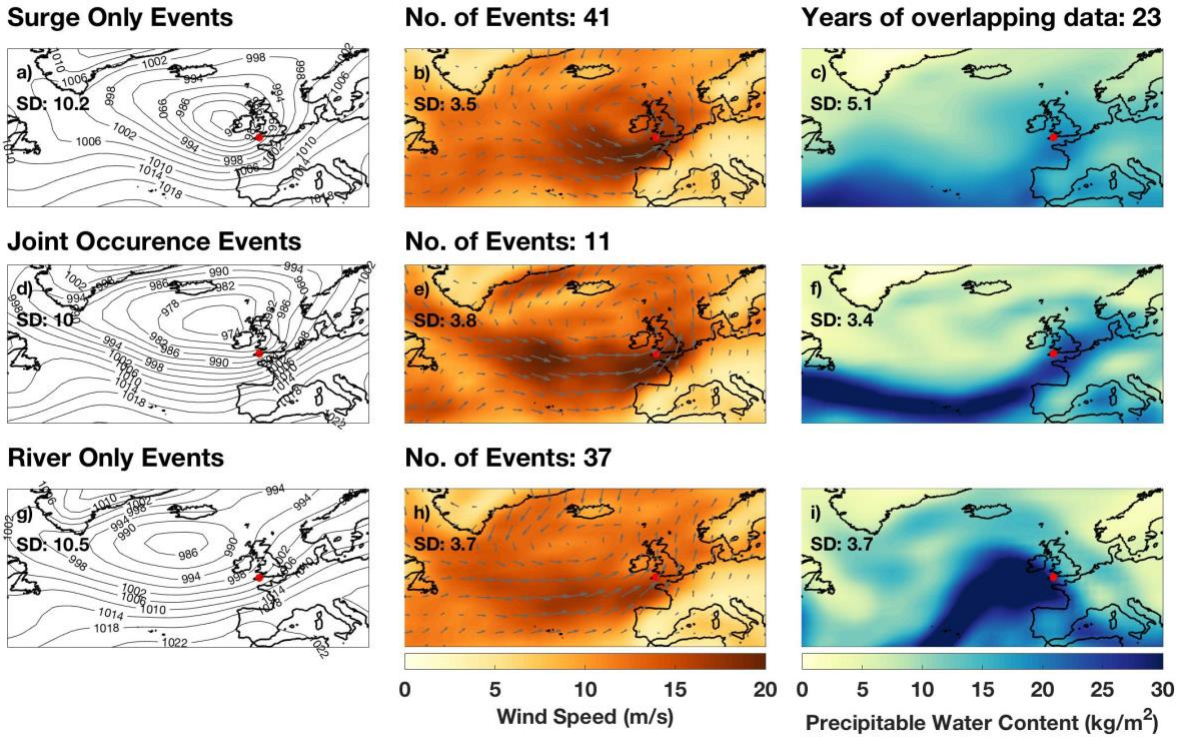

Figure 4.7: Meteorology conditions for Devonport [5]: first column, sea level pressure (mbar); second column, wind speed (m/s) and direction (grey arrows); third column, precipitable water content (kg/m^2); during (a, b and c) high skew surge events only, (d, e and f) both high skew surge and high river discharge events, and (g, h and i) extreme high river discharge events only. SD correspond to the averaged standard deviation over the grid for each variable across the selected events.

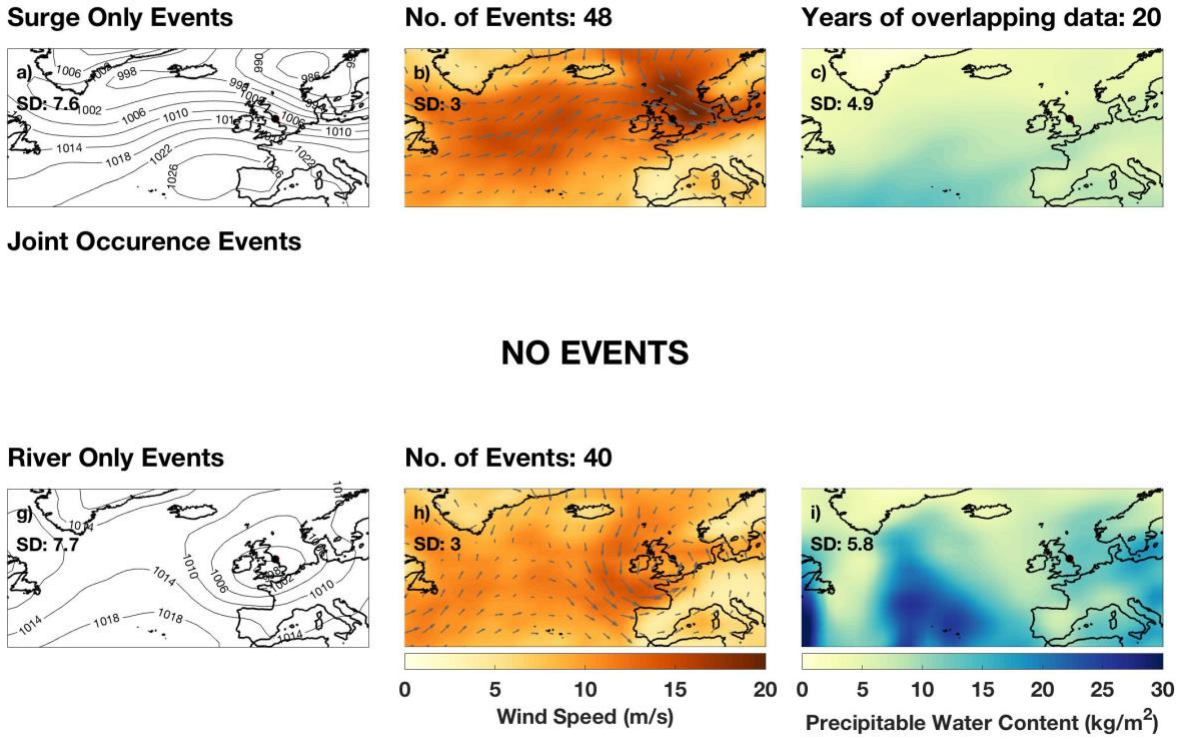

Figure 4.8: Meteorology conditions for Whitby [30]: first column, sea level pressure (mbar); second column, wind speed (m/s) and direction (grey arrows); third column, precipitable water content (kg/m^2); during (a, b and c) high skew surge only events, (d, e and f) both high skew surge and high river discharge events, and (g, h and i) extreme high river discharge only events. SD correspond to the averaged standard deviation over the grid for each variable across the selected events.

In contrast, at Whitby, the meteorological patterns in SLP are very different across the two event types (note that no joint high skew surge and high river discharge were observed here; Figure 8), showing that the storms that lead to high skew surges are distinct from the storms that lead to high rainfall and therefore river discharge. For events with high skew surge only, the storm centre is situated over Scandinavia (Figure 4.8a), producing strong north-westerly winds across the North Sea (Figure 4.8b). PWC is low for the entire eastern coast (Figure 4.8c). For events with high river only, a weaker low- pressure system is centred over central UK (Figure 4.8g). The wind speeds are therefore low on the eastern coast (Figure 4.8h). However, the PWC is high over much of the UK. For sites on the western coast of the UK, the storms typically have similar SLP characteristics between the three event types, whereas for sites on the eastern coast, the storms are more distinct.

The tracks of the storms responsible for each of the three event types are digitised at these two selected sites. These storm tracks are shown in Figure 4.9 for Devonport (Figure 4.9a–c) and Whitby (Figure 4.9d–f). The mean storm tracks are overlaid in each instance. At Devonport, the mean storm tracks are typically similar, moving in an easterly–north-easterly direction and cross over the north or just to the north of Scotland (Figure 4.9a, b, and c). The slight variation is likely due to the resolution of the average track. In contrast, at Whitby, the mean storm tracks for the high skew surge events and high river discharge events are very different. The mean storm track for the high skew surge events passes to the north of Scotland (Figure 4.9d), while the events with high river only cross central UK (Figure 4.9f), all in a west–east direction.

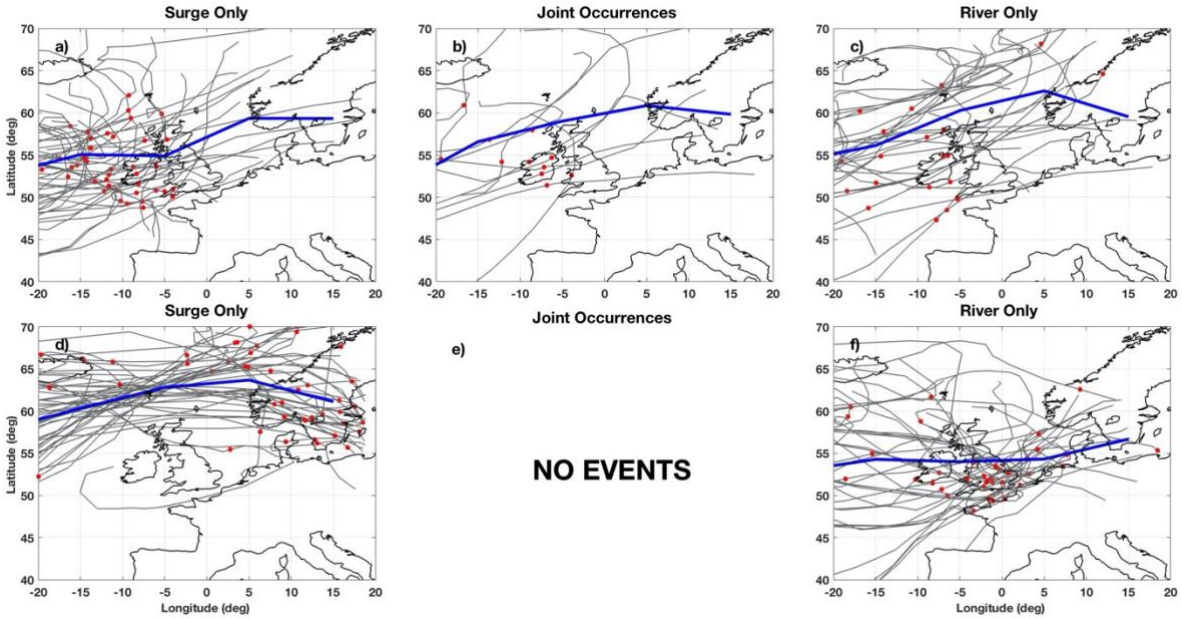

Figure 4.9: Storm tracks for Devonport [5] (a, b and c) and Whitby [30] (d, e and f) over Northern Europe. The first column (a, d) shows high skew surge only events. The second column (b, e) both high skew surge and high river discharge events. The third column (c, f) shows high river discharge only events. The blue line represents the mean storm track. Grey lines show individual storm tracks with the location of the storm at peak skew surge and/or peak river discharge shown by the red dot.

4.3.3 Localised correlations

The analysis of weather types (described in Sect. 4.2) has helped to explain national-scale spatial variations in the occurrence of compound events (i.e. the west–east difference shown in Figure 4.4), but to understand variations locally, other variables must be considered. Therefore,

how the strength and phase of dependence between skew surge and river discharge is influenced by the characteristics of the corresponding river catchments is assessed.

The three selected catchment characteristics (BFI, catchment area, and catchment elevation variation) are plotted in Figure 4.10a, b, and c, respectively. The river sites that drain onto the central southern coast typically have the greatest BFI (nearly 1, i.e. extremely porous chalk), whilst those on the north-western coast typically have the lowest (0–0.2, i.e. predominately clay soils; Figure 4.10a). Catchments are largest on the Severn River, the river Bann in Northern Ireland, and the eastern coast of Scotland, whereas smaller catchments are found in Cornwall, western Scotland, and around Weymouth (Figure 4.10b). The largest elevation variation is seen on the river Spey in Scotland, and altitude variation is low across the eastern coast of UK between Immingham and Dover (Figure 4.10c). Visually, there is no obvious strong spatial correlation be- tween any of the three catchment characteristics (Figure 10) and either the rank correlation between daily maximum skew surge and daily maximum river discharge (Figure 4.4a) or the number of joint occurrences per decade between extreme skew surge and extreme river discharge (Figure 4.4b).

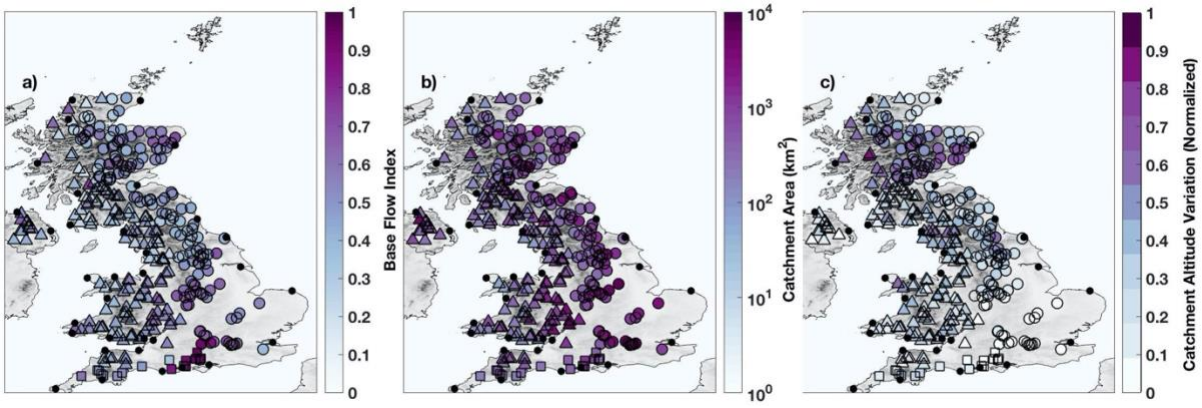

Figure 4.10: (a) Base flow index; (b) catchment area size (logged km^2); and (c) catchment altitude variation (normalised). Note that the triangles, circles and squares show the river stations that discharge onto the west, east and south coasts, respectively.

The rank correlation for daily maximum skew surge and daily maximum river discharge (at the 0-day lag) is plotted against the three catchment characteristics for each site in Figure 4.11a, b, and c. The day of maximum lag for the rank correlation is plotted against the three catchment characteristics for each site in Figure 4.11d, e, and f. Corresponding correlation coefficients (CCs) are listed in Table 4.3, first for all sites and then just the river sites closest to the 33 tide gauge sites. There is a negative correlation (CC=−0.5, significant at 95 %) between dependence and BFI. This is in line with the hypothesis that the lower the BFI of the site (e.g. the flashier

the catchment), the more likely that high skew surges will occur around the same time as high river discharge. There is a statistically significant negative correlation (CC = −0.31) between dependence and catchment area. Again, this is in line with the hypothesis that high skew surges are more likely to occur around the same time as high river discharge in small catchments. There is a weak but statistically significant positive correlation (CC = 0.16) between dependence and catchment altitude variation. Again, this is in line with the hypothesis that the steeper the catchment, the more likely that high skew surges will occur around the same time as high river discharge. The correlation is higher (CC = 0.34, significant at 95 %) for just the 33 river sites closest to each tide gauge site. The correlations between the three catchment characteristics and the day of maximum lag are not as strong (Table 4.3; Figure 4.11d, e and f). There is a weak statistically significant correlation (CC = 0.21, significant at 95 %) between the day of the maximum lag and BFI. Sites with larger BFI typically have larger positive lags. There is also a weak, statistically significant correlation (CC = 0.11, significant at 95 %) between the day of the maximum lag and catchment area. Sites with large catchment area typically have larger positive lags.

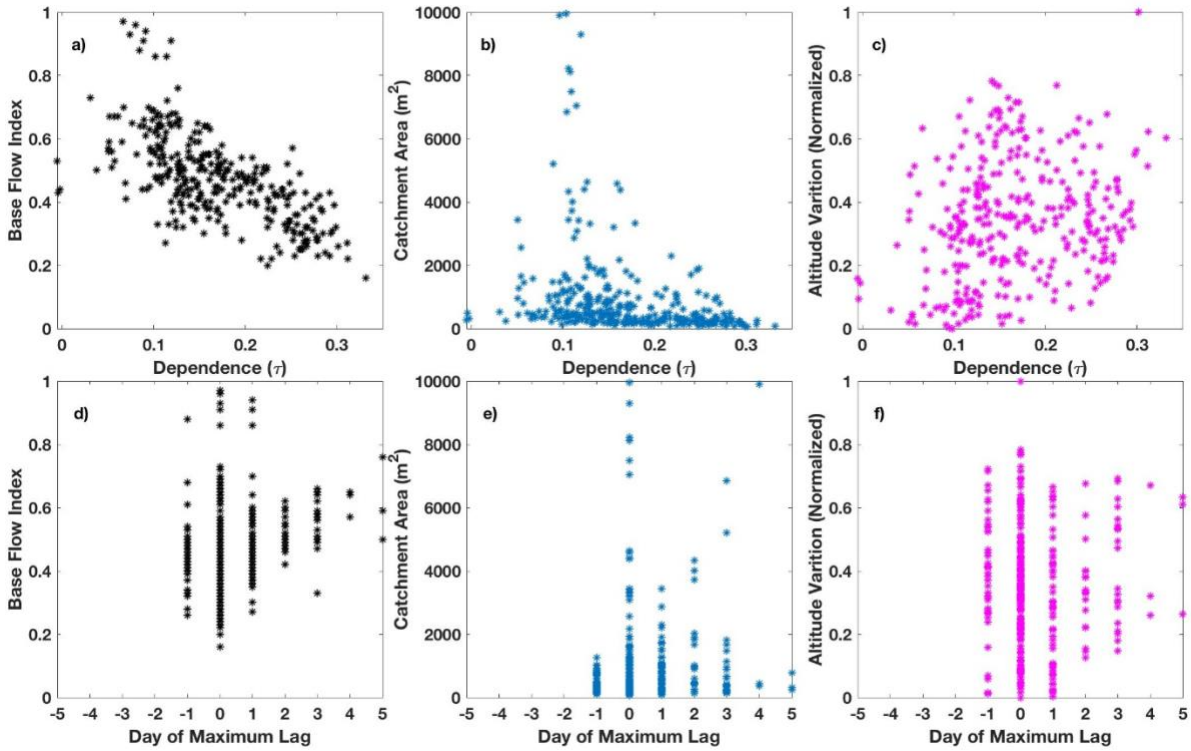

Figure 4.11: Kendall's Rank Correlation τ between daily maximum skew surge and daily maximum river discharge with: (a) base flow index; (b) catchment area size (logged km^2); (c) catchment altitude variation (normalised); and correlation of the day of lag with the largest

Kendall's Rank Correlation τ with: (d) base flow index; (e) catchment area size (logged km^2); (f) catchment altitude variation (normalised), for all sites.

Table 4.3: Correlation between catchment variables and: (i) the number of joint occurrences per decade between high skew surges and river discharge; and (ii) the lag day when there is the maximum number of joint occurrences between high skew surge and high river discharge. Bold text indicates statistical significance at a 95% confidence interval.

Catchment Variable	All Sites		Coastal Sites	
	Dependence	**Lag**	**Dependence**	**Lag**
BFI	**-0.50**	**0.21**	**-0.48**	0.17
Catchment Area Size	**-0.31**	**0.12**	**-0.33**	0.13
Altitude Variation	**0.16**	-0.032	**0.34**	0.17

4.4 Discussion

In this chapter, the potential for compound flooding arising from the joint occurrence of extreme total water level or skew surge and river discharges around the coast of UK has been assessed. Like earlier studies (i.e. Svensson and Jones, 2002, 2004; Petroliagkis et al., 2016; Paprotny et al., 2018), the joint occurrence of high skew surges and high river discharge have been identified to occur more frequently on the south-western and western coasts of the UK compared to the eastern coast. However, for the first time, it's shown that this spatial variability is driven by meteorological differences in storm characteristics. On the western coast of the UK, the storms that generate high skew surges and high river discharge are typically similar in characteristics (i.e. there is a low-pressure system to the north-west of Ireland with strong south-westerly winds affecting the south- western coast) and track across the UK on comparable path- ways. In contrast, on the eastern coast, the storms that typically generate high skew surges (i.e. when there is a low pressure over Scandinavia producing strong north-westerly winds across the North Sea) are distinct from the types of storms that tend to generate high river discharge in this area (i.e. when there is a weaker low-pressure system over central UK).

For the first time, relationships have been identified across the UK between the strength and phase of the dependence between high skew surge and high river discharge and the characteristics of the corresponding river catchments. High skew surges are found to occur

more frequently with high discharge in catchments with a lower base flow index, smaller area, and steeper elevation gradient. In catchments with a high base flow index, large area, and shallow elevation gradient, the peak river flow tends to occur several days after high skew surge. It's also found that for inland river discharge sites on the eastern coast, the maximum number of joint occurrences happens when river discharge occurs −1 days before peak skew surge. This is because the maximum storm surge in the North Sea occurs after the storm has crossed the North Sea into Scandinavia, whereas the high rainfall occurs a day earlier when the storm is centred over the UK.

The key concern for compound flooding is when estuaries or coastal regions experience both high storm surge and high river discharge around the same time (i.e. the 0-day lag), which is likely to lead to disproportionately large adverse flood consequences. Of the 33 tide gauge sites considered, dependence between high skew surge and high river discharge is at its maximum at the 0-day lag at 19 sites. At most other sites, high river discharge occurs between +1 and +5 days after peak skew surge, and therefore compound flooding is not as much of a concern. However, there are still important implications for flood management and emergency response if a large fluvial flood occurs several days after a major coastal flood, as this is likely to stretch emergency services.

The meteorological analysis undertaken indicates subtle differences in the types of storms that tend to generate compound events compared to non-compound events, particularly for sites on the western coast of the UK (see Figure 4.6). As compound events tend to exacerbate the adverse consequences of a flood, it is vital that they are forecasted accurately, and that appropriate warning is provided. Further- more, the best response to a compound event might differ from a non-compound event. Therefore, being able to accurately forecast that an event might be a compound event, as opposed to a non-compound event, is crucial. With these insights and improvement in forecast opportunities discussed below, these aspects of emergency response should be analysed in more detail.

In this study, the same daily historical weather-pattern catalogue are used as Neal et al., (2018) and Richardson et al. (2018) to calculate the modal weather pattern at each site for (1) high skew surge events only, (2) joint-occurrence events, and (3) high river discharge events only. This is done in order to briefly assess whether Coastal Decider could be expanded to give early warnings of events with the potential to generate compound flooding from both high sea level and high river discharge. Results are shown in Figure 4.12. Nearly all the events are dominated by the higher-numbered weather patterns, which tend to be the more stormy types and which

are most likely to occur in the winter. Clear distinctions are found along coastal regions. Weather pattern 30 occurs for sites along the south-western and western UK coast for each of the three types of events. This is one of the stormiest weather patterns, with a large depression situated to the north of Scotland. This causes a strong westerly flow across the UK, with frontal rainfall being particularly heavy in western parts of the UK. Weather pattern 20 is dominant along the central western coast, particularly from the Bristol Channel northwards. This weather pattern is similar to weather pat- tern 30, but with the depression centre being further north, therefore shifting the wind and rain impacts further north. Sites in Scotland typically feature weather patterns 20 (cyclonic westerly) and 21 (cyclonic south-westerly). Along the eastern coast, high skew surge and river discharge events experience different weather patterns, with pattern 14 (cyclonic northerly) generally being seen during high skew surge events compared to patterns 11 (low pressure centred over the UK), 24 (southerly tracking cyclone centred over the North Sea), and 30 (very cyclonic westerly), which are generally related to high river events. These results indicate that it may be possible to extend the forecasting capability of Coastal Decider to also include indications for the likelihood of compound events. Small-scale weather features will need to be included in the mean composites for each weather pattern (e.g. weather pattern 30, which is a very stormy cyclonic south-westerly type, will have a mean composite that is formed from many subtle variations in the overall broad- scale stormy south-westerly flow; this means that the small- scale (and perhaps rarer) features will still be represented within a broader-scale weather pattern).

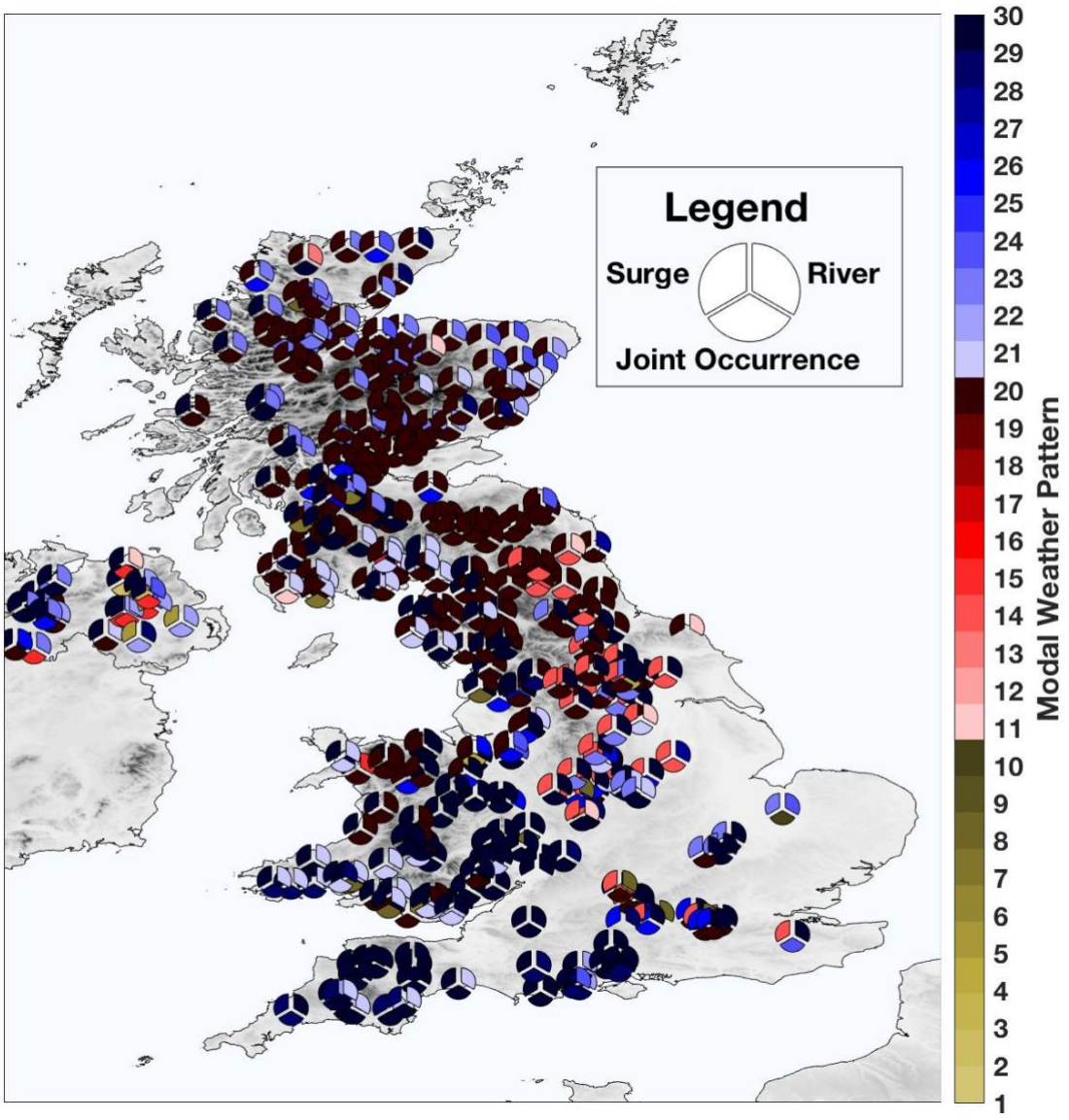

Figure 4.12: The modal weather pattern type (indicated by the colours in the legend) for extreme surge only events (top left segment), extreme river flow only events (top right segment), and extreme joint occurrence events (bottom segment) observed at the study locations.

So far, just considered high water levels which produce the potential for flooding have been considered. In periods of high runoff in the UK, such as 1998, 2000, and 2007, floods happened repetitively near the tidal limit of rivers due to tidal locking at high tide, such as the floods in Lewes in 2000 (White, 2007). However, these may not be compound events as defined here. To briefly assess the extent of flooding during compound events, the dates of joint occurrences at Devonport (which had a higher number of joint occurrences per decade) were compared with reports of coastal flooding in the SurgeWatch database (Haigh et al., 2015, 2017). SurgeWatch records the social, economic, and environmental consequences of 330 coastal floods that have

impacted the UK in the last 100 years. Of the nine joint-occurrence events when there was both high skew surge and high river discharge observed at Devonport, seven events had reports of coastal flooding. Events with significant flooding included the following: 24–25 December 1999, which caused extensive flooding in Lymington, Dorset, as discussed below, and the 14th February 2014 storm, which led to the destruction of the main railway line in Dawlish (Devon Maritime Forum, 2014), note that this event also had large waves. No flooding was reported for the Great Storm of 15–16 October 1987 (Burt & Mansfield, 1988). There was extensive wind damage to the UK during this event, but little coastal flooding because the event coincided with neap tides.

As stated earlier, compound flooding can occur not only during two (or more) extreme events but also when just one flood source is extreme (for example, extreme river discharge combines with a moderate storm surge) or when two moderate flooding sources combine to create a flood event. It should be noted that the latter two types of compound flooding involving moderate events were beyond the scope of this paper and so were not considered in the methods. These types of events are important, however, and need to be recognised in future studies into flood risk.

4.5 Conclusions

This chapter has assessed the potential for compound flooding arising from the joint occurrence of extreme total water level or skew surge and river discharges around the coast of UK. It's found that the joint occurrence of high skew surges and high river discharge occurs more frequently during the study period (15–50 years) at sites on the south-western and western coasts of the UK (between three and six joint events per decade), compared to sites along the eastern coast (between zero and one joint events per decade). For the first time, this study showed that the spatial variability in the dependence and number of joint occurrences of high skew surges and high river discharge is driven by meteorological differences in storm characteristics. On the western coast of the UK, the storms that generate high skew surges and high river discharge are typically similar in characteristics and track across the UK on comparable pathways. In contrast, on the eastern coast, the storms that typically generate high skew surges are mostly distinct from the types of storms that tend to generate high river discharge. High skew surges are found to occur more frequently with high river discharge at catchments with a lower base flow index, smaller catchment area, and steeper elevation

gradient. In catchments with a high base flow index, large catchment area, and shallow elevation gradient, the peak river flow tends to occur several days after the high skew surge. The previous lack of consideration of compound flooding means that flood risk has likely been underestimated around UK coasts, particularly along the south-western and western coasts. Furthermore, the additional damages caused due to compound events are unknown. It is therefore crucial that this be addressed in future assessments of flood risk and flood management approaches.

5. The potential for compound flooding around the UK from all flood sources.

5.1 Introduction

Relatively few studies have considered more than two sources. Key papers which have included more than two flooding sources include Hawkes (2005) who assessed: wave height and sea level; river flow and surge; rainfall and sea level and wind-sea and swell using JOIN-SEA, a joint probability calculating software. A spatial pattern was found in combinations, such as river discharge and surge, with stronger dependence found on the west coast. However, no spatially coherent pattern was found in wave height and sea level. Petrogiliakis et al. (2016) examined the dependence between three source variables: storm surge, river discharge and waves, around Europe including 10 sites around the UK. The strongest dependence was found in the southwest for all combinations. No study has considered waves coupled with river discharge or rainfall. In summary whilst compound flooding research has grown in recent years, typically, studies have only considered two of the flood sources. Those that have covered three or more (such as Hawkes, 2005) have not considered all the potential flood pair combinations (for example, waves occurring with river discharge). Finally, whilst the role the NAO on individual flooding sources has been well studied (Haylock & Goodess, 2004; P. L. Woodworth et al., 2007), no study has considered the role climate oscillations have on compound flooding.

The overall objective of this chapter is to assess the compound flood potential around the coast of the UK arising from the joint occurrence of all possible pairs of the four main flood sources. To achieves this, the sub-objectives in this study are therefore fourfold, as follows:

1. To map the spatial dependence between all possible pairs of the four main source variables around the UK coast, comparing different methods for quantifying the dependence between these two variables.
2. To investigate the meteorological conditions that drive compound and non-compound events across the UK.
3. To investigate the influence of the North Atlantic Oscillation on compound flooding; and

4. To quantify how much the return levels of the source variables are underestimated if variables are considered independent versus dependent.

The approach incorporates the four main flood source drivers (storm-tides, waves, river discharge, and surface run-off) affecting coastal regions. However, this will not account for the pluvial source directly, as pluvial flooding is a much smaller scale process. Instead, like Wahl et al. (2015), this study will use rainfall at each analysis site as a proxy for surface runoff. The influence of groundwater and subsurface contributions is not explicitly addressed, as this is only important in very localised areas (areas of outcrop chalk). Furthermore, a wave hindcast is used due to the lack of observations. There can be some limitations using nearshore data, at depth limited sites, large waves can have the same impact at the shoreline as smaller waves dues to breaking. In addition, macro tidal regions may see no impact from waves due to the low water height.

The structure of this chapter is as follows: Section 4.2 will discuss the different datasets used to describe the flood sources. Section 4.3 will describe the methodology used to answer the three sub-objectives. The results are described in Section 4.4 and discussed in Section 4.5. Finally, conclusions and future implications are examined in Section 4.6.

5.2 Methodology

The analysis was undertaken in four main stages, each addressing one of the four-chapter sub-objectives outlined above. These stages are described in turn in the sections below.

5.2.1 Data selection

From the datasets described in Sections 3.1-3.4, data were extracted at coastal sites. With the fewest sites available, the tide gauges are used as the primary site, and the nearest observation/modelled point of each of the other three datasets (wave, river and rainfall) is selected which met the follow criteria:

1. A data overlap >15 years; and
2. The selected observation/modelled points had to be hydrologically relevant to each other at each site. For example, a river gauge may be located close to two coastlines however as the river only flows out into one of these coasts, the wave node is selected from this coast. It should be noted that there may be situations where the same coastal management unit is responsible for two sets of coastline, and so riverine flooding on one coastline simultaneous

to riverine flooding on another might be relevant. This type of compound flooding is outside the scope of this study however.

The selected sites can be seen in Figure 5.2 and Table 10.1, with the number of years of overlap in each site pairings seen in Figure 5.1. Due to the above criteria, nine tide gauge sites featured no river discharge site (Dover, Newhaven, St Mary's, Port Erin, Port Ellen, Stornoway, Lerwick, Lowestoft and Harwich), and hence were removed from the analysis. Therefore, 33 sites have been considered in surge/river combination.

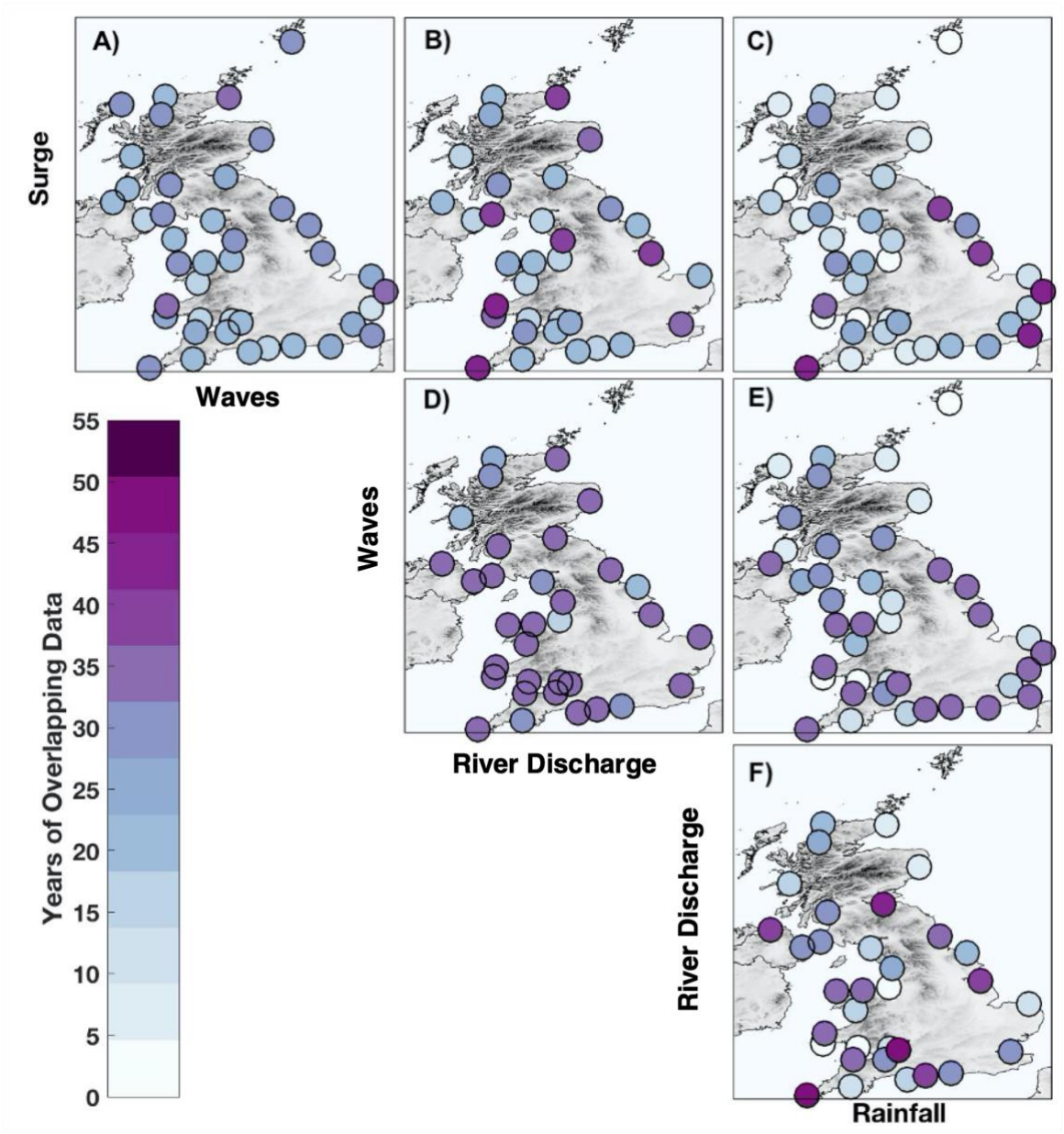

Figure 5.1: Overview of length of time series with overlapping data between each pair of source variables.

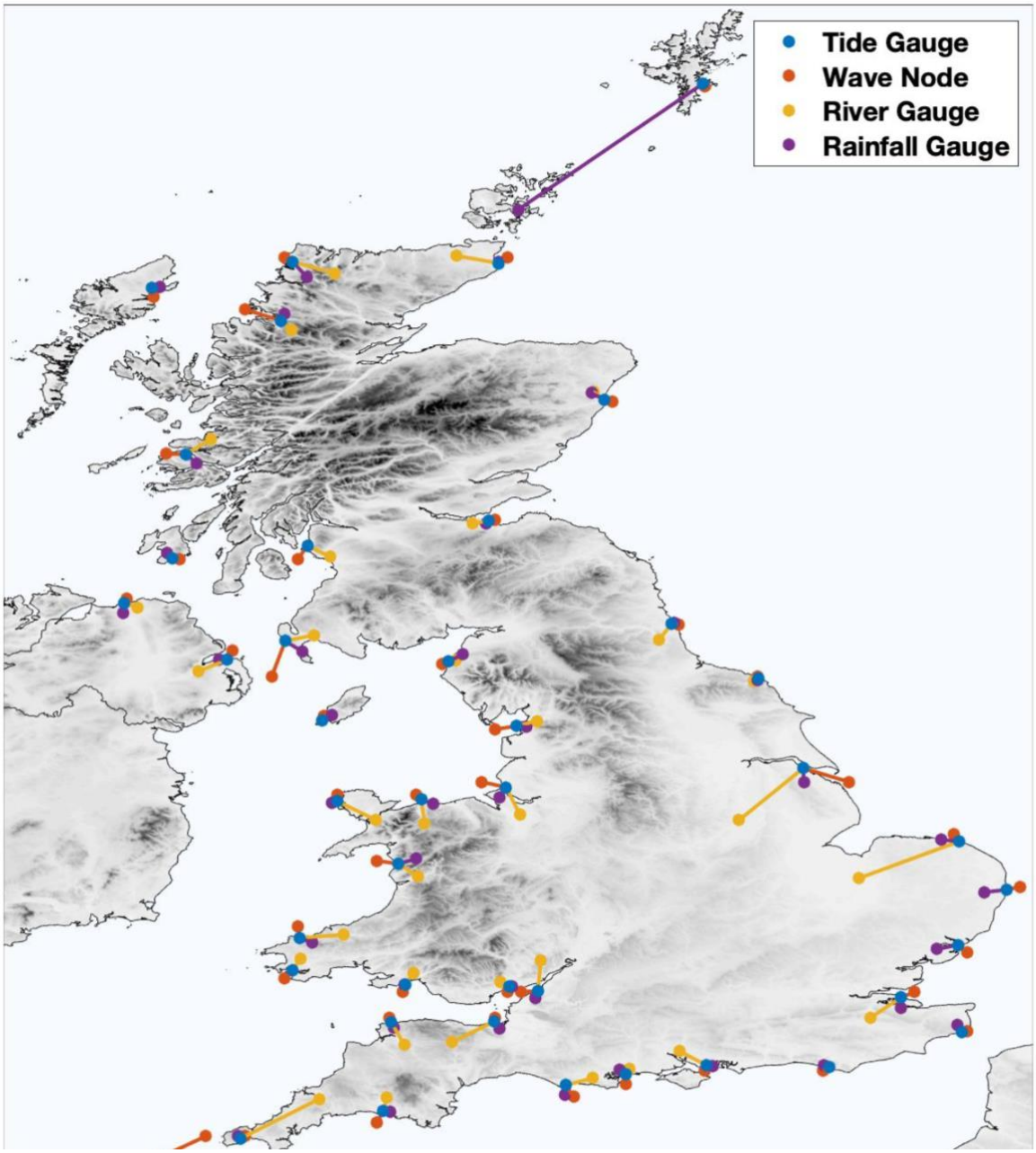

Figure 5.2: Overview of the matched tide, wave, river discharge and rainfall gauge sites employed in this study.

5.2.2 Dependence and joint occurrence

The first sub-objective is to map the spatial dependence between all possible pairs of the four main source variables around the UK coast, comparing different methods for quantifying the dependence between these two variables. For sea level, the skew surge parameter is used, See Chapter 4.2.2 for extraction methods. For waves, daily maximum heights are extracted from

the high-frequency time-series. JOIN-SEA (HR Wallingford, 1998) identified waves at high water in macrotidal regions to be the hazard (and conversely less risk posed at low water). As the tidal cycle was not considered in the wave height, this might impact the use of daily maximum significant wave height. The river discharge records were obtained in the format of daily mean values, and so no pre-processing was necessary on these records. Likewise, rainfall data were acquired as daily total accumulation, and no additional processing was required.

Extreme levels were extracted for each of the four datasets (i.e. skew surge, wave height, river discharge and rainfall) daily time series, at each site, using a peaks-over-threshold (POT) approach (Figure 5.3). The 99th percentile is used in each case, this threshold was selected based on the findings in Section 4.2.1, which used a variable threshold but the found the threshold varied by just 0.3th. A declustering algorithm is used, with a storm length of 48 hours to guarantee independent events.

Across the four source variables there are six possible pair combinations, as follows:

1. Surge and wave (referred as SUvsWA);
2. Surge and river discharge (SUvsRD);
3. Surge and rainfall (SUvsRA);
4. Wave and river discharge (WAvsRD);
5. Waves and rainfall (WAvsRA); and
6. River discharge and rainfall (RDvsRA).

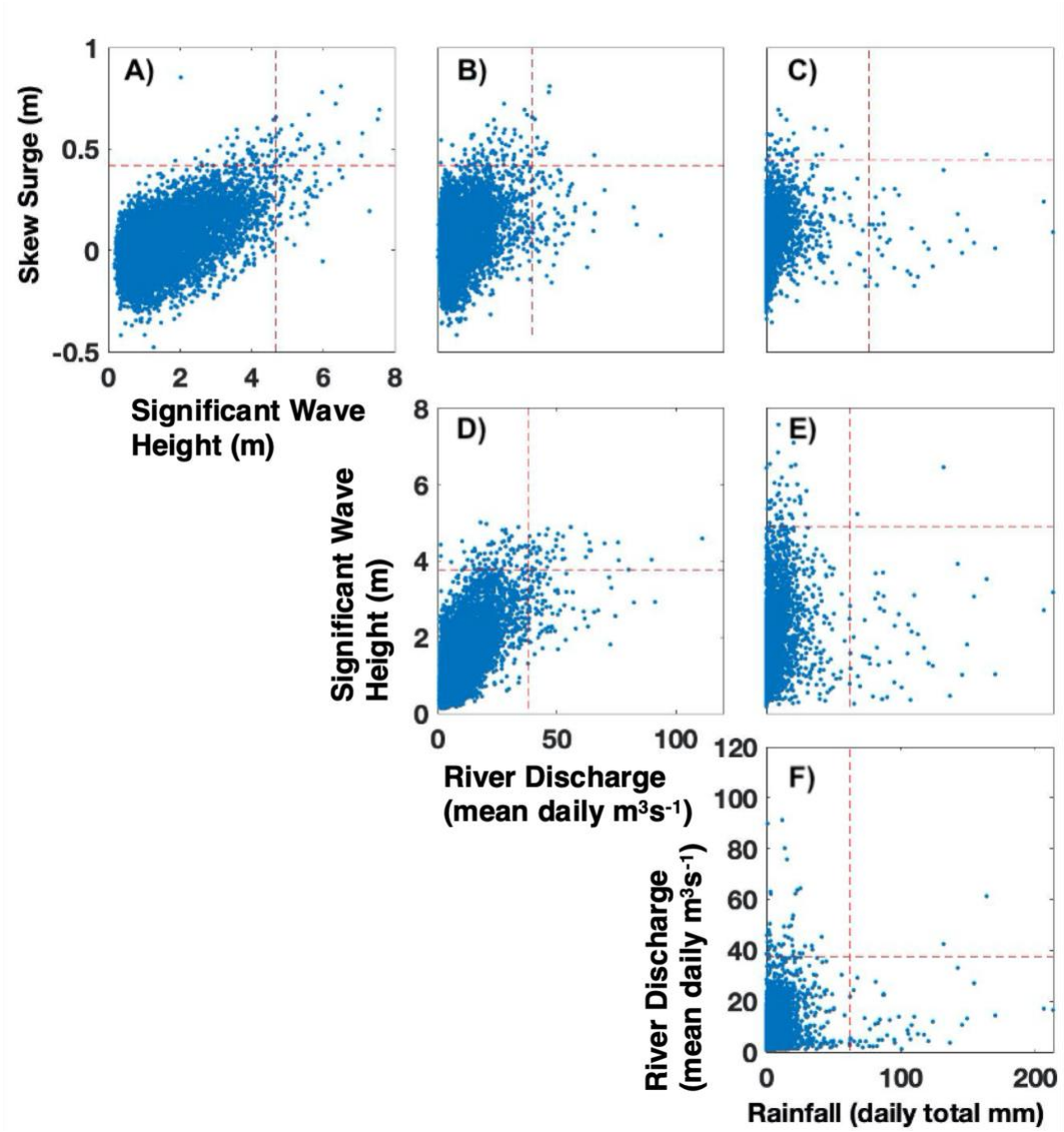

Figure 5.3: Daily maximum (a) surge vs waves, (b) surge vs river discharge, (c) surge vs rainfall, (d) wave vs river discharge, (e) wave vs rainfall, and (f) rainfall vs river discharge, for Devonport. The dotted red lines represent the 99th percentile of each variable.

Two different approaches were used to assess the relationship between the six variable pairs. The 'dependence method' and the 'joint occurrence method', full descriptions of the methodology can be seen in Sect. 4.2.2

5.2.3 Meteorological analysis

The second sub-objective is to investigate the meteorological conditions that drive compound and non-compound events across the UK. To do this, a similar approach was followed to that

previously applied in Hendry et al. (2019). For each site, fields of SLP, wind speed and PWC are extracted for the 6-hour period closest to the peak of each: (1) extreme single source event (e.g. surge only events); and (2) each joint occurrence event (e.g. SUvsWA). Full description of the methodology can be seen in Sect. 4.2.3.

5.2.4 NAO analysis

The third subobjective is to investigate the influence of the North Atlantic Oscillation on compound flooding. To achieve this, the average North Atlantic Oscillation (NAO) index of each winter season (December to March) was calculated and divided into NAO negative years (NAO<-0.5), NAO neutral (-0.5<NAO< 0.5) and NAO positive (NAO>0.5). For the date of each extreme event identified, the winter NAO index value is extracted (for both single source extreme events and joint occurring events). The modal NAO phase observed for each extreme type is calculated and compared to understand the impact of NAO on compound events.

5.2.5 Return Periods

The fourth sub-objective is to quantify how much return levels of the source variables are underestimated if the dependence between variables is not considered. To do this, first the pair of sources are assumed to be fully independent, and calculate the exceedance probability of each flood source separately, by using the POT methods as described in Section 3.1 using the 99^{th} percentile. A Generalised Pareto Distribution (GPD) is then fitted to the extracted extremes. The 10-year return levels are identified for each of the four main sources (dashed red line, Figure 5.4). The joint probability between pairs is then calculated by the probability of one flood source exceeding the 10-year level multiplied by another flood source exceeding the 10-year level (i.e. the 100-year joint event). Second, the joint return period of difference sources are calculated, by applying copular theory to stations where the dependence between variables is statistically significance ($\alpha < 0.05$). Three different copulas are applied; (1) Gumbel (upper tail dependence), (2) Frank (no tail dependence) and (3) Clayton (lower tail dependence), selected for each pair by comparing the non-parametric tail dependence coefficients. A Cramer-von-Mises test is used to assess goodness of fit (Genest et al., 2009). The copula model is then used to calculate the probability of the 10-year levels being reached

in both flood sources (thick red line in Figure 5.4). Finally, the factor difference in return period is calculated between the dependence and independence case.

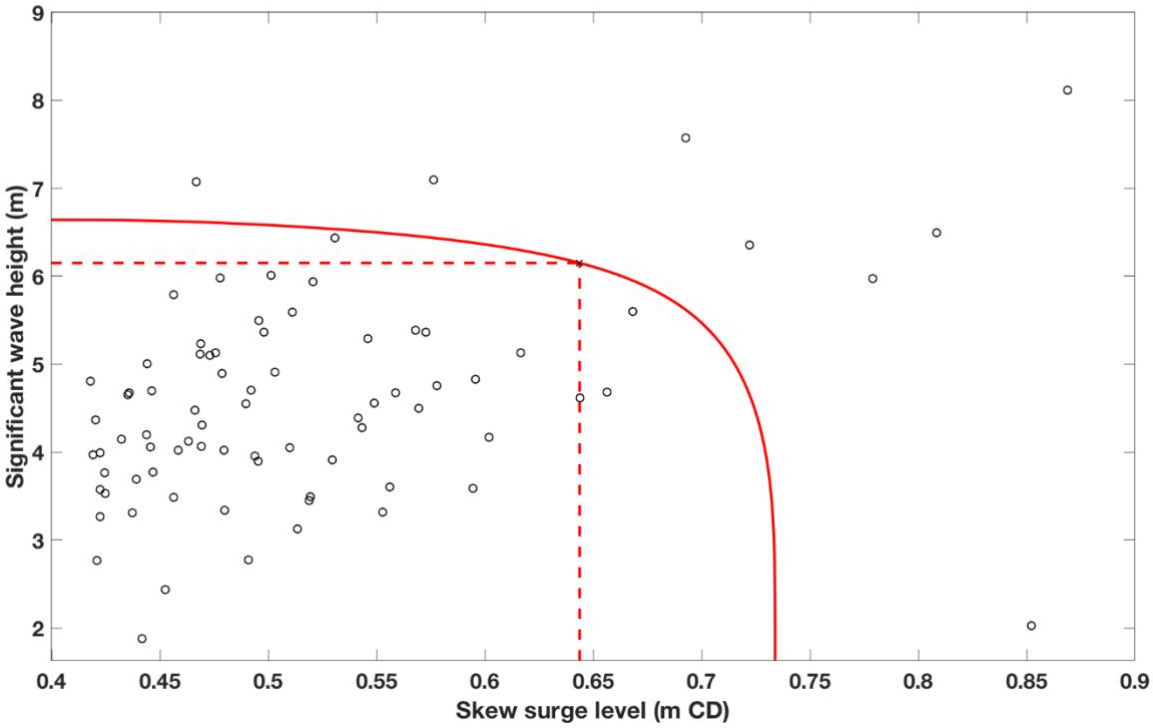

Figure 5.4: Summary of methods for return period extraction. Black circles represent the extracted extreme surge and wave datasets, the dashed red line represents the independent 10-year return levels. The solid red line represents the dependent probability of reaching those levels

5.3 Results

5.3.1 Dependence and Joint Occurrences

Two methods are used to assess the dependence between each of the six pairs of variables, across the 33 sites. The results of the first method, the dependence method, are shown in Figure 5.5; only sites with statistically significant (at 95% confidence) are shown. For each of the six pairs of variables, the dependence at 0-day lag shows a clear spatial pattern, with generally greater dependence between all the six pairs of variables at sites on the west coast of the UK, compared to the east. The strongest dependence is found between WAvsRD and WAvsRA,

particularly for sites in the southwest, with sites having values of 0.35-0.5, whilst east coast sites typically have dependence values of 0.05-0.2.

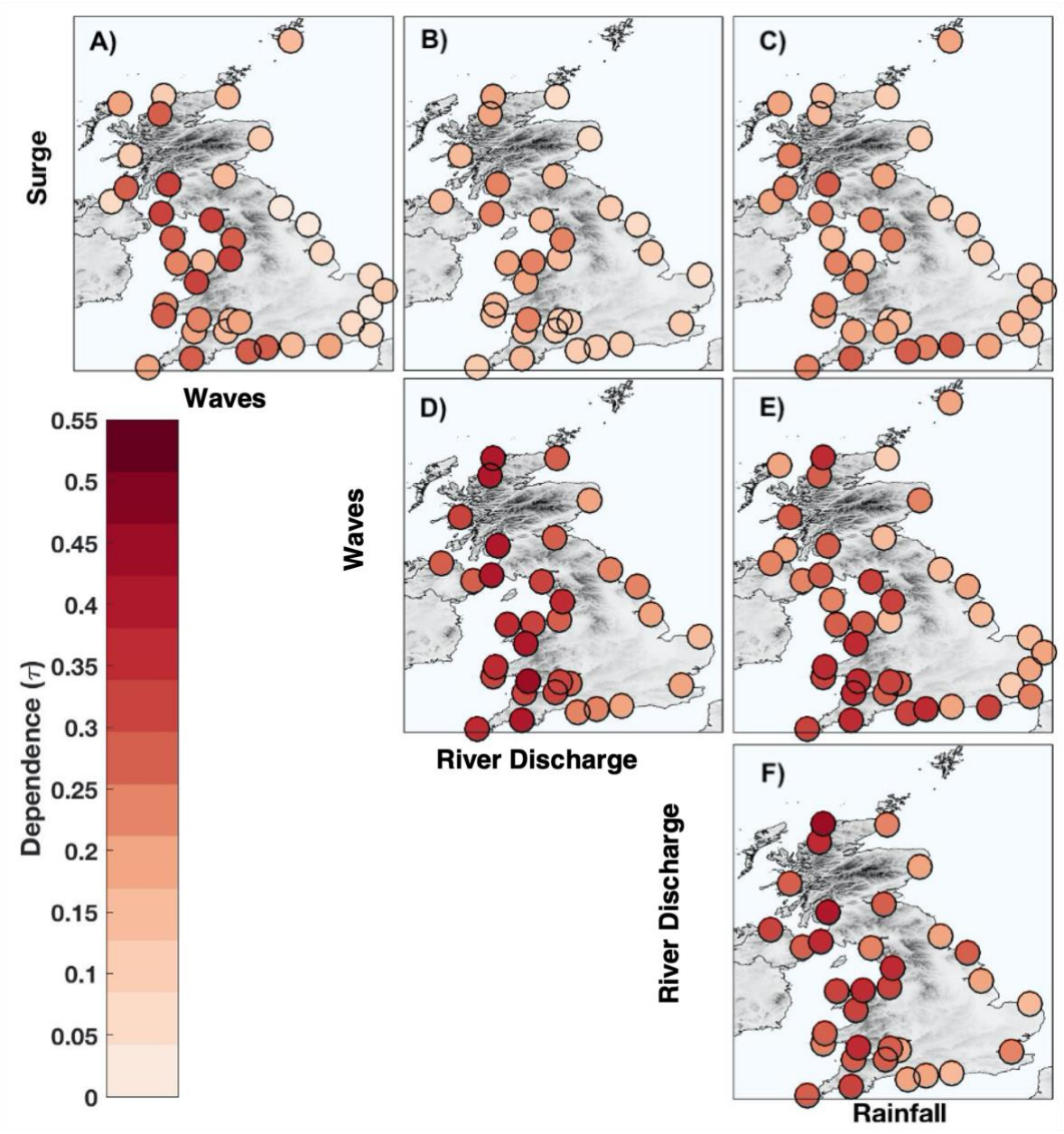

Figure 5.5: The dependence (Kendall's Tau) between each of the source variable pairs.

The results of the second method, the joint occurrence method, are shown in Figure 5.6. The greatest number of joint occurrences is found between surge and wave (Figure 5.6a), with a maximum of 17 joint occurrences per decade being seen at Liverpool. There's also a clear split between west and east coast sites, with sites along the west coast (Portsmouth to Kinlochbervie) experiencing 6-17 events per decade, compared to east coast sites (Wick to Newhaven), which

experienced 0-8 events per decade. The 5 remaining source pairs have far fewer joint occurrences. WAvsRD (Figure 5.6d) contains the next greatest number of joint occurrences per decade, particularly in the south west, with Devonport experiencing around 9 events per decade. Sites from Dover clockwise around to North Shields mostly feature 3-7 events per decade. East coast sites Whitby, Immingham, and Cromer feature no joint occurrences over their data lengths. SUvsRD (Figure 5.6b) experiences a similar west/east spatial pattern to WAvsRD, with the greatest number of joint occurrences being found on the southwest coast, with the greatest number of joint occurrences at Bournemouth (7 events per decade). The spatial pattern varies slight from WAvsRD, with northeast sites experiencing far fewer events (all but one site had 1 or 0 events per decade). RDvsRA (Figure 5.6f) exhibits a different spatial pattern compared to any of the other flood pair combinations. The most joint occurrences are found at sites in Northern Ireland (9 events per decade), the north of England and south of Scotland (3-4 events per decade). Sites in the north of Scotland and south of England have far lower number of joint occurrences (0 – 3 events per decade). SUvsRA (Figure 5.6c) and WAvsRA (Figure 5.6e) both feature relatively low numbers of joint occurrences (<3 events per decade) across all sites around the UK, with 25 and 18 sites showing zero joint occurrences respectively. No discernible national scale spatial pattern is evident.

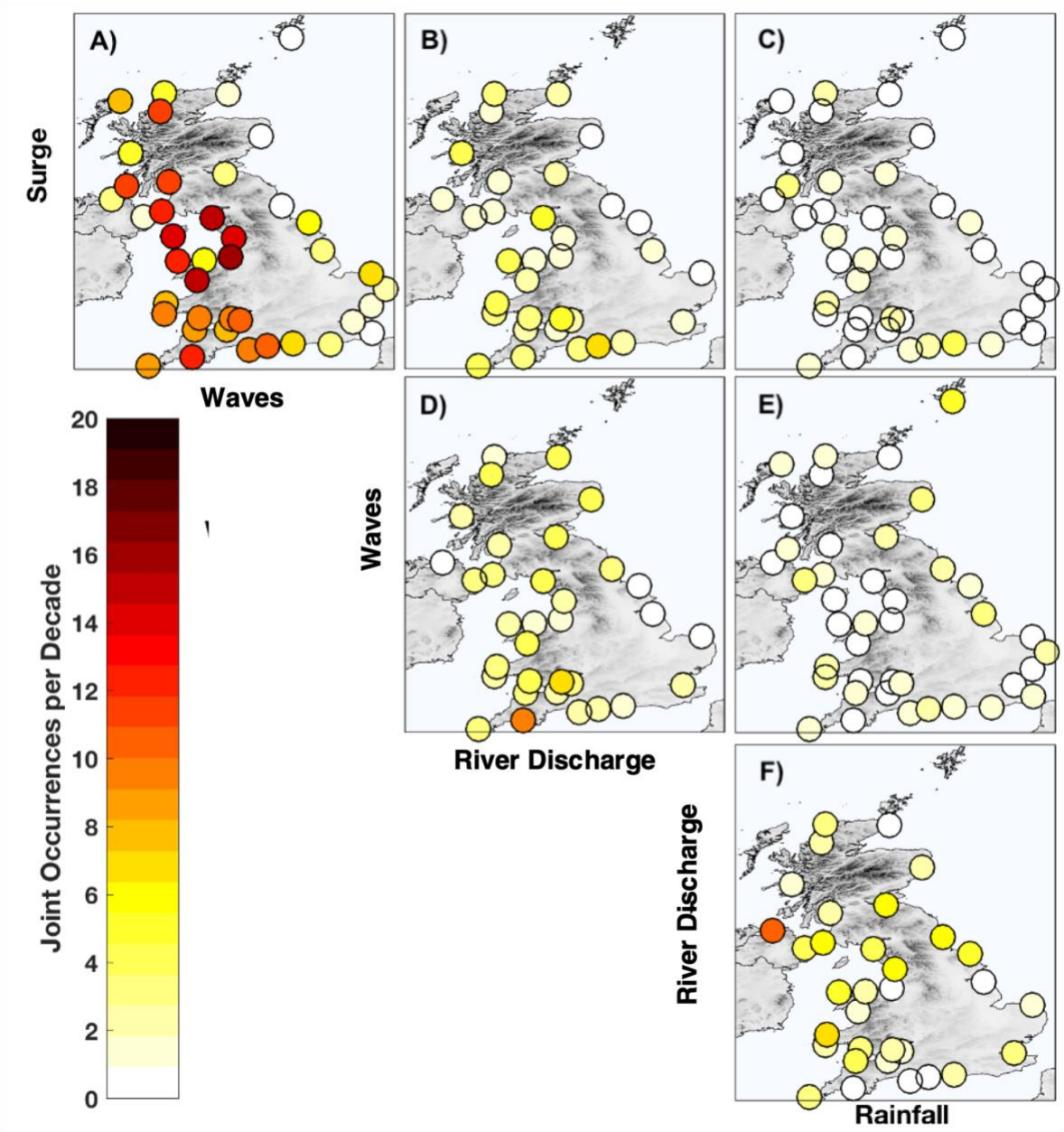

Figure 5.6: The joint occurrence per decade for each source variable pair.

The dependence is also calculated between each of the six pairs of variables using time lags from −5 to +5 days. The day when there is the maximum dependence between pairs of variables is shown in Figure 5.7 for all sites. No clear spatial pattern is evident for the six pair combinations. Along the west coast, SUvsWA (Figure 5.7a) for example, experiences the greatest dependence on day 0 or when waves occurred 1 day after the surge, whilst for sites in the southeast (Southampton to Harwich) the greatest dependence is found when waves occur 1 day before the surge. For sites on the east coast (Lowestoft to North Shields) the greatest dependence is found when waves occur 1 day prior to the surge. A distinct west/east difference is evident for SUvsRA (Figure 5.7c), with sites Wick to Portsmouth along the east and south

coast all having the greatest dependence when the surge occurred the same day as rainfall. For sites on the west coast the greatest dependence is when rainfall occurred a day after the surge. SUvsRD (Figure 5.7b) does not feature such a clear spatial pattern, although 40% of sites along the south and west coasts also have a maximum dependence when river discharge occurs 1-3 days after the surge. For RDvsRA (Figure 5.7f), most sites have largest dependence at 0-day lag. However, 8 of the sites experience maximum dependence when rainfall occurs before river discharge. There is no clear spatial pattern however and is mostly likely due to the local river's response time to rainfall.

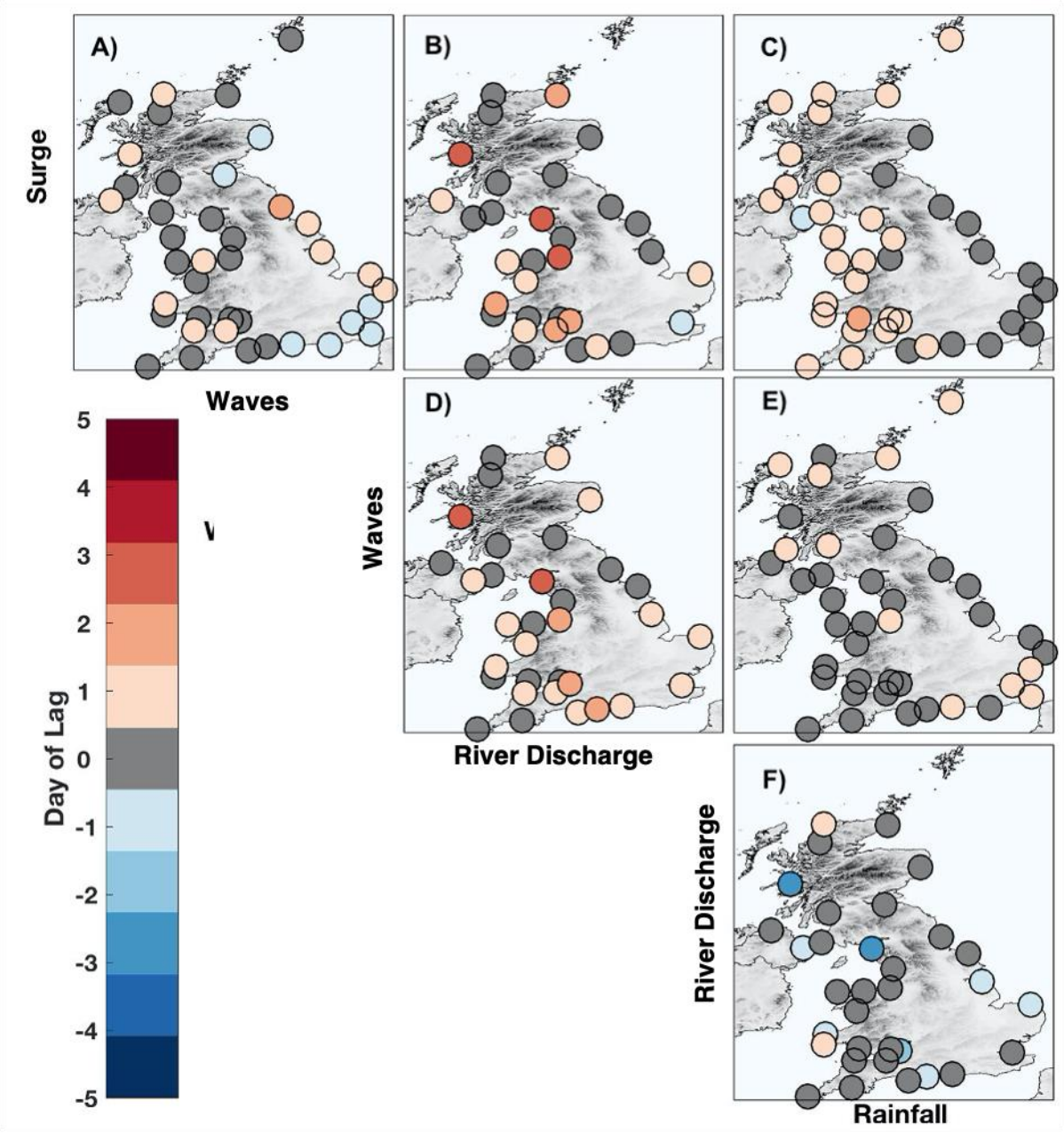

Figure 5.7: The lag day of maximum dependence between each pair of source variables. (a) surge vs waves; (b) surge vs river discharge; (c) surge vs rainfall; (d) waves vs river discharge;

(e) waves vs rainfall, and (f) river discharge vs rainfall. The flood source variables labelled on the x axis is lagged ±5 days around the y axis flood source variable. For example, (a) is showing the peak dependence when waves are lagged ±5 days after the skew surge.

5.3.2 Meteorological Analysis

Next, the meteorological conditions that drive compound (i.e., joint occurrence of source pairs) and non-compound events (i.e. single source events only) events across the UK are investigated. To illustrate the results of this component, two contrasting sites are focused on: Devonport on the UK south-west coast, which has high dependence and joint occurrences across all flood source pairs; and Cromer, on the UK eastern coast, which has low dependence and joint occurrences between flood source pairs.

Composite plots of wind speed, PWC and SLP pressure are shown in Figure 5.8 and Figure 5.9 at Devonport, for the four single source events and then for the six pairs of joint event types, respectively. For the single source extreme events at Devonport (Figure 5.8), all events featured a depression situated in the North Atlantic. For surge and wave events the depression is located northwest of Ireland (~55N 11W), whilst for river and rainfall events the depression is positioned southwest of Iceland (~ 60N 25W). The depression is weaker for rainfall events, compared to the other three source events. All event types featured a band of rainfall running along the isobars southeast of the low. The events differed in wind strength, with far stronger winds (up to 20m/s) being seen for the surge and wave events over Devonport and in the western English Channel, whilst river and rainfall events had lower wind speeds (15m/s for river events, 5-10/s for rainfall). For the joint occurrence events at Devonport (Figure 5.8), SUvsWA, SUvsRD, WAvsRD and WAvsRA events all feature similar weather pattern types compared to the single source events; with a low-pressure systems situation over the North Atlantic and the strong, south-westerly winds funnelling up the western English Channel. Synoptic weather patterns during WAvsRA events differs slightly, with significantly more PWC over the entire British Isles, rather than the band of PWC seen in the SUvsWA, SUvsRD and WAvsRD event (however only one joint event is observed). RDvsRA events features a depression further west (~60N 35W) than for the other joint occurrence or single event. The band of PWC features over just the southwest of the UK with less intense rainfall.

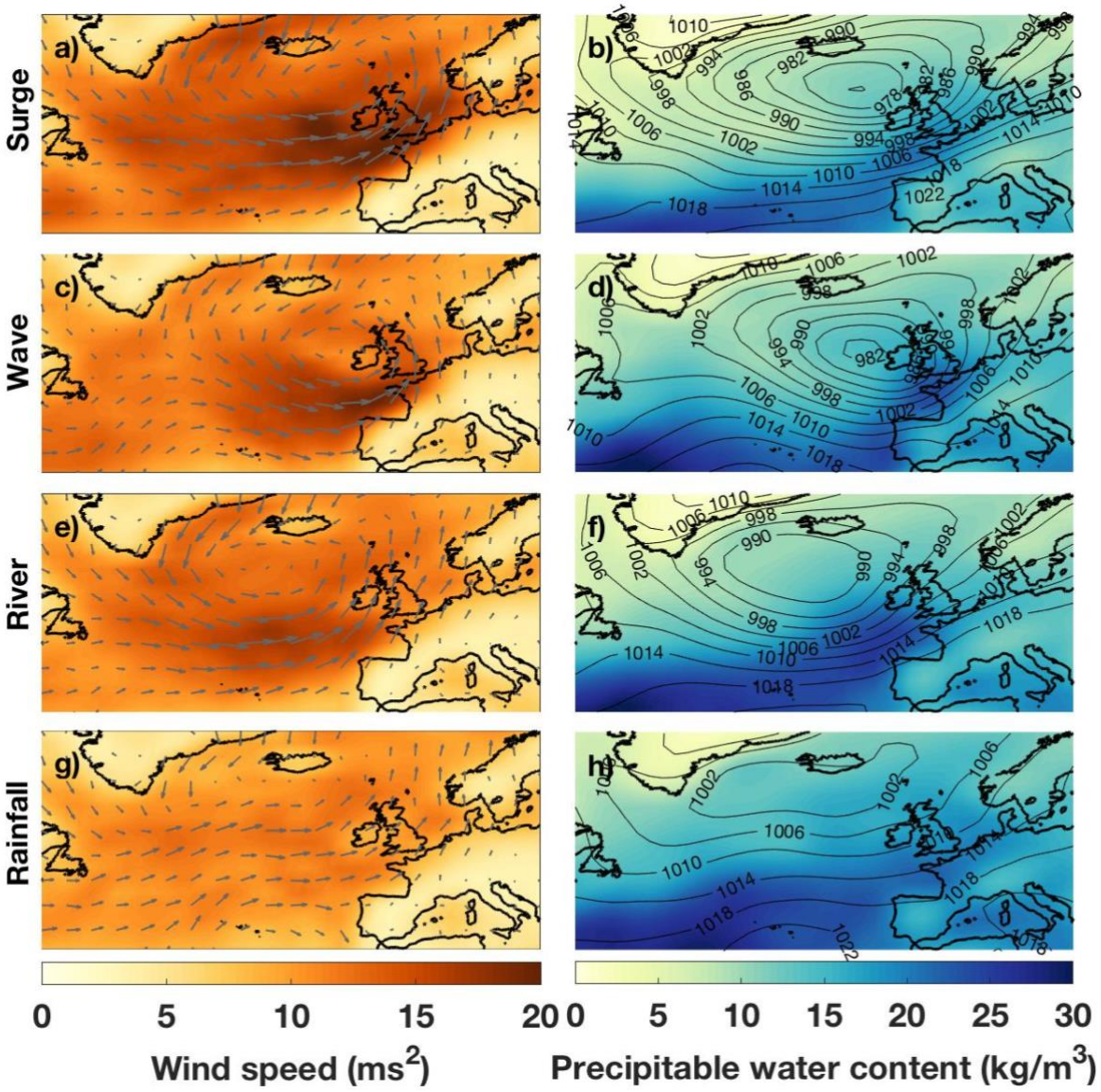

Figure 5.8: Meteorology conditions for Devonport [Site 5]: (a, c, e, g) wind speed (m s^{-1}) and direction (grey arrows), (b, d ,f, h) precipitable water content (kgm^{-2}) and sea-level pressure contours (mbar) during (a, b) extreme skew surge events, (c, d) extreme wave events, (e, f) extreme river discharge events, (g, h) extreme rainfall events.

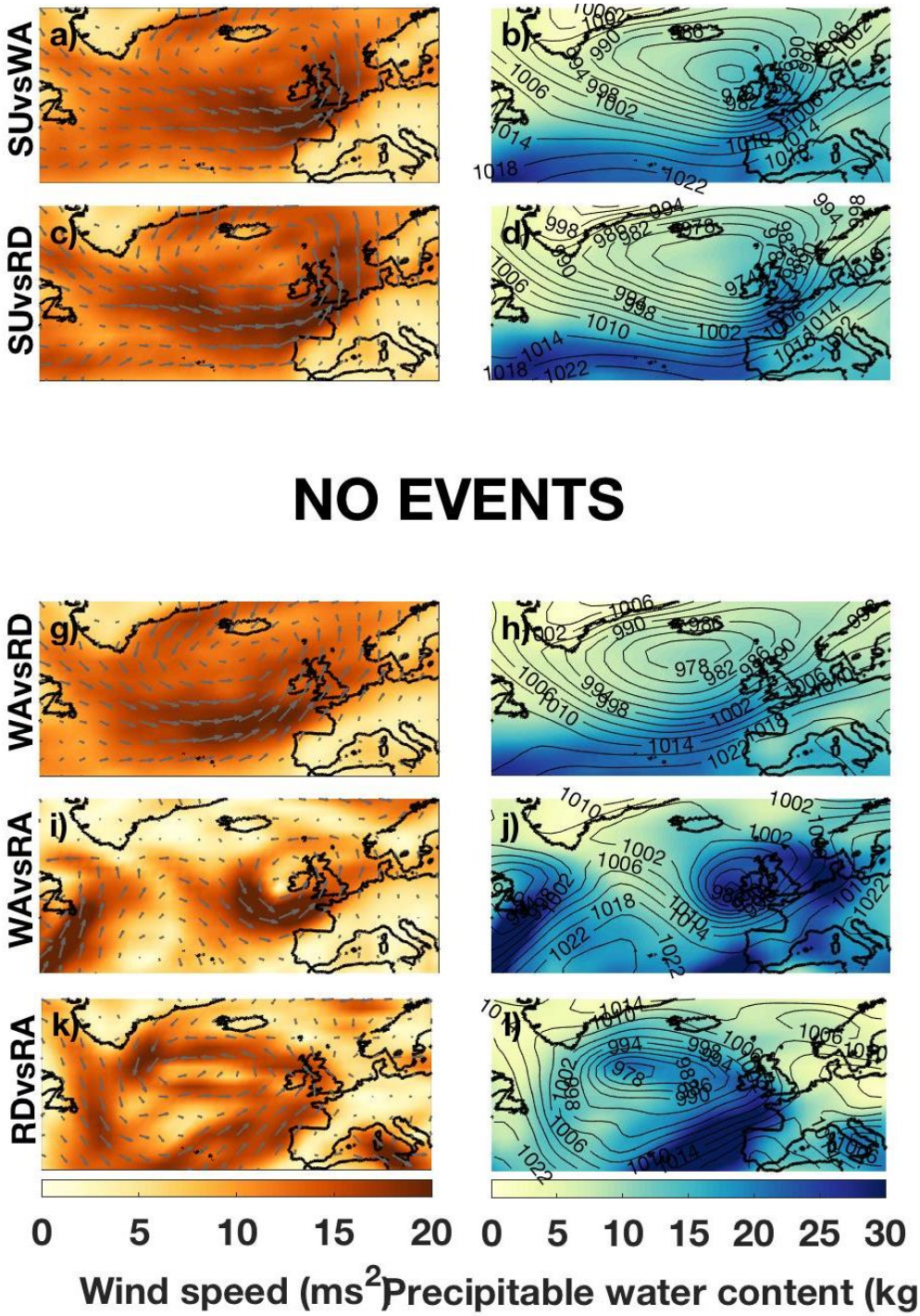

Figure 5.9: Meteorology conditions for Devonport joint extreme occurrences [Site 5]: (a, c, e, g) wind speed (m s^{-1}) and direction (grey arrows), (b, d ,f, h) precipitable water content (kgm^{-2}) and sea-level pressure contours (mbar) during (a, b) skew surge vs wave, (c, d) skew surge vs river discharge, (e, f) skew surge vs rainfall, (g, h) wave vs river discharge, (i, j) wave vs rainfall, (k, k) river discharge vs rainfall.

Composite plots of wind speed, PWC and SLP pressure are shown in Figure 5.10 Figure 5.11 at Cromer, for the four single source events and then for the six pairs of joint event types, respectively. The synoptic weather patterns for the single source events at Cromer (Figure 5.10) differ significantly from each other. Surge and wave extreme events feature a depression over Scandinavia (~65N 15W), with strong northerly winds funnelling down the North Sea and low PWC levels over Cromer. Extreme river events feature a low over the North Atlantic, with weak winds. Rainfall events on the other hand, have a far less defined weather pattern, with high PWC levels across the entire British Isles and low winds. It should be noted, Rainfall events experience a higher standard deviation than the other flood sources (6.3 in PWC compared to 5.4 in surge, the next highest), suggesting more variable conditions. The meteorological conditions of joint occurrence events at Cromer are seen in Figure 5.11. In contrast to Devonport, only SUvsWA (Figure 5.11a) and RDvsRA (Figure 5.11k) features the same weather pattern as it's single sources. All other combinations bear little resemblance to both sources, for example WAvsRD features a low depression over. Either no events or just one event were seen in Cromer for SUvsRD, SUvsRA or WAvsRA pairs.

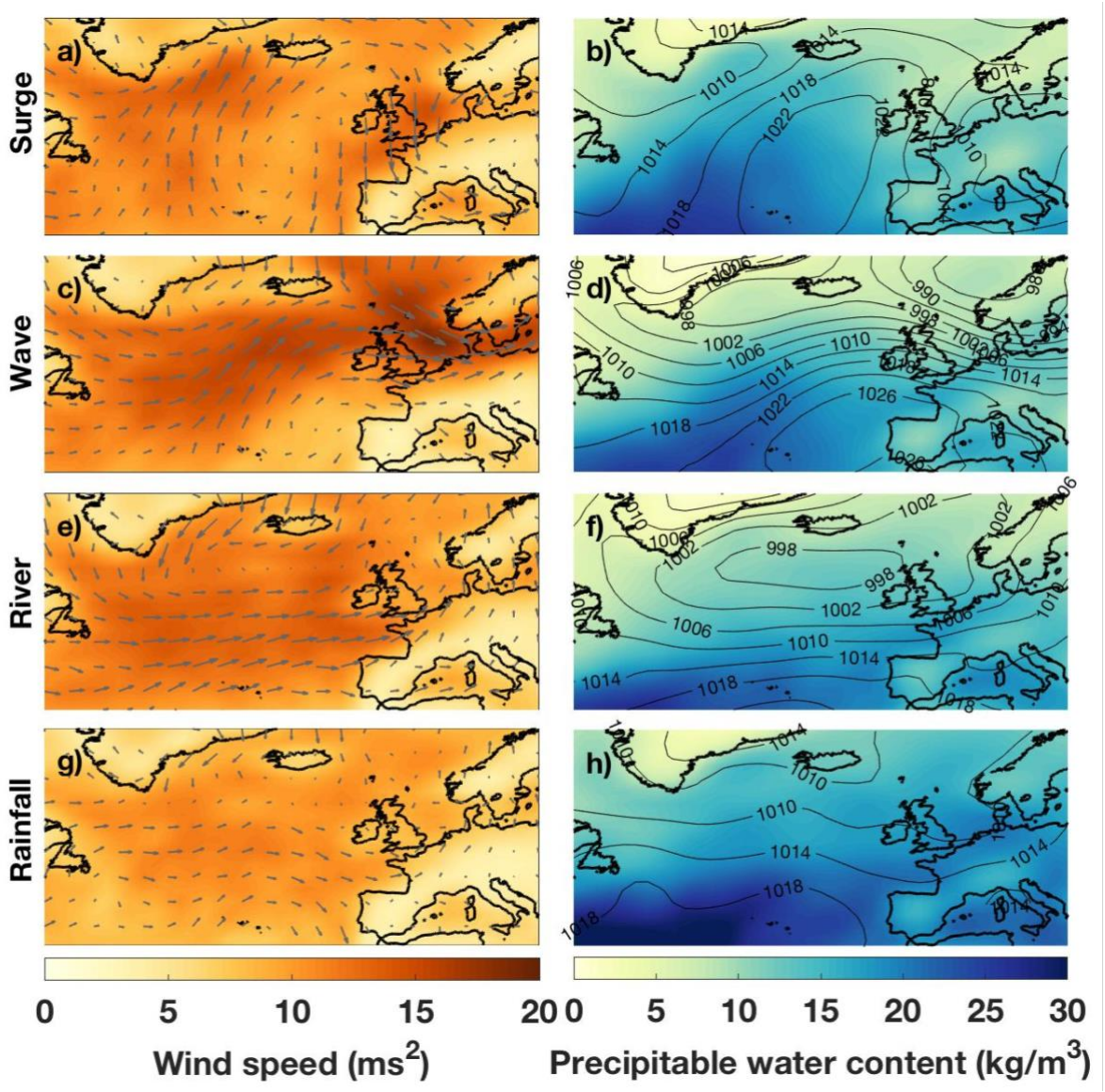

Figure 5.10: Meteorology conditions for Cromer [Site 38]: (a, c, e, g) wind speed (m s^{-1}) and direction (grey arrows), (b, d ,f, h) precipitable water content (kgm^{-2}) and sea-level pressure contours (mbar) during (a, b) extreme skew surge events, (c, d) extreme wave events, (e, f) extreme river discharge events, (g, h) extreme rainfall events.

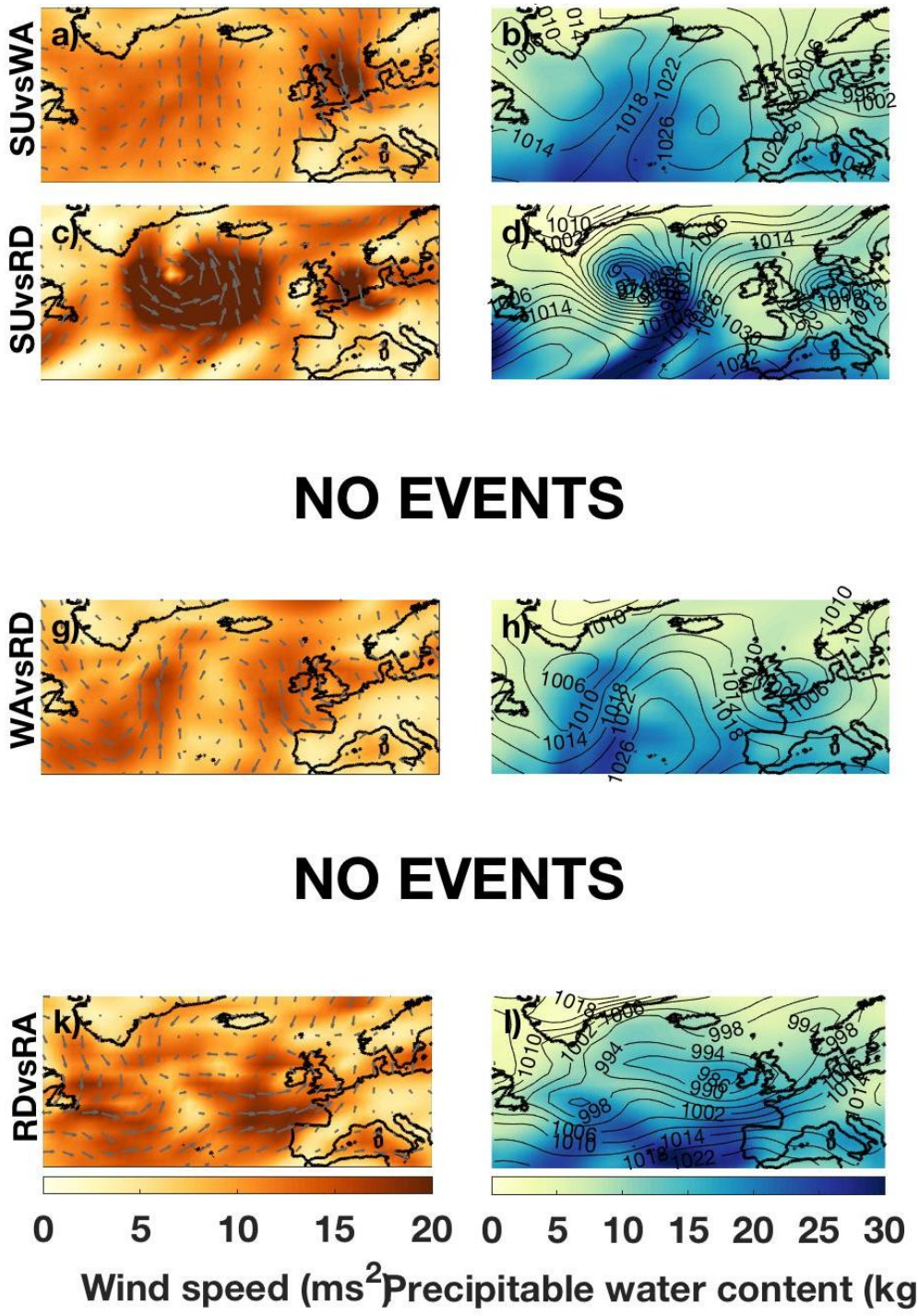

Figure 5.11: Meteorology conditions for Cromer joint extreme occurrences [Site 38]: (a, c, e, g) wind speed (m s^{-1}) and direction (grey arrows), and (b, d ,f, h) precipitable water content (kgm^{-2}) and sea-level pressure contours (mbar) during (a, b) skew surge vs wave, (c, d) skew surge vs river discharge, (e, f) skew surge vs rainfall, (g, h) wave vs river discharge, (i, j) wave vs rainfall, (k, k) river discharge vs rainfall.

5.3.3 NAO Analysis

The NAO index value was identified for each of the compound (i.e. joint occurrence of source pairs) and non-compound events (i.e. single source events only) to gauge the impact of the NAO on the weather patterns leading to compound flooding. The same two contrasting sites (Devonport in the southwest and Cromer in the east) are used. At Devonport (Table 5.1), surge, wave and river events were found to occur most often (66.6%, 44.5% and 55.5% respectively) during strong positive winter NAO years, whilst rainfall events tended to occur during weak NAO years (62.9% of events). For compound events, SUvsWA, WAvsRD and WAvsRA occurred on strong positive winter NAO years (50%, 57.6% and 66.6% respectively) whilst SUvsRD events typically occurred in weak NAO winters (69.2%).

Table 5.1: The number of single source and joint occurrence extreme events (percentage in brackets) which fall under a negative winter NAO (wNAO <-0.5); a weak winter NAO (-0.5<wNAO<0.5) and positive winter NAO (wNAO>0.5) for Devonport [Site 5].

Extreme flood source event	Negative winter NAO (wNAO <-0.5)	Weak Winter NAO (-0.5<wNAO<0.5)	Positive winter NAO (wNAO>0.5)
Storm surge	3 (7.7%)	10 (25.6%)	**26 (66.6%)**
Significant wave height	11 (24.4%)	14 (31.1%)	**20 (44.5%)**
River discharge	9 (12.5%)	23 (31.9%)	**40 (55.5%)**
Rainfall	0	**22 (62.9%)**	13 (37.1%)
Surge vs wave height	6 (17.6)	11 (32.4%)	**17 (50%)**
Surge vs river discharge	1 (7.7%)	**9 (69.2%)**	3 (23.1%)
Surge vs rainfall	No events		
Wave height vs river discharge	4 (12.1%)	10 (30.3%)	**19 (57.6%)**
Wave height vs rainfall	1 (33.3%)	0	**2 (66.6%)**
River discharge vs rainfall	1 (33.3.%)	0	**2 (66.6%)**

Cromer, on the other hand (Table 5.2), experienced strong positive NAO's for the majority of surge and wave events (45.7% and 72.2% respectively) whilst river and rainfall events were typically weak events (51.3% and 53.2% respectively). For compound events, 52% of SUvsWA events are found to occur in strong positive winter NAO years, whilst SUvsRD was mostly during weak NAO years (66.6%). the other compound flood pairs featured too few events to draw conclusions.

Table 5.2: The number of single source and joint occurrence extreme events (percentage in brackets) which fall under a negative winter NAO (wNAO <-0.5); a weak winter NAO (-0.5<wNAO<0.5) and positive winter NAO (wNAO>0.5) for Cromer [Site 38].

Extreme flood source event	Negative winter NAO (wNAO <-0.5)	Weak Winter NAO (-0.5<wNAO<0.5)	Positive winter NAO (wNAO>0.5)
Storm surge	6 (8.6%)	**32 (45.7%)**	**32 (45.7%)**
Significant wave height	4 (5.6%)	16 (22.2%)	**52 (72.2%)**
River discharge	17 (23.0%)	**38 (51.3%)**	19 (25.7%)
Rainfall	2 (4.3%)	**25 (53.2%)**	20 (42.5%)
Surge vs wave height	1 (5.3%)	8 (42.1%)	**10 (52.6%)**
Surge vs river discharge	0	0	**1 (100%)**
Surge vs rainfall	No events		
Wave height vs river discharge	0	**2 (66.6%)**	1 %33.3%)
Wave height vs rainfall	No events		
River discharge vs rainfall	0	1	**1 (100%)**

.

5.3.4 Return Periods

Finally, how much return levels of the source variables are underestimated if the dependence between variables is not considered, is investigated. For each of the six source pairings, the return period factor increases when dependence between variables is accounted (as shown in Figure 5.12). The spatial patterns in results match closely those for dependence shown in Figure 5.5). The greatest increase in return period is found for sites on the west coast in all flood pair combinations. The greatest spatial variability is found in SUvsWA (Figure 5.12a). Sites on the north west coast (e.g., Liverpool, Heysham and Workington) increase 4-5 times when assuming independence compared to accounting for dependence between source pairs. In comparison, sites on the east coast (e.g., Immingham, Whitby and North Shields) have a probability increase of just 0.5-2 times. The greatest magnitude of probability increase is found for WAvsRD (Figure 5.12d), where sites across the entire west coast from Newlyn in the south to Kinlochbervie in North Scotland see a factor increase in probability of 5-6 times. WAvsRA experiences similar probability increase of up to 5-6 times, however this is primarily in Wales and the southwest. RAvsRD (Figure 5.12f), has the least distinct spatial pattern with increase of up to 5 times being found on both the east and west coasts. SUvsRD and SUvsRA (Figure 5.12b and c) experience the lowest increases in probability of around 3-4 times on the west coast and 2-3 times on the east coast.

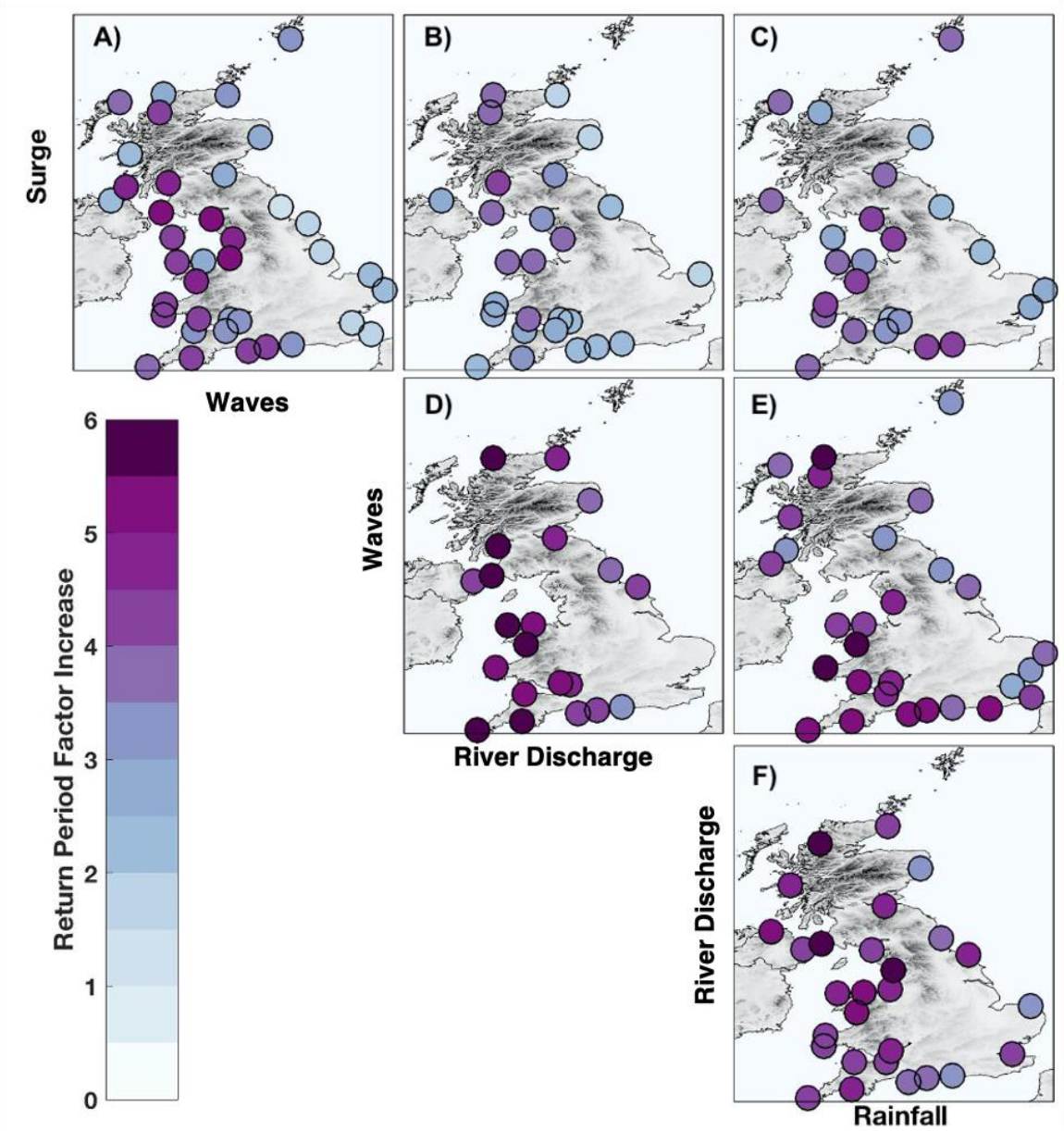

Figure 5.12: Factor decrease in return period when flood source variables are considered independent (using a GEV model) to dependent (using a copula model).

5.4 Discussion

This chapter has assessed the potential for compound flooding arising from the main flood source combinations around the coast of the UK. This has been achieved by analysing the joint occurrence of extreme events, and the dependency between the flood pair combinations. For all combinations a spatial pattern is seen in the dependence, with sites along the west and south

west coasts having greater dependence between source variables compared to the east. The same spatial pattern is found for most pairs in joint occurrences, however for RDvsRA and WAvsRA, no definitive pattern is seen. This confirms the spatial pattern found in previous studies (Hawkes, 2005; Petroliagkis et al., 2016).

For the first time the types of weather patterns which can lead to different types of compound events are identified. On the west coast, it's shown that surge, wave and riverine flooding (Figure 5.8a, c and e) are all generated by similar weather patterns.

Extreme rainfall events (Figure 5.8g) typically feature reduced wind strength, this suggest why extreme rainfall events do not occur in compound events as frequently, as strong winds are not present to generate surge and waves (Figure 5.9c, e and f). On the other hand, the extremes on the east coast typically experience different weather patterns. Surge and wave extremes (Figure 5.11a and c) typically feature a low over Scandinavia, whilst river and rainfall events are far weaker systems with a lower further west over the UK or Atlantic.

The NAO is the primary mode of atmospheric variability in the North Atlantic, expressed as the difference in mean sea level pressure between Iceland and the Azores. An increase in the winter NAO typically results in a greater number of storms crossing northern Europe at higher latitudes, resulting in increased surge and wave activity in the southern North Sea. A reduction in NAO leads to fewer and weaker storms which cross at lower latitudes (Hurrell, 1995; Jones et al., 1997). Haylock and Goodess (2004) analysed the correlation between the NAO and the number of days with extreme rainfall in Europe. In the southwest UK, they found weak positive correlation, matching to the results for Devonport, whilst no correlation was found on the east coast of the UK, agreeing with the results for Cromer. This is consistent with the results presented here. For example, at Devonport, the majority of surge, wave and river extreme events occur during positive winter NAO phases. Precipitation events were found to be associated with weaker NAO winters at both sites.

The joint probability of extreme flood source pairs is calculated in two ways, when sources are considered independent of each other and dependent on each other. The change in joint probability is then calculated (Figure 5.12). The probability of both flood sources reaching a 10-year level is found to increase when sources were considered dependent, compared to independent, across all sites and for all flood combinations. The east/west spatial variability is also seen in all pairs of source variables, similarly to spatial variations in dependence (Figure 5.5). When looking at the relationship between surge and waves globally, Marcos et al (2019)

found a far greater ratio of increase in return periods (~15 times higher when considering independent vs dependent compared to 2-3 in Figure 5.12) on the south east UK coast. However, they used a 50-year return period, which may show a greater change between independent and dependent relationships.

This study has been a broad analysis of compound flooding in the UK from the main sources of flooding, to identify national scale spatial patterns, therefore only the primary variable was assessed. However, each flood source can be impacted by a range of variables (Figure 2.1). For example, daily total rainfall is used as proxy for pluvial flooding, based on the nearest rain gauge to each tide gauge, however surface run off is affected by a range of variables, including rainfall duration, surface type (i.e. proportion of tarmacked and paved surfaces), ground saturation, ground composition, urban drainage systems (Gaitan et al., 2016)). To more fully evaluate the pluvial flood risk, detailed localised modelling would be required considering all the variables mentioned above. As this study was looking on a national scale however, this was not feasible.

Similarly, flooding created by waves is also affected by wave period and direction as well as localised topography of the shoaling coastline. Period and direction were not investigated, due to validation of the hindcast modelled dataset used in the study showed period and direction performed poorly against the observed data. As with pluvial flooding, wave run up is highly dependent on localised coastal topography and would require finer scale modelling to more accurately account for wave flooding.

For sea level, the analysis focused on the skew surge rather than total water level (TWL). In Chapter 3, both skew surge and TWL were analysed and a relationship found in both, however it was much stronger in the skew surge as the probability of the surge occurring coincidently with a high astronomical tide was removed. For demonstrating the overall relationship between the flooding sources this is appropriate. However, it should be noted that this doesn't necessarily establish if flooding events occurred. Haigh et al. (2016) found for the UK, the majority of coastal flooding events occurred when a moderate surge aligned with a spring astronomical high tide, rather than an extreme surge. Therefore, analysing simply an extreme surge may cause flooding events to be overlooked. Haigh et al. (2016) also found that whilst extreme skew surges had increase over time, flood events had not, due to improvements in flood defences and forecasting. Using extreme compound events as opposed to occurrences of actual flooding may not be a true representation of flooding.

An additional limitation to the research is the length of the datasets used. An average overlapping data length of 23 years was obtained between source variables, this does have the potential to overlook several multi-decadal features such as the lunar nodal cycle and the Atlantic Multidecadal Oscillation (AMO). If total water level is considered, the impact of the 18.6 year lunar nodal cycle can have great impact on astronomical tides (Haigh et al., 2011), and so a minimum of 2 lunar nodal cycles are required. Furthermore, decadal clustering of extremes (i.e. groupings of extreme events in some decades and not others) was found in the surge time-series in the UK (M. P. Wadey et al., 2014), which suggested these might be linked to regional changes in climate, such as the NAO and the AMO, further illustrating the need for longer time-series. More recently, a new climatic index has been developed, Western Europe Pressure Anomaly (WEPA) (Castelle et al., 2017). WEPA captures the sea level pressure gradient between Ireland and the Canary Islands, and outperforms climatic index (such as the NAO) when studying extreme waves, particularly for the 2013/14 winter season. Future work could consider the impacts of WEPA on compound flooding.

5.5 Conclusions

This chapter has assessed the potential for compound flooding around the UK coast arising from the joint occurrence of pairs of the four main sources of flooding, namely: storm surge, waves, river-discharge and surface runoff. It was found that the joint occurrence and dependence of all six pairs of joint variables occurs more frequently during the study period (15–50 years) at sites on the south-western and western coasts of the UK, compared to sites along the eastern coast. The strongest dependence is between waves and river discharge, whilst the greatest number of joint occurrences is between surge and waves. It's shown, for the first time, that the spatial variability in the dependence and number of joint occurrences of extreme flood sources is driven by meteorological differences in storm characteristics. In the west, the flood sources are typically driven by the same weather patterns, however on the east coast, the different flood sources are driven by differing weather systems (i.e., surge and waves are typically generated by a low-pressure system over Scandinavia, whilst river and rainfall had less well defined weather patterns, with no low pressure centre), reducing the likelihood of compound events. The influence of the NAO on compound flooding is also examined. It's found that compound events excluding rainfall on the west coast are more likely to occur during a positive NAO winter. On the east coast, whilst surge and wave events occur during a positive

NAO winter, rainfall and river discharge events are more likely during a weak NAO winter. Finally, it's found that return periods of variables are underestimated, particularly for sites on the west coast, when the dependence between variables is ignored. Failure to account compound flooding could result in an underestimation of the flood risk by 5-6 times for some flood combinations such as wave vs river discharge, when comparing an independent to dependent relationship.

The results presented in this chapter have shown that all flood sources must be considered collectively when assessing the risk from flooding, and to do so otherwise could result in a significant underestimation of the risk, with disastrous consequences. This risk is not uniform however, and a greater emphasis of compound flooding research should be placed on the west coast of the UK. It is therefore crucial that future flood management approaches and forecasting techniques consider compound flooding and its drivers.

6. Using meteorological drivers to identify potential past and future compound flood events in the UK.

6.1 Introduction

The analyses presented in Chapters 3 and 4 assessed the occurrences of compound extreme events around the UK coast using observed data. A key outcome of this component of the study was that that certain types of weather conditions favour the joint occurrence of storm surge and river discharge, while other weather patterns do not, and this therefore influences the stretches of coastline were compound flooding is more likely to occur. For example, findings show that compound flooding is more likely to occur on the west coast of the UK, where storms over the North Atlantic cause both strong south-westerly winds and a band of rain from the southwest. In contrast, on the east coast, compound flooding is less likely to occur because the storms that generate large storm surges, do not generate high river discharge. The analysis therefore gave key insight into understanding of compound events. However, a key limitation of the analysis undertaken in Chapters 3 and 4, is the data availability. The average overlapping data length of sea levels and river flow in Chapter 3 was 29 years. This creates uncertainties when attempting to interpret whether there is evidence for long-term changes in the frequency of compound flooding. The dataset is often too short to discern whether compound flooding is becoming more or less likely to occur and to determine what the impact of multidecadal cycles, and in particular, atmospheric variability due to the North Atlantic Oscillation (NAO) and Atlantic Multidecadal Oscillation (AMO), is. These climate teleconnection patterns influence the storm track and amount of rainfall, and so could indirectly affect compound flooding. Furthermore, sea levels are influenced by multi-decadal astronomical tidal cycles, such as the 18.6 lunar nodal cycle, which can influence flooding. Haigh et al. (2011) recommends that 36 years of data are used in sea level analyses (e.g., at least two complete nodal cycles), to capture this variability. Failure to do so, could result in a greater or larger number of flooding events being identified, and in changes being falsely interpreted as a variation in the flooding climate, rather than the increased (or decreased) water level due to the astronomical tide resulting in greater (or lower) storm tides.

One way of overcoming the lack of long observed data, is to use non quality-controlled evidence over many hundreds or thousands of years. For example, in the UK, databases such as Surgewatch (Haigh et al., 2016; Haigh et al., 2017; https://www.surgewatch.org/) have qualitatively identified major coastal flood events going back as far as 1014 using a wide range of 'soft' sources, such as periodicals, newspapers, monthly weather and hydrological reports professional reports and other online sources (such as blogs and social media). Brázdil et al. (2006) performed a similar historical flood database on riverine flooding in Europe. Whilst these methods have issues with data accuracy, they do provide context to modern extreme events. To quantitatively improve extreme estimations, datasets can be extended with historic events or paleofloods, thus reducing uncertainties and better representing potential outliers. This technique has been used for both river (Benito et al., 2004; Hosking & Wallis, 1986; Payrastre et al., 2011; Stedinger & Baker, 1987) and skew surges (Hamdi et al., 2015)

An alternative method is to assess data on a regional scale and combine observed timeseries to create a single continuous longer sea level dataset. Combining several local datasets has produced a technique known as Regional Frequency Analysis (RFA), whereby different locations in a region are clustered together to use all of the available data (Bernardara et al., 2011; Weiss et al., 2014). This method is based on the index flood principle (Dalrymple, 1960) which uses a local index at each site to preserve any individualities in a region. There are limitations with this technique, for example the probability distribution of the extreme values must be the same at all sites within a region to allow the fitting of a distribution curve (Frau et al., 2018; Hosking & Wallis, 1997). The RFA technique has been combined with paleoflood records by Nguyen et al., (2014) for river discharge; Hamdi et al. (2016) for oceanic and meteorological parameters and Frau et al. (2018) for storm surges. No study however, has used these methods yet to expand compound flooding databases.

Another limitation of just using observations in compound flooding studies, is that one cannot then consider how the frequency of compound flooding may change in the future. To date, Bevacqua et al. (2019, 2020) are the only studies assessing how compound flooding may change in the future with climate change. Storm surges were simulated through a DFLOW FM model, waves through Wavewatch III and astronomical tides were simulated using FES2012 model. The three models were uncoupled. All were forced using climate projections from CMIP5 multi-model ensembles, under RCP 8.5 conditions. Precipitation was taken directly from the projections. Statistical analysis was then applied to the modelled datasets using an "AND" return period (where both variables must pass an extreme threshold) to identify the

compound return periods. They found that the greatest compound flooding probability is seen in the Mediterranean, however climate projections showed an increase in compound flood probability along parts of the northern European coast.

As described in Section 2.7.5, an alternative method to observe compound events is to assess the source drivers which lead to such events, i.e., by identifying the weather patterns which lead to compound flood events via techniques as seen in Neal et al. (2016) and Hemer et al (2008). Therefore, the objective of this chapter is to evaluate how compounding flooding might vary in the future and extend historic compound flooding records. To address this objective there are three sub-objectives as follows:

1. To establish a method to extend compound flood records in the UK beyond traditional observed data methods, by using synoptic weather patterns as a proxy;
2. To analyse whether the frequency of storms that tend to lead to compound flooding has changed over the period 1851 to 2017; and
3. To assess any potential future changes in compound flooding up to the year 2095 under RCP2.6 and 8.5 conditions (explained in Section 5.2.2).

The structure of this chapter is as follows: Section 5.2 discusses the different datasets used in this analysis. Section 5.3 describes the methodology used to address the three sub-objectives. The results are described in Section 5.4 and discussed in Section 5.5. Finally, conclusions and future implications are examined in Section 5.6.

6.2 Methodology

The analysis was undertaken in three main stages described in turn in the sections below, each addressing one of the three-chapter sub-objectives outlined in Section 5.1.

6.2.1 Define reference compound conditions

The reference conditions were produced from the joint occurrence of extreme storm surges and river discharge calculated in Chapter 3. Four sites were selected, spaced at roughly equal distances, chosen according to the number of joint occurring extreme events. A high number of joint extreme events were required, to provide enough test events for technique validation. Sites were therefore only picked along the west coast, as much fewer compound events are observed along the east coast (Figure 4.4). The 4 sites (from south to north) were Devonport, Fishguard, Heysham and Kinlochbervie (Figure 6.1). At each site, the reference conditions

were defined as the composite meteorological conditions identified in Chapter 3 for the joint occurrence events of extreme storm surge and river discharge; based upon MSLP, WS and PWC (Figure 6.2Figure 6.3,Figure 6.4Figure 6.5). Unlike in Chapters 3 and 4, here the entire temporal data extent (1851-2017) is analysed.

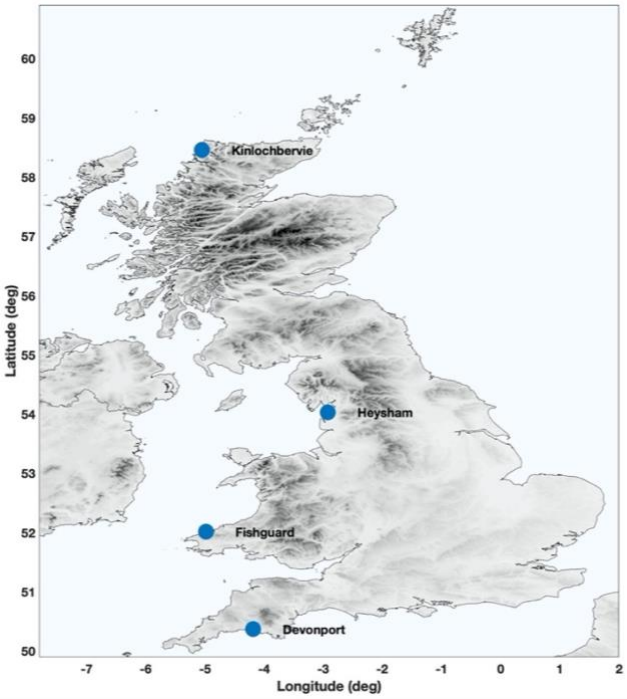

Figure 6.1: Location of the study sites for Section 5.

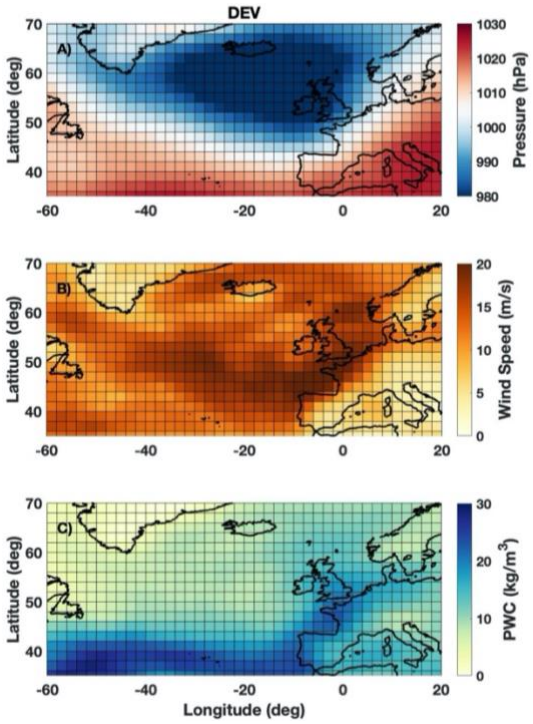

Figure 6.2: Reference Meteorological conditions for Devonport for: (a) Sea level pressure (hPa); (b) Wind speed (m/s); and (c) Precipitable water content (kg/m^3).

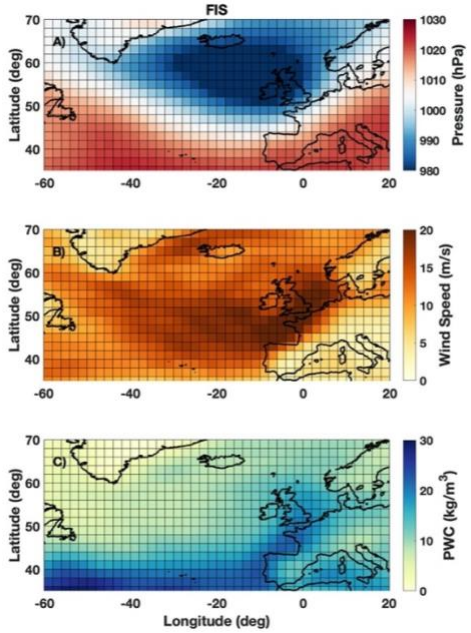

Figure 6.3: Reference Meteorological conditions for Fishguard a) Sea level pressure (hPa) b) Wind speed (m/s) c) Precipitable water content (kg/m^3).

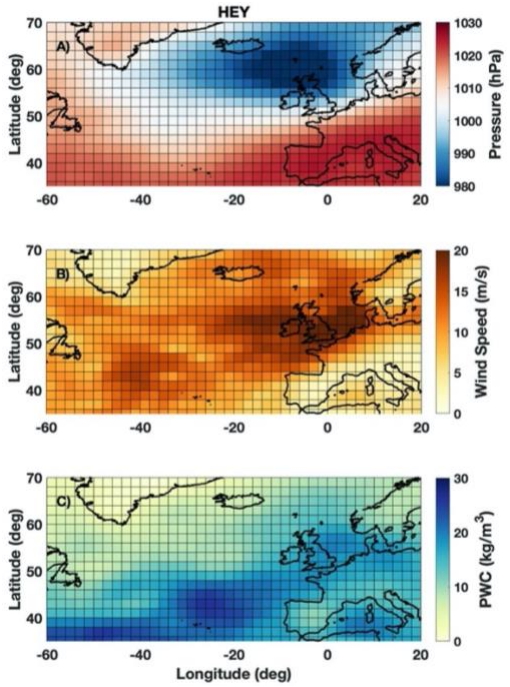

Figure 6.4: Reference Meteorological conditions for Heysham a) Sea level pressure (hPa) b) Wind speed (m/s) c) Precipitable water content (kg/m^3).

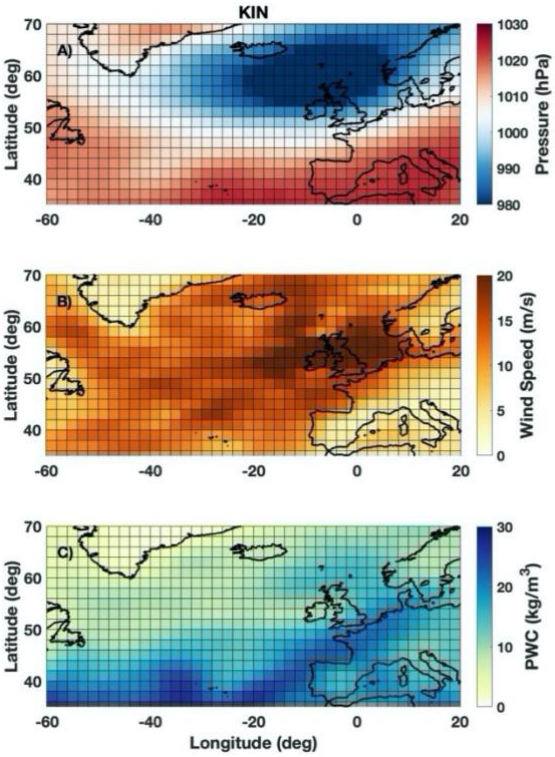

Figure 6.5: Reference Meteorological conditions for Kinlochbervie a) Sea level pressure (hPa) b) Wind speed (m/s) c) Precipitable water content (kg/m^3).

6.2.2 Establish a method to extend compound flood records

The first sub-objective is to establish a method to extend compound flood records in the UK beyond traditional observed data methods, by using synoptic weather patterns as a proxy. Two different techniques were used to compare meteorological conditions to the reference conditions (Figure 6.2,Figure 6.3,Figure 6.4 Figure 6.5). The first approach calculated the distance from the reference conditions measured using the Pearson's Correlation (PC) method based on the technique of (Wu et al., 2018). This provided the degree of similarity of spatial structures (i.e., high- and low-pressure systems in the similar places). The second method used the difference in magnitude as measured using a sum of square difference (SSD) method, based on a modified Kirchoffer score (Hemer et al., 2008). Each time stamp (1850 to 2017) of the 20th century reanalysis dataset contained three variables (MSLP, WS and PWC). This provided almost 170 years of MSLP, WS and PWC data at 6 hourly intervals, resulting in 241,920 unique meteorological conditions to sample and test against. As shown in Chapters 3 and 4, weather systems were resolved adequately in the 20th Century Reanalysis. Each timestamp was then tested using both the PC and SSD method, thus resulting in 6 tests scores comparing the reference conditions to the conditions during the time stamp.

For the PC method, a modified version of Wu et al (2018) was used. Individual timestamps were not normalized, to maintain a seasonal variation. The Pearson product-moment correlation (Equation 1) was calculated between every grid point in the selected region between the reference conditions and each timestamp. This created a single correlation number at each time stamp.

Equation 1: $\rho(A,B) = \frac{1}{N-1}\sum_{i=1}^{N}(\frac{A_i-\mu_A}{\sigma_A})(\frac{B_i-\mu_i}{\sigma_B})$

where μ_A and σ_A are the mean and standard deviation of A (the reference conditions), respectively, and μ_B and σ_B are the mean and standard deviation of B (the sample timestamp).

The SSD method is partially based on the Kirchhoffer sum-of squares technique (Kirchhofer, 1973; Yarnal, 1993). This procedure calculates the total difference between the gridded synoptic maps and reference conditions. Each time stamp is compared to the reference condition using the sum of squares equation, as follows:

Equation 2: $S = \sum_{i=1}^{N}(Z_{i,a} - Z_{i,b})^2$

where S is the Kirchhofer score, Zi,a is the normalised grid value of point i at time a (reference conditions), Zi,b is the grid value of point i at time b, and N is the number of data points in the grid.

Hemer et al (2008) also introduced a Kirchhofer score for each row and column as they found it possible that a comparison of two grids could generate a low value of S, indicating overall statistical similarity, but have very different patterns in certain sectors of the synoptic chart. It was decided this was not necessary in this study, as the PC method would eliminate any distance variations that might lead to false positive results. Furthermore, tests found the thresholds for the row and column scores were very sensitive to changes in region size.

To ensure the correct region was investigated, three regions were tested. These regions were: (i) the entire North Atlantic basin (Region A); (ii) 40N-60N 30W-20E (Region B); and (iii) 34N-66N 30W-20E (Region C) (Figure 6.6). These regions were tested against the PC method, by correlating their reference conditions against the observed events which made up the reference conditions.

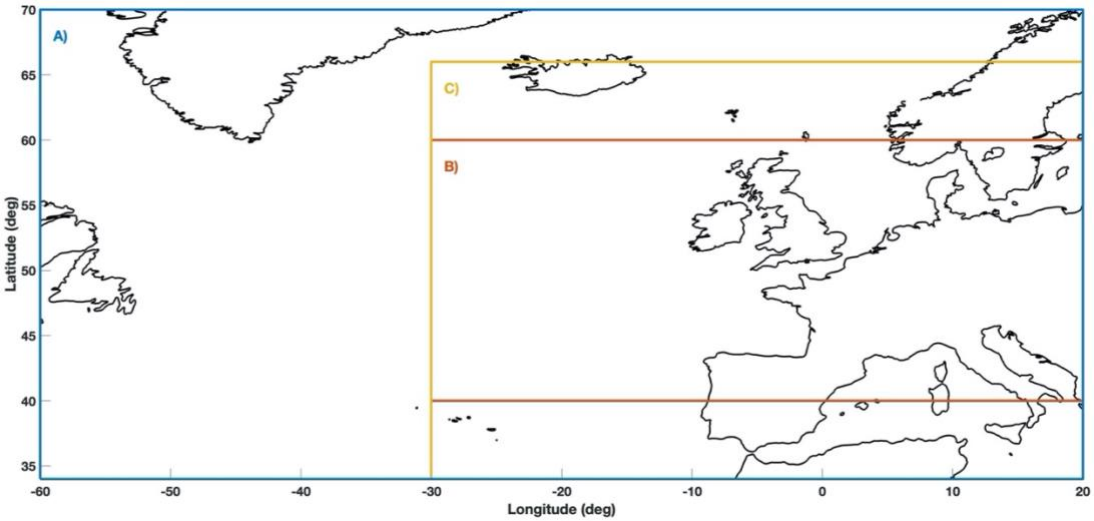

Figure 6.6: Different study regions used: a) entire North Atlantic basin (34N-70N 60W-20E); b) 40N-60N 30W-20E; and c) 34N-66N 30W-20E.

A threshold has to be set to determine if the meteorological conditions at a timestamp are similar to the reference conditions to be flagged as a compound event. Three different methods were tested for threshold determination. The first threshold used the lowest correlation/ highest SSD when the reference conditions were compared to the historic known compound extreme events from which the reference event composite was created (Figure 6.8Figure 6.9Figure 6.10 Figure 6.11). Outliers were removed if they were more than 1.5 interquartile ranges above the upper quartile (75^{th} percentile) or below the lower quartile (25^{th} percentile). The second threshold was set using a percentile method. The 99^{th} percentile of the correlations for each time stamp was extracted, and this was used as the passing threshold. For the SSD this was set at the 1^{st} percentile (a higher SSD indicates greater deviation from the reference conditions). This method therefore ensured only the highest correlations/lowest SSD events were identified, however, it did mean some of the historic events might be missed off. The final threshold method involved using a variable percentile threshold. For the period of observed sea level and river flow data, the number of compound events is known. The correlation/SSD results were trimmed to this period and a threshold calculated so that the same or similar number of compound events were identified as had been observed. This method resulted in a different threshold for each site.

To ensure compound events were only captured once, a declustering algorithm was used. Of those passing the threshold tests, time stamps were first sorted by their correlation/SSD score,

to ensure the largest scores were kept. Results were then removed within ± 24 hours of each other. 24 hours was selected to remain consistent with the declustering algorithms used in Chapters 3 and 4. Remaining flagged events were then chronologically re-sorted.

The resulting flagged events were then validated. This was initially done using the observed time period. The number and temporal location of flagged events were compared to observed compound events. The different methodologies' success was based on these results.

6.3.3 Temporal trends of compound flooding in the UK

The second sub-objective is to analyse whether the frequency of storms that tend to lead to compound flooding has changed over the period 1851 to 2017. The number of flagged events is initially calculated as an annual and decadal count, and trend lines are fitted. The number of events is then compared to climatic indices to see if these are a contributing factor. Both the NAO and AMO are considered. First, just a visual comparison is made, comparing troughs and peaks in the indices and number of compound events, then second, the NAO and AMO are correlated against the number of events annually.

6.3.4 Future changes in compound flooding in the UK

The third and final sub-objective is to assess any potential future changes in compound flooding up to the year 2095 under RCP2.6 and 8.5 conditions. This was done by applying the same methodology above to the HADGEM2-ES climate projections described in Section 5.3.1 and 5.3.2. The RCP2.6 and RCP8.5 scenarios were used to show the extreme cases and test if this method can show future changes in compound flooding. Modifications to the methodology were made to allow for the differences in the datasets. As described in section 5.2.2, daily data was used to ensure all three variables (MSLP, WS and PWC) are available, compared to 6-hourly in the 20th century reanalysis. When using the 20th century reanalysis, the declustering algorithm removed flagged data points which were within 24 hours of another flagged point. As this could not be done for daily, the declustering was extended to ±48 hours instead of 24 hours. With precipitation flux being used instead of PWC, the PC and SSD were much lower when compared to the 20th century reanalysis. This prevented the thresholds for PWC being used on the HADGEM2-ES dataset, therefore just MSLP and PWC were used.

6.3 Results

6.3.1 Establish a method to extend compound flood records

The first sub-objective was to establish a method to extend compound flood records in the UK beyond traditional observed datasets, by using synoptic weather patterns as a proxy. To achieve this, two different methods were established to extend the compound flooding dataset using weather patterns: (1) the Pearson's Correlation (PC) method to measure the spatial distance a weather system is from the reference conditions; and (2) the sum of square difference (SSD) method to measure the difference in magnitude from the reference conditions. By combining these two methods, the weather systems most similar to the conditions resulting in compound extreme events can be identified in the 20th Century reanalysis dataset extending from 1851 to 2017.

The first step was to identify the region most appropriate for UK weather systems. Initially, the weather patterns across the entire North Atlantic basin (Region A) were analysed. The region was tested using the correlation method (PC) on known compound flood event dates. On these test events, Region A produced a relatively low correlation (Figure 6.7), due to large areas in the western North Atlantic unrelated to the UK's weather regime. Next, Region B used the eastern half of the North Atlantic through to Scandinavia. This captured the weather regimes most related to the UK when focused on MSLP and WS, however PWC was still lower, due to missing off the band of rain which travels diagonally from southwest to northeast (Figure 6.6c). This was found to reduce the correlation (Figure 6.7b) on the test events, therefore the latitude limits were increased to 34N-66N (Region C) to capture the region from the Azores in the south to Iceland in the north. This generated acceptable correlations for all events and variables.

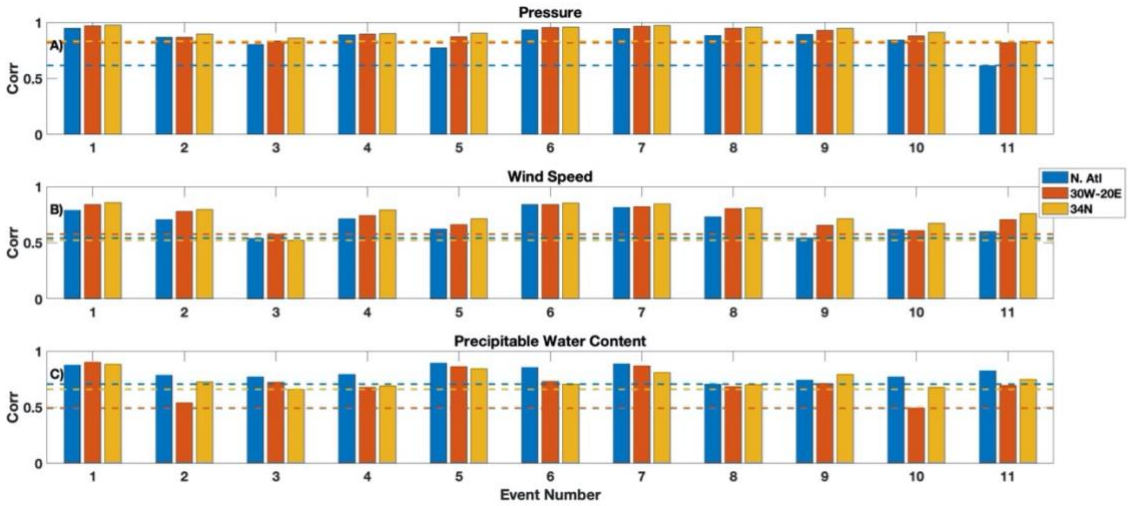

Figure 6.7: Correlation at Devonport comparing the reference composite of a) mean sea level pressure, b) wind speed and c) precipitable water content against known compound extreme events (labelled 1-11) during the observed period (1987-2016) for the three different regions of interest.

The next step required calculating a threshold for when the PC and SSD test results classified as a compound flood event. The meteorological conditions during each individual observed compound flood events were used as test events against the reference compound conditions at each of the four selected sites (Figure 6.8 for Devonport, Figure 6.9 for Fishguard, Figure 6.10 for Heysham and Figure 6.11 for Kinlochbervie) for the PC and SSD tests.

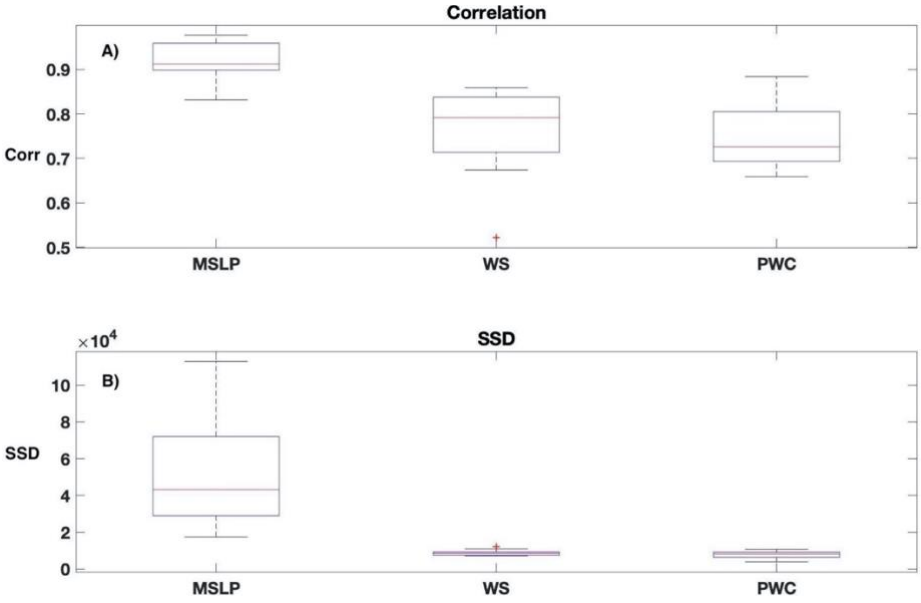

Figure 6.8: Boxplot of a) Correlation and b) SSD values at Devonport comparing the reference composite of mean sea level pressure (MSLP), wind speed (WS) and precipitable water content (PWC) against known compound extreme events during the observed period.

The central red line represents the median, the top and bottom edges of the box represent the 25th and 75th percentiles, the whiskers represent the most extreme data points not considered outlets, red crosses represent outliers (more than 1.5 times the interquartile range away from the bottom or top of the box).

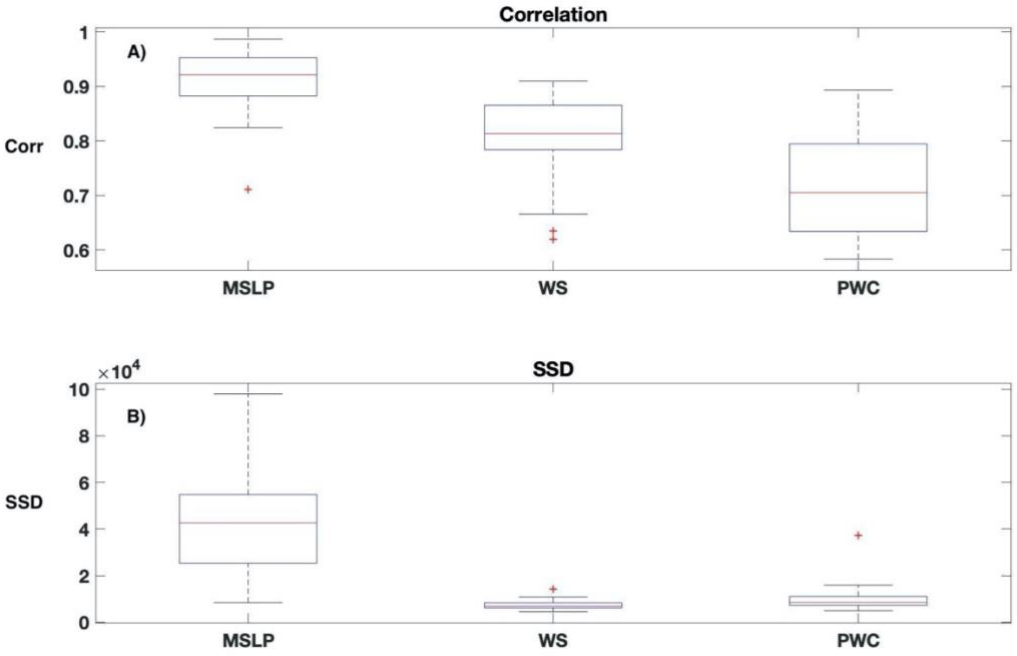

Figure 6.9: Boxplot of a) correlation and b) SSD values at Fishguard comparing the reference composite of mean sea level pressure (MSLP), wind speed (WS) and precipitable water content (PWC) against known compound extreme events during the observed period. The central red line represents the median, the top and bottom edges of the box represent the 25th and 75th percentiles, the whiskers represent the most extreme data points not considered outlets, red crosses represent outliers (more than 1.5 times the interquartile range away from the bottom or top of the box).

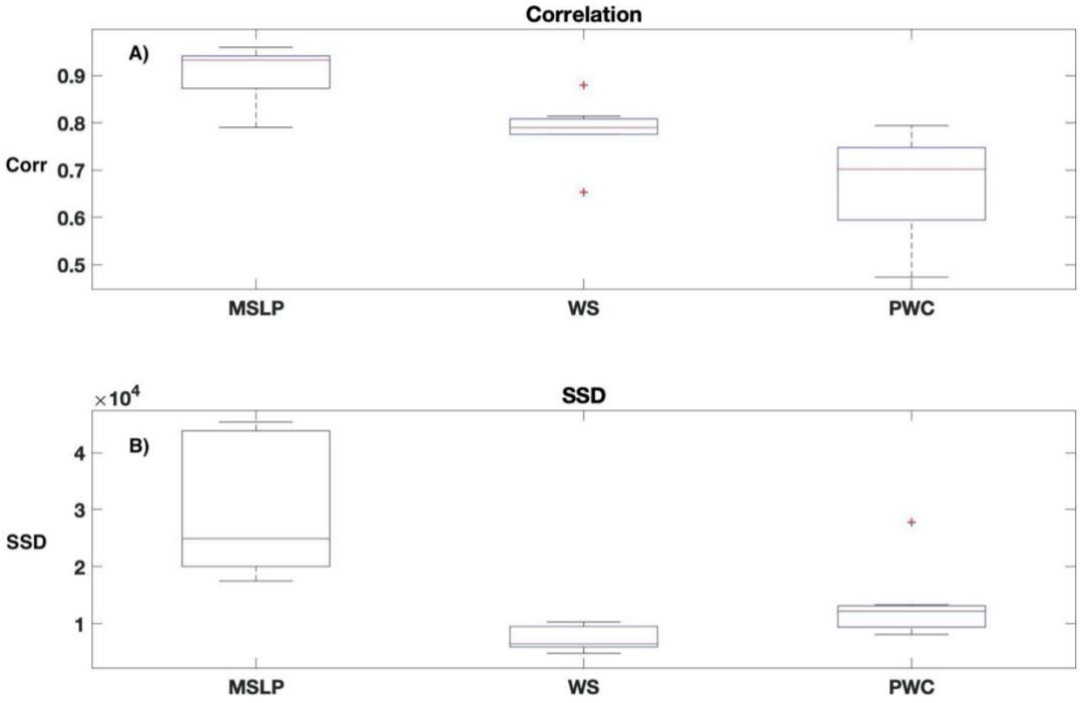

Figure 6.10: Boxplot of a) Correlation and b) SSD values at Heysham comparing the reference composite of mean sea level pressure (MSLP), wind speed (WS) and precipitable water content (PWC) against known compound extreme events during the observed period. The central red line represents the median, the top and bottom edges of the box represent the 25th and 75th percentiles, the whiskers represent the most extreme data points not considered outlets, red crosses represent outliers (more than 1.5 times the interquartile range away from the bottom or top of the box).

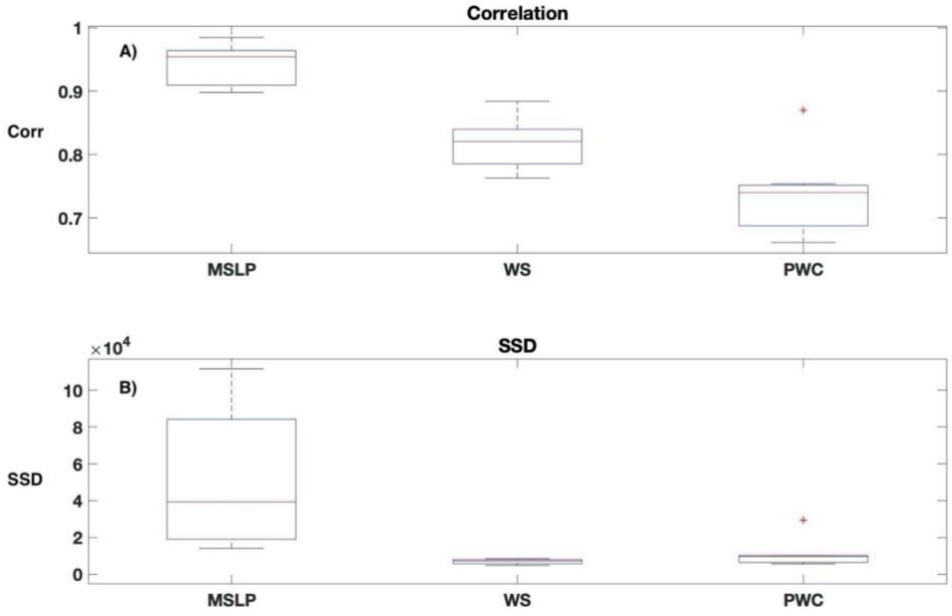

Figure 6.11: Boxplot of a) correlation and b) SSD values at Kinlochbervie comparing the reference composite of mean sea level pressure (MSLP), wind speed (WS) and precipitable water content (PWC) against known compound extreme events during the observed period. The central red line represents the median, the top and bottom edges of the box represent the 25th and 75th percentiles, the whiskers represent the most extreme data points not considered outlets, red crosses represent outliers (more than 1.5 times the interquartile range away from the bottom or top of the box).

The lowest correlating (or highest for the SSD method) event was selected as the threshold (hereafter referred to as threshold method 1). This was then applied to the 20th century reanalysis dataset for the time period of overlapping observed sea level and river flow datasets. To ensure the threshold was accurately identifying compound events, the number of flagged events is compared to the number of events found the observed dataset (Figure 6.12 shown for Devonport). For all sites, threshold method 1 was found to overestimate the number of compound event occurring. For example, at Devonport, 11 events were identified in the observed tide/river gauge records, whilst using the PC/SSD method, 66 events were found during the same 26-year time period (Figure 6.12).

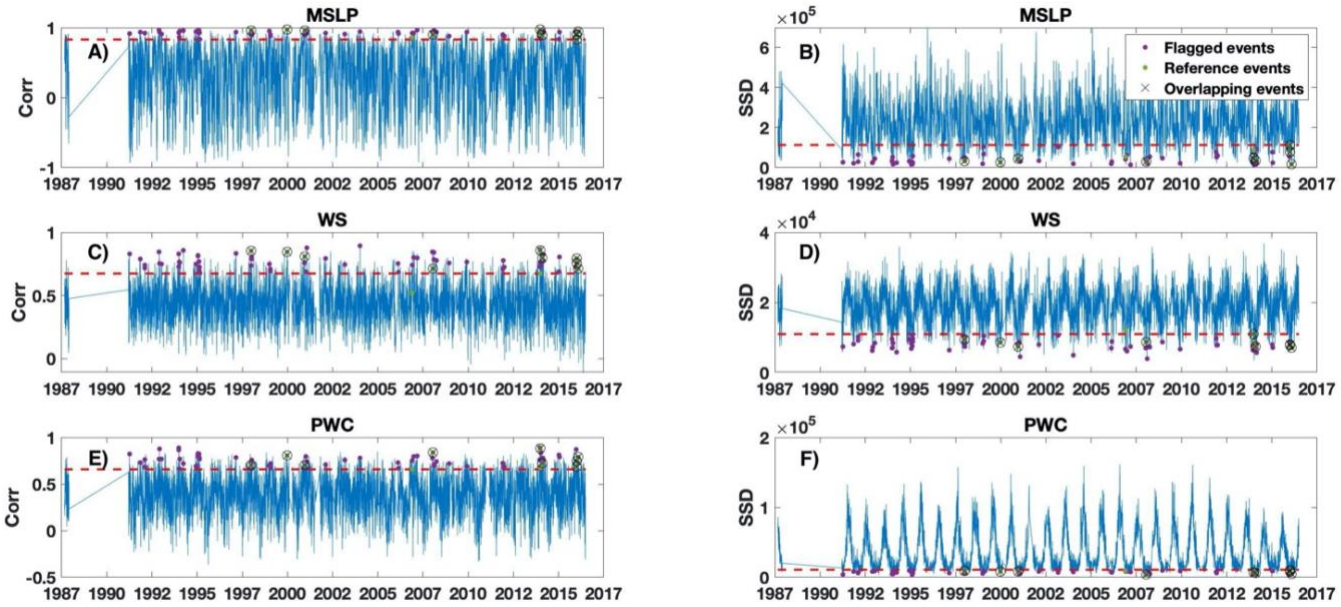

Figure 6.12: Number of events at Devonport above the threshold method 1 for all tests. a), c) and e) are using the PC test, b), d) and f) are using the SSD test for the observed data period.

To reduce the number of events in the time period a fixed threshold (referred to as threshold method 2) was used. Initially time stamps with correlations and SSD greater than the 99th percentile in all 6 tests were used. Whilst this did bring the number closer to the observed record, it still resulted in an overestimation of events (44 for Devonport compared to 11 observed events, Figure 6.13).

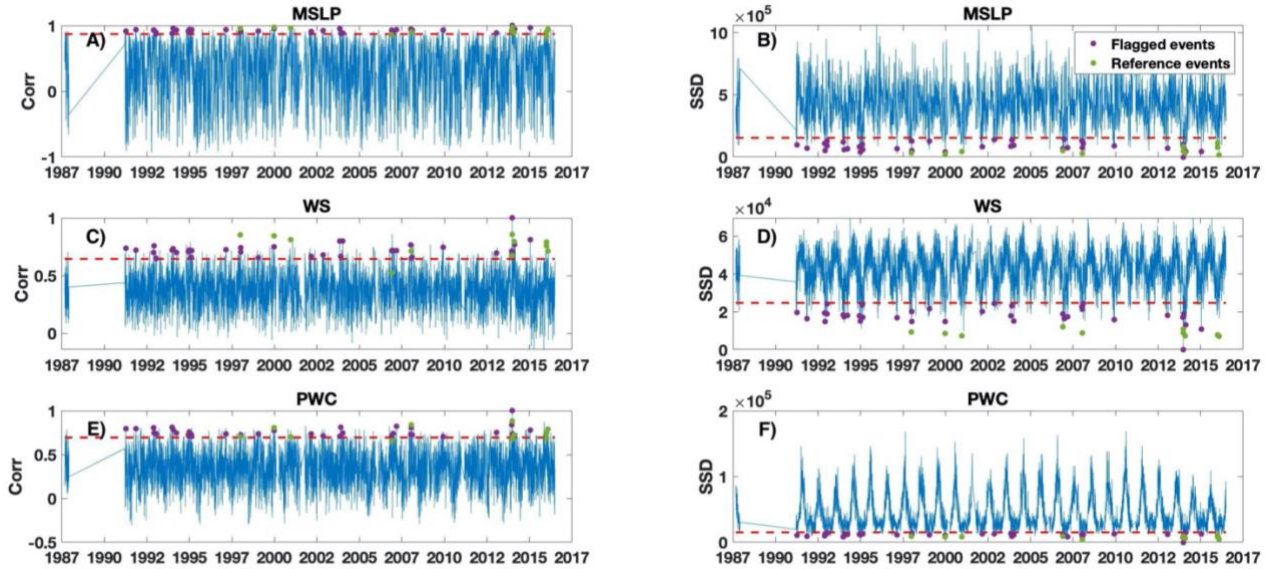

Figure 6.13: Number of events at Devonport above the threshold method 2 for all tests. a), c) and e) are using the PC test, b), d) and f) are using the SSD test for the observed data period.

Finally, a variable threshold approach (threshold method 3) was tested (Figure 6.14). To ensure storms were captured in the correct locations, the PC test thresholds were kept as those in threshold method 1. Only the SSD threshold was adjusted from the reference events, as this is a measure of the magnitude of the storms. It should be noted that the threshold was found to be different at each site (

), suggesting the range in magnitude of storms leading to compound flood events varies from site to site. Using this method, the number of events identified using the PC/SSD approach was matched the number of events in observed data.

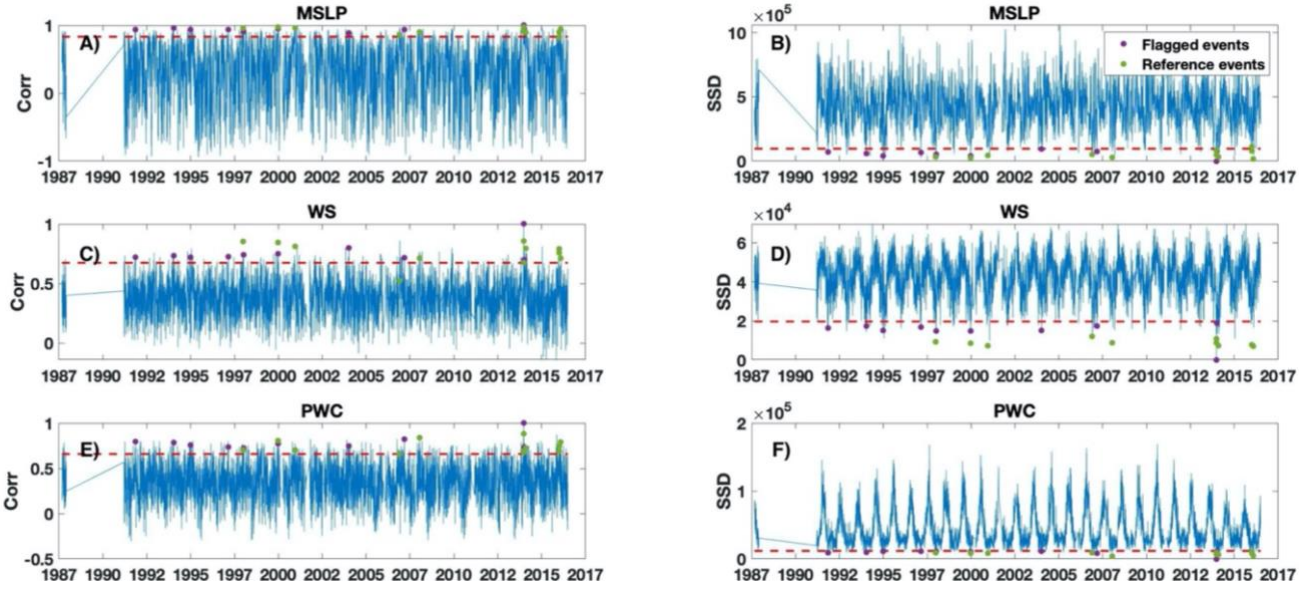

Figure 6.14: Number of events at Devonport above the threshold method 3 for all tests. a), c) and e) are using the PC test, b), d) and f) are using the SSD test for the observed data period.

Table 6.1: the threshold selected using threshold method 3.

Site	SSD percentile threshold
Devonport	99.1th
Fishguard	98.5th
Heysham	99th
Kinlochbervie	96th

6.3.2 Temporal trends of compound flooding in the UK

The second sub-objective was to analyse whether the frequency of storms that tend to lead to compound flooding has changed over the period 1851 to 2017. This was achieved by using the variable threshold methodology (threshold method 3) established in Section 5.4.1. and extended to the entire 20th Century reanalysis dataset period (1851 to 2017) (Figure 6.15).

To assess temporal changes, the number of events per year were plotted for the four sites (chosen forthe high number jointly occurring extreme surge and discharge events at each of the four sites Figure 4.4) and are shown in Figure 6.16a-d. The maximum number of events per year was 3 across all sites. At each of the four sites there is no statistically significant temporal trend evident, but there is year to year variability. For example, at Fishguard (Figure 6.16b), the number of events per year drops from 3 to 0 in consecutive years between 1975 and 1976.

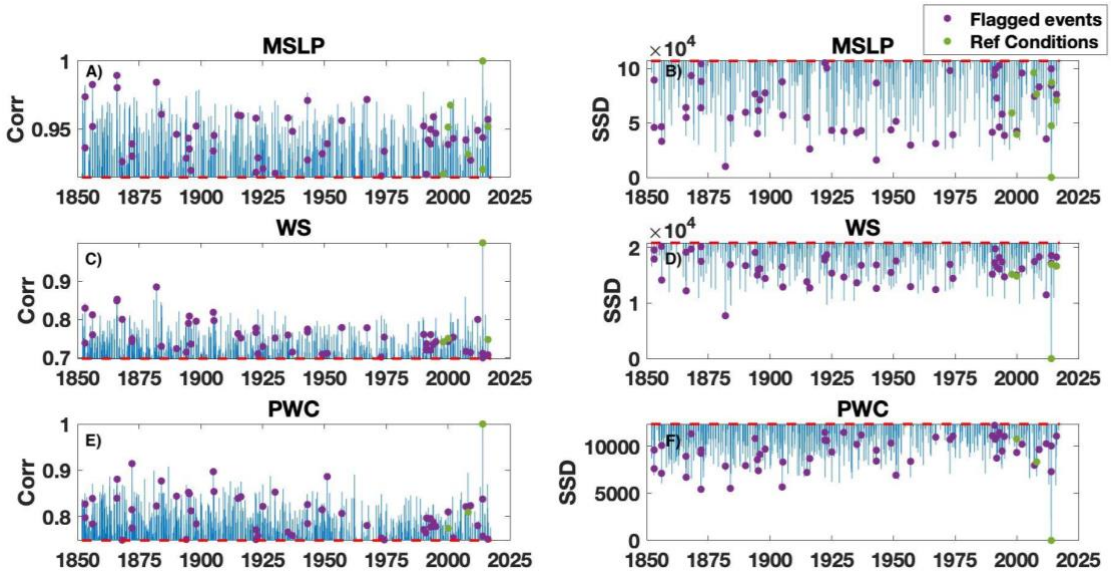

Figure 6.15: Number of events at Devonport above the threshold method 3 for all tests. a), c) and e) are using the PC test, b), d) and f) are using the SSD test. For the entire 20th Century reanalysis time series (1851-2017), zoomed into above the thresholds.

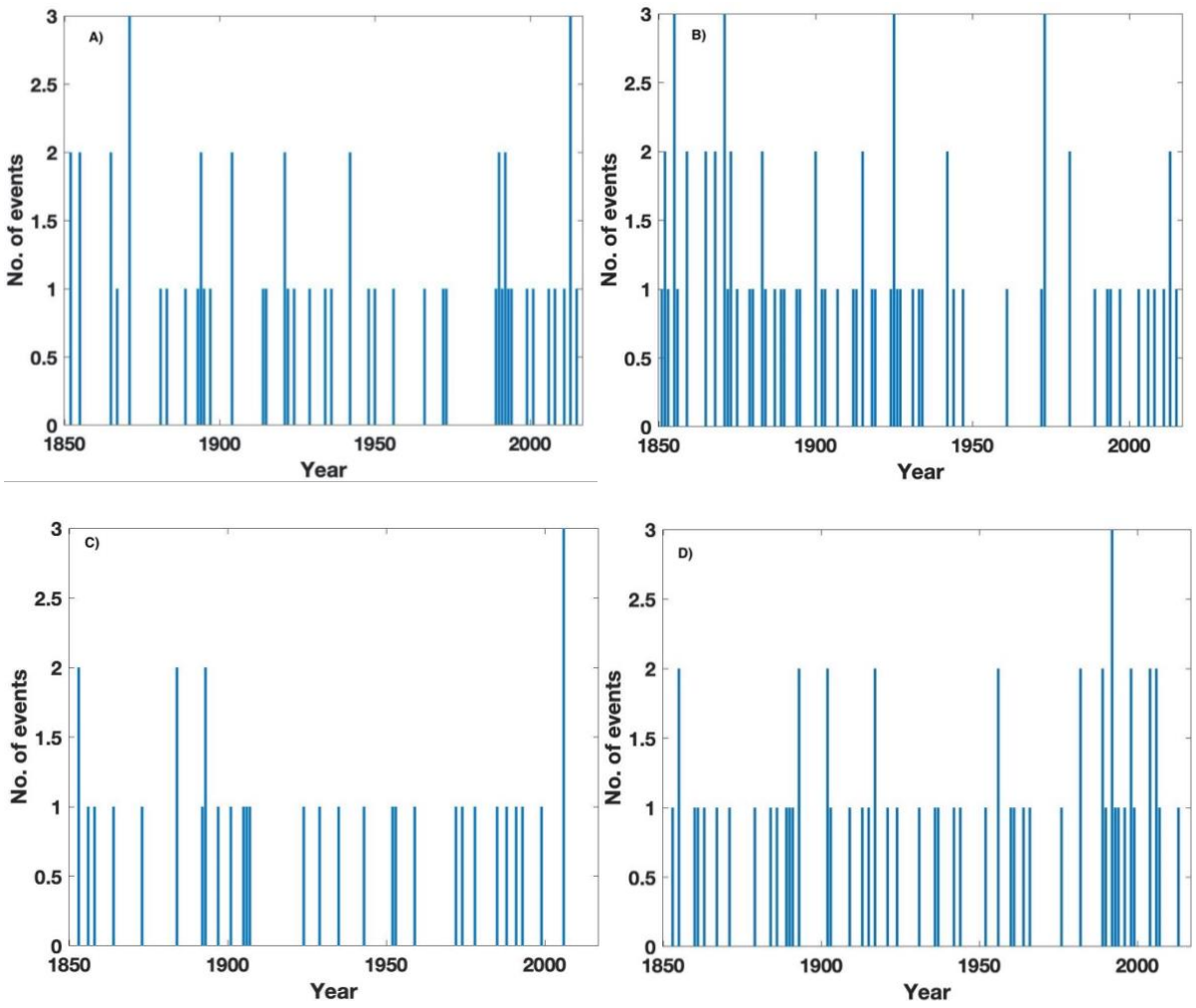

Figure 6.16: Frequency of compound events per year at a) Devonport b) Fishguard c) Heysham d) Kinlochbervie.

The number of events per decade is shown in Figure 6.17a-d for all sites. Devonport (Figure 6.17a) featured a maximum of 6 events per decade (1990's), and a minimum of 1 event per decade (1950's and 1960's). Fishguard (Figure 6.17b) has the most events per decade, with 10 events per decade in the 1850's. Qualitatively, it appears from Figure 6.17b that the number of events per decade declines over the entire time period, however, no statistically significant trend was computed. Heysham (Figure 6.17c), had the fewest events per decade (between 4-0). Finally, at Kinlochbervie (shown in Figure 6.17d), the most events (9) occurred in the 1990's towards the end of the dataset, with a minimum of 1 event per decade in the 1970's and 2010's. Furthermore, Fishguard and Heysham also featured decades with no events in 1950's (Fishguard) and 1910's, 1960 's and 2010's (Heysham).

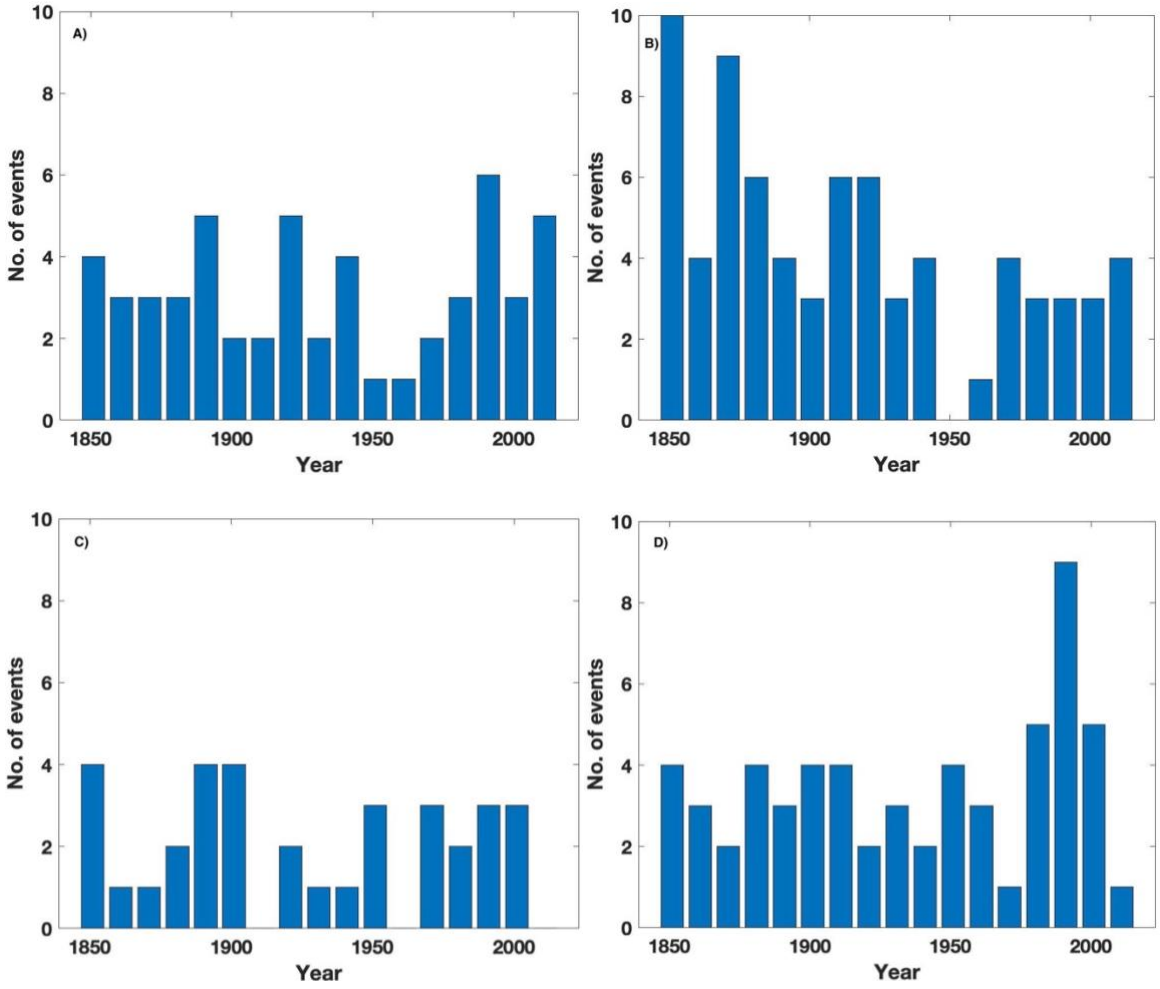

Figure 6.17: Frequency of compound events per decade at a) Devonport b) Fishguard c) Heysham d) Kinlochbervie.

When comparing between sites, the events identified are not uniform. For example, at Devonport (Figure 6.16a) between 1989 and 1994, at least 1 event was identified each year. This clustering was not seen at any other site. The inter-site variation would suggest the composite weather patterns are unique enough to discern compound flooding on at least a regional basis. The total number of events identified throughout the timeseries is listed in Table 6.2. The greatest number of events was found at Fishguard (73) whilst the fewest were found at Heysham (34). This appears to be no relationship to the variable thresholds in

.

Table 6.2: The number of compound events observed through the entire 20th Century Reanalysis time series (1851-2017) as a total and average per year over the time period.

Site	Total number of events	Average number of events per year (over the entire time period)
Devonport	54	0.32
Fishguard	73	0.42
Heysham	34	0.20
Kinlochbervie	59	0.35

The number of events per year was correlated against the winter NAO for the corresponding year at each site and comparisons are shown in Figure 6.18a-d. Whilst all sites show positive correlation, it is relatively weak, with Devonport and Kinlochbervie having the strongest correlation (r= 0.33 and 0.29 respectively) and Fishguard and Heysham the weakest r= 0.15 and 0.22 respectively, both of which are statistically insignificant). For the winter AMO the correlation is shown in (Figure 6.19a-d) and is weaker than the NAO results. All sites show a negative correlation with the NAO, with the greatest at r = -0.11 (Devonport) and weakest at Fishguard with r = 0.

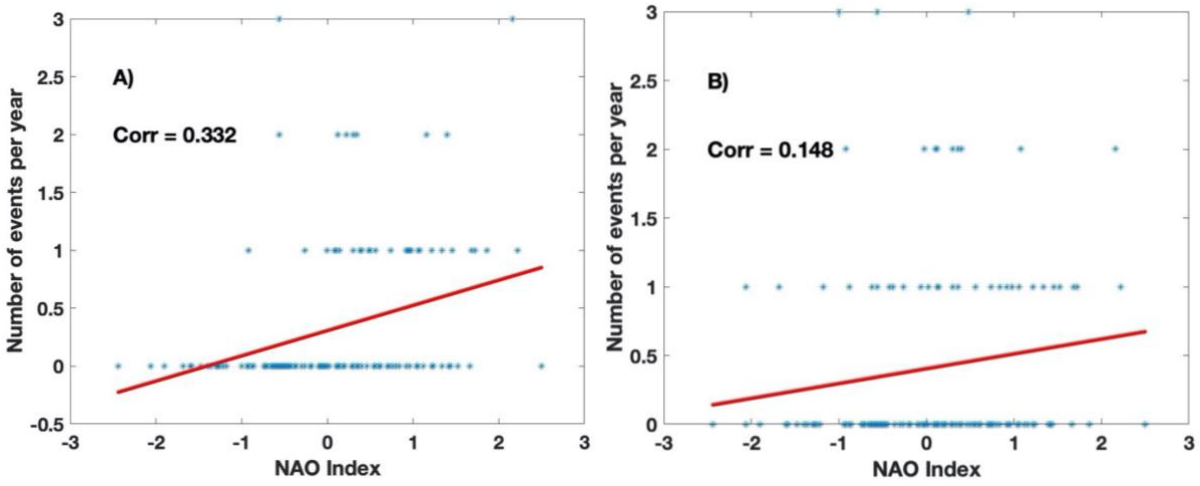

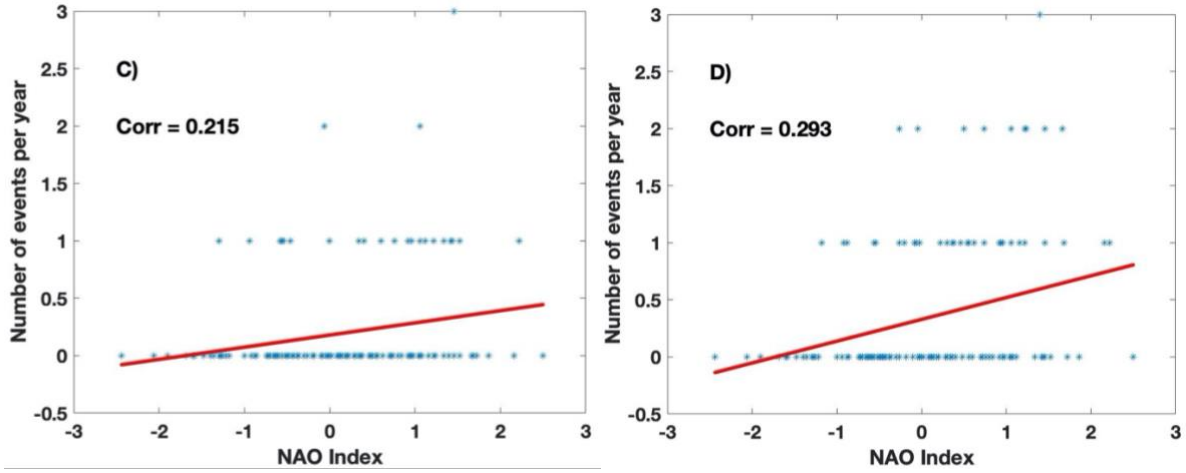

Figure 6.18: Scatter plot of the winter NAO index against number of events per decade at a) Devonport b) Fishguard c) Heysham d) Kinlochbervie. The red line indicates the linear regression between the two variables, correlation between the two variables is also displayed.

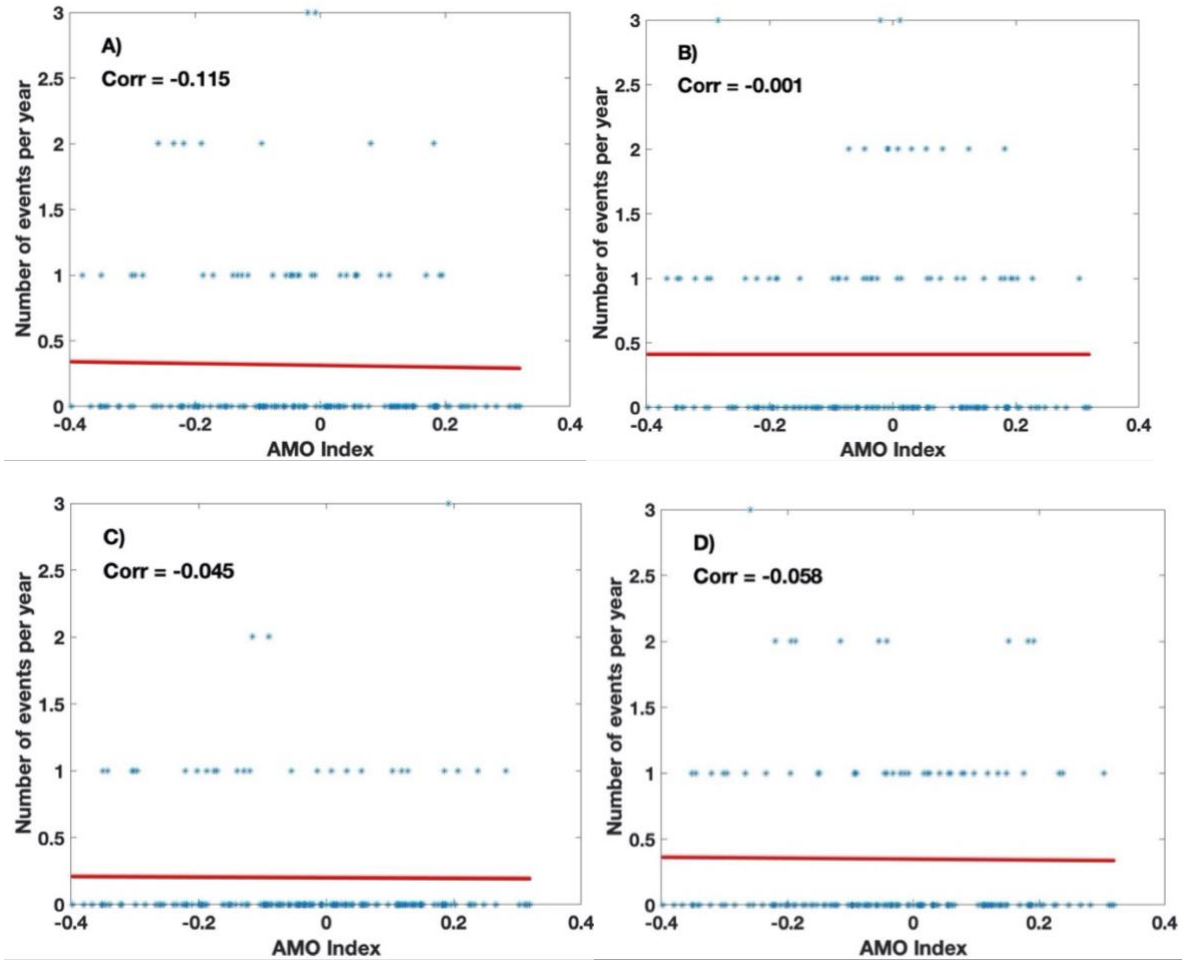

Figure 6.19: Scatter plot of the AMO index against number of events per decade at a) Devonport b) Fishguard c) Heysham d) Kinlochbervie. The red line indicates the linear regression between the two variables, correlation between the two variables is also displayed.

6.3.3 Future changes in compound flooding in the UK

The final sub-objective was to assess whether there is any evidence that events with compound flooding potential could change in the future (up to the year 2095) under the RCP 2.6 and 8.5 climate change scenarios. As discussed in Section 5.3.3, because HADGEM2-ES only uses precipitation flux instead of PWC, the rainfall component had to be discounted from this investigation. Therefore, the following results cannot be compared directly to the historic and present-day compound flooding conditions. Instead results under RCP 2.6 and 8.5 are compared to each other, to assess if this methodology is viable. Figure 6.20 andFigure 6.21 show identified compound events under the RCP 2.6 and 8.5 scenarios respectively. A total of 86 compound events were found during the century for RCP 2.6 and 69 compound events for RCP 8.5. When observing both annual and decadal compound flood occurrences (Figure 6.22a and b), no increasing or decreasing trend is evident. Both climate scenarios appear, however, to have more compound flood events in the first half of the 21st Century compared to the second half. For RCP2.6, 54 events were seen in the first half, compared to 32 in the second half, whilst for RCP8.5, 45 were seen in the first half of the century, compared to 24 in the second. Both scenarios show a trough between 2055 and 2065 before increasing towards the end by 2085. The greatest difference between RCP 2.6 and 8.5 occurs between 2045 and 2055 when RCP 2.6 has 13 events compared to 6 events in RCP 8.5.

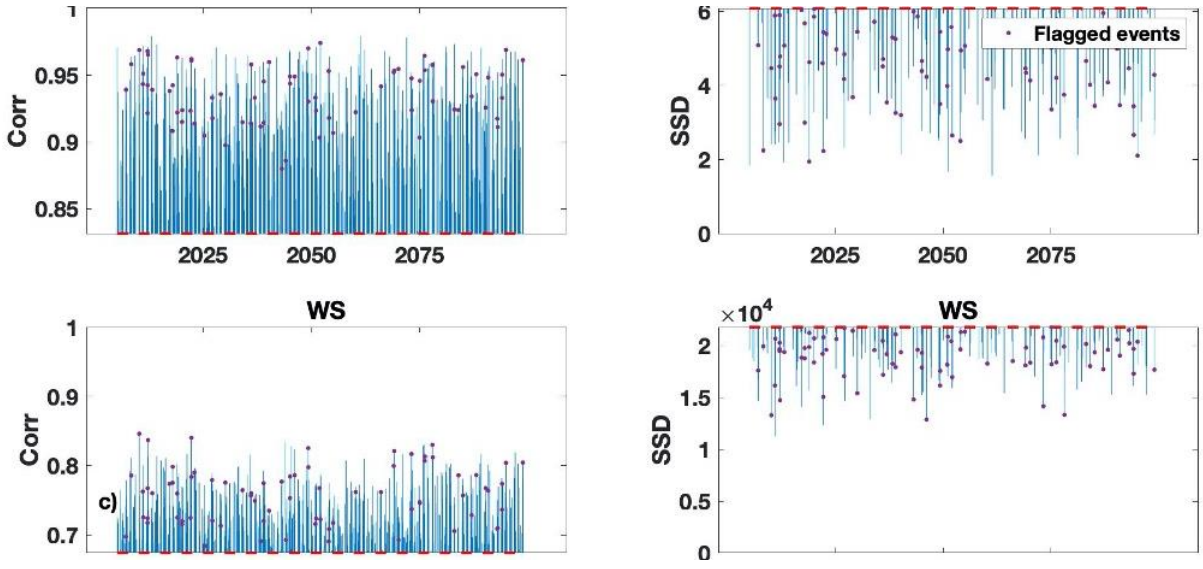

Figure 6.20: Correlation and Sum of Squared difference tests for a) and b) mean sea level pressure and c) and d) wind speed for HADGEM20-ES RCP 2.6 scenario to compound flooding reference conditions at Devonport.

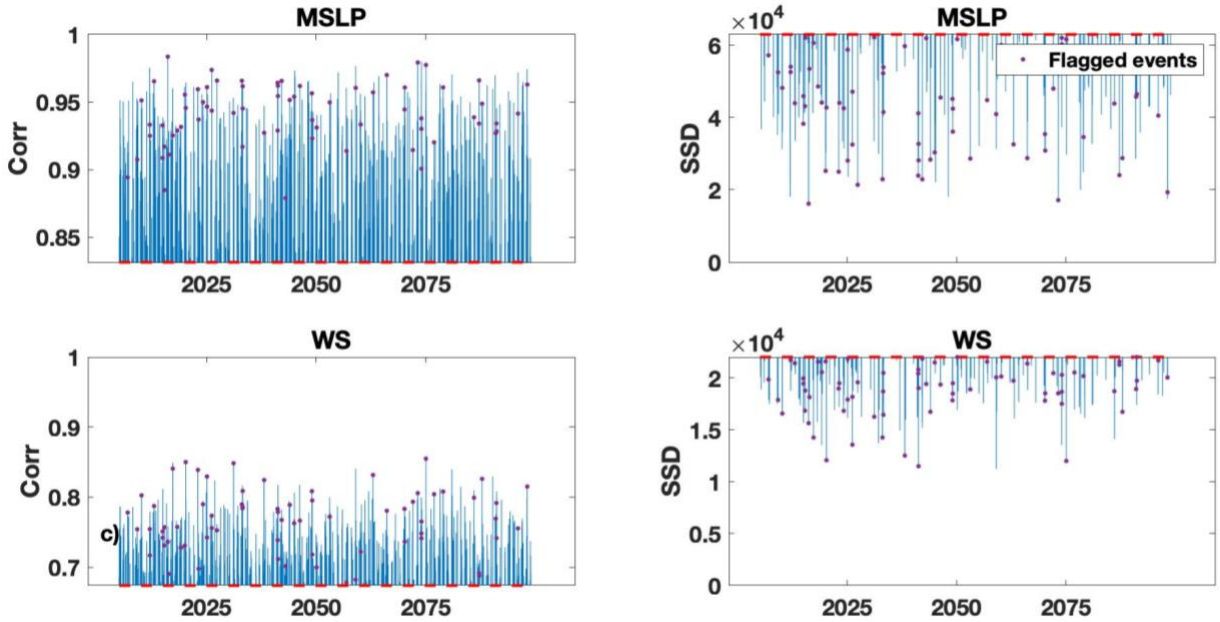

Figure 6.21: Correlation and Sum of Squared difference tests for a) and b) mean sea level pressure and c) and d) wind speed for HADGEM20-ES RCP 8.5 scenario to compound flooding reference conditions at Devonport.

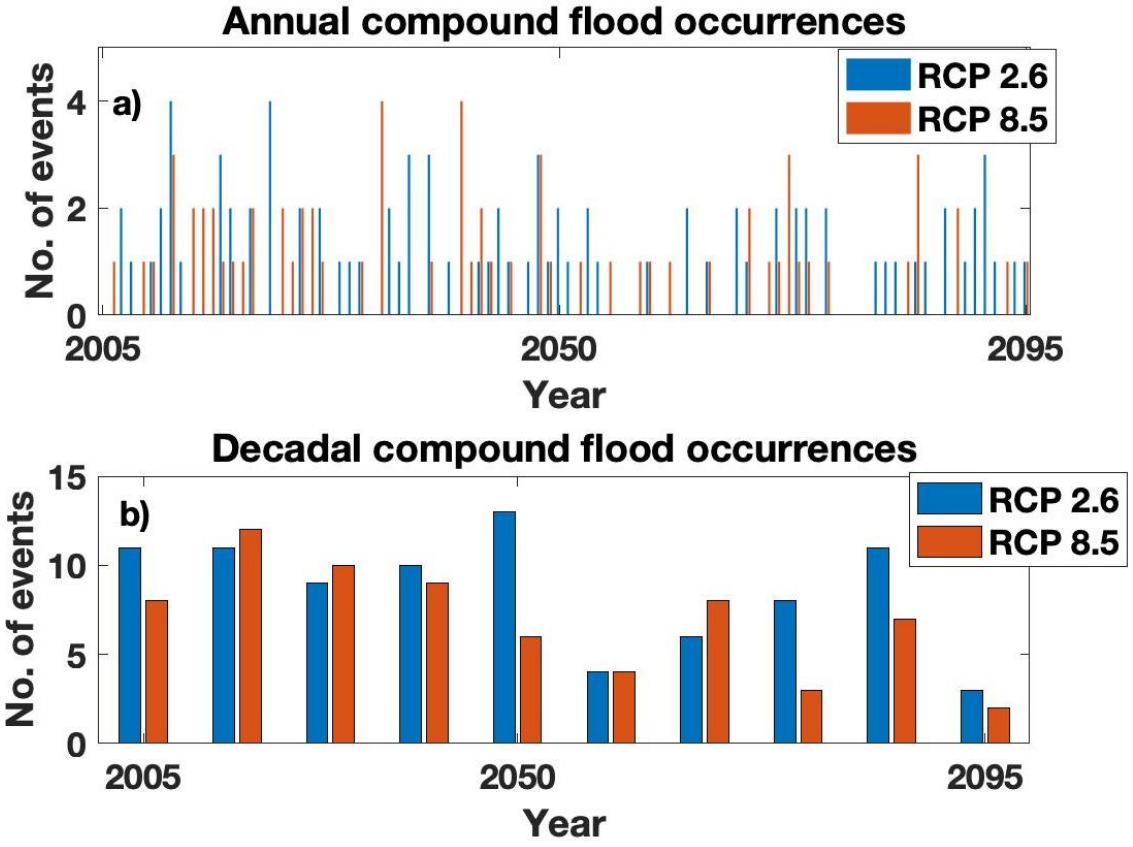

Figure 6.22: Frequency of compound events a) per year b) per decade identified in RCP2.6 and RCP8.5 scenarios from HADGEM2-ES projection.

6.4 Discussion

This chapter has developed a novel method for identifying events with compound flood potential using meteorological approaches, and assessed how the frequency of events has changed on centennial scales in the past and future, during periods when no direct observed records are available. Section 5.4.1 tested a range of thresholds for classifying a weather pattern as a compound flood event. The initial threshold used the weather patterns from observed events as the base threshold, however this was found to be too broad. The method found to be most effective was to vary the magnitude threshold (SSD) to match the number of observed events. This creates errors, as know compound events are not picked up.

Selecting an appropriate threshold is difficult for compound flooding compared to other weather pattern methods (see for example Neal et al., 2016), where only one variable and test was selected (predominantly sea level pressure). Studies which have looked at compound flooding weather pattern typologies (such as Wu et al., 2018) have just used sea level pressure, however, as shown in Section 4.4.2, wind speed and rainfall have a large impact in the UK on whether a storm will produce a single source event or a compound event.

No statistically significant trend was seen in the number of events occurring over the past time period 1851 to 2017. Due to the novelty of this study in extending the compound flooding records, no other studies are available to compare the results to directly. Instead they can be compared to changes in single source flood events. Haigh et al. (2010) analysed temporal changes in extreme water levels in the Channel, and found an increase in extreme water levels through the 20th century primarily due to the mean sea level rise. When looking at temporal changes in the surge component (which is most related to the weather patterns), they found considerable intra and inter-decadal variability in surge activity, however, no evidence of increasing trends. Furthermore, Woodworth & Blackman (2002) had similar finding for Liverpool over the period of 1768- 1999, with no overall increasing trend in surge. These studies corresponds to the results found in Section 5.4.2, which highlight decadal variability (Figure 6.16 Figure 6.17) but no overall longer-term trend.

Wadey et al. (2014) studied a century of sea level data for Newlyn, Cornwall, which serves a good comparison for the performance of the methodology at Devonport (100 km away). They also found clustering of extreme sea level events in the periods 1925-1945 and 1995-2005, whilst fewer events in the mid 20th Century (1945-1985). This is in agreement with Figure 6.16Figure 6.17, suggesting this methodology has merits.

A nationwide assessment of trends in UK river extreme flows was conducted by Hannaford & Marsh (2008). Over the periods of 1959-2003 and 1969-2003 they found an increasing trend in the frequency of POT (peak over threshold) events, particularly in maritime-influenced uplands areas of the north and west, however trends were not as strong for lowland areas. They also found strong correlation with the NAO, which likely linked the increasing trends to the more positive NAO phase prevalent from 1960's onwards. When comparing the same time period used in Hannaford & Marsh (2008) to Figure 6.16Figure 6.17, all sites show fewer events in the first half (1960-1980) of the century compared to the second half (1980-present). This would likely produce a similar positive trend to Hannaford and Marsh (2008).

A detailed study of one the UK's longest continuous river discharge records (1883- present) at Teddington on the Thames River revealed no long-term change in flood magnitude (Marsh & Harvey, 2012). Whilst this site is not related to any of the study sites, it does agree with the findings that no long-term trend in compound events is seen across any site.

The annual number of meteorological events with compound flooding potential was correlated against both the NAO and AMO to understand how climate oscillations can impact the frequency of events over the longer term. Positive correlation was found at all four sites (Figure 6.18), however, overall the correlation was weak ($p = 0.14 - 0.33$). This is in line with Table 6.2, which showed that whilst the majority of extreme surge and river events occurred during strong positive NAO years, the majority of compound events occurred during weak NAO winter years. Woodworth et al. (2007) found positive correlation between extreme surge and NAO around the UK, however, it was weakest on the west coast. This perhaps explains why the correlations in Figure 6.18 were relatively weak, despite Hannaford & Marsh (2008) finding strong correlation between extreme river flows and the NAO.

The AMO showed no correlation with the annual number of events. This was surprising as it's suggested long term variability of sea surface temperature in the North Atlantic can be associated with development and occurrence of extra-tropical storms over multidecadal time series (Brooks et al., 2020; Shaffrey & Sutton, 2006). Further studies, such as Peings & Magnusdottir (2014), suggest that AMO precedes the NAO by 10-15 years. Therefore, further analysis may require using time-lagged correlations.

The final sub-objective investigated if the same methodology could be applied to understand possible changes in the frequency of compound flooding in the future, using Devonport as a case study. Due to the difference in representation of precipitation (precipitation flux vs

precipitable water content), the reference compound flooding conditions were not able to apply a precipitation variable and focused on mean sea level pressure and wind speed. With this in mind, no comparison is made between the hindcast projection records. Surprisingly more compound events (86 compared to 69) were observed in RCP 2.6. This reason for this is unknown. However, when the SSD test was removed, and events identified on correlation alone, RCP 8.5 identified more events, suggesting the threshold methodology needs improving.

When looking at temporal trends, fewer events were seen in the latter half of the century. This is in contrast to the findings of Bevacqua et al. (2019), who found that the southwest of the UK was a hotspot for compound flooding probability increase under RCP 8.5 condition. It should be noted they identified precipitation as the primary driver of compound flooding probability change in the UK, whilst no precipitation variable was used in the future projection portion of this work.

6.5 Conclusions

This chapter has developed, for the first time, a methodology for studying compound flooding using weather patterning approaches, allowing changes in the frequency of events to be assessed over longer periods of time where no traditional observed direct records of compound flood events are available. This work has been carried out to demonstrate if the methodology is feasible and if it produces results similar to long term time series of the individual flood sources.

When investigating the entire 20th Century reanalysis timeseries length (1851 – 2017), it is found that no significant increasing or decreasing trend in compound flood events is found for any of the sites considered. There is interannual and interdecadal variability at all sites, with a maximum of 10 events per decade (Fishguard) whilst two sites (Fishguard and Heysham) feature decades with no compound flood events. Furthermore, the number of events per year were correlated to two different climate indices (the North Atlantic Oscillation, NAO and the Atlantic Multi-decadal Oscillation, AMO). Whilst the NAO showed stronger correlation (maximum of 0.34 at Devonport) no sites showed statistically significant correlation with either the NAO or AMO.

The method used three different variables (mean sea level pressure, wind speed and precipitable water content) and two different tests (location, using a correlation method; and

magnitude, using a sum of square difference method). This resulted in six different tests being applied to each timestamp and so raised the sensitivity of passing all six thresholds. All three variables were selected due to the impact they had on compound flood events compared to single source flood events (see Section 4.4.2). Further work could identify which variables and tests are most appropriate to allow for the most accurate results when comparing the 20th Century Reanalysis to observed events.

Once the two tests (PC and SSD) had been applied to the time series, a threshold had to be selected to identify what classes as a compound flood event. Due to the sensitivity the most appropriate method was found to be to manually adjust the threshold of the SSD tests until the same number of events was found as in the observed records. Unfortunately, this method is not as accurate, since the observed events were not always identified in the reanalysis timeseries. This highlights how sensitive the method is to threshold selection. Further work should identify the best threshold approach.

The meteorological reanalysis used the 20th Century Reanalysis and this was selected for its long temporal length (1851 to 2017). However, it is relatively coarse spatially (2^{o}). As a result, the reference conditions used as "compound flood conditions" may not have captured the conditions adequately, particularly as Section 5.4.1 highlighted how sensitive the methodology is. Further work should explore using a higher spatial resolution hindcast, such as ERA5 by ECMWF (Hersbach et al., 2018), which runs from 1950 to present. But there is a balance between have a long enough timeseries to explore the temporal trends in compound flooding, but a high enough spatial resolution to accurately capture the location and magnitude of the storm system. Furthermore, some events might be lost for overlapping time series which date further back than 1950.

As an application demonstrator, the methodology was only applied to compound flooding relating to the simultaneous occurrence of extreme storm surges and river flow at four sites around the UK. Additional work could develop the methods to incorporate the different combinations of compound flooding (including wave and pluvial). Furthermore, increase the number of sites both nationally and globally.

The work on future climate projections showed the method has potential, however it requires further refinement to use as a reliable assessment of future compound flooding changes. To address the mismatching rainfall parameter used in the 20th Century Reanalysis and HADGEM2-ES, a different reanalysis could be selected which uses precipitation flux. 20th

Century Reanalysis was selected to derive the reference conditions based on its long time series (going back to 1851) for use in historic compound flooding. For future projections, this length is not required. A reanalysis product such as ERA5 (Hersbach et al., 2018) provide precipitation flux, and has a temporal coverage of 1950-present, which is enough for most of the overlapping observed datasets (tide and river gauges). ERA5 also has the added benefit of having a much higher temporal and spatial resolution (hourly and 0.25^{o} respectively).

The results in this chapter have shown a method which could have far reaching applications. It has been demonstrated for use on historic weather data, but could also be used as a forecasting tool. The UK Met Office is already using weather pattern analysis tools such as Decider (Neal et al., 2016). If the methods set out can be refined, they could help to forecast potential compound flood events, which have traditionally been difficult to forecast. Finally, the same methodology could be further applied to future climate data, to gain a better understanding of potential future compound flooding.

7. Conclusions, implications and future work

7.1 Conclusions

The overall aim of this thesis has been to determine which regions of the UK coast are more subject to compound flooding, which combination of source variables are most apparent, and what variables (e.g. meteorological conditions, catchment characteristics) control the spatial patterns evident in compound events. This information is vital to support flood risk management, planning and emergency preparedness and response for now and in the future.

The first objective was to assess the potential for compound flooding arising from the joint occurrence of high sea levels and high river discharge around the coast of UK and the driving mechanisms involved. Results from two different statistical approaches, showed that there is clear evidence that joint occurrences of extreme sea levels and river discharge occur at a greater frequency on the western coast of the UK (between three and six joint events per decade) when compared to the eastern coast (between zero and one joint event per decade). To understand the relationship between extreme sea levels and river discharge, the meteorological conditions leading to individual extreme events were compared to joint extreme events. Along the south and western coasts, the storms which generate extreme surge or river discharge were found to be similar in characteristics in terms of sea-level pressure, wind speeds and rainfall. On the other hand, storms along the eastern coast which produced high surges were typically distinct from those which resulted in extreme river flow. The tracks of storms were also compared and this showed storms causing west coast flood events followed a similar route, whilst on the eastern coast, storms typically follow different pathways for the two flood types. The storm systems characteristics and tracks show that the meteorological conditions driving flood variables are the key factor controlling the likelihood of compound flooding (by extreme storm surges and river discharge) is likely in a given area of the UK.

At a more localised spatial scale, variation in the number of joint occurrences and dependency was investigated. This was achieved by correlating the joint extreme occurrence, at various time lags, with catchment characteristics (e.g., catchment size, base flow index and elevation gradient). Catchments with a larger area, high base flow index and shallow gradient were found to have a weaker relationship between surge and river discharge, as peak discharge tended to occur several days after the skew surge had peaked.

Additionally, the application of compound flood forecasting was tested using the Met Office's Decider tool, which uses 30 weather patterns to forecast potential consequences. It was found that on the west coast, the same or similar weather patterns (for example at Devonport: weather patterns 21 and 30) were responsible for surge only, river only and compound events. In contrast, on the east coast the weather patterns varied greatly for the different flood types.

The second objective expanded on the first to quantify the risk of underestimating compound flooding around the coast of the UK arising from the joint occurrence of all possible pairs of the four main flood sources. This was achieved by expanding upon the methodology of Chapter 3 to include precipitation (as a proxy for pluvial flooding) and wave height. It was found that the joint occurrence (and dependency) of six pairs of variables (i.e. surge vs wave, surge vs river discharge, surge vs rainfall, wave vs river discharge, wave vs rainfall and river discharge vs rainfall) occurs more frequently along the south and west coasts of the UK when compared to the east coast. The greatest number of joint occurrences and strongest dependency were found to be between skew surge and waves, showing a substantially stronger relationship compared to the other flood combinations. The next strongest relationship was found between waves and river discharge.

It is also shown for the first time that the variation in compound extreme events is primarily driven by meteorological difference in storm characteristics for all variable combinations. On the west coast all four flood sources are primarily driven by the same weather patterns, whilst on the east coast the coastal flood sources (storm surges and waves) are generated by differing weather systems to terrestrial (pluvial and fluvial). The influence of the North Atlantic Oscillation (NAO) on compound flooding was also investigated. Results showed that compound events on the west coast (excluding rainfall) are more likely during a positive winter NAO. On the east coast, surge and wave events are more likely to occur during a positive winter NAO, whilst rainfall and river discharge events are more likely during a weak winter NAO.

Finally, the return period of extreme events is found to be underestimated if dependence between variables is ignored. The flood frequency could be 5-6 times greater along the west coast, if variables are considered together as opposed to calculated as if independent of each other. This is a particularly important finding for flood management and planning.

The third objective was to assess how compound flooding varied in historical records (1851-2017) and might vary in the future (up to 2095), by using an indirect metrological based analysis to extend historic direct compound flooding records. This was achieved by developing

a novel method of identifying potential compound flooding events, by using the synoptic weather patterns which typically generate the flooding sources as a proxy. The method measured both magnitude and location of weather systems around the British Isles. It was found that the results were extremely sensitive to the threshold selected to identify compound flood events, and is an area of further refinement moving forwards. The results in Chapter 5 match to studies looking at long-term trends in both extreme river flow and surges, this suggest the methodology could be used in the future.

A key finding is that over the past 170 years (i.e., since 1851) no evidence was found that the weather patterns that typically generate compound events have increased or decreased over time, but there is year to year variability. When comparing the number of compound events over the last 170 years to climatic indices, weak positive correlation was found against the NAO, whilst no statistically significant correlation was found for the Atlantic Multidecadal Oscillation (AMO). Stronger positive correlation was expected with the NAO, as the individual flood sources (surge and flow) typically produce strong positive correlation against the NAO.

Finally, the approach was applied to future climate projections (up to 2095) under two difference emissions scenarios (RCP 2.6 and 8.5). Results showed no significant increase in compound flood potential, which disagrees with a recent study (Bevacqua et al., 2019). However, a number of key issues restricted successful implementation of this approach. These include identifying a precipitation variable which is valid for both the reference conditions (from the 20th Century Reanalysis) and climate projections; and improving the threshold identification for classifying a compound flood event. With refinement, results highlight the potential to use this method to assess possible future changes in compound flood analysis with further refinement. This study used the skew surge component, which does not take into account sea level rise. Sea level rise projections by the IPCC (2021), up to 2100 are between 0.3 and 1.8m, which will cause the number of coastal flooding events to increase greatly.

Limitations in this study were primarily down to data availability. The location of the data source can have a huge impact on the timeseries. For example, using a wave node in deep water vs shallow water will result in the wave parameters changing, as well as having implications on the performance of the wave model, as models frequently perform inadequately in shallow water (if using a model over observed data). In addition, the location of the river gauge has a huge impact on identifying compound events, as the timing of co-occurring events is greatly impacted by how downstream the river gauge is.

The frequency of the data source also has implications on the study. Gauged daily flow was used for river flow, whilst meteorological data was available at 6 hourly. Therefore, the results extreme river events may not have a link to the meteorological conditions found.

The duration of available data also had an impact, a minimum of 15 years of overlapping data was used. This is placed a limit on the accuracy of the extreme value analysis performed in Chapter 4. 10-year return periods were used, as extrapolating large return periods might lead to large uncertainties (such as 50 and 100 years, which are commonly used for by flood planning authorities).

This study has analysed changes in the hazard source (i.e., the surge and the meteorological conditions leading to that surge). The pathway of the hazard has not been considered, or how this might change through the time series, for example through natural or man-made changed in flood defences.

Chapter 5 focused on meteorological data to understand future changes in compound flooding, however the coastal/river response needs consideration, as the hazard might be dampened or amplified due to future changes in conditions (for example, through sea level rise).

Particularly novel and key output from this thesis are:

1. A new understanding for the UK that will benefit national flood hazard management. This included the first detailed assessment of meteorological drivers of compound flooding in the UK. The weather patterns and storm tracks which lead to compound and single source flood events were analysed, and found to be the primary reason for variability in compound flooding around the UK. For the first time, the characteristics of river catchments were used to assess compound flooding, this provided clarity to why some river/estuaries are more likely to result in compound flooding than other on a more localised scale which couldn't be explained by the meteorological drivers. Furthermore the first assessment of all four primary flood sources into one unified study. Whilst studies have included multiple sources, none had previously incorporated all four drivers (storm tides, waves, pluvial and fluvial) and established if there are any connections between all four. Furthermore, this thesis has quantified for the first time how the flood risk can be significant underestimated if flood sources are treated as independent compared to as compound events
1. New methods/approached transferable to other locations for global impact. This includes the use of a novel method to extend compound flooding records beyond

directly observed records, which has previously been a key limiting factor in assessing temporal trends in compound flooding. This methodology involved using the weather patterns leading to compound events to expand timeseries records. Furthermore, these methods were shown to have the potential to be used to predict changes in compound flood occurrences, using future climate projections.

7.2 Implications

Establishing the spatial variability of compound flooding involving skew surge and river discharge can have significant implications and benefits for all aspects of flood management. The results highlight the different requirement for flood defence planning at different locations. On the west coast, where compound flooding has been shown to be more prevalent, defence planning and upgrading must incorporate the potential for compound flooding. In contrast, on the east coast flooding defence planning should focus on the single flood sources, where the threat of, for example, of a large storm surge is far greater than of a compound event.

The flood event in Lymington, UK in 1999, highlights the need to plan for compound events. An investment in flood defences protected the town against extreme sea levels, including new sluice gates on the river. In December 1999, a storm surge forced the gates shut on the river over several tidal cycles, whilst intense rainfall caused the river to build on the fluvial side, which eventually burst its banks and caused flooding of property (Ruocco et al., 2011a; Turner, 2000) The research in this thesis has highlighted that on the south coast (where Lymington is found), extreme surges and river discharge are caused by the same physical mechanisms and so this type of event is likely and needs protecting against. Areas identified in the thesis as being at higher likelihood of compound flooding should be modelled in greater detail to help plan future flood risk accordingly.

Flood defences are not the only aspect of management, however. This research can also improve the emergency response to flooding. The application of Coastal Decider (Neal et al., 2016) to compound flooding events in Section 3.3.4 showed the potential to use weather pattern forecasting to identify regions likely to be flooded and allow response resources such as pumps and barriers to be mobilised to affected sites quicker. Additionally, emergency planning may differ for compound events. For examples, roads that were typically used for evacuation during

coastal flooding only events might become blocked if river flooding also occurs simultaneously. This could result in areas being cut off from emergency services, increasing risk to life and infrastructure. This is highlighted by the Fukushima Daiichi nuclear disaster in 2011, when 9.0 magnitude earthquake triggered a tsunami hitting eastern Japan. The nuclear powerplant was damaged by the tsunami, however, the response plan was disrupted in part due to blocked roads from the earthquake. Whilst not a pure compound flood event, the lack of planning for compounding natural hazard events (in this case, a tsunami combined with an earthquake) resulted in a major nuclear disaster and 18,500 deaths (Funabashi & Kitazawa, 2012). Emergency planning should therefore encompass scenarios based on the single source and compound flood events.

The findings in Chapter 3 indicated that the characteristics of river catchments can have a large impact on the likelihood of compound flooding. Rivers which respond more rapidly to rainfall (i.e. have a steep hydrograph) through smaller, steeper catchments with a more clay-based geology are more likely to coincide with a surge peak. Areas such as South Wales experienced high levels of compound flood variability when looking at surge vs river discharge, this is because of the difference in catchment characteristics, therefore in these regions, when distributing flood defence resources, "flashy rivers" (those which respond quickly to rainfall) should be focused on for compound flood defences. This could include "hard" flood defences, such as increasing embankment sizes or dredging, or soft engineering approaches such as flood plain zoning or managed realignments.

Objective 2 highlighted and quantified, for the first time, that flood likelihood is significantly underestimate if the four drives are considered independent, particularly for the west coast of the UK. Therefore, future flood risk planning collectively should consider all types of flooding potential, rather than calculating each individually, as has been traditionally done in the past. The Environment Agency is currently updating its guidance on joint probability events. The methods and insights of this research can inform such analysis.

Until now, assessment of compound flooding has been limited by the amount of overlapping data of the four flood variables, either observed or modelled. This frequently amounted in short data lengths. For example, Ward et al. (2018) is the largest global study and has mean overlap of 39 years between river discharge stations and tide gauges. Shorter datasets prevent conclusions being drawn on temporal changes in compound events. By extending this record to almost 170 years using a unique weather patterning approach on the 20th century Reanalysis

dataset, far more robust insight can be drawn on flood events and the influence of systematic trends vs multidecadal regional climate variability; in this study, the latter effect dominates.

Flood forecasting using weather patterns has advantages over more common numerical weather predictions (NWP) as they provide longer lead times. Longer lead in times are extremely useful to governments and response agencies. Large-scale multi-regional coordinated responses can take several days to weeks to coordinate, which is a not a time scale currently possible from forecasts using regularly updating coupled ocean-atmosphere models (Neal et al., 2018). The use of predetermined weather patterns allows for forecast to be made from further out than traditional NWP's. The Met Office Coastal Decider tool has already been shown to be an effective forecasting tool for storm surges and waves for as much as 32 days out, by using 30 weather patterns with associated likelihoods of extreme surge and waves occurring around the UK (Neal et al., 2018). The ability to forecast for compound flood events from any combination of storm surges, waves, rivers and pluvial flooding would significantly improve the UK Flood Forecasting Centres capabilities, and improve responses to floods, potentially lowering the impact in terms of damages, injuries and deaths.

Understanding long term future changes in compound flooding events is a key part of managing them. The individual sources of flooding have been relatively well studied with regards to future climate change. For example, storm surges and waves will be more likely to cause floods due to rising mean sea levels (Hinkel et al., 2014; Vitousek et al., 2017) and storm intensity may increase (Lennart Bengtsson et al., 2006; Shaw et al., 2016). Furthermore, the probability of extreme precipitation events has been found to increase, raising the likelihood of pluvial and fluvial flood events (Otto et al., 2018). However, just one study to date has investigated compound flooding under climate change (i.e., Bevacqua et al., 2019). Surge and precipitation models were forced with CMIP5 projections from the business-as-usual RCP 8.5 scenario. They found an increased probability of compound flooding in the UK would increase. This highlights the need for increased studies on future changes in compound flooding. Using weather types as a proxy for compound flooding as shown in this thesis is a key way this can this assessment can be done.

7.3 Further work

This research has raised a number of further research questions, and avenues of investigation for future work. These are summarised below.

1. The first objective of this study (Chapter 3) investigated the national scale likelihood of extreme sea levels occurring around the same time as extreme river flow. Whilst extreme flow indicates the likelihood of flooding, the capacity and anthropogenic flood defences of the rivers are not specified, therefore it is unknown at what point river flow will lead to a river breaching its bank. Further studies should use hydrodynamic modelling to study compound flooding in more localised regions, focusing on the catchments found to have high incidents of compound flooding (such as Wales, southwest and northwest of England). This would allow accurate analysis on when river and coastal flood defences would be breached, as well as the extent and depth of flooding.
2. The work in Objective 1 (Chapter 3) highlighted the important impact catchment characteristics can have on the response of rivers and thus on compound flooding. The study looked at three different variables (i.e., Base Flow Index, catchment size and elevation variation). Whilst these were considered the most important variables, additional catchment characteristics may be of importance in specific locations. These could include land usage, for example woodlands will slow down water reaching a river and flatten the flood curve, whilst human developments typically speed up the time it takes water in the catchment to reach the river. Geomorphology would also need further investigation. Whilst Base Flow Index and elevation variation gave broad characterisation of a catchment's sediment and gradient, more detailed data, such as bedrock type and high resolution topography would provide greater insight. Additionally, human adaptations to the river and water course (such as weirs, dams and reservoirs) and will have a large impact on the flood hydrograph.
3. The analysis in Objective 2 (Chapter 4) looked at all the possible combinations of pairs of flooding sources. However, it did not consider higher dimensions of occurrences (i.e., 3 or more sources). This can involve more complex statistical models which have been done at local scales (Bevacqua et al., 2017) which could be hard to do on a national scale. Future studies should look at multidimensional compound flooding studies on a larger scale.
4. This study used observed discrete datasets for all the variables (excluding waves). With 44 tide gauges in the UK National Tide Gauge Network, and a coastline of ~12,000 km (CIA, 2020), data is only available on average every ~270 km. Using a modelled hindcast datasets could provide a continuous record of compound flooding along the

UK coastline, which would be of more use to UK flood and coastal erosion management. For example, Couasnon et al. (2019) used the CaMa-Flood model v362 (Yamazaki et al., 2014) for river discharge and the Global Tide and Surge Model (GTSM) (Muis et al., 2016).

5. Throughout this thesis, rainfall has been used as a proxy for pluvial flooding, as has been applied in other compound flood studies (e.g. Wahl et al., 2015). Whilst this is acceptable on a large scale; to truly account for pluvial flooding, a more accurate metric would be required. Typically, pluvial flooding is assessed using inundation models, which consider factors such ground type and slope. Future compound flooding studies should find a way to incorporate more accurate pluvial flooding measurements on a large scale.
6. Objective 2 (Chapter 4) used significant wave height to represent waves, however, as specified earlier, wave period, direction and spreading can all have impact on the wave climate and potential impact. Future work using all wave parameters (a longer observed record, or hindcast with more accurate representation of all wave parameters) would help to identify regions at risk of compound flooding involving waves. Furthermore, Coastal bathymetry and geomorphology can also have an impact on the nature of a wave hitting the coastline, for example, a steep beach run up versus a shallow run up. Finally, the impact of an open coast versus a fetch limited coast (such as the Irish Sea), which can reduce wave parameters such as wave period.
7. Objective 3 (Chapter 5) investigated a novel method of assessing compound flooding using the weather patterns that typically drive compound events. The technique however was difficult to implement successfully due to compound events requiring multiple weather parameters (mean sea level pressure, wind speed and precipitable water content) to define the synoptic patterns. When combined with two different tests (magnitude and location) this created six thresholds to define compound events. Further work should analyse if all the tests are required. For example, when comparing the reference conditions against known compound events (Figure 6.7), the correlation for mean sea level pressure was larger compared to wind speed and precipitable water content, however had a far great sum of square difference score (i.e., events differed more from the reference conditions), compared to the other variables. This would suggest that mean sea level pressure was far more sensitive to changes in magnitude than location. Another difficulty was setting the threshold to classify a weather pattern as a compound event. Finding a balance between avoiding false positive results but

capturing known compound events was challenging when using the six tests mentioned above. Further work should study how the thresholds could be calculated to accurately assess compound flooding in weather patterns.

8. This thesis also attempted to apply the same weather pattern technique to future climate projection (HADGEM2-ES). However, the projection and the meteorological reanalysis used (20th Century Reanalysis) did not have the same precipitation parameters available (precipitation flux, and precipitable water content). Therefore, the reference compound flooding conditions generated from the reanalysis data did not match. The 20th Century reanalysis was selected to for its long temporal coverage, however further work into future compound flooding should use a shorter meteorological dataset (such as ERA5) to better match climate projections.

References

Ambaum, M. H. P., Hoskins, B. J., & Stephenson, D. B. (2001). Arctic Oscillation or North Atlantic Oscillation? *Journal of Climate*, *14*(16), 3495–3507. https://doi.org/10.1175/1520-0442(2001)014<3495:AOONAO>2.0.CO;2

Arns, A., Dangendorf, S., Jensen, J., Talke, S., Bender, J., & Pattiaratchi, C. (2017). Sea-level rise induced amplification of coastal protection design heights. *Scientific Reports*, *7*, 1–9. https://doi.org/10.1038/srep40171

Barnston, A. G., & Livezey, R. E. (1987). Classification, seasonality and persistence of low-frequency atmospheric circulation patterns. *Monthly Weather Review*, *115*(6), 1083–1126. https://doi.org/10.1175/1520-0493(1987)115<1083:CSAPOL>2.0.CO;2

Baumann, J., Chaumillon, E., Bertin, X., Schneider, J. L., Guillot, B., & Schmutz, M. (2017). Importance of infragravity waves for the generation of washover deposits. *Marine Geology*, *391*(May), 20–35. https://doi.org/10.1016/j.margeo.2017.07.013

Baxter, P. J. (2005). The east coast Big Flood, 31 January–1 February 1953: a summary of the human disaster. *Phil. Trans. R. Soc.*, *363*, 1293–1312. https://doi.org/https://doi.org/10.1098/rsta.2005.1569

Bengtsson, Lars. (2016). Probability of combined high sea levels and large rains in Malmö, Sweden, southern Öresund. *Hydrological Processes*, *30*(18), 3172–3183. https://doi.org/10.1002/hyp.10815

Bengtsson, Lennart, Hodges, K. I., & Roeckner, E. (2006). Storm tracks and climate change. *Journal of Climate*, *19*(15), 3518–3543. https://doi.org/10.1175/JCLI3815.1

Benito, G., Lang, M., Barriendos, M., Llasat, M. C., Francés, F., Ouarda, T., Thorndycraft, V. R., Enzel, Y., Bardossy, A., Coeur, D., & Bobée, B. (2004). Use of systematic, palaeoflood and historical data for the improvement of flood risk estimation. Review of scientific method. *Natural Hazards*, *31*(3), 623–643. https://doi.org/10.1023/B:NHAZ.0000024895.48463.eb

Bernardara, P., Andreewsky, M., & Benoit, M. (2011). Application of regional frequency analysis to the estimation of extreme storm surges. *Journal of Geophysical Research: Oceans*, *116*(2), 1–11. https://doi.org/10.1029/2010JC006229

Bevacqua, E., Maraun, D., Hobæk Haff, I., Widmann, M., & Vrac, M. (2017). Multivariate

statistical modelling of compound events via pair-copula constructions: Analysis of floods in Ravenna (Italy). *Hydrology and Earth System Sciences*, *21*(6), 2701–2723. https://doi.org/10.5194/hess-21-2701-2017

Bevacqua, E., Maraun, D., Vousdoukas, M. I., Voukouvalas, E., Vrac, M., Mentaschi, L., & Widmann, M. (2019). Higher probability of compound flooding from precipitation and storm surge in Europe under anthropogenic climate change. *Science Advances*, *5*(9). https://doi.org/10.1126/sciadv.aaw5531

Bevacqua, E., Vousdoukas, M., Zappa, G., Hodges, K., Shepherd, T., Maraun, D., Mentaschi, L., & Feyen, L. (2020). *Global projections of compound coastal meteorological extremes*. 1–20. https://doi.org/10.31223/OSF.IO/4X2U8

Bezak, N., Brilly, M., & Šraj, M. (2014). Comparaison entre les méthodes de dépassement de seuil et du maximum annuel pour les analyses de fréquence des crues. *Hydrological Sciences Journal*, *59*(5), 959–977. https://doi.org/10.1080/02626667.2013.831174

Bilskie, M. V., & Hagen, S. C. (2018). Defining Flood Zone Transitions in Low-Gradient Coastal Regions. *Geophysical Research Letters*, *45*(6), 2761–2770. https://doi.org/10.1002/2018GL077524

Blake, E. S., & Zelinksy, D. A. (2018). Hurricane Harvey (AL092017). In *National Hurricane Center Tropical Report* (Vol. AL092017). https://doi.org/10.1097/jpn.0000000000000424

Brázdil, R., Kundzewicz, Z. W., & Benito, G. (2006). Historical hydrology for studying flood risk in Europe. *Hydrological Sciences Journal*, *51*(5), 739–764. https://doi.org/10.1623/hysj.51.5.739

British Oceanographic Data Centre. (2018). *UK Tide Gauge Network*. https://www.bodc.ac.uk/data/hosted_data_systems/sea_level/uk_tide_gauge_network/

Brooks, A., Roberts, H., & Brooke, J. (2020). The impacts of climate change on fisheries, relevant to the coastal and marine environment around the UK. *Marine Climate Change Impacts Partnership (MCCIP) Science Review*, *2020*(January), 566–592. https://doi.org/10.14465/2020.arc24.tra

Brown, J., Eastwood, L. A., Martin, A., Gold, I., Bird, C., Thompson, C., & Farrington, B. (2018). WireWall: a new approach to measuring coastal wave hazard. *3rd International Conference on Protection against Overtopping, 6-8 June 2018, UK*, *3*(66), 6–8.

Brown, J. M., Souza, A. J., & Wolf, J. (2010). Surge modelling in the eastern Irish Sea: Present and future storm impact. *Ocean Dynamics*, *60*(2), 227–236. https://doi.org/10.1007/s10236-009-0248-8

Brown, S., & Nicholls, R. J. (2015). Subsidence and human influences in mega deltas: The case of the Ganges-Brahmaputra-Meghna. *Science of the Total Environment*, *527–528*, 362–374. https://doi.org/10.1016/j.scitotenv.2015.04.124

Brown, S., Nicholls, R. J., Goodwin, P., Haigh, I. D., Lincke, D., Vafeidis, A. T., & Hinkel, J. (2018). Quantifying Land and People Exposed to Sea-Level Rise with No Mitigation and 1.5°C and 2.0°C Rise in Global Temperatures to Year 2300. *Earth's Future*, *6*(3), 583–600. https://doi.org/10.1002/2017EF000738

Buishand, T. A. (1984). Bivariate Extreme-Value Data and the Station-Year Method. *Journal of Hydrology*, *69*, 77–95.

Burt, S. D., & Mansfield, D. . (1988). The Great Storm of 15-16 October 1987. *Weather*, *43*, 90–110.

Burzel, A., & Becker, B. P. J. (2014). *Of Flooding On Critical Infrastructure How does access to this work benefit you ? Let us know !*

Callaghan, D. P., Nielsen, P., Short, A., & Ranasinghe, R. (2008). Statistical simulation of wave climate and extreme beach erosion. *Coastal Engineering*, *55*(5), 375–390. https://doi.org/10.1016/j.coastaleng.2007.12.003

Camus, P., Haigh, I. D., Nasr, A., Wahl, T., Darby, S. E., & Nicholls, R. J. (2021). Regional analysis of multivariate compound flooding potential: sensitivity analysis and spatial patterns. *Natural Hazards and Earth System Sciences Discussions*, *2021*(October 2000), 1–32. https://nhess.copernicus.org/preprints/nhess-2021-50/

Cangialosi, J. P., Latto, A. S., & Berg, R. (2017). *National Hurrican Centrer Tropical Cyclone Report: Hurricane Irma (AL112017)*. https://www.nhc.noaa.gov/data/tcr/AL112017_Irma.pdf

Castelle, B., Dodet, G., Masselink, G., & Scott, T. (2017). A new climate index controlling winter wave activity along the Atlantic coast of Europe: The West Europe Pressure Anomaly. *Geophysical Research Letters*, *44*(3), 1384–1392. https://doi.org/10.1002/2016GL072379

CCO. (2020). *The Channel Coastal Observatory*. https://www.channelcoast.org/cco/

CEFAS. (2020a). *Wavenet*. http://wavenet.cefas.co.uk

CEFAS. (2020b). *Wavenet QA/QC Procedures*. https://www.cefas.co.uk/data-and-publications/wavenet/qa-qc-procedure/

CEH. (2018). *NRFA*. https://nrfa.ceh.ac.uk/data/search

Chartteron, J., Clarke, C., Daly, E., Dawks, S., Elding, C., Fenn, T., Hick, E., Miller, J., Morris, J., Ogunyoye, F., & Salado, R. (2016). The costs and impacts of the winter 2013 to 2014 floods. In *Environment Agency*. https://www.gov.uk/government/publications/the-costs-and-impacts-of-the-winter-2013-to-2014-floods

Chen, W. B., & Liu, W. C. (2014). Modeling flood inundation induced by river flow and storm surges over a river basin. *Water (Switzerland)*, *6*(10), 3182–3199. https://doi.org/10.3390/w6103182

Church, J. A., Clark, P. U., Cazenave, A., Gregory, J. M., Jevrejeva, S., Levermann, A., Merrifield, M. A., Milne, G. A., Nerem, R. S., Nunn, P. D., Payne, A. J., Pfeffer, W. T., Stammer, D., & Unniskrishnan, A. S. (2013). Sea Level Change. In *Climate Change 2013: The Physical Science Basis. Contribution of Working Group I to the Fifth Assessment Report of the Intergovernmental Panel on Climate Change* (pp. 493–499). https://doi.org/10.1016/B978-0-12-409548-9.10820-6

CIA. (2020). *The World Fact Book - UK*. https://www.cia.gov/the-world-factbook/countries/united-kingdom/#geography

Coles, S., Bawa, J., Trenner, L., & Dorazio, P. (2001). *An introduction to statistical modeling of extreme values* (Vol. 208).

Coles, S., Heffernan, J., & Tawn, J. (1999). Dependence Measures for Extreme Value Analyses. *Extremes*, *2*(4), 339–365. https://doi.org/10.1023/A:31009963131610

Compo, G. P., Whitaker, J. S., Sardeshmukh, P. D., Matsui, N., Allan, R. J., Yin, X., Gleason, B. E., Vose, R. S., Rutledge, G., Bessemoulin, P., BroNnimann, S., Brunet, M., Crouthamel, R. I., Grant, A. N., Groisman, P. Y., Jones, P. D., Kruk, M. C., Kruger, A. C., Marshall, G. J., … Worley, S. J. (2011). The Twentieth Century Reanalysis Project. *Quarterly Journal of the Royal Meteorological Society*, *137*(654), 1–28. https://doi.org/10.1002/qj.776

Couasnon, A., Eilander, D., Muis, S., Veldkamp, T. I. E., Haigh, I. D., Wahl, T., Winsemius,

H., & Ward, P. J. (2019). Measuring compound flood potential from river discharge and storm surge extremes at the global scale and its implications for flood hazard. *Natural Hazards and Earth System Sciences Discussions*, 1–24. https://doi.org/10.5194/nhess-2019-205

Dawson, D. A., Hunt, A., Shaw, J., & Gehrels, W. R. (2018). The Economic Value of Climate Information in Adaptation Decisions: Learning in the Sea-level Rise and Coastal Infrastructure Context. *Ecological Economics*, *150*(March), 1–10. https://doi.org/10.1016/j.ecolecon.2018.03.027

Dawson, D., Shaw, J., & Roland Gehrels, W. (2016). Sea-level rise impacts on transport infrastructure: The notorious case of the coastal railway line at Dawlish, England. *Journal of Transport Geography*, *51*(February 2014), 97–109. https://doi.org/10.1016/j.jtrangeo.2015.11.009

Devon Maritime Forum. (2014). *Reviewing the impacts, responses and resilience of people and places in Devon to the winter storms of 2013/2014*.

Dixon, H., Hannaford, J., & Fry, M. J. (2013). The effective management of national hydrometric data: experiences from the United Kingdom. *Hydrological Sciences Journal*, *58*(7), 1383–1399. https://doi.org/10.1080/02626667.2013.787486

Emanuel, K. (2017). Assessing the present and future probability of Hurricane Harvey's rainfall. *Proceedings of the National Academy of Sciences of the United States of America*, *114*(48), 12681–12684. https://doi.org/10.1073/pnas.1716222114

Enfield, D. B., Mesta-Nunez, A. M., & Trimble, P. J. (2001). The Atlantic multidecadal oscillation and its relation to rainfall and river flows in the continental U.S. *Geophysical Research Letters*, *28*(10), 2077–2080.

Environment Agency, Chatterton, J., Viviattene, C., Morris, J., Penning-Rowsell, E. C., Tapsell, S. M., Ii, T. L. J., Walker, G., Calvert, M., Tsapakis, I., Cheng, T., Bolbol, A., Bourne, N., Gillan, W., Notley, S. O., Taylor, N., & ... (2013). The costs and impacts of the winter 2013 to 2014 floods, Report – SC140025/R1. In *Applied Ergonomics* (Vol. 28). https://trl.co.uk/sites/default/files/PPR348.pdf%0Ahttp://dx.doi.org/10.1016/j.jtrangeo.2012.11.003%0Ahttp://dx.doi.org/10.1016/j.apergo.2015.03.019

Fang, J., Wahl, T., Fang, J., Sun, X., Kong, F., & Liu, M. (2020). Compound flood potential

from storm surge and heavy precipitation in coastal China. *Hydrology and Earth System Sciences Discussions*, *July*, 1–24. https://doi.org/10.5194/hess-2020-377

Finlay, B. J. (2020). *Autumn and winter floods 2019-20*. *March*.

Frau, R., Andreewsky, M., & Bernardara, P. (2018). The use of historical information for regional frequency analysis of extreme skew surge. *Natural Hazards and Earth System Sciences*, *18*(3), 949–962. https://doi.org/10.5194/nhess-18-949-2018

Fritz, H. M., Blount, C. D., Thwin, S., Thu, M. K., & Chan, N. (2009). Cyclone Nargis storm surge in Myanmar. *Nature Geoscience*, *2*(7), 448–449. https://doi.org/10.1038/ngeo558

Funabashi, Y., & Kitazawa, K. (2012). Fukushima in review: A complex disaster, a disastrous response. *Bulletin of the Atomic Scientists*, *68*(2), 9–21. https://doi.org/10.1177/0096340212440359

Gaitan, S., van de Giesen, N. C., & ten Veldhuis, J. A. E. (2016). Can urban pluvial flooding be predicted by open spatial data and weather data? *Environmental Modelling & Software*, *85*, 156–171. https://doi.org/10.1016/J.ENVSOFT.2016.08.007

Ganguli, P., & Merz, B. (2019). Trends in Compound Flooding in Northwestern Europe during 1901–2014. *Geophysical Research Letters*, 0–2. https://doi.org/10.1029/2019gl084220

Genest, C., Rémillard, B., & Beaudoin, D. (2009). Goodness-of-fit tests for copulas: A review and a power study. *Insurance: Mathematics and Economics*, *44*(2), 199–213. https://doi.org/10.1016/j.insmatheco.2007.10.005

Gill, J. C., & Malamud, B. D. (2014). Reviewing and visualizing the interactions of natural hazards. *Reviews of Geophysics*, *69*, 680–722. https://doi.org/10.1002/2013RG000445

Gill, J. C., & Malamud, B. D. (2017). Anthropogenic processes, natural hazards, and interactions in a multi-hazard framework. *Earth-Science Reviews*, *166*, 246–269. https://doi.org/10.1016/j.earscirev.2017.01.002

Gouldby, B., Méndez, F. J., Guanche, Y., Rueda, A., & Mínguez, R. (2014). A methodology for deriving extreme nearshore sea conditions for structural design and flood risk analysis. *Coastal Engineering*, *88*, 15–26. https://doi.org/10.1016/j.coastaleng.2014.01.012

Gouldby, Ben, Wyncoll, D., Panzeri, M., Franklin, M., Hunt, T., Hames, D., Tozer, N.,

Hawkes, P., Dornbusch, U., & Pullen, T. (2017). Multivariate extreme value modelling of sea conditions around the coast of England. *Proceedings of the Institution of Civil Engineers - Maritime Engineering*, *170*(1), 3–20. https://doi.org/10.1680/jmaen.2016.16

Gustard, A., Bullock, A., & Dixon, J. M. (1992). Low flow estimation in the United Kingdom. *Institute of Hydrology, Wallingford*, *108*, 1–292. http://nora.nerc.ac.uk/id/eprint/6050/1/IH_108.pdf

Haigh, I. D., Eliot, M., & Pattiaratchi, C. (2011). Global influences of the 18.61 year nodal cycle and 8.85 year cycle of lunar perigee on high tidal levels. *Journal of Geophysical Research*, *116*(C6), C06025. https://doi.org/10.1029/2010JC006645

Haigh, I. D., Ozsoy, O., Wadey, M. P., Nicholls, R. J., Gallop, S. L., Wahl, T., & Brown, J. M. (2017). An improved database of coastal flooding in the United Kingdom from 1915 to 2016. *Scientific Data*, *4*. https://doi.org/10.1038/sdata.2017.100

Haigh, I. D., Wadey, M. P., Gallop, S. L., Loehr, H., Nicholls, R. J., Horsburgh, K., Brown, J. M., & Bradshaw, E. (2015). A user-friendly database of coastal flooding in the United Kingdom from 1915-2014. *Scientific Data*, *2*, 1–13. https://doi.org/10.1038/sdata.2015.21

Haigh, I. D., Wadey, M. P., Wahl, T., Ozsoy, O., Nicholls, R. J., Brown, J. M., Horsburgh, K., & Gouldby, B. (2016). *Analysis : Spatial and temporal analysis of extreme sea level and storm surge events around the coastline of the UK*. 1–14. https://doi.org/10.1038/sdata.2016.107

Haigh, I., Nicholls, R., & Wells, N. (2010). Assessing changes in extreme sea levels: Application to the English Channel, 1900-2006. *Continental Shelf Research*, *30*(9), 1042–1055. https://doi.org/10.1016/j.csr.2010.02.002

Hallegatte, S., Green, C., Nicholls, R. J., & Corfee-Morlot, J. (2013). Future flood losses in major coastal cities. *Nature Climate Change*, *3*(9), 802–806. https://doi.org/10.1038/nclimate1979

Hamdi, Y., Bardet, L., Duluc, C. M., & Rebour, V. (2015). Use of historical information in extreme-surge frequency estimation: The case of marine flooding on the La Rochelle site in France. *Natural Hazards and Earth System Sciences*, *15*(7), 1515–1531. https://doi.org/10.5194/nhess-15-1515-2015

Hamdi, Y., Duluc, C. M., Bardet, L., & Rebour, V. (2016). Use of the spatial extremogram to

form a homogeneous region centered on a target site for the regional frequency analysis of extreme storm surges. *International Journal of Safety and Security Engineering*, *6*(4), 777–781. https://doi.org/10.2495/SAFE-V6-N4-777-781

Hannaford, J., & Marsh, T. (2008). High-flow and flood trends in a network of undisturbed catchments in the UK. *International Journal of Climatology*, *28*, 1325–1338. https://doi.org/10.1002/joc

Hao, Z., & Singh, V. P. (2016). Review of dependence modeling in hydrology and water resources. *Progress in Physical Geography*, *40*(4), 549–578. https://doi.org/10.1177/0309133316632460

Hawkes, P. J. (2005). Use of Joint Probability Methods in Flood Management: A Guide to Best Practice. In *Flood and Coastal Defence R&D Programme* (Issue FD2308/TR2).

Hawkes, P. J. (2008). Joint probability analysis for estimation of extremes. *Journal of Hydraulic Research*, *46*(sup2), 246–256. https://doi.org/10.1080/00221686.2008.9521958

Hawkes, P. J., Gouldby, B. P., Tawn, J. A., & Owen, M. W. (2002). The joint probability of waves and water levels in coastal engineering design. *Journal of Hydraulic Research*, *40*(3), 241–251. https://doi.org/10.1080/00221680209499940

Hawkes, P., Svensson, C., & Surendran, S. (2005). The joint probability of pairs of variables relevant to flood risk: dependence mapping and best practice. *Proceedings of the 40th Defra Flood and Coastal Management Conference*.

Haylock, M. R., & Goodess, C. M. (2004). Interannual variability of European extreme winter rainfall and links with mean large-scale circulation. *International Journal of Climatology*, *24*(6), 759–776. https://doi.org/10.1002/joc.1033

Heffernan, J. E., & Tawn, J. A. (2004). A conditional approach for multivariate extreme values. *Journal of the Royal Statistical Society. Series B: Statistical Methodology*, *66*(3), 497–530. https://doi.org/10.1111/j.1467-9868.2004.02050.x

Hemer, M. A., Simmonds, I., & Keay, K. (2008). A classification of wave generation characteristics during large wave events on the Southern Australian margin. *Continental Shelf Research*, *28*(4–5), 634–652. https://doi.org/10.1016/j.csr.2007.12.004

Hendry, A., Haigh, I. D., Nicholls, R. J., Winter, H., Neal, R., Wahl, T., Joly-Lauge, A., & Darby, S. E. (2019). Assessing the characteristics and drivers of compound flooding

events around the UK coast. *Hydrology and Earth System Sciences*, *23*(7), 3117–3139. https://doi.org/10.5194/hess-23-3117-2019

Hersbach, H., Bell, B., Berrisford, P., Biavati, G., Horányi, A., Muñoz Sabater, J., Nicolas, J., Peubey, C., Radu, R., Rozum, I., Schepers, D., Simmons, A., Soci, C., Dee, D., & Thépaut, J.-N. (2018). *ERA5 hourly data on pressure levels from 1979 to present.* Copernicus Climate Change Service (C3S) Climate Data Store (CDS). https://doi.org/10.24381/cds.bd0915c6

Hess, P., & Brezowsky, H. (1969). Katalog der grosswetterlagen Europas. *Berichte Des Deutschen Wetterdienstes*, *113*.

Hinkel, J., Lincke, D., Vafeidis, A. T., Perrette, M., Nicholls, R. J., Tol, R. S. J., Marzeion, B., Fettweis, X., Ionescu, C., & Levermann, A. (2014). Coastal flood damage and adaptation costs under 21st century sea-level rise. *Proceedings of the National Academy of Sciences of the United States of America*, *111*(9), 3292–3297. https://doi.org/10.1073/pnas.1222469111

Horsburgh, K. J., & Wilson, C. (2007). Tide-surge interaction and its role in the distribution of surge residuals in the North Sea. *Journal of Geophysical Research: Oceans*, *112*(8), 1–13. https://doi.org/10.1029/2006JC004033

Hosking, J. R. M., & Wallis, J. R. (1986). The Value of Historical Data in Flood Frequency Analysis. *Water Resources Research*, *22*(11), 1606–1612. https://doi.org/https://doi.org/10.1029/WR022i011p01606

Hosking, J. R. M., & Wallis, J. R. (1997). *Regional Frequency Analysis An Approach Based on L-Moments*. Cambridge University Press. https://doi.org/https://doi.org/10.1017/CBO9780511529443

Houston, D., Werritty, A., Bassett, D., Geddes, A., Hoolachan, A., & Mcmillan, M. (2011). *Pluvial (rain-related) flooding in urban areas: the invisible hazard*. www.jrf.org.uk

HR Wallingford. (1998). *The joint probability of waves and water levels: JOIN-SEA Version 1.0 - User manual. Report TR 71*. http://eprints.hrwallingford.co.uk/483/1/TR71_-_REPRO_-_JOIN-SEA_-_Version_1-bpg.pdf

Hurrell, J. W. (1995). Decadal trends in the North Atlantic oscillation: Regional temperatures and precipitation. *Science*, *269*(5224), 676–679. https://doi.org/10.1126/science.269.5224.676

Hurrell, J. W., & Deser, C. (2010). North Atlantic climate variability: The role of the North Atlantic Oscillation. *Journal of Marine Systems*, *79*(3–4), 231–244. https://doi.org/10.1016/j.jmarsys.2009.11.002

Ikeuchi, H., Hirabayashi, Y., Yamazaki, D., Muis, S., Ward, P. J., Winsemius, H. C., Verlaan, M., & Kanae, S. (2017). Compound simulation of fluvial floods and storm surges in a global coupled river-coast flood model: Model development and its application to 2007 Cyclone Sidr in Bangladesh. *Journal of Advances in Modeling Earth Systems*, *9*, 1847–1862. https://doi.org/10.1002/2013MS000282.Received

James, P. M. (2007). An objective classification method for Hess and Brezowsky Grosswetterlagen over Europe. *Theoretical and Applied Climatology*, *88*(1–2), 17–42. https://doi.org/10.1007/s00704-006-0239-3

Jenkinson, A. F., & Collinson, F. P. (1977). An initial climatology of gales over the North Sea. *Synoptic Climatology Branch Memorandum*, *62*(18).

Jones, P. D., Jonsson, T., & Wheeler, D. (1997). Extension to the North Atlantic Oscillation Using Early Instrumental Pressure Observations from Gibraltar and South-west Iceland. *INTERNATIONAL JOURNAL OF CLIMATOLOGY*, *17*, 1433–1450. https://doi.org/10.1007/1-4020-3266-8_150

Jonkman, S. N., Maaskant, B., Boyd, E., & Levitan, M. L. (2009). Loss of life caused by the flooding of New Orleans after hurricane Katrina: Analysis of the relationship between flood characteristics and mortality. *Risk Analysis*, *29*(5), 676–698. https://doi.org/10.1111/j.1539-6924.2008.01190.x

Keef, C., Svensson, C., & Tawn, J. A. (2009). Spatial dependence in extreme river flows and precipitation for Great Britain. *Journal of Hydrology*, *378*(3–4), 240–252. https://doi.org/10.1016/j.jhydrol.2009.09.026

Kendall, M. G. (1938). A New Measure of Rank Correlation. *Biometrika*, *30*(1/2), 81. https://doi.org/10.2307/2332226

Kendon, M., & McCarthy, M. (2015). The UK's wet and stormy winter of 2013/2014. *Weather*, *70*(2), 40–47. https://doi.org/10.1002/wea.2465

Kew, S. F., Selten, F. M., Lenderink, G., & Hazeleger, W. (2013). The simultaneous occurrence of surge and discharge extremes for the Rhine delta. *Natural Hazards and Earth System Sciences*, *13*(8), 2017–2029. https://doi.org/10.5194/nhess-13-2017-2013

Khanal, S., Ridder, N., de Vries, H., Terink, W., & van den Hurk, B. (2018). Storm surge and extreme river discharge: a compound event analysis using ensemble impact modelling. *Hydrology and Earth System Sciences Discussions*, *April*, 1–25. https://doi.org/10.5194/hess-2018-103

Klerk, W. J., Winsemius, H. C., van Verseveld, W. J., Bakker, A. M. R., & Diermanse, F. L. M. (2015). The co-incidence of storm surges and extreme discharges within the Rhine–Meuse Delta. *Environmental Research Letters*, *10*(3), 035005. https://doi.org/10.1088/1748-9326/10/3/035005

Kowalewska-Kalkowska, H. (2018). Frequency and Strength of Storm Surges in the Oder River Estuary Area. *Acta Scientiarum Polonorum Formatio Circumiectus*, *3*(December), 55–65. https://doi.org/10.15576/asp.fc/2018.17.3.55

Kumbier, K., Carvalho, R. C., Vafeidis, A. T., & Woodroffe, C. D. (2018). Investigating compound flooding in an estuary using hydrodynamic modelling: A case study from the Shoalhaven River, Australia. *Natural Hazards and Earth System Sciences*, *18*(2), 463–477. https://doi.org/10.5194/nhess-18-463-2018

Lamb, H. (1972). British Isles weather types and a register of the daily sequence of circulation patterns 1861-1971. *METEOROL. OFF., GEOPHYS. MEM.*, *116*, 1–85.

Lamb, Hubert. (1991). *Historic Storms of the North Sea, British Isles and Northwest Europe*. Cambridge University Press.

Lamb, Keef, C., Tawn, J., Laeger, S., Meadowcroft, I., Surendran, S., Dunning, P., & Batstone, C. (2010). A new method to assess the risk of local and widespread flooding on rivers and coasts. *Journal of Flood Risk Management*, *3*(4), 323–336. https://doi.org/10.1111/j.1753-318X.2010.01081.x

Leonard, M., Westra, S., Phatak, A., Lambert, M., van den Hurk, B., Mcinnes, K., Risbey, J., Schuster, S., Jakob, D., & Stafford-Smith, M. (2014). A compound event framework for understanding extreme impacts. In *Wiley Interdisciplinary Reviews: Climate Change* (Vol. 5, Issue 1, pp. 113–128). John Wiley & Sons, Inc. https://doi.org/10.1002/wcc.252

Li, F., van Gelder, P. H. A. J. M., Ranasinghe, R., Callaghan, D. P., & Jongejan, R. B. (2014). Probabilistic modelling of extreme storms along the Dutch coast. *Coastal Engineering*, *86*, 1–13. https://doi.org/10.1016/j.coastaleng.2013.12.009

Lian, J. J., Xu, K., & Ma, C. (2013). Joint impact of rainfall and tidal level on flood risk in a

coastal city with a complex river network: a case study of Fuzhou City, China. *Hydrol. Earth Syst. Sci*, *17*, 679–689. https://doi.org/10.5194/hess-17-679-2013

Lu, Q. C., Peng, Z. R., & Zhang, J. (2015). Identification and prioritization of critical transportation infrastructure: Case study of coastal flooding. *Journal of Transportation Engineering*, *141*(3), 1–8. https://doi.org/10.1061/(ASCE)TE.1943-5436.0000743

Lumbroso, D. M., & Vinet, F. (2011). A comparison of the causes, effects and aftermaths of the coastal flooding of England in 1953 and France in 2010. *Natural Hazards and Earth System Sciences*, *11*(8), 2321–2333. https://doi.org/10.5194/nhess-11-2321-2011

Malagon Santos, V., Haigh, I., & Wahl, T. (2017). Spatial and Temporal Clustering Analysis of Extreme Wave Events around the UK Coastline. *Journal of Marine Science and Engineering*, *5*(3), 28. https://doi.org/10.3390/jmse5030028

Mangor, K., Drønen, N. K., Kaergaard, K. H., & Ristensen, N. E. (2017). *Shoreline Management Guidlines*. DHI.

Marcos, M., Rohmer, J., Vousdoukas, M., Mentaschi, L., Le Cozannet, G., & Amores, A. (2019). Increased extreme coastal water levels due to the combined action of storm surges and wind-waves. *Geophysical Research Letters*, *1*, 2019GL082599. https://doi.org/10.1029/2019GL082599

Marsh, T., Hannaford, J., Llewellyn, P. N., Lane, P. H., & Lees, P. M. (2007). The summer 2007 fl oods in England & Wales – a hydrological appraisal FUNDING & DATA SOURCES. *Ecology*.

Marsh, T., & Harvey, C. L. (2012). The Thames flood series: A lack of trend in flood magnitude and a decline in maximum levels. *Hydrology Research*, *43*(3), 203–214. https://doi.org/10.2166/nh.2012.054

Masina, M., Lamberti, A., & Archetti, R. (2015). Coastal flooding: A copula based approach for estimating the joint probability of water levels and waves. *Coastal Engineering*, *97*, 37–52. https://doi.org/10.1016/J.COASTALENG.2014.12.010

Mason, T., & Dhoop, T. (2017). Quality Control of Wave Data. In *CCO*.

Mason, T., & Dhoop, T. (2018). *Occurrence of Bimodal Seas around the English Coastline - Channel Coast Observatory Technical Note TN 02*. *June*, 1–8.

Mazas, F., & Hamm, L. (2017). An event-based approach for extreme joint probabilities of

waves and sea levels. *Coastal Engineering*, *122*(April), 44–59. https://doi.org/10.1016/j.coastaleng.2017.02.003

Mcgarrigle, P., Bradshaw, E., Bradley, L., Hargreaves, G., Macleod, L., Bell, C., & Hibbert, A. (2015). *UK Coastal Monitoring and Forecasting: 2015 Annual Report for the UK Tide Gauge Network*.

McGranahan, G., Balk, D., & Anderson, B. (2007). The rising tide: assessing the risks of climate change and human settlements in low elevation coastal zones. *Environment and Urbanization*, *19*(1), 17–37. https://doi.org/10.1177/0956247807076960

Met Office, & CEH. (2014). The Recent Storms and Floods in the UK. In *Met Office UK - February 2014* (Issue February). https://doi.org/10.1038/scientificamerican04051913-315

Moftakhari, H. R., Salvadori, G., AghaKouchak, A., Sanders, B. F., & Matthew, R. A. (2017). Compounding effects of sea level rise and fluvial flooding. *Proceedings of the National Academy of Sciences*, 201620325. https://doi.org/10.1073/pnas.1620325114

Mongo, E., Cambaza, E., Nhambire, R., Singo, J., & Machava, E. (2020). Outbreak of Cholera Due to Cyclone Idai in Central Mozambique (2019). In S. Reddy (Ed.), *Evaluation of Health Services* (Vol. 32, pp. 137–144). Intech. https://doi.org/10.5772/intechopen.89358

Muis, S., Verlaan, M., Winsemius, H. C., Aerts, J. C. J. H., & Ward, P. J. (2016). A global reanalysis of storm surges and extreme sea levels. *Nature Communications*, *7*(May), 11969. https://doi.org/10.1038/ncomms11969

Munich Re. (2017). *NatCatSERVICE*. www.munichre.com/natcatservice.

National Tidal and Sea Level Facility. (2018). *UK National Tide Gauge Network*. http://www.ntslf.org/data/uk-network-real-time

Neal, R., Dankers, R., Saulter, A., Lane, A., Millard, J., Robbins, G., & Price, D. (2018). Use of probabilistic medium- to long-range weather-pattern forecasts for identifying periods with an increased likelihood of coastal flooding around the UK. *Meteorological Applications*, *25*(4), 534–547. https://doi.org/10.1002/met.1719

Neal, R., Fereday, D., Crocker, R., & Comer, R. E. (2016). A flexible approach to defining weather patterns and their application in weather forecasting over Europe. *Meteorological Applications*, *23*(3), 389–400. https://doi.org/10.1002/met.1563

Nerem, R. S., Beckley, B. D., Fasullo, J. T., Hamlington, B. D., Masters, D., & Mitchum, G. T. (2018). Climate-change-driven accelerated sea-level rise detected in the altimeter era. *Proceedings of the National Academy of Sciences of the United States of America*, *115*(9), 2022–2025. https://doi.org/10.1073/pnas.1717312115

Nguyen, C. C., Gaume, E., & Payrastre, O. (2014). Regional flood frequency analyses involving extraordinary flood events at ungauged sites: further developments and validations. *Journal of Hydrology*, *508*, 385–396. https://doi.org/https://doi.org/10.1016/j.jhydrol.2013.09.058

Nicholls, R. J., Lincke, D., Hinkel, J., Brown, S., Vafeidis, A. T., Meyssignac, B., Hanson, S. E., Merkens, J. L., & Fang, J. (2021). A global analysis of subsidence, relative sea-level change and coastal flood exposure. *Nature Climate Change*, *11*(4), 338–342. https://doi.org/10.1038/s41558-021-00993-z

NOAA. (2018a). *20th Century Reanalysis, Version 2c*. https://www.esrl.noaa.gov/psd/data/20thC_Rean/

NOAA. (2018b). *Costliest U.S. tropical cyclones tables updated*. https://doi.org/10.1080/00049187308702635

Olbert, A. I., Comer, J., Nash, S., & Hartnett, M. (2017). High-resolution multi-scale modelling of coastal fl ooding due to tides , storm surges and rivers in fl ows . A Cork City example. *Coastal Engineering*, *121*(January), 278–296. https://doi.org/10.1016/j.coastaleng.2016.12.006

Orimoloye, S., Horrillo-Caraballo, J., Karunarathna, H., & Reeve, D. E. (2021). Wave overtopping of smooth impermeable seawalls under unidirectional bimodal sea conditions. *Coastal Engineering*, *165*(September 2020), 103792. https://doi.org/10.1016/j.coastaleng.2020.103792

Otto, F. E. L., Van Der Wiel, K., Van Oldenborgh, G. J., Philip, S., Kew, S. F., Uhe, P., & Cullen, H. (2018). Climate change increases the probability of heavy rains in Northern England/Southern Scotland like those of storm Desmond - A real-time event attribution revisited. *Environmental Research Letters*, *13*(2). https://doi.org/10.1088/1748-9326/aa9663

Paprotny, D., Vousdoukas, M. I., Morales-Nápoles, O., Jonkman, S. N., & Feyen, L. (2018). Compound flood potential in Europe. *Hydrology and Earth System Sciences*

Discussions, *April*, 1–34. https://doi.org/10.5194/hess-2018-132

Paprotny, D., Vousdoukas, M. I., Morales-Nápoles, O., Jonkman, S. N., & Feyen, L. (2020). Pan-European hydrodynamic models and their ability to identify compound floods. *Natural Hazards*, *101*(3), 933–957. https://doi.org/10.1007/s11069-020-03902-3

Pawlowicz, R., Beardsley, B., & Lentz, S. (2002). Classical tidal harmonic analysis including werror estimates in MATLAB using T_TIDE. *Computers and Geosciences*, *28*(8), 929–937. https://doi.org/10.1016/S0098-3004(02)00013-4

Payrastre, O., Gaume, E., & Andrieu, H. (2011). Usefulness of historical information for flood frequency analyses: Developments based on a case study. *Water Resources Research*, *47*(8), 1–15. https://doi.org/10.1029/2010WR009812

Peings, Y., & Magnusdottir, G. (2014). Forcing of the wintertime atmospheric circulation by the multidecadal fluctuations of the North Atlantic ocean. *Environmental Research Letters*, *9*(3). https://doi.org/10.1088/1748-9326/9/3/034018

Perez, J., Menendez, M., & Losada, I. J. (2017). GOW2 : A global wave hindcast for coastal applications. *Coastal Engineering*, *124*(March), 1–11. https://doi.org/10.1016/j.coastaleng.2017.03.005

Petroliagkis, T. I., Voukouvalas, E., Disperati, J., & Bidlot, J. (2016). *Joint Probabilities of Storm Surge, Significant Wave Height and River Discharge Components of Coastal Flooding Events. EUR 27824 EN*. https://doi.org/doi:10.2788/677778

Poate, T. G., McCall, R. T., & Masselink, G. (2016). A new parameterisation for runup on gravel beaches. *Coastal Engineering*, *117*, 176–190. https://doi.org/10.1016/j.coastaleng.2016.08.003

Probst, P., & Annunziato, A. (2019). *Tropical Cyclone Idai: analysis of the wind, rainfall and storm surge impact*. https://reliefweb.int/sites/reliefweb.int/files/resources/joint_research_centre_analysis_of_wind_rainfall_and_storm_surge_impact_09_april_2019.pdf

Pugh, D., & Woodworth, P. (2014). *Sea-Level Science: Understanding Tides, Surges, Tsunamis and Mean Sea-Level Changes* (2nd ed.). Cambridge University Press.

Pugh, DT. (2004). *Changing Sea Levels: Effects of Tides, Weather and Climate*. Cambridge University Press.

Ray, T., Asce, M., Stepinski, E., Sebastian, A., Bedient, P. B., & Asce, F. (2011). *Dynamic Modeling of Storm Surge and Inland Flooding in a Texas Coastal Floodplain*. https://doi.org/10.1061/(ASCE)HY.1943-7900.0000398

Richardson, D., Fowler, H. J., Kilsby, C. G., & Neal, R. (2018). A new precipitation and drought climatology based on weather patterns. *International Journal of Climatology*, *38*(2), 630–648. https://doi.org/10.1002/joc.5199

Richardson, Doug, Fowler, H. J., Kilsby, C. G., Neal, R., & Dankers, R. (2020). Improving sub-seasonal forecast skill of meteorological drought: A weather pattern approach. *Natural Hazards and Earth System Sciences*, *20*(1), 107–124. https://doi.org/10.5194/nhess-20-107-2020

Robins, P. E., Lewis, M. J., Freer, J., Cooper, D. M., Skinner, C. J., & Coulthard, T. J. (2018). Improving estuary models by reducing uncertainties associated with river flows. *Estuarine, Coastal and Shelf Science*, *207*, 63–73. https://doi.org/10.1016/j.ecss.2018.02.015

Rueda, A., Camus, P., Tomás, A., Vitousek, S., & Méndez, F. J. (2016). A multivariate extreme wave and storm surge climate emulator based on weather patterns. *Ocean Modelling*, *104*, 242–251. https://doi.org/10.1016/j.ocemod.2016.06.008

Ruocco, A. C., Nicholls, R. J., Haigh, I. D., & Wadey, M. P. (2011a). Reconstructing coastal flood occurrence combining sea level and media sources: A case study of the Solent, UK since 1935. *Natural Hazards*, *59*(3), 1773–1796. https://doi.org/10.1007/s11069-011-9868-7

Ruocco, A. C., Nicholls, R. J., Haigh, I. D., & Wadey, M. P. (2011b). Reconstructing coastal flood occurrence combining sea level and media sources: a case study of the Solent, UK since 1935. *Natural Hazards*, *59*(3), 1773–1796. https://doi.org/10.1007/s11069-011-9868-7

Ruosteenoja, K., Räisänen, J., Venäläinen, A., & Kämäräinen, M. (2016). Projections for the duration and degree days of the thermal growing season in Europe derived from CMIP5 model output. *International Journal of Climatology*, *36*(8), 3039–3055. https://doi.org/10.1002/joc.4535

Saleh, F., Ramaswamy, V., Wang, Y., Georgas, N., Blumberg, A., & Pullen, J. (2017). A multi-scale ensemble-based framework for forecasting compound coastal-riverine

flooding: The Hackensack-Passaic watershed and Newark Bay. *Advances in Water Resources*, *110*(March), 371–386. https://doi.org/10.1016/j.advwatres.2017.10.026

Samuels, P. G., & Burt, N. (2002). A new joint probability appraisal of flood risk. *Proceedings of the Institution of Civil Engineers: Water and Maritime Engineering*, *154*(2), 109–115. https://doi.org/10.1680/maen.154.2.109.38642

Santer, B. D., Wigley, T. M. L., & Jones, P. D. (1993). Correlation methods in fingerprint detection studies. *Climate Dynamics*, *8*(6), 265–276. https://doi.org/10.1007/BF00209666

Seneviratne, S., Nicholls, N., Easterling, D., Goodess, C., Kanae, S., Kossin, J., Luo, Y., Marengo, J., McInnes, K., Rahimi, M., Reichstein, M., Sorteberg, A., Vera, C., & Zhang, X. (2012). Changes in climate extremes and their impacts on the natural physical environment. *Managing the Risk of Extreme Events and Disasters to Advance Climate Change Adaptation.*, 109–230. https://www.ipcc.ch/pdf/special-reports/srex/SREX-Chap3_FINAL.pdf

Serafin, K. A., Ruggiero, P., Parker, K., & Hill, D. F. (2019). What's streamflow got to do with it? A probabilistic simulation of the competing oceanographic and fluvial processes driving extreme along-river water levels. *Hazards Earth Syst. Sci*, *19*, 1415–1431. https://doi.org/10.5194/nhess-19-1415-2019

Shaffrey, L. C., & Sutton, R. (2006). Bjerkness compensation and the decadal variability of the energy transports in a coupled climate model. *Journal of Climate*, *19*(7), 1167–1181. https://doi.org/10.1175/JCLI3652.1

Shaw, E. M., Beven, K. J., Chappell, N. A., & Lamb, R. (2011). *Hydrology in practice* (third). Spon Press.

Shaw, T. A., Baldwin, M., Barnes, E. A., Caballero, R., Garfinkel, C. I., Hwang, Y. T., Li, C., O'Gorman, P. A., Rivière, G., Simpson, I. R., & Voigt, A. (2016). Storm track processes and the opposing influences of climate change. *Nature Geoscience*, *9*(9), 656–664. https://doi.org/10.1038/ngeo2783

Sibley, A., & Cox, D. (2014). Flooding along English Channel coast due to long-period swell waves. *Weather*, *69*(3), 59–66. https://doi.org/10.1002/wea.2145

Silva-Araya, W. F., Santiago-Collazo, F. L., Gonzalez-Lopez, J., & Maldonado-Maldonado, J. (2018). Dynamic modeling of surface runoff and storm surge during hurricane and

tropical storm events. *Hydrology*, *5*(1), 1–28. https://doi.org/10.3390/hydrology5010013

Smith, R. L. (1986). Extreme value theory based on the r largest annual events. *Journal of Hydrology*, *86*(1–2), 27–43.

Stedinger, J. R., & Baker, V. R. (1987). Surface water hydrology: Historical and paleoflood information. *Reviews of Geophysics*, *25*(2), 119–124. https://doi.org/https://doi.org/10.1029/RG025i002p00119

Stevens, A. J., Clarke, D., & Nicholls, R. J. (2016). Trends in reported flooding in the UK: 1884–2013. *Hydrological Sciences Journal*, *61*(1), 50–63. https://doi.org/10.1080/02626667.2014.950581

Stewart, S. R. (2017). Hurricane Matthew. *National Hurricane Center*, *October 2016*, 1–96. http://www.nhc.noaa.gov/data/tcr/AL142016_Matthew.pdf

Stokes, K., Poate, T., Masselink, G., King, E., Saulter, A., & Ely, N. (2021). Forecasting coastal overtopping at engineered and naturally defended coastlines. *Coastal Engineering*, *164*. https://doi.org/10.1016/j.coastaleng.2020.103827

Svensson, C, & Jones, D. A. (2004). Dependence between sea surge, river flow and precipitation in south and west Britain. *Hydrology and Earth System Sciences Discussions European Geosciences Union*, *8*(5), 973–992.

Svensson, Cecilia, & Jones, D. A. (2002). Dependence between extreme sea surge, river flow and precipitation in eastern Britain. *International Journal of Climatology*, *22*(10), 1149–1168. https://doi.org/10.1002/joc.794

Svensson, Cecilia, & Jones, D. A. (2005). Joint Probability : Dependence between extreme sea surge , river flow and precipitation : *R&D Technical Report FD2308/TR3 to DEFRA. CEH Wallingford*, *Wallingford*, *UK*.

Taylor, K. E. (2001). Summarizing multiple aspects of model performance in a Single Diagram. *Journal of Geophysical Research*, *106*(D7), 7183–7192.

Torres, J. M., Bass, B., Irza, N., Fang, Z., Proft, J., Dawson, C., Kiani, M., & Bedient, P. (2015). Characterizing the hydraulic interactions of hurricane storm surge and rainfall-runoff for the Houston-Galveston region. *Coastal Engineering*, *106*, 7–19. https://doi.org/10.1016/j.coastaleng.2015.09.004

Turner, R. (2000). *Environment Agency Southern Region Christmas Floods 1999 Volume*

Two.

van den Hurk, B., van Meijgaard, E., de Valk, P., van Heeringen, K.-J., & Gooijer, J. (2015). Analysis of a compounding surge and precipitation event in the Netherlands. *Environmental Research Letters*, *10*(3), 035001. https://doi.org/10.1088/1748-9326/10/3/035001

Vitousek, S., Barnard, P. L., Fletcher, C. H., Frazer, N., Erikson, L., & Storlazzi, C. D. (2017). Doubling of coastal flooding frequency within decades due to sea-level rise. *Scientific Reports*, *7*(1). https://doi.org/10.1038/s41598-017-01362-7

Wadey, M. P., Haigh, I. D., & Brown, J. M. (2014). A century of sea level data and the UK's 2013/14 storm surges: An assessment of extremes and clustering using the Newlyn tide gauge record. *Ocean Science*, *10*(6), 1031–1045. https://doi.org/10.5194/os-10-1031-2014

Wadey, M P, Brown, J. M., Haigh, I. D., Dolphin, T., & Wisse, P. (2015). Assessment and comparison of extreme sea levels and waves during the 2013/14 storm season in two UK coastal regions. *Natural Hazards and Earth System Sciences*, *15*(10), 2209–2225. https://doi.org/10.5194/nhess-15-2209-2015

Wadey, Matthew P. (2013). *Understanding Defence Failures and Coastal Flood Events: a Case Study Approach*. University of Southampton.

Wahl, T., Jain, S., Bender, J., Meyers, S. D., & Luther, M. E. (2015). Increasing risk of compound flooding from storm surge and rainfall for major US cities. *Nature Climate Change*, *5*(12), 1093–1097. https://doi.org/10.1038/nclimate2736

Wahl, T., Mudersbach, C., & Jensen, J. (2012). Assessing the hydrodynamic boundary conditions for risk analyses in coastal areas: A multivariate statistical approach based on Copula functions. *Natural Hazards and Earth System Science*, *12*(2), 495–510. https://doi.org/10.5194/nhess-12-495-2012

Ward, P. J., Couasnon, A., Eilander, D., Haigh, I. D., Hendry, A., Muis, S., Veldkamp, T. I. E., Winsemius, H. C., & Wahl, T. (2018). Dependence between high sea-level and high river discharge increases flood hazard in global deltas and estuaries. *Environmental Research Letters*, *13*(8), 084012. https://doi.org/10.1088/1748-9326/aad400

Weiss, J., Bernardara, P., & Benoit, M. (2014). Modeling intersite dependence for regional frequency analysis of extreme marine events. *Water Resources Research*, *50*, 5926–

5940. https://doi.org/10.1002/ 2014WR015391

White, C. J. (2007). *The Use of Joint Probability Analysis to Predict Flood Frequency in Estuaries and Tidal Rivers* [University of Southanpton]. http://eprints.soton.ac.uk

Wolf, J., Brown, J. M., & Howarth, M. J. (2011). The wave climate of Liverpool Bay-observations and modelling. *Ocean Dynamics*, *61*(5), 639–655. https://doi.org/10.1007/s10236-011-0376-9

Wolf, J., Woolf, D., & Bricheno, L. (2020). The impacts of climate change on fisheries, relevant to the coastal and marine environment around the UK. *Marine Climate Change Impacts Partnership (MCCIP) Science Review*, *2020*(January), 456–481. https://doi.org/10.14465/2020.arc07.saw

Woodworth, P. L., Flather, R. A., Williams, J. A., Wakelin, S. L., & Jevrejeva, S. (2007). The dependence of UK extreme sea levels and storm surges on the North Atlantic Oscillation. *Continental Shelf Research*, *27*(7), 935–946. https://doi.org/10.1016/j.csr.2006.12.007

Woodworth, Philip L., & Blackman, D. L. (2002). Changes in extreme high waters at Liverpool since 1768. *International Journal of Climatology*, *22*(6), 697–714. https://doi.org/10.1002/joc.761

Wu, W., McInnes, K., O'Grady, J., Hoeke, R., Leonard, M., & Westra, S. (2018). Mapping Dependence Between Extreme Rainfall and Storm Surge. *Journal of Geophysical Research: Oceans*, *123*(4), 2461–2474. https://doi.org/10.1002/2017JC013472

Wyncoll, D., Haigh, I., Gouldby, B., Hames, D., Laeger, S., Wall, A., & Hawkes, P. (2016). *Spatial analysis and simulation of extreme coastal flooding scenarios for national-scale emergency planning*. *01001*, 1–6.

Yamazaki, D., O'Loughlin, F., Trigg, M. A., Miller, Z. F., Pavelsky, T. M., & Bates, P. D. (2014). Development of the Global Width Database for Large Rivers. *Water Resources Research*, *50*, 3467–3480. https://doi.org/10.1002/2013WR014664

Zappa, G., Shaffrey, L. C., Hodges, K. I., Sansom, P. G., & Stephenson, D. B. (2013). A multimodel assessment of future projections of north atlantic and european extratropical cyclones in the CMIP5 climate models. *Journal of Climate*, *26*(16), 5846–5862. https://doi.org/10.1175/JCLI-D-12-00573.1

Zheng, F., Westra, S., Leonard, M., & Sisson, S. A. (2014). Modeling dependence between

extreme rainfall and storm surge to estimate coastal flooding risk. *Water Resources Research*, *50*(3), 2050–2071. https://doi.org/10.1002/2013WR014616

Zheng, F., Westra, S., & Sisson, S. A. (2013). Quantifying the dependence between extreme rainfall and storm surge in the coastal zone. *Journal of Hydrology*, *505*, 172–187. https://doi.org/10.1016/j.jhydrol.2013.09.054

Zscheischler, J., Martius, O., Westra, S., Bevacqua, E., Raymond, C., Horton, R. M., van den Hurk, B., AghaKouchak, A., Jezequel, A., Mahecha, M., Maraun, D., Ramos, A., Ridder, N., Thiery, W., & Vignotto, E. (2020). A typology of compound weather and climate events. *Nature Reviews Earth & Environment*, *1*, 333–347.

Zscheischler, J., Westra, S., van den Hurk, B. J. J. M., Seneviratne, S. I., Ward, P. J., Pitman, A., AghaKouchak, A., Bresch, D. N., Leonard, M., Wahl, T., & Zhang, X. (2018). Future climate risk from compound events. *Nature Climate Change*, *8*, 469–477. https://doi.org/10.1038/s41558-018-0156-3

8. Appendix A

Table 8.1: List compound flooding studies per variables analysed and in chronological order. The scale number indicates studies that are: (1) localised; (2) regional; or (3) global in scale.

Variables		Reference	scale	year
Sea Level & Precipitation	1	Bevacqua et al., 2019	2	2019
	3	Wu et al., 2018	2	2018
	4	Tu et al., 2018	1	2018
	5	Bengtsson, 2016	1	2016
	6	van der Hurk et al., 2015	1	2015
	7	Wahl et al., 2015	2	2015
	8	Zheng et al., 2015	1	2015
	9	Zheng et al., 2014	1	2014
	10	Xu et al., 2014	1	2014
	11	Zheng et al., 2013	2	2013
	12	Lian et al., 2013	1	2013
Sea Level & River Discharge	1	Ganguli and Merz, 2019a	2	2019
	2	Hendry et al., 2019	2	2019
	3	Couasnon et al., 2019	3	2019
	4	Khanal et al., 2018	1	2018
	5	Ward et al., 2018	3	2018
	7	Couasnon et al., 2018	1	2018
	8	Bevacqua et al., 2017	1	2017
	9	Moftakhari et al., 2017	2	2017
	10	Klerk et al., 2015	1	2015
	11	Kew et al., 2013	1	2013

	12	Lamb et al., 2010	2	2010
Variables		Reference	scale	year
	13	White, 2007	2	2007
	14	Defra/Environmental Agency, 2003	2	2005
	15	Svensson and Jones, 2004	2	2004
	16	Samuels and Bart, 2002	1	2002
	17	Svensson and Jones, 2002	2	2002
	18	Mantz and Wakeling, 1979	1	1979
	19	Kowalewska-Kalkowska and Wiśniewski, 2009	1	2009
Sea Level & Waves	1	Marcos et al., 2019	3	2019
	3	Petroliagkis, 2018	2	2018
	4	Mazas and Hamm, 2017	1	2017
	5	Arns et al., 2017	1	2017
	6	Wyncoll et al., 2016	2	2016
	7	Rueda et al., 2016	1	2016
	8	Masina et al., 2015	1	2015
	9	Li et al., 2014	1	2014
	10	Serafin and Ruggiero, 2014	1	2014
	11	Gouldby et al., 2014	1	2014
	12	Wahl et al., 2012	1	2012
	13	Hawkes and Svensson, 2005	2	2005
	14	Defra, 2005	2	2005
	15	Hawkes_et_al_2002	2	2002
	16	Owen et al., 1997	2	1997

	17	Hawkes and Hague, 1994	2	1994
Variables		Reference	scale	year
	18	HRL, 1990	1	1990
Precipitation & River Discharge	1	Keef et al., 2009	2	2009
Runoff & Precipitation	1	Liu et al., 2018	1	2018
Sea Level, Waves, River & Precipitation	1	Paprotny et al., 2018	2	2018
	2	Paprotny et al., 2020	2	2020
Modelling	1	Kumbier et al. (2018)		2018
	2	Olbert et al. (2017)		2017
	3	Chen and Liu, 2014		2014
	4	Acreman, 1994		1994
	5	Bilskie and Hagen (2018)		2018
	6	Silva –Araya et al (2018)		2018
	7	Ikeuchi et al. (2017)		2017
	8	Bacopoulos et al. (2017)		2017
	9	Saleh et al. (2017)		2017
	10	Torres et al. (2015)		2015
	11	Thompson and Frazier (2014)		2014
	12	Ray et al., 2011		2011
	13	Sopelana et al 2018	1	2018
	14	Kowalewska-Kalkowska and Kowalewski (2006)	1	2006
	15	Kowalewska-Kalkowska and Kowalewski (2011)	1	2011

9. Appendix B

Table 9.1: The pairs of tide gauge sites and river discharge stations used in Chapter 3.

Tide Gauge	Tide Gauge Latitude (deg)	Tide Gauge longitude (deg)	River Gauge ID	River	River Gauge Location	River Gauge Latitude (deg)	River Gauge longitude (deg)
Aberdeen	57.14	-2.08	12002	Dee	Park	57.08	-2.33
Aberdeen	57.14	-2.08	12001	Dee	Woodend	57.05	-2.60
Aberdeen	57.14	-2.08	12003	Dee	Polhollick	57.06	-3.08
Aberdeen	57.14	-2.08	11001	Don	Parkhill	57.22	-2.19
Aberdeen	57.14	-2.08	13007	North Esk	Logie Mill	56.77	-2.49
Aberdeen	57.14	-2.08	9002	Deveron	Muiresk	57.54	-2.49
Aberdeen	57.14	-2.08	11002	Don	Haughton	57.27	-2.40
Aberdeen	57.14	-2.08	13008	South Esk	Brechin	56.73	-2.65
Aberdeen	57.14	-2.08	12007	Dee	Mar Lodge	56.99	-3.49
Aberdeen	57.14	-2.08	11003	Don	Bridge of Alford	57.24	-2.72
Aberdeen	57.14	-2.08	9001	Deveron	Avochie	57.51	-2.78
Aberdeen	57.14	-2.08	10003	Ythan	Ellon	57.36	-2.09
Aberdeen	57.14	-2.08	12008	Feugh	Heugh Head	57.03	-2.52
Aberdeen	57.14	-2.08	13012	South Esk	Gella Bridge	56.78	-3.03
Avonmouth	51.51	-2.71	54057	Severn	Haw Bridge	51.95	-2.23
Avonmouth	51.51	-2.71	54032	Severn	Saxons Lode	52.05	-2.20
Avonmouth	51.51	-2.71	55023	Wye	Redbrook	51.80	-2.69
Avonmouth	51.51	-2.71	54001	Severn	Bewdley	52.38	-2.32
Avonmouth	51.51	-2.71	54095	Severn	Buildwas	52.64	-2.52
Avonmouth	51.51	-2.71	55002	Wye	Belmont	52.04	-2.75
Avonmouth	51.51	-2.71	54005	Severn	Montford	52.72	-2.87
Avonmouth	51.51	-2.71	55007	Wye	Erwood	52.09	-3.35
Avonmouth	51.51	-2.71	54028	Vyrnwy	Llanymynech	52.77	-3.11

Avonmouth	51.51	-2.71	53018	Avon	Bathford	51.40	-2.31
Avonmouth	51.51	-2.71	54029	Teme	Knightsford Bridge	52.20	-2.39
Avonmouth	51.51	-2.71	54002	Avon	Evesham	52.09	-1.94
Avonmouth	51.51	-2.71	54014	Severn	Abermule	52.55	-3.23
Avonmouth	51.51	-2.71	54008	Teme	Tenbury	52.31	-2.59
Avonmouth	51.51	-2.71	55003	Lugg	Lugwardine	52.06	-2.66
Avonmouth	51.51	-2.71	55012	Irfon	Cilmery	52.15	-3.47
Avonmouth	51.51	-2.71	55016	Ithon	Disserth	52.21	-3.43
Avonmouth	51.51	-2.71	54080	Severn	Dolwen	52.45	-3.49
Avonmouth	51.51	-2.71	54012	Tern	Walcot	52.71	-2.60
Avonmouth	51.51	-2.71	54038	Tanat	Llanyblodwel	52.79	-3.11
Avonmouth	51.51	-2.71	55026	Wye	Ddol Farm	52.30	-3.50
Avonmouth	51.51	-2.71	55029	Monnow	Grosmont	51.92	-2.85
Avonmouth	51.51	-2.71	55021	Lugg	Butts Bridge	52.23	-2.73
Avonmouth	51.51	-2.71	55032	Elan	Caban Dam	52.27	-3.57
Bangor	54.66	-5.67	205004	Lagan	Newforge	54.55	-5.95
Bangor	54.66	-5.67	203018	Six-Mile Water	Antrim	54.72	-6.22
Bangor	54.66	-5.67	203097	Upper Bann	Moyallen	54.39	-6.39
Barmouth	52.72	-4.05	64001	Dyfi	Dyfi Bridge	52.60	-3.85
Barmouth	52.72	-4.05	63001	Ystwyth	Pont Llolwyn	52.38	-4.07
Barmouth	52.72	-4.05	65001	Glaslyn	Beddgelert	53.01	-4.10
Bournemouth	50.71	-1.87	43021	Avon	Knapp Mill	50.75	-1.78
Bournemouth	50.71	-1.87	43003	Avon	East Mills Total	50.93	-1.77
Bournemouth	50.71	-1.87	43007	Stour	Throop	50.76	-1.84
Cromer	52.93	1.30	33035	Ely Ouse	Denver Complex	52.58	0.35
Cromer	52.93	1.30	33026	Bedford Ouse	Offord	52.29	-0.22

Cromer	52.93	1.30	33039	Bedford Ouse	Roxton	52.17	-0.30
Cromer	52.93	1.30	33002	Bedford Ouse	Bedford	52.13	-0.46
Devonport	50.37	-4.19	47001	Tamar	Gunnislake	50.53	-4.22
Devonport	50.37	-4.19	46003	Dart	Austins Bridge	50.48	-3.76
Devonport	50.37	-4.19	47019	Tamar	Polson Bridge	50.64	-4.33
Devonport	50.37	-4.19	46002	Teign	Preston	50.56	-3.62
Devonport	50.37	-4.19	47015	Tavy	Ludbrook	50.49	-4.15
Devonport	50.37	-4.19	47006	Lyd	Lifton Park	50.64	-4.28
Fishguard	52.01	-4.98	62001	Teifi	Glanteifi	52.05	-4.56
Heysham	54.03	-2.92	72004	Lune	Caton	54.08	-2.72
Heysham	54.03	-2.92	71001	Ribble	Samlesbury	53.77	-2.62
Heysham	54.03	-2.92	71009	Ribble	New Jumbles Rock	53.83	-2.45
Heysham	54.03	-2.92	73010	Leven	Newby Bridge	54.27	-2.97
Heysham	54.03	-2.92	71006	Ribble	Henthorn	53.85	-2.42
Heysham	54.03	-2.92	72005	Lune	Killington	54.31	-2.58
Heysham	54.03	-2.92	73005	Kent	Sedgwick	54.28	-2.75
Heysham	54.03	-2.92	72011	Rawthey	Brigflatts	54.31	-2.55
Heysham	54.03	-2.92	71008	Hodder	Hodder Place	53.85	-2.45
Heysham	54.03	-2.92	71004	Calder	Whalley Weir	53.82	-2.41
Heysham	54.03	-2.92	71011	Ribble	Arnford	54.00	-2.25
Heysham	54.03	-2.92	72002	Wyre	St Michaels	53.86	-2.82
Heysham	54.03	-2.92	72015	Lune	Lunes Bridge	54.42	-2.60
Heysham	54.03	-2.92	74001	Duddon	Duddon Hall	54.30	-3.24
Hinkley	51.22	-3.13	45001	Exe	Thorverton	50.80	-3.51
Hinkley	51.22	-3.13	45002	Exe	Stoodleigh	50.95	-3.51
Hinkley	51.22	-3.13	45011	Barle	Brushford	51.02	-3.53
Holyhead	53.31	-4.62	65006	Seiont	Peblig Mill	53.14	-4.25
Ilfracombe	51.21	-4.11	50001	Taw	Umberleigh	50.99	-3.99

Ilfracombe	51.21	-4.11	50002	Torridge	Torrington	50.95	-4.14
Ilfracombe	51.21	-4.11	50006	Mole	Woodleigh	50.97	-3.91
Ilfracombe	51.21	-4.11	50010	Torridge	Rockhay Bridge	50.84	-4.12
Immingham	53.63	-0.19	28022	Trent	North Muskham	53.14	-0.80
Immingham	53.63	-0.19	28009	Trent	Colwick	52.95	-1.08
Immingham	53.63	-0.19	28007	Trent	Shardlow	52.86	-1.33
Immingham	53.63	-0.19	27009	Ouse	Skelton	53.99	-1.13
Immingham	53.63	-0.19	28019	Trent	Drakelow Park	52.78	-1.65
Immingham	53.63	-0.19	27003	Aire	Beal Weir	53.72	-1.20
Immingham	53.63	-0.19	27007	Ure	Westwick Lock	54.10	-1.46
Immingham	53.63	-0.19	27071	Swale	Crakehill	54.15	-1.35
Immingham	53.63	-0.19	27079	Calder	Methley	53.73	-1.38
Immingham	53.63	-0.19	28067	Derwent	Church Wilne	52.88	-1.34
Immingham	53.63	-0.19	27080	Aire	Lemonroyd	53.75	-1.42
Immingham	53.63	-0.19	27002	Wharfe	Flint Mill Weir	53.92	-1.36
Immingham	53.63	-0.19	27089	Wharfe	Tadcaster	53.89	-1.27
Immingham	53.63	-0.19	28085	Derwent	St Mary's Bridge	52.93	-1.47
Immingham	53.63	-0.19	27041	Derwent	Buttercrambe	54.02	-0.88
Immingham	53.63	-0.19	27034	Derwent	Stamford Bridge	54.27	-1.71
Immingham	53.63	-0.19	27021	Don	Doncaster	53.53	-1.14
Immingham	53.63	-0.19	27028	Aire	Armley	53.80	-1.57
Immingham	53.63	-0.19	28117	Derwent	Whatstandwell	53.09	-1.51
Immingham	53.63	-0.19	27043	Wharfe	Addingham	53.94	-1.86
Immingham	53.63	-0.19	28080	Tame	Lea Marston Lakes	52.54	-1.69
Immingham	53.63	-0.19	28018	Dove	Marston on Dove	52.86	-1.65

Immingham	53.63	-0.19	27090	Swale	Catterick Bridge	54.39	-1.65
Immingham	53.63	-0.19	28011	Derwent	Matlock Bath	53.12	-1.56
Immingham	53.63	-0.19	28012	Trent	Yoxall	52.76	-1.80
Immingham	53.63	-0.19	28074	Soar	Kegworth	52.83	-1.27
Immingham	53.63	-0.19	28093	Soar	Pillings Lock	52.76	-1.16
Immingham	53.63	-0.19	27062	Nidd	Skip Bridge	54.00	-1.26
Immingham	53.63	-0.19	27029	Calder	Elland	53.69	-1.81
Immingham	53.63	-0.19	27001	Nidd	Hunsingore Weir	53.97	-1.35
Immingham	53.63	-0.19	28008	Dove	Rocester Weir	52.95	-1.83
Immingham	53.63	-0.19	27035	Aire	Kildwick Bridge	53.91	-1.98
Immingham	53.63	-0.19	28043	Derwent	Chatsworth	53.21	-1.61
Immingham	53.63	-0.19	28014	Sow	Milford	52.79	-2.04
Immingham	53.63	-0.19	28003	Tame	Water Orton	52.52	-1.75
Immingham	53.63	-0.19	27006	Don	Hadfields Weir	53.41	-1.41
Immingham	53.63	-0.19	27053	Nidd	Birstwith	54.04	-1.65
Kinlochbervie	58.46	-5.05	96002	Naver	Apigill	58.48	-4.21
Kinlochbervie	58.46	-5.05	96004	Strathmore	Allnabad	58.35	-4.65
Leith	55.99	-3.18	15006	Tay	Ballathie	56.51	-3.39
Leith	55.99	-3.18	15003	Tay	Caputh	56.54	-3.49
Leith	55.99	-3.18	21009	Tweed	Norham	55.72	-2.16
Leith	55.99	-3.18	15012	Tummel	Pitlochry	56.70	-3.72
Leith	55.99	-3.18	21021	Tweed	Sprouston	55.61	-2.39
Leith	55.99	-3.18	15007	Tay	Pitnacree	56.66	-3.76
Leith	55.99	-3.18	15016	Tay	Kenmore	56.60	-3.99
Leith	55.99	-3.18	18011	Forth	Craigforth	56.14	-3.97
leith	55.99	-3.18	21006	Tweed	Boleside	55.59	-2.80
Leith	55.99	-3.18	16004	Earn	Forteviot Bridge	56.35	-3.55

Leith	55.99	-3.18	18003	Teith	Bridge of Teith	56.19	-4.06
Leith	55.99	-3.18	16001	Earn	Kinkell Bridge	56.33	-3.73
Leith	55.99	-3.18	21008	Teviot	Ormiston Mill	55.55	-2.47
Leith	55.99	-3.18	15034	Garry	Killiecrankie	56.75	-3.80
Leith	55.99	-3.18	21003	Tweed	Peebles	55.65	-3.18
Leith	55.99	-3.18	15024	Dochart	Killin	56.46	-4.33
Leith	55.99	-3.18	18010	Forth	Gargunnock	56.13	-4.07
Leith	55.99	-3.18	21007	Ettrick Water	Lindean	55.57	-2.82
Leith	55.99	-3.18	15025	Ericht	Craighall	56.61	-3.35
Leith	55.99	-3.18	18008	Leny	Anie	56.26	-4.29
Leith	55.99	-3.18	15011	Lyon	Comrie Bridge	56.61	-3.98
Leith	55.99	-3.18	21005	Tweed	Lyne Ford	55.64	-3.26
Leith	55.99	-3.18	21012	Teviot	Hawick	55.43	-2.76
Leith	55.99	-3.18	15010	Isla	Wester Cardean	56.61	-3.15
Leith	55.99	-3.18	18015	Eas Gobhain	Loch Venachar	56.23	-4.26
Leith	55.99	-3.18	15039	Tilt	Marble Lodge	56.82	-3.82
Leith	55.99	-3.18	15023	Braan	Hermitage	56.56	-3.61
Leith	55.99	-3.18	18005	Allan Water	Bridge of Allan	56.16	-3.96
Leith	55.99	-3.18	15041	Lyon	Camusvrachan	56.60	-4.25
Leith	55.99	-3.18	21022	Whiteadder Water	Hutton Castle	55.79	-2.19
Leith	55.99	-3.18	21011	Yarrow Water	Philiphaugh	55.54	-2.89
Leith	55.99	-3.18	19001	Almond	Craigiehall	55.96	-3.34
Leith	55.99	-3.18	15013	Almond	Almondbank	56.42	-3.51

Leith	55.99	-3.18	18001	Allan Water	Kinbuck	56.23	-3.95
Leith	55.99	-3.18	16003	Ruchill Water	Cultybraggan	56.36	-4.00
Leith	55.99	-3.18	21020	Yarrow Water	Gordon Arms	55.51	-3.09
Liverpool	53.45	-3.02	67027	Dee	Ironbridge	53.13	-2.87
Liverpool	53.45	-3.02	67033	Dee	Chester Suspension Bridge	53.19	-2.88
Liverpool	53.45	-3.02	67015	Dee	Manley Hall	52.97	-2.97
Liverpool	53.45	-3.02	69002	Irwell	Adelphi Weir	53.49	-2.26
Liverpool	53.45	-3.02	67001	Dee	Bala	52.91	-3.58
Liverpool	53.45	-3.02	69007	Mersey	Ashton Weir	53.44	-2.34
Liverpool	53.45	-3.02	68001	Weaver	Ashbrook	53.17	-2.49
Liverpool	53.45	-3.02	67006	Alwen	Druid	52.98	-3.43
Liverpool	53.45	-3.02	68003	Dane	Rudheath	53.24	-2.50
Llandudno	53.33	-3.83	66011	Conwy	Cwmlanerch	53.11	-3.79
Llandudno	53.33	-3.83	66025	Clwyd	Pont Dafydd	53.26	-3.43
Llandudno	53.33	-3.83	66001	Clwyd	Pont-y-Cambwll	53.23	-3.39
Llandudno	53.33	-3.83	66012	Lledr	Pont Gethin	53.07	-3.81
Milford Haven	51.71	-5.05	60003	Taf	Clog-y-Fran	51.81	-4.56
Milford Haven	51.71	-5.05	61002	Eastern Cleddau	Canaston Bridge	51.80	-4.80
Milford Haven	51.71	-5.05	61001	Western Cleddau	Prendergast Mill	51.82	-4.97
Millport	55.75	-4.91	84013	Clyde	Daldowie	55.83	-4.12
Millport	55.75	-4.91	85001	Leven	Linnbrane	55.99	-4.58
Millport	55.75	-4.91	84005	Clyde	Blairston	55.80	-4.07
Millport	55.75	-4.91	84003	Clyde	Hazelbank	55.69	-3.85

Millport	55.75	-4.91	84018	Clyde	Tulliford Mill	55.64	-3.76
Millport	55.75	-4.91	89003	Orchy	Glen Orchy	56.45	-4.86
Millport	55.75	-4.91	84004	Clyde	Sills of Clyde	55.66	-3.70
Millport	55.75	-4.91	83006	Ayr	Mainholm	55.46	-4.59
Millport	55.75	-4.91	86002	Eachaig	Eckford	56.02	-4.99
Millport	55.75	-4.91	83005	Irvine	Shewalton	55.60	-4.63
Millport	55.75	-4.91	84001	Kelvin	Killermont	55.91	-4.31
Millport	55.75	-4.91	84014	Avon Water	Fairholm	55.74	-3.99
Millport	55.75	-4.91	85002	Endrick Water	Gaidrew	56.05	-4.44
Millport	55.75	-4.91	82002	Doon	Auchendrane	55.41	-4.63
Millport	55.75	-4.91	84015	Kelvin	Dryfield	55.94	-4.18
Millport	55.75	-4.91	82001	Girvan	Robstone	55.26	-4.81
Millport	55.75	-4.91	84012	White Cart Water	Hawkhead	55.84	-4.40
Millport	55.75	-4.91	83009	Garnock	Kilwinning	55.65	-4.69
Millport	55.75	-4.91	83013	Irvine	Glenfield	55.60	-4.49
Millport	55.75	-4.91	85003	Falloch	Glen Falloch	56.34	-4.72
Millport	55.75	-4.91	83004	Lugar Water	Langholm	55.47	-4.36
Millport	55.75	-4.91	83003	Ayr	Catrine	55.50	-4.34
Mumbles	51.57	-3.98	60010	Tywi	Capel Dewi	51.86	-4.20
Mumbles	51.57	-3.98	59001	Tawe	Ynystanglws	51.68	-3.90
Mumbles	51.57	-3.98	60002	Cothi	Felin Mynachdy	51.88	-4.17
Mumbles	51.57	-3.98	60007	Tywi	Dolau Hirion	52.01	-3.81
Mumbles	51.57	-3.98	58002	Neath	Resolven	51.70	-3.72
Mumbles	51.57	-3.98	58001	Ogmore	Bridgend	51.50	-3.58
Mumbles	51.57	-3.98	58012	Afan	Marcroft Weir	51.60	-3.78

Mumbles	51.57	-3.98	60006	Gwili	Glangwili	51.87	-4.28
Newlyn	50.10	-5.54	49001	Camel	Denby	50.48	-4.80
Newport	51.55	-2.99	56001	Usk	Chainbridge	51.74	-2.95
Newport	55.01	-1.44	23003	North Tyne	Reaverhill	55.05	-2.15
Newport	51.55	-2.99	57005	Taff	Pontypridd	51.60	-3.33
Newport	51.55	-2.99	56002	Ebbw	Rhiwderin	51.59	-3.07
Newport	51.55	-2.99	57007	Taff	Fiddlers Elbow	51.65	-3.32
Newport	51.55	-2.99	57006	Rhondda	Trehafod	51.61	-3.37
Newport	51.55	-2.99	57008	Rhymney	Llanedeyrn	51.53	-3.12
North Shields	55.01	-1.44	23001	Tyne	Bywell	54.95	-1.94
North Shields	55.01	-1.44	23004	South Tyne	Haydon Bridge	54.98	-2.22
North Shields	55.01	-1.44	24009	Wear	Chester le Street	54.85	-1.56
North Shields	55.01	-1.44	24001	Wear	Sunderland Bridge	54.73	-1.59
North Shields	55.01	-1.44	23006	South Tyne	Featherstone	54.94	-2.51
North Shields	55.01	-1.44	22001	Coquet	Morwick	55.33	-1.63
North Shields	55.01	-1.44	23022	North Tyne	Uglydub	55.18	-2.45
North Shields	55.01	-1.44	23005	North Tyne	Tarset	55.17	-2.35
North Shields	55.01	-1.44	24008	Wear	Witton Park	54.67	-1.73
North Shields	55.01	-1.44	23008	Rede	Rede Bridge	55.14	-2.21
North Shields	55.01	-1.44	22009	Coquet	Rothbury	55.31	-1.89
Portpatrick	54.84	-5.12	81002	Cree	Newton Stewart	54.96	-4.48
Portpatrick	54.84	-5.12	81004	Bladnoch	Low Malzie	54.86	-4.52
Portpatrick	54.84	-5.12	81006	Water of	Minnoch Bridge	55.04	-4.57

				Minnoch			
Portpatrick	54.84	-5.12	81003	Luce	Airyhemming	54.90	-4.84
Portrush	55.21	-6.66	203040	Lower Bann	Movanagher	54.98	-6.55
Portrush	55.21	-6.66	201010	Mourne	Drumnabuoy House	54.81	-7.46
Portrush	55.21	-6.66	203093	Main	Shane's Viaduct	54.74	-6.31
Portrush	55.21	-6.66	203010	Blackwater	Maydown Bridge	54.41	-6.74
Portrush	55.21	-6.66	201009	Owenkillew	Crosh	54.73	-7.35
Portrush	55.21	-6.66	201008	Derg	Castlederg	54.71	-7.59
Portrush	54.84	-5.12	82003	Stinchar	Balnowlart	55.11	-4.97
Portrush	55.21	-6.66	203012	Ballinderry	Ballinderry Bridge	54.66	-6.56
Portrush	55.21	-6.66	203020	Moyola	Moyola New Bridge	54.66	-6.52
Portrush	55.21	-6.66	201006	Drumragh	Campsie Bridge	54.60	-7.29
Portrush	55.21	-6.66	236005	Colebrooke	Ballindarragh Bridge	54.27	-7.49
Portrush	55.21	-6.66	202002	Faughan	Drumahoe	54.98	-7.28
Portrush	55.21	-6.66	204001	Bush	Seneirl Bridge	55.16	-6.52
Portrush	55.21	-6.66	201005	Camowen	Camowen Terrace	54.60	-7.29
Portrush	55.21	-6.66	203011	Main	Dromona	54.92	-6.37
Portrush	55.21	-6.66	203092	Main	Dunminning	54.94	-6.36
Portrush	55.21	-6.66	236007	Sillees	Drumrainey Bridge	54.31	-7.69
Portrush	55.21	-6.66	201002	Fairywater	Dudgeon Bridge	54.63	-7.37
Portrush	55.21	-6.66	203027	Braid	Ballee	54.85	-6.29

Portsmouth	50.80	-1.11	42004	Test	Broadlands	50.97	-1.50
Portsmouth	50.80	-1.11	42023	Itchen	Riverside Park	50.94	-1.37
Portsmouth	50.80	-1.11	42024	Test	Chilbolton Total	51.15	-1.45
Portsmouth	50.80	-1.11	42010	Itchen	Highbridge & Allbrook Total	50.99	-1.34
Sheerness	51.45	0.74	39001	Thames	Kingston	51.41	-0.31
Sheerness	51.45	0.74	39072	Thames	Royal Windsor Park	51.49	-0.59
Sheerness	51.45	0.74	39121	Thames	Walton	51.39	-0.42
Sheerness	51.45	0.74	39111	Thames	Staines	51.43	-0.51
Sheerness	51.45	0.74	39130	Thames	Reading	51.46	-0.97
Sheerness	51.45	0.74	39002	Thames	Days Weir	51.64	-1.18
Sheerness	51.45	0.74	39046	Thames	Sutton Courtenay	51.65	-1.25
Sheerness	51.45	0.74	39129	Thames	Farmoor	51.76	-1.36
Sheerness	51.45	0.74	39008	Thames	Eynsham	51.77	-1.35
Sheerness	51.45	0.74	40003	Medway	Teston / East Farleigh	51.25	0.45
Sheerness	51.45	0.74	39016	Kennet	Theale	51.43	-1.07
Sheerness	51.45	0.74	39079	Wey	Weybridge	51.37	-0.46
Sheerness	51.45	0.74	39104	Mole	Esher	51.38	-0.37
Sheerness	51.45	0.74	39103	Kennet	Newbury	51.40	-1.32
Tobermory	56.62	-6.06	91002	Lochy	Camisky	56.88	-5.05
Tobermory	56.62	-6.06	92001	Shiel	Shielfoot	56.76	-5.83
Tobermory	56.62	-6.06	90003	Nevis	Claggan	56.82	-5.09
Ullapool	57.90	-5.16	94001	Ewe	Poolewe	57.76	-5.61
Ullapool	57.90	-5.16	93001	Carron	New Kelso	57.43	-5.44
Ullapool	57.90	-5.16	95001	Inver	Little Assynt	58.17	-5.16
Ullapool	57.90	-5.16	95002	Broom	Inverbroom	57.81	-5.06

Weymouth	50.61	-2.45	44001	Frome	East Stoke Total	50.68	-2.19
Weymouth	50.61	-2.45	43009	Stour	Hammoon	50.93	-2.26
Weymouth	50.61	-2.45	45004	Axe	Whitford	50.75	-3.05
Whitby	54.49	-0.61	25009	Tees	Low Moor	54.49	-1.44
Whitby	54.49	-0.61	25001	Tees	Broken Scar	54.52	-1.60
Whitby	54.49	-0.61	25008	Tees	Barnard Castle	54.54	-1.93
Whitby	54.49	-0.61	25018	Tees	Middleton in Teesdale	54.62	-2.08
Whitby	54.49	-0.61	27092	Esk	Briggswath	54.46	-0.65
Wick	58.44	-3.09	6007	Ness	Ness-side	57.45	-4.26
Wick	58.44	-3.09	8006	Spey	Boat o Brig	57.55	-3.14
Wick	58.44	-3.09	4001	Conon	Moy Bridge	57.56	-4.54
Wick	58.44	-3.09	8010	Spey	Grantown	57.32	-3.61
Wick	58.44	-3.09	5003	Glass	Kerrow Wood	57.35	-4.74
Wick	58.44	-3.09	8005	Spey	Boat of Garten	57.25	-3.75
Wick	58.44	-3.09	8002	Spey	Kinrara	57.15	-3.85
Wick	58.44	-3.09	7002	Findhorn	Forres	57.61	-3.64
Wick	58.44	-3.09	5002	Farrar	Struy	57.43	-4.68
Wick	58.44	-3.09	3003	Oykel	Easter Turnaig	57.96	-4.70
Wick	58.44	-3.09	8004	Avon	Delnashaugh	57.40	-3.36
Wick	58.44	-3.09	7001	Findhorn	Shenachie	57.38	-3.95
Wick	58.44	-3.09	2001	Helmsdale	Kilphedir	58.14	-3.70
Wick	58.44	-3.09	2002	Brora	Bruachrobie	58.01	-3.88
Wick	58.44	-3.09	3002	Carron	Sgodachail	57.89	-4.55
Wick	58.44	-3.09	97002	Thurso	Halkirk	58.52	-3.49
Wick	58.44	-3.09	8013	Feshie	Feshie Bridge	57.12	-3.90
Wick	58.44	-3.09	3004	Cassley	Rosehall	57.98	-4.59
Wick	58.44	-3.09	4005	Meig	Glenmeanie	57.53	-4.87
Wick	58.44	-3.09	4003	Alness	Alness	57.70	-4.26

Wick	58.44	-3.09	8007	Spey	Invertruim	57.04	-4.16
Wick	58.44	-3.09	8009	Dulnain	Balnaan Bridge	57.30	-3.70
Wick	58.44	-3.09	4004	Blackwater	Contin	57.57	-4.59
Wick	58.44	-3.09	6009	Moriston	Levishie	57.22	-4.65
Wick	58.44	-3.09	7004	Nairn	Firhall	57.57	-3.87
Wick	58.44	-3.09	5004	Glass	Fasnakyle	57.32	-4.80
Wick	58.44	-3.09	96001	Halladale	Halladale	58.48	-3.90
Workington	54.65	-3.57	76007	Eden	Sheepmount	54.90	-2.95
Workington	54.65	-3.57	80002	Dee	Glenlochar	54.96	-3.98
Workington	54.65	-3.57	78003	Annan	Brydekirk	55.02	-3.27
Workington	54.65	-3.57	79002	Nith	Friars Carse	55.15	-3.69
Workington	54.65	-3.57	75002	Derwent	Camerton	54.66	-3.49
Workington	54.65	-3.57	77002	Esk	Canonbie	55.07	-2.94
Workington	54.65	-3.57	79006	Nith	Drumlanrig	55.27	-3.80
Workington	54.65	-3.57	75003	Derwent	Ouse Bridge	54.68	-3.24
Workington	54.65	-3.57	76003	Eamont	Udford	54.67	-2.66
Workington	54.65	-3.57	76005	Eden	Temple Sowerby	54.65	-2.61
Workington	54.65	-3.57	75005	Derwent	Portinscale	54.60	-3.16
Workington	54.65	-3.57	77003	Liddel Water	Rowanburnfoot	55.07	-2.92
Workington	54.65	-3.57	78006	Annan	Woodfoot	55.29	-3.42
Workington	54.65	-3.57	79005	Cluden Water	Fiddlers Ford	55.10	-3.68
Workington	54.65	-3.57	76015	Eamont	Pooley Bridge	54.62	-2.82
Workington	54.65	-3.57	78005	Kinnel Water	Bridgemuir	55.15	-3.43
Workington	54.65	-3.57	76008	Irthing	Greenholme	54.91	-2.80
Workington	58.44	-3.09	4006	Bran	Dosmucheran	57.60	-5.01
Workington	54.65	-3.57	80001	Urr	Dalbeattie	54.93	-3.84
Workington	54.65	-3.57	79003	Nith	Hall Bridge	55.39	-4.08

Workington	54.65	-3.57	79004	Scar Water	Capenoch	55.23	-3.82
Workington	54.65	-3.57	75004	Cocker	Southwaite Bridge	54.64	-3.35
Workington	54.65	-3.57	74005	Ehen	Braystones	54.44	-3.53

10. Appendix C

Table 10.1: The pairs of tide gauge, river discharge and rainfall stations and wave nodes used in Chapter 4.

Site No.	Tide gauge	Tide gauge latitude (deg.)	Tide gauge longitude (deg.)	Wave node latitude (deg.)	Wave node longitude (deg.)	River gauge latitude (deg.)	River gauge longitude (deg.)	Rainfall station latitude (deg.)	Rainfall station longitude (deg.)
1	Newhaven	50.78	0.06	50.75	0.0	N/A	N/A	50.8	0.01
2	Portsmouth	50.8	-1.11	50.75	-1.13	50.94	-1.37	50.79	-1.04
3	Bournemouth	50.71	-1.87	50.63	-1.88	50.76	-1.84	50.75	-1.94
4	Weymouth	50.61	-2.45	50.5	-2.38	50.68	-2.19	50.52	-2.45
5	Devonport	50.37	-4.19	50.25	-4.25	50.49	-4.15	50.35	-4.12
6	Newlyn	50.1	-5.54	50.13	-5.5	50.48	-4.8	50.13	-5.57
7	St Marys	49.92	-6.32	50.13	-5.88	N/A	N/A	49.91	-6.29
8	Ilfracombe	51.21	-4.11	51.25	-4.13	50.99	-3.99	51.16	-4.09
9	Hinkley	51.22	-3.13	51.25	-3.13	51.02	-3.53	51.15	-3.08
10	Avonmouth	51.51	-2.71	51.5	-2.88	51.8	-2.69	51.44	-2.74
11	Newport	51.55	-2.99	51.5	-3	51.59	-3.07	51.55	-2.96
12	Mumbles	51.57	-3.98	51.5	-4	51.68	-3.9	51.57	-3.98
13	Milford Haven	51.71	-5.05	51.63	-5.13	51.82	-4.97	51.71	-5.05
14	Fishguard	52.01	-4.98	52.13	-5	52.05	-4.56	51.97	-4.87
15	Barmouth	52.72	-4.05	52.75	-4.25	52.6	-3.85	52.77	-3.87
16	Holyhead	53.31	-4.62	53.38	-4.63	53.14	-4.25	53.3	-4.68
17	Llandudno	53.33	-3.83	53.38	-3.88	53.11	-3.79	53.29	-3.71

18	Liverpool	53.45	-3.02	53.5	-3.25	53.19	-2.88	53.35	-3.08
19	Heysham	54.03	-2.92	54	-3.13	54.08	-2.72	54.02	-2.82
20	Workington	54.65	-3.57	54.63	-3.63	54.66	-3.49	54.71	-3.43
21	Port Erin, Isle of Man	54.09	-4.77	54.13	-4.75	N/A	N/A	54.13	-4.67
22	Bangor	54.66	-5.67	54.75	-5.63	54.55	-5.95	54.67	-5.75
23	Portrush	55.21	-6.66	55.25	-6.63	55.16	-6.52	55.11	-6.66
24	Portpatrick	54.84	-5.12	54.5	-5.25	54.9	-4.84	54.74	-4.96
25	Milport	55.75	-4.91	55.63	-5	55.65	-4.69	55.75	-4.91
26	Port Ellen	55.63	-6.19	55.63	-6.13	N/A	N/A	55.68	-6.25
27	Tobermory	56.62	-6.06	56.63	-6.25	56.76	-5.83	56.54	-5.96
28	Stornoway	58.21	-6.39	58.13	-6.38	N/A	N/A	58.21	-6.32
29	Ullapool	57.9	-5.16	58	-5.5	57.81	-5.06	57.96	-5.13
30	Kinlochbervie	58.46	-5.05	58.5	-5.13	58.35	-4.65	58.31	-4.92
31	Lerwick	60.15	-1.14	60.13	-1.13	N/A	N/A	58.95	-2.9
32	Wick	58.44	-3.09	58.5	-3	58.52	-3.49	58.45	-3.09
33	Aberdeen	57.14	-2.08	57.13	-2	57.22	-2.19	57.21	-2.2
34	Leith	55.99	-3.18	56	-3.13	55.96	-3.34	55.97	-3.21
35	North Shields	55.01	-1.44	55	-1.38	54.85	-1.56	55.02	-1.42
36	Whitby	54.49	-0.61	54.5	-0.63	54.46	-0.65	54.47	-0.62
37	Immingham	53.63	-0.19	53.5	0.25	53.14	-0.8	53.5	-0.18
38	Cromer	52.93	1.3	53	1.25	52.58	0.35	52.95	1.12
39	Lowestoft	52.47	1.75	52.5	1.88	N/A	N/A	52.45	1.54
40	Harwich	51.95	1.29	51.88	1.38	N/A	N/A	51.91	1.09
41	Sheerness	51.45	0.74	51.5	0.88	51.25	0.45	51.35	0.75
42	Dover	51.11	1.32	51.13	1.38	N/A	N/A	51.19	1.28
43	Jersey	49.18	-2.12	49.38	-1.88	N/A	N/A	49.2	-2.13